UNIVERSITÉ **LAVAL**

Amélioration de la résistance à la fissuration des bétons projetés: composition des mélanges et mise en place «Improving the Cracking Resistance of Shotcrete: Mix Designs and Placement»

Thèse

Bruce Gandhi Menu

Doctorat en génie civil
Philosophiæ doctor (Ph. D.)

Québec, Canada

Résumé

Le béton projeté est une méthode de mise en place rapide, économique et polyvalente qui offre de multiples avantages par rapport au béton conventionnel dans divers types de constructions nouvelles et dans les réparations. Un des grands avantages du béton projeté est de permettre une mise en place sur des surfaces fortement irrégulières en utilisant peu on même aucun coffrage. Cependant, ces mêmes caractéristiques rendant le béton projeté avantageux et polyvalent peuvent le rendre vulnérable à la fissuration due au retrait restreint. Cette vulnérabilité vient de la *restriction* élevée inhérente à de nombreuses applications (projection adhérente sur substrat rigide). En effet, le béton développera des contraintes internes s'il ne peut manifester ses changements volumétriques librement, ce qui peut conduire à de la fissuration lorsque ces contraintes atteignent la résistance en traction du matériau. La fissuration des réparations due au retrait restreint est sans aucun doute un des plus grands défis auxquels l'industrie des réparations en béton fait face aujourd'hui. La fissuration peut raccourcir les années de service d'une structure en béton (corrosion accélérée, délamination, etc.) et engendre souvent des coûts des maintenances supplémentaires importants. Il existe peu d'informations fiables dans la littérature sur les paramètres qui influencent la fissuration due au retrait restreint des bétons projetés ainsi que sur leur comportement à long terme en service. Ce manque d'informations à propos de l'influence des différentes composantes du mélange et de la mise en place des bétons projetés rend difficile, voire impossible, la prédiction du comportement à long terme des bétons projetés face aux problèmes de fissuration. De plus, l'ensemble des paramètres individuels affectant la fissuration due au retrait restreint est très difficile à identifier. Pour cette raison, il est devenu impératif de caractériser le comportement volumétrique des bétons projetés au moyen d'essais de retrait restreint. Dans cette thèse, l'évolution de différentes propriétés à l'état frais et durci telles que la consistance de projection, le rebond, la résistance à la compression, la résistance à la traction par fendage, le module élastique, le retrait libre et le retrait restreint est étudiée. Ce projet se concentre particulièrement sur les mélanges et leur composition, la méthode de mise en place et le potentiel de fissuration due au retrait restreint. Le potentiel de fissuration sera évalué au moyen d'une procédure d'essai annulaire qui a récemment été adaptée et amélioré pour les bétons projetés. À partir des données expérimentales générées, une analyse approfondie du développement des contraintes et de la résistance à la fissuration des bétons projetée sera conduite.

Mots clés : béton projeté, fissuration, retrait restreint, restriction, réparations, rebond, retrait libre, essai annulaire.

Abstract

Shotcrete is a fast, cost-saving, sustainable and versatile concrete placement method that offers numerous advantages over conventional concrete in a variety of new construction and repair works. One of the major benefits of the shotcrete process is that it can be sprayed over irregular surfaces and can cover large surfaces with little or no formwork. Howbeit, these same versatile features also often make shotcrete vulnerable to restrained shrinkage cracking. Cracking occurs mainly because of the highly *restrained* conditions that are inherent in many shotcrete applications (spraying on a rigid substrate). If shrinkage is restrained, internal tensile stresses are progressively induced in the element which can lead to cracking when the stresses eventually exceed the tensile strength of the material. Cracking of repair materials is unarguably one of the major challenges facing the repair industry worldwide today. Cracking can shorten the service life of concrete structures (accelerated corrosion, delamination, etc.) and often requires significant additional costly maintenance. Yet, reliable material data on parameters that influence the long-term service life and cracking in-place shotcrete is scarce. This lack of information on the influence of mixture composition as well as the placement process makes it difficult, if not impossible, to predict the long-term cracking behaviour of shotcrete. Furthermore, key mixture parameters that lead to cracking have been very difficult to identify. For this reason, it has become imperative for material characterization to be made on the basis of a restrained shrinkage test. In this thesis, different fresh and hardened shotcrete properties such as spraying consistency, rebound, compressive strength, splitting tensile strength, elastic modulus, free shrinkage, and restrained shrinkage deformation are investigated. The project focuses particularly on mix designs and compositions, placement process and the potential for cracking due to restrained shrinkage. The shrinkage ring test method which has been recently adapted and improved for shotcrete will be used to evaluate the cracking potential. Based on the experimental data that will be generated, an in-depth analysis of stress development and cracking resistance of shotcrete will be conducted.

Keywords: shotcrete, restrained shrinkage, cracking, restrained conditions, repair materials, free shrinkage, rebound, ring test.

Table of Contents

List of Tables

List of Figures

To God, my loved ones and my family

Acknowledgment

I would like to thank everyone that contributed and helped make this dissertation possible. First, my deepest gratitude goes to my supervisor Prof Marc Jolin and co-supervisor Prof Benoît Bissonnette for their advice, guidance, and complete support of my personal and professional development. Their constructive criticisms, effective discussions and suggestions greatly helped me to complete my work successfully. I would also like to thank my ad-hoc co-supervisor Dr Laurent Molez for his advice, guidance, and help in understanding modelling of concrete early age behaviour.

I am also indebted to Mr Jean-Daniel Lemay and Mr Mathieu Thomassin for their outstanding technical support. Their help and experience have been essential to this dissertation and to my development. I would also like to thank Mr. Alexandre Pépin Beaudet for all his help and devotion in the spraying aspect of this project. Working with Samy-Joseph Essalik has made my time at the Université Laval a truly memorable experience. Thanks to my colleagues Pasquale Basso-Trujillo, Antoine Gagnon, and Thomas Jacob Vaillancourt. My sincere gratitude also goes to all the administrative staffs, especially Lyne Dupuis for her kindness and help.

Special thanks to my family and love ones for all their love, support, and encouragement throughout my life to this point. Without their guidance and encouragement, this work and everything it entails would have been impossible. I will always be grateful for everything they have done and owe them a debt that can never be repaid.

Preface

This research project is intended to accomplish a comprehensive study on the shrinkage and the associated potential for cracking of shotcrete mixtures by evaluating their early age shrinkage and tensile creep properties. This Ph.D. dissertation is written as an article-based thesis and consists of five research papers (main body) and one scientific conference paper (appendix). The author of this dissertation is the main author of all of the above-mentioned articles. The contributions of the first author to the articles consisted of carrying out the research works, gathering the results, doing the analyses, writing the computer codes, plotting the graphs, drafting, and revising of the articles. Co-authors Dr. M. Jolin and Dr. B. Bissonnette supervised the research work, improved the methods of interpretation of the results and the research methodology, and critically revised the papers. Co-author Dr. L. Molez supervised the writing of the computer codes, analysis and interpretation of data, and critically revised the papers, Co-authors Mr. A. Pepin- Beaudet and Mr. T. Jacob-Vaillancourt participated in the experimental work, acquisition of data and initial drafting of articles during their M.Sc. work.

The layout of the articles was revised extensively to reflect imposed the Ph.D. dissertations. Also, for the sake of uniformity, the same citations style was used for all the articles presented in the dissertation.

Introduction

A brief insight of the problem at hand and the objective of this thesis are provided in this chapter. This will include brief review of previous research efforts to reduce the shrinkage and, ultimately, the cracking tendency of concrete and/or shotcrete mixtures.

Background

The motivation for this project is the effort to reduce the cracking potential of shotcrete, notably in view of repair applications. Shotcrete has proven to be an advantageous technique for concrete repairs, and with the ever-increasing need for concrete infrastructure rehabilitation and the solid technological background available today, this application technique is in great demand. A great majority of shotcrete repairs have performed satisfactorily over the past years. However, extensive shrinkage cracking is still encountered in some situations, eventually leading to debonding, premature deterioration and failures of shotcrete repairs in service. Early age cracking of repairs is a major concern of the shotcrete repair industry. Cracking is caused mainly by restraint to volume changes resulting from dimensional incompatibility between the repair material and the substrate. The new concrete (*repair material*) seeks to shrink freely, whereas the old existing concrete in the structure being repaired (*substrate*) is in a more stable volumetric state. Through adhesion, the repair concrete is prevented from contracting by the old concrete, resulting in the development of internal tensile stresses. If the induced stresses exceed the tensile strength of the repair material, cracks will appear. The likelihood of cracking depends largely on the rate of development of strength (tensile), elastic modulus and creep properties in the repair material, with respect to the existing substrate properties.

Research Objectives

The ultimate goal of this PhD thesis is to gain a better and more up-to-date understanding of the shrinkage and cracking sensitivity of shotcrete. The project seeks to help formulate guidelines that can be employed to predict the likelihood of restrained shrinkage cracking occurrence in shotcrete applications. The improved knowledge from the project will help engineers develop and use repair shotcrete with significantly low sensitivity to shrinkage cracking. Following a review of the information available today, the specific objectives will be reached by focusing mainly on the following:

- Optimize the *free ring shrinkage test* procedure and correlate the results with the *restrained ring test* results;

- Correlate the cracking potential with mixture proportions and mechanical properties;

- Investigate the key mix design parameters that influence shrinkage and the cracking behaviour of shotcrete;

- Explore the influence of the placement method (i.e., cast-in-place and sprayed) on shrinkage and the cracking characteristics of shotcrete;

- Develop a numerical tool for the study of the shrinkage and the cracking potential of shotcrete mixtures;

In parallel, two supplementary specific objectives were naturally linked to this work:

- Explore the effect of curing and protection on shrinkage and the quality of the in-place shotcrete (M.Sc. project of Jacob-Vaillancourt running in parallel);

- Evaluate the significance of the shrinkage ring tests (restrained and unrestrained) as suitable tools for characterizing the sensibility to cracking of repair materials (M.Sc. project of Alexandre Pépin-Beaudet running in parallel).

The originality of this project is the focus on characterizing key factors that lead to cracking of shotcrete through the use of *free* and *restrained* shrinkage tests. Moreover, the data will provide sufficient information on the cracking potential of mixtures that will lead to the optimization and improvement of shotcrete mixture designs with reduced sensitivity to cracking.

Previous Works (CRIB, Université Laval)

The problem of shrinkage and cracking of concrete and/or shotcrete has already been the subject of several master's and doctoral thesis at the CRIB (Research Centre on Concrete Infrastructure) of Université Laval. Most notably, Bissonnette (1996) [1] and Modjabi-Sangnier (2010) [2]) has shown that the cracking potential of a concrete mixture cannot be solely weighed by the amplitude of its drying shrinkage because of stress relaxation due to tensile creep. These results demonstrated the importance of considering tensile creep in predicting the risk of cracking, particularly in repairs. The results further showed that concrete tensile creep potential is mostly dependent on certain mixture parameters.

In a subsequent experimental program led by Girard [3], the AASHTO shrinkage ring test procedure (AASHTO T334-08 [4], *formerly AASHTO PP 34–99* [5]) was used as a basis towards the development of an approach for the quantitative assessment of dimensional compatibility and sensitivity to cracking of *shotcrete*. The results of the study showed that the modified procedure to cast the AASHTO ring test specimen through pneumatic projection can be used successfully to evaluate the sensitivity to cracking of shotcrete mixtures. Although this test method has only been used at Université Laval's shotcrete laboratory up to now, it is the aim of this thesis work to further improve the proposed approach proposed and help eventually develop it into a standardized testing method.

Previous research works (such as reference [2, 3]) attempted to combine the free shrinkage ring measurements and restrained ring shrinkage results to perform analytical viscoelastic calculations, but the approach was not conclusive. The calculated creep values calculated from these data were found to be variable and sometimes inconsistent. The current study will thus intend to investigate the cause of the inconsistencies. This will in addition provide a better understanding of the difference between the measured

free ring shrinkage and that obtained from a uniaxial shrinkage test (particularly with the same volume/surface ratio exposed to drying) and allow to assess the necessity to use the former in restrained shrinkage investigations involving ring specimens.

Organization of Contents

This Ph.D. dissertation is written as an article-based thesis. The thesis begins with an introduction which includes a background, research objectives and structure of the thesis. Chapter 1 provides an up-to-date account of the present state of knowledge on shotcrete technology and on early-age shrinkage and cracking. Some techniques used in mitigating shrinkage of shotcrete are also highlighted. Chapter 2 provides an overview of the materials used and the detailed experimental programs outlined to address the issues of shrinkage and the associated potential risk of cracking of shotcrete. Chapters 3 to 7 contains the main research findings of the thesis which are presented through five research papers either published or submitted for publication in recognized scientific journal. A supplementary paper presented in a renowned scientific conference is found in Appendix A. Chapter 8 presents a discussion of the results compiled from the different papers. The dissertation is completed by a summary and a conclusion of the overall research, along with some possible future research avenues. The research papers included in this Ph.D. thesis are as follows.

Chapter 3 Article #1 pp 36 - 49

B. Menu, M. Jolin, and B. Bissonnette. 2017. Studies on the influence of drying shrinkage test procedure, specimen geometry, and boundary conditions on free shrinkage, published in *Advances in Materials Science and Engineering*, Article ID 9834159.

The paper describes the research that has been carried out to optimize the *free ring shrinkage test* procedure. The study demonstrates the influence of the free shrinkage test procedure, the specimen geometry, the boundary conditions, and the surface area-to-volume ratio exposed to drying on the free shrinkage of shotcrete.

Chapter 4 Article #2 pp 50 - 69

B. Menu, M. Jolin, and B. Bissonnette. 2020. Assessing the early-age shrinkage cracking potential of concrete using ring specimens under different boundary conditions published in *Advances in Materials Science and Engineering*, Article ID 4842369.

This paper deals with the potential for cracking due to restraints and is a continuation of the previous paper on free shrinkage. The paper presents information to improve our interpretation of cracking behaviour in *restrained shrinkage ring specimens* and a theoretical approach for evaluating the *stress rate* development

of the concrete rings. The findings are used to provide guidance towards the implementation of a suitable drying method for shotcrete ring tests.

Chapter 5 Article #3 pp 70 - 82

B. Menu, T. Jacob-Vaillancourt, M. Jolin, and B. Bissonnette. July 2020. The role of curing methods in early age moisture loss and drying shrinkage, published in *ACI Materials Journal*, V. 117, No. 4.

It was shown in article #2 that longer moist curing can delay shrinkage and counteract the risk of early-age cracking. This paper is an extended research to investigate the effectiveness of the most commonly used curing methods on early-age water evaporation and the subsequent shrinkage in freshly applied shotcrete. Among the range of curing methods investigated, moist curing performed better. Dry curing was found to be the least effective and most detrimental, while effectiveness of curing compound was found to be dependent on the w/cm ratio, being less efficient in low w/cm ratio mixture, but beneficial in higher w/cm ratio concrete.

Chapter 6 Article #4 pp 83 - 115

B. Menu, A. Pepin- Beaudet, M. Jolin, and B. Bissonnette. Experimental study on the effect of mixture parameters on shrinkage and cracking resistance of dry-mix shotcrete, submitted to *Cement and Concrete Composites* on September 28, 2020.

While previous articles focused on the influence of specimen geometry, drying layout and curing on shrinkage and cracking of shotcrete. This paper reports results of an experimental study conducted to investigate the influence of key mixture parameters on shrinkage, stress development, and age at cracking of dry-mix shotcrete mixtures using the *ring shrinkage test* method. In this study, for the first time, an investigation was initiated on the use of crack-reducing admixture in dry-mix shotcrete mixtures. The investigation showed that the addition of silica fume or combine silica fume and fly ash increases the cracking potential of the dry-mix shotcrete, whereas the use polymer, shrinkage-reducing admixture or crack-reducing admixture reduces it. This study also confirms that it is possible to produce shotcrete ring specimens that comply with the AASHTO T 334 ring test standard.

Chapter 7 Article #5 pp 116 - 140

B. Menu, B. Bissonnette and M. Jolin, . Evaluation of early-age viscoelastic characteristics of concrete using ring specimens, submitted to *Journal of Materials in Civil Engineering* on October 26, 2020.

This paper illustrates how *free* shrinkage ring and *restrained* ring shrinkage measurements from the previous papers can provide data on the *tensile creep* and *relaxation* behaviour of different shotcrete mixtures. It was found that mixtures with a higher level of creep or relaxation and lower shrinkage exhibited

lower risk of shrinkage cracking in otherwise equal conditions. This indicates that higher tensile creep capacity is only useful in reducing the risk for cracking if the shrinkage is not increased in the same proportion. The study also demonstrated that tensile creep is an essential component in the evaluation of the risk and sensitivity to cracking of shotcrete under restrained conditions.

As complement to the publications mentioned above, a publication on numerical modelling of shotcrete is presented in Appendix A.

Appendix A Article #6 pp 160 - 169

B. Menu, M. Jolin, B. Bissonnette, and L. Molez. 2018. Évaluation de la sensibilité et potentiel à la fissuration des bétons projetés au jeune âge, published in proceeding of the Conférence Internationale Francophone NoMaD 2018, Liège Université, Liège, Belgique, p. 9.

The present paper is intended to give an overview of the numerical method developed to analyze the behaviour of concrete ring specimens under free and restrained shrinkage. The proposed model and the identified materials parameters validated were used to simulate the shrinkage cracking behaviour of selected shotcretes mixtures from previous papers. It has been found that numerical results agree well with experimental results in terms of cracking ages for both cast and sprayed rings, indicating that the proposed numerical approach is reliable for analyzing cracking in concrete ring specimens subject to restrained shrinkage.

Some additional publications have been made during the project (not presented here). These publications are:

B. Menu, M. Jolin, B. Bissonnette, and N. Ginouse. June 2017. Evaluation of early age shrinkage cracking tendency of concrete, Proceedings of the CSCE Annual Conference on Leadership in Sustainable Infrastructure, Vancouver, Canada, pp. EMM649-1-EMM649-8.

B. Menu, Pépin Beaudet, M. Jolin, B. Bissonnette, and L. Molez. 2018. Évaluation quantitative de la sensibilité à la fissuration du béton au moyen de l'essai de retrait restreint annulaire, in 19ème Journées Scientifiques du Regroupement Francophone pour la Recherche et la Formation sur le Béton ((RF)²B), Anglet, France, 10 pages.

Chapter 1 Literature Review

1.1 Introduction

This chapter provides an up-to-date account of the present state of knowledge on shotcrete and its deformational properties. This will include a general description and insight into shotcrete technology and what renders shotcrete susceptible to cracking due to shrinkage cracking. Other phenomena and factors that need to be considered in analyzing restrained shrinkage cracking is also discussed and basic terms will be defined. To avoid repetition, this chapter will only focus on specific issues since elements of the literature review are also presented in the various articles.

1.2 Shotcrete Technology

Researchers, engineers, construction managers, developers, and architects have tried over the years to enhance and introduce more efficient concrete placement and construction methods, with the aim of reducing the costs and turnaround time. This led to the introduction of a special type of concreting method known as shotcrete (also known as sprayed concrete in many parts of the world). Shotcrete was first introduced into the construction industry in 1910 [6]. Since its inception, shotcrete applications have expanded consistently, with constant improvements and innovations of the technique and mixture design. Today, shotcrete is receiving more attention in almost all domains of the construction industry. In fact, shotcrete has become an indispensable tool in the repair and rehabilitation of concrete structures. The mining and tunnelling industries are other major users of shotcrete, especially for ground stabilization as a temporary support or final lining. Shotcrete technology has also grown into an important technique wherever irregular and complex geometries are involved. Further, the time needed for shotcreting works is much *faster*, making it very attractive in construction projects where scheduling is critical.

Shotcrete is a mortar or concrete that is pneumatically sprayed or projected at high velocity through a pressure resistant conveying hose onto a surface, where it is compacted on impact. Thus, the high velocity is essential for the shotcrete process as it allows the material to stick to the sprayed surface and ensures adequate compaction or consolidation and allows the material to stick to the sprayed surface. Without a proper compaction and consolidation, quality shotcrete cannot be produced [7]. Adequate in-place shotcrete is well-compacted and free of cracks, and it encapsulates the reinforcement and adheres well to the receiving substrate.

1.2.1 Why not Shotcrete?

There is often a debate on how exactly shotcrete differs from ordinary cast-in-place concrete. In reality, shotcrete is unique in some respects: it has its own mixture designs, its own implementation techniques, its own testing and recommendations. Notwithstanding, shotcrete simply remains a method for placing

concrete or mortar. In fact, if properly applied, the durability and physical properties of shotcrete are comparable to those of conventional cast-in-place concrete of similar composition. In most cases, the shotcrete placement method provides a significant number of advantages in wide areas of applications where normal cast-in-place techniques cannot be employed, for instance where access to the work area is difficult and where thin layers or variable thicknesses are required.

Shotcrete is also useful in situations where formwork is not expensive or not practical, and it can offer savings on labour. In the case of repairs, shotcrete can provide superior durability and bonding to existing concrete. The many pros and cons of shotcrete are covered elsewhere [6, 8, 9].

1.2.2 Shotcrete Process

Shotcrete can be produced using two different techniques, the wet-mix and the dry-mix processes. Be it the wet-mix or the dry-mix process, the shotcrete material is conveyed through a hose and then projected onto a surface. The major differences between the two processes have to do with the method of conveying the material through the hose and the location where water is added to the mixture. A schematic set-up of both shotcreting processes is presented in Fig. 1.1. The most widely used method in repairs is the dry-mix process, where the dry materials are conveyed through the delivery hose and wetted at the water ring before exiting at the nozzle. The dry materials may be prebagged or mixed on site. The wet-mix process involves the mixing of all of the ingredients (except for certain admixtures) before they enter the delivery hose. Thus, all mixing water is present in the concrete before its introduction into the pump for the wet-mix shotcrete; while for the dry-mix shotcrete process, water is introduced near the end of the delivery hose [8].

Today, the trend towards automated or remote-controlled spraying equipment for shotcreting is gaining grounds, especially in the mining and tunnelling sector. Nevertheless, shotcrete mix produced with conventional batching equipment and applied from a hand-held nozzle remains and still is the most common and widely used method for repairs.
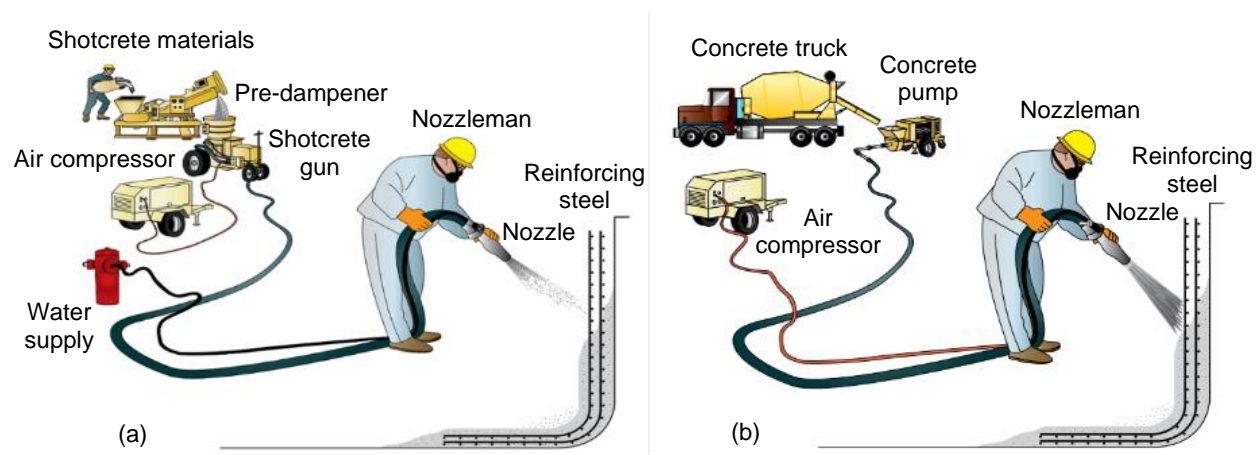
Fig. 1.1 Typical setup for a) dry-mix shotcrete operations; b) wet-mix shotcrete operations

7

1.2.2.1 Consistency

In the dry-mix process, the nozzleman has control over mixing water and thus of the consistency of the mixture at the nozzle to meet variable field conditions whereas in the wet-mix process, the mixing water is controlled at the mixing equipment [9, 10]. The *consistenc*y (i.e., degree of wetness or plasticity) of an in-place shotcrete is of utmost importance as it may affect both its strength and shrinkage properties. Shotcrete with a relatively dry (stiff) shooting consistency may adversely affect rebar encapsulation as well as increase rebound [11]. As clearly shown in Fig. 1.2, the amount of material rebound varies linearly with the shooting consistency for a given shotcrete mixture. Reportedly, spraying the dry-mix shotcrete at its so-called *wettest stable consistency* helps minimizing rebound losses and most importantly, allows proper encasement of the reinforcing steel [8]. To ensure comparability among mixtures with different compositions, a consistency criterion may be set, for which the nozzleman is allowed to adjust the water flow (as opposed to equal w/cm ratio in conventional concrete) [12].
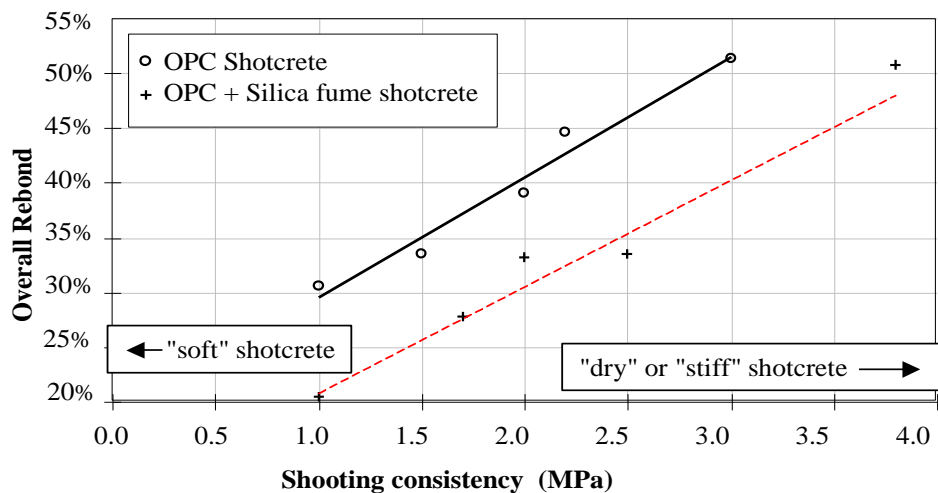
Fig. 1.2 Rebound as a function of the shooting consistency of the mixture [8]

1.2.2.2 Rebound

A very distinctive aspect of shotcrete is that a certain portion of the materials misses the target or does not adhere to the surface during spraying. The amount of materials bouncing off the receiving surface is known as *rebound*. Rebound is perhaps one of the biggest challenges facing the shotcrete industry today. How much rebound is acceptable for a shotcrete application is not entirely clear, but it is desired to minimize rebound. Generally, the dry-mix process produces greater rebound losses than the wet-mix process. The amount of rebound by weight of total sprayed materials is generally in the range of 5 to 15% for the wet-mix process [6, 8] and 15 to 40% for the dry-mix process [8, 12, 13]. How much is acceptable for a given shotcrete application may vary, but it is desirable to minimize rebound. Unfortunately, rebound in shotcrete

is not only expected but is inevitable and to a certain extent. For example, aggregates bouncing off the surface may create a sticky surface for subsequent shotcrete material to become compacted into the surface [13]. Thus, some rebound is necessary to achieve the needed consolidation and desired properties of the shotcrete.

Nevertheless, it must be emphasized that rebound affects the *final in-place mixture composition* by reducing the amount of coarse aggregate and consequently, the as-shot mechanical properties. Furthermore, rebound also has a major economical consequence on the final construction cost. More importantly, shotcrete often exhibits higher shrinkage tendency in comparison with ordinary concrete due to rebound. This is primarily because a high proportion of the rebounding materials corresponds to the coarse aggregates which play key roles in opposing shrinkage of concrete and diluting the paste content. Many factors related to the shooting parameters (air velocity, shooting angle, orientation, and thickness of shooting) and mix design proportion parameters (e.g. cement, silica fume, set accelerator, and water content) will affect the overall rebound [6, 13]. As can be seen in Fig. 1.2, silica fume as well as the shooting consistency (water content) influence shotcrete rebound.

1.2.3 Cementitious Materials

Like any other ordinary concrete, pozzolanic materials such as slag, fly ash and silica fume are often incorporated into shotcrete mixtures. *Silica fume*, a highly pozzolanic mineral additives is added at a typical dosage of about 5 to 10% by weight of cement to produce superior quality shotcrete as it improves the cohesion and adhesion of shotcrete mixture. In addition, adding silica fume also reduces the amount of rebound during the spraying process as shown clearly in Fig. 1.2. Silica fume is also added to increase strength, impermeability and enhances the thickness of build-up in a single pass, without having to resort to the use of high addition rates of accelerators [6]. Thus, silica fume shotcrete is ideal for overhead shotcrete applications. *Fly ash*, on the other hand, is primarily added to facilitate pumping shotcrete materials over long distances. Moreover, fly ash can also reduce rebound of shotcrete and improve its durability. The dosage of fly ash is typically between 15 to 25% by weight of the total binder, through a replacement level of as high as 40% is possible in the wet-mix process. It should be mentioned that fly ash can reduce the early-age strength development of shotcrete. *Slag* is not often used in shotcrete, but can improve its long-term hardened properties.

1.2.4 Admixtures

The advent of modern shotcrete technology has been driven by increasing use of chemical admixtures in shotcreting. *Water-reducers* and *superplasticizers* are commonly used in the wet-mix process to improve workability and cohesiveness. They are primarily used in silica fume shotcrete to reduce the water demand (because silica fume has a high-water demand) and the cement content, thereby reducing shrinkage. Obviously, the overall effect is dependent on the dosage. *Air entraining admixtures* are added to shotcrete to enhance its pumpability, freeze/thaw durability and scaling resistance in the presence of de-icing

9

chemicals [14]. *Set accelerators* are employed in both dry-mix and wet-mix. They are primarily used to shorten the setting time and increase early strength. Reports, however, suggest that the use of accelerators at high dosages can reduce the long-term strength of the shotcret [8, 15]. Accelerators can also increase drying shrinkage and hence the potential for shrinkage cracking [6].

1.3 Shrinkage Cracking: Phenomena and Influencing Factors

1.3.1 Volume Change of Cementitious Materials

All cement-based materials undergo significant volume changes (i.e., contraction or expansion) in response to chemical reactions, temperature variations, and moisture variations within their porosity, even without the presence of any external forces.

Desiccation shrinkage it the one of the most significant cause involved in cracking of cementitious materials. It is a gradual process, so naturally, time is a key factor in shrinkage as it can take place over a long period of time. The rate of shrinkage is higher at early age and evolves at a constantly decreasing rate with time. There are three types of desiccation shrinkage caused by a reduction in relative humidity inside the porosity of cement-based materials: plastic shrinkage, autogenous shrinkage, and drying shrinkage. In reality, all these types of shrinkage are interrelated and may occur simultaneously. For example, drying shrinkage can occur simultaneously with autogenous shrinkage when concrete is subjected to drying conditions immediately after curing.

In addition to the various forms of desiccation shrinkage, cement-based materials are subject to thermal volume changes and carbonation shrinkage. All these volume changes are discussed in more detail in the following subsections.

1.3.2 Desiccation Shrinkage

1.3.2.1 Mechanisms of Desiccation Shrinkage

Despite decades of research into the origins of shrinkage, current knowledge suggests that the mechanisms still remain not completely understood. The most prominent shrinkage mechanisms that have been proposed to explain the shrinkage phenomena are related to capillary tension, disjoining pressure, and (change in) surface free energy. The *capillary tension* mechanism is based on the Kelvin-Laplace law, which indicates that the capillary stress increase as the pore size decreases. The theory stipulates that concrete shrinkage is a result of the evaporation of "*free*" water from the pores. The pores are emptied such that larger pores are gradually emptied first, then progressively followed by the smaller ones. Partial eEmptying of pores results in the formation of a meniscus between the liquid-gas interfaces, which induces a tensile stresses in the liquid phase. This is in turn balanced by compressive forces induced in the solid, which gives rise macroscopically to shrinkage.

The *disjoining pressure* theory stipulates that '*excess*' pressure caused by the natural tendency to adsorb more water beyond saturation exists in the narrower gel pores. According to the theory, the disjoining pressure in hindered adsorption areas is a function of the pore radius, increasing as the latter gets smaller [16]. This pressure is caused by surface forces acting in the adsorbed water confined within the small narrow spaces which creates repulsive forces. So, when capillaries begin to dry out due to decreases in R.H., the water contained in areas of hindered adsorption moves to freely adsorbing zones. The movement of water relieves the disjoining pressure between the solid particles which causes shrinkage as the water layer becomes thinner. In other words, when the pore humidity decreases, the disjoining pressure is reduced, causing shrinkage.

Shrinkage deformation may also result from changes in *surface energy* of calcium silicate hydrate (C-S-H) gel particles at low R.H. levels. Evaporation of adsorbed water from C-S-H gel surfaces causes surface energy to increase, which leads in turn to a compression of the solid particles and gives rise macroscopically to shrinkage.

1.3.2.2 Plastic Shrinkage

Plastic shrinkage occurs due to loss of water by evaporation from *freshly* placed concrete within the first few hours, up to setting. The magnitude of the plastic shrinkage is affected by the rate of evaporation, which is influenced by the air temperature, temperature of concrete at the evaporating surface, relative humidity (R.H.), and wind velocity. It is generally believed that plastic shrinkage *cracking* is likely to occur when the rate of evaporation exceeds the rate at which the bleeding water rises to the surface [17]. According to CSA A23.1-14 [18], the conditions for plastic shrinkage should be considered to exist when the rate of surface moisture evaporation exceeds about 0.50 kg/m^2/h, whiles the ACI 305R [19] suggests a value of 1.0 kg/m^2/h. Shotcrete is particularly prone to plastic shrinkage because of the inherent reduced rate of bleeding and excessive surface moisture evaporation. The problem is further aggravated by the relatively large areas of unprotected fresh shotcrete that are often exposed to drying immediately after spraying. The use silica fume in shotcrete can potentially increase its plastic shrinkage potential. In most cases, plastic shrinkage is higher the larger the cement content is in the mixture (i.e., smaller aggregate content by volume). To some extent, however, the risk of plastic shrinkage cracking can be reduced through proper curing and protection practices.

1.3.2.3 Self-desiccation Shrinkage

Autogenous shrinkage occurs as a result of *self-desiccation* or internal drying of concrete during hydration. Thus, the volume change occurs without any moisture transfer with the surrounding environment, and is normally observed in high strength or high-performance concrete with low water-to-cement ratio [20]. Autogenous shrinkage must not be confused with chemical shrinkage. The latter is the intrinsic volume deficit of the hydration reaction, the products of hydration occupying less space than the reactants. In the plastic phase, the macroscopical volume change is equal to the chemical shrinkage. After setting, the

11

rigidity of the paste opposes the contraction and the chemical shrinkage results instead in the apparition of empty spaces in the porosity (if not supplied with external water), which equates to a reduction in the relative humidity within the pore network, which is hence referred to self-desiccation [21].

The risk of autogenous shrinkage is known to increase with a decrease in the water-to-cementitious materials (w/cm) ratio [22, 23]. It is, therefore, not surprising that autogenous shrinkage is a major concern in high strength or high-performance concrete with low w/cm ratios. Yet, the contribution of autogenous shrinkage is still often neglected in design of concrete structures.

1.3.2.4 Drying Shrinkage

All cementitious materials experience drying shrinkage as the hardened concrete element is subjected to unsaturated exposure conditions. Drying shrinkage can be described as a time-dependent mechanical response of a concrete subjected to drying condition(s). When concrete is exposed to unsaturated ambient air, some of the water (moisture or adsorbed water) contained in the pores begins to exit by evaporation causing the concrete to exhibit a contraction referred to as drying shrinkage. Drying occurs as soon as the internal R.H. inside the concrete pores is higher than that of the surrounding air and proceed until a thermodynamical equilibrium is established. Conversely, when exposed to a medium with a higher relative humidity, concrete will absorb water. Drying shrinkage is a long-term process and the severity of the shrinkage depends on the rate of drying and drying conditions. The drying rate is largely influenced by the volume-to-surface of the concrete exposed to drying environment and the water to binder ratio. Since the rate of drying necessarily varies across the thickness of a concrete member, differential volumetric changes take place [24]. As a result, the internal mass of the concrete being kept more humid will partly restrain the shrinkage that occurs the surface, resulting in tensile stresses at the surface. The magnitude and kinetics of shrinkage that may occur depend on the mixture materials and proportions.

It should be added that drying shrinkage can occur simultaneously with autogenous shrinkage when concrete is subjected to drying conditions, the competition being more significant the earlier the age of the material at the time drying is initiated.

1.3.2.5 Thermal Volume Changes

Cementitious materials are not immune to the effects of temperature changes, which result from the chemical reaction of hydration of the binder (internal source of heat) or from the exposure conditions (external source or sink of heat).

The hydration process generates heat that can subject concrete elements to a substantial temperature variation. Heat of hydration causes the concrete temperature inside the mass to initially rise and expand. As the rate of hydration decelerates and the heat is released progressively by diffusion, concrete subsequently cools down and undergoes contraction. The difference between the temperature within the concrete and its surroundings may lead to significant thermal gradients, thereby causing non-uniform

volume changes and a potentially harmful state of stress. The heat of hydration released is dependent on the mineral composition of cement and the size of the concrete element. In practice, cracking resulting from early temperature changes primarily affects massive structures, where the heat generated cannot be easily dissipated. Thus, thermal cracking due to cement hydration is usually not significant in thin concrete members, where shotcrete is more frequently employed.

Through their service life, cementitious materials are subject to thermal variations in response to the exposure conditions (variable ambient temperature, solar radiations, etc.). As a result, they undergo volumes changes proportional to their thermal expansion coefficient. Again, depending on the conditions, thermal gradients may arise and induce significant internal stresses.

1.3.2.6 Carbonation Shrinkage

Carbonation shrinkage occurs as a result of a carbon dioxide reacting in the presence of pore moisture. The carbonation process starts at the surface moving inwards and is very slow under natural conditions. As the reaction itself, carbonation shrinkage essentially affects the surface, but can slowly penetrate the concrete depending on the moisture content and CO_2 exposure. Carbonation makes concrete vulnerable to corrosion of reinforcement(s) because it reduces the overall pH of the pore water, but the induced shrinkage is usually not a major cause of deterioration of shotcrete structures and repairs.

1.3.3 Why is Shotcrete Sensitive to Shrinkage?

Shotcrete is prone to shrinkage due in part to the shotcrete mix composition itself, the placement process and finishing operations. One main advantage of shotcrete is the capacity to cover large surfaces (e.g., a wall or abutment repair) without the use of formwork. However, once the finishers have completed their work on the shotcrete surface, unless suitable curing is achieved promptly, a relatively large area of unprotected fresh concrete/shotcrete is left unprotected and surface water evaporation will quickly lead to differential shrinkage through the relatively thin (typically 75-150 mm) shotcrete layer. Furthermore, the shotcrete mixture composition itself contains some of the essential ingredients known to aggravate shrinkage. For example, shotcrete mixes are typically high cement content mixtures with low coarse aggregate content (maximum nominal aggregate size of 10-14 mm), and often contains mineral additives, set accelerators and other admixtures. As a result, shotcrete mixtures generally exhibit higher shrinkage compared to conventional concrete mixtures [6, 9, 25]. This explains the need for a better understanding of how the mix design factors are influencing shrinkage in shotcrete. For instance, set accelerators influence both the mechanisms and kinetics of early cement hydration process. It would seem logical that the influential factors upon shrinkage of shotcrete may be different from those of ordinary cast-in-place concrete since they may develop a different internal structure.

1.3.4 Restrained Shrinkage Cracking

The primary concern regarding shrinkage of cementitious materials in real-life service conditions is the potential for cracking. Shrinkage would not be a problem if there were no restraint. This, however, is never the case in practice due to the highly restrained conditions that are inherent in most concrete elements. This particularly true in the case of shotcrete repairs where shrinkage due to drying of the new repair material is restrained by the old stable material *(i.e. substrate)*. When concrete is prevented from undergoing free volumetric changes, internal tensile stresses are progressively induced. Depending on the degree of restraint within the material, shrinkage strains may induce quite significant tensile stresses in the concrete. These stresses add up to the inherent state of stress that results from the highly non-linear moisture gradient.

Cracking occurs when the maximum tensile stress induced by the restrained deformation exceeds the concrete tensile strength (as shown in Fig. 1.3). Considering the low tensile strength of concrete, should cement-based materials be purely elastic, the amount of shrinkage leading to cracking would be much less than the actual long-term shrinkage values recorded in standard shrinkage tests such as ASTM C157. In reality, the tensile stress developed due to restrained shrinkage can be relaxed by tensile creep as illustrated in Fig. 1.3. This beneficial effect prevents or at least delays cracking quite significantly.

From a structural point of view, shrinkage cracking will almost always occur at the weakest point within the areas of the concrete element subjected to stress reaching the material's strength. The prediction of such a location and the exact conditions which will lead to cracking falls under the purview of fracture mechanics [26, 27] , which emphasize the key role of stress concentration and material composition with regards to crack formation. This, however, is not explored here since the conditions leading to the formation of a crack depend on material properties difficult to evaluate experimentally, particularly in the early ages when the material evolves rapidly. It is instead the presence, or not, of a crack in the repair material that is of interest here.

The presence of cracks provide easy access for oxygen, moisture, chlorides, and other aggressive chemicals into the matrix, and can therefore impact the long-term durability and service life of concrete structures [28, 29]. In addition, cracking can also have a huge financial implication in terms of repairs. Even from a purely aesthetic point of view, cracking of concrete surface is often unacceptable. Shrinkage cracking remains arguably one of the major problems in the concrete industry today.

It is thus desirable to prevent or at least minimize concrete shrinkage cracks. Concrete/shotcrete engineers and researchers must recognize the need to predict the occurrence of shrinkage cracking in order to design mixtures with low cracking potential. Also, in the case of repair and rehabilitation of existing concrete structures, selecting the right repair material with low shrinkage characteristics and higher dimensional compatibility [30] can help prevent cracking and loss of bond.
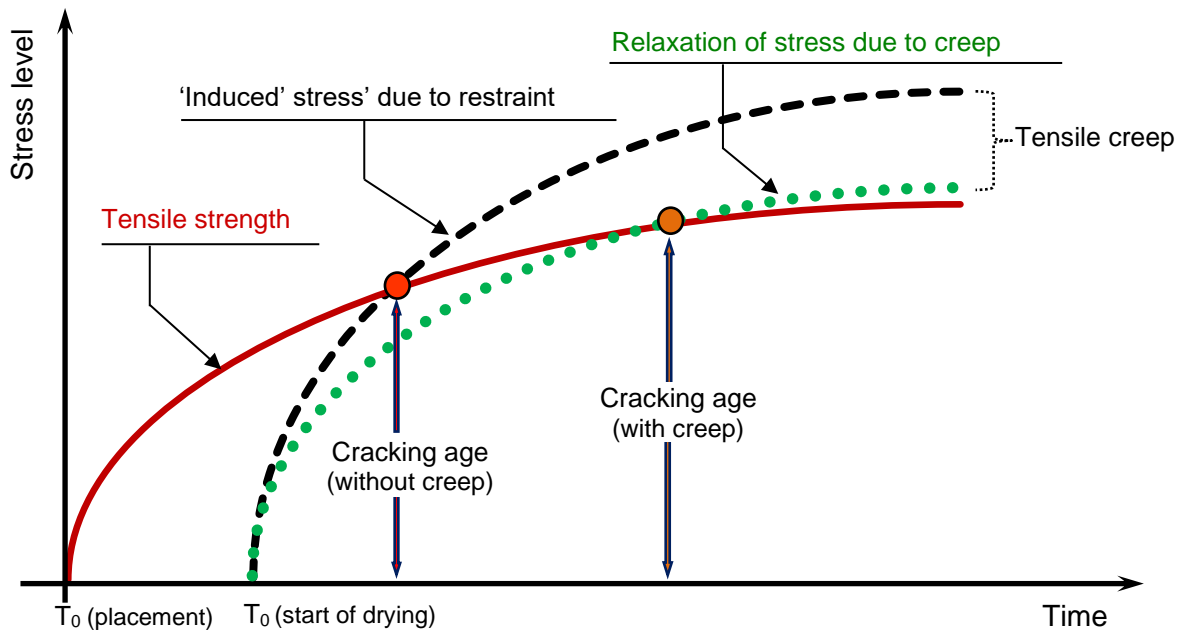
Fig. 1.3 Time dependence of cracking on restrained shrinkage and creep/relaxation

1.3.4.1 Influence of Creep and Stress Relaxation on Cracking

Cracking under restrained shrinkage depends on the combined effect of shrinkage and tensile creep, or conversely, relaxation. In reality, shrinkage and creep/relaxation phenomena typically occur simultaneously. In fact, both shrinkage and creep/relaxation originate from the same source, the hydrated cement paste [31]. The term creep refers to a time-dependent increase in deformation under constant stress, whiles relaxation refers to a decrease of stresses under constant deformation [32]. It is necessary to mention that creep may be subdivided into a non-drying part, called basic creep, and a drying part, called drying creep, but this level of detail is not the scope of this thesis and may be found elsewhere [1, 17, 33]. The following discussion will refer essentially to the term creep, as both phenomena are the manifestations of the same material viscoelastic characteristics.

On the one hand, creep may be detrimental if it causes significant losses of prestressing or if it results in excessive deformation and deflection (that may impair the structural integrity or behaviour of the structure). On the other hand, creep may be beneficial and desirable, most especially in repairs and some reinforced concrete elements, because it tends to provide a certain capability of redistribution of stresses, particularly under restrained conditions. In many instances, the improved shrinkage cracking performance of concrete is due to creep-relaxation. Indeed, research has shown that creep can mitigate the detrimental effects of shrinkage in concrete [1, 34] by partially relieving the induced tensile stresses. The ability to relieve stress concentrations contributes to prevent or at least delay cracking (see Fig. 1.3). Creep also increases the mechanical compatibility between the repair materials and the substrate by allowing it, to some degree, to

15

adapt when subjected to restrained shrinkage [1]. To sum it all up, the importance of creep in the assessment of the risk of cracking of concrete cannot be overemphasized. Therefore, to allow for a more appropriate state-of-the-art design of concrete repairs, a better knowledge and evaluation of the tensile creep behaviour of concrete is required.

1.3.4.2 Restrained Shrinkage Cracking - Other Influencing Factors

From many published works [29, 34-37], five major parameters are considered to mostly influence the restrained shrinkage cracking potential of concrete and repair materials, namely shrinkage (rate and magnitude), elastic modulus, tensile creep, tensile strength and the degree of restraint (external and internal). However, there is currently no universally accepted agreement on the relative individual influence of each of these parameters on the potential for cracking. Besides, the complex interaction between these parameters in practice makes it very difficult to define a specific shrinkage limit or threshold of acceptability. Understanding how these parameters affect the shrinkage cracking of a cementitious materials is vital. There is therefore clearly a need to further explore the correlations between shrinkage cracking and these parameters.

1.3.5 Factors Affecting Shrinkage

Shrinkage is a fairly complex phenomenon that depends on a combination of several key factors. These factors include the concrete's surrounding environment, size and geometry of the concrete elements (i.e. volume-to-surface area ratio), admixtures, pozzolans, curing conditions, cement paste and aggregate content [28, 36, 38].

In general, a high degree of correlation has been found between concrete environment and drying shrinkage [28, 36]. In fact, for a given concrete, the magnitude of drying shrinkage is higher the lower the *relative humidity* [28, 39]. When a concrete element is exposed to an environment with a lower relative humidity (R.H. gradient between the concrete porosity and the surrounding air), it loses progressively its moisture content through diffusion in the pore network and evaporation at the surface. This drying process continues until equilibrium is reached, at a high rate initially and then at a constantly decreasingly rate. The moisture loss from the material's porosity is the main driving force for drying shrinkage.

Drying shrinkage is also dependent on the concrete element *size and geometry*, more specifically the ratio of the surface that will be exposed to drying to the overall volume (S_e/V). This is because the rate of water loss is controlled by the length of the path travelled by the water to get to the surface [31]. So, for a given concrete element, the smaller the S_e/V ratio, the higher the shrinkage will be at a given age. Conversely, in massive structures such as dams, the ratio is such that the exposed massive parts will undergo negligible drying and shrinkage during the life of the structure.

Aggregate-cement ratio has the greatest effect on the total shrinkage (i.e. effect of both autogenous and drying shrinkages) of cement-based materials. This is due to the restraining role of aggregates on shrinkage

and the potential for shrinkage of the cement paste. A higher aggregate volume fraction causes a dilution of the cement paste and the overall total water content of the mixture. The twin influences of the aggregate content and w/cm ratio is shown in Fig. 1.4a. It is obvious that the higher the amount of aggregate, everything else being kept the same, the lower the shrinkage will be expected to be. Similarly, the magnitude of shrinkage is directly related to the paste volume (see Fig. 1.4b).

Conflicting results can be found in the literature regarding the effect of w/cm ratio upon shrinkage (compare Fig. 1.4 a) and b). Some research indicates a more significant influence of w/cm ratio on shrinkage [17, 23, 29], while others found the effect of w/cm ratio to be relatively small [36, 40]. This suggests that the overall water content *per se* may not be a primary factor [17] with regards to shrinkage because it is possible that several factors that are dependent upon w/cm ratios and that affects shrinkage (pore size distribution, porosity, creep, water diffusion, etc.) [36] might have cross-effects in such a way that different trends are observed.

The use of mineral additives as a binder also affects the shrinkage behaviour of cement-based materials. The viewpoints about the influence of mineral admixtures on shrinkage and their working mechanisms remain disputable. However, it is known that *silica fume* tends to increase the overall shrinkage of cement-based materials. To illustrate this fact, Fig. 1.5 shows the autogenous shrinkage recorded for concrete specimens with and without silica fume (SF) at various ages. As clearly shown in the figure, the addition of silica fume significantly increased the ultimate shrinkage deformation measured.

Fly ash, on the other hand, typically tends to decrease shrinkage depending on the replacement level literature [41-44] which. The use of *slag* can also decrease shrinkage of cement-based materials [43]. However, at cement replacement of about 50-75% of the total mass of binder, slag can increase the autogenous shrinkage [16].

The choice of using a set *accelerator* in shotcrete can be very important with respect to shrinkage, because accelerators increase the hydration rate. When the hydration rate is increased, the rate of heat liberation at early ages will also increase, which can in turn contribute to increase early-age shrinkage.

There are conflicted conclusions with respect to air entrainment admixtures. Some indicate that they have little or no effect on shrinkage, but others show that they can reduce shrinkage. Similarly, it is rather difficult to state the exact influence of *superplasticizers* on shrinkage based on comparison of the data available in the literature since in each case different mixtures and moisture conditions have been used. Generally, superplasticizers may affect early age shrinkage (by some 10 to 20 per cent [17]) depending on the dosage. From a structural point of view, understanding the individual and combined influence these factors are essential for selecting the right material construction and repairs to resolve the early-age cracking problems.
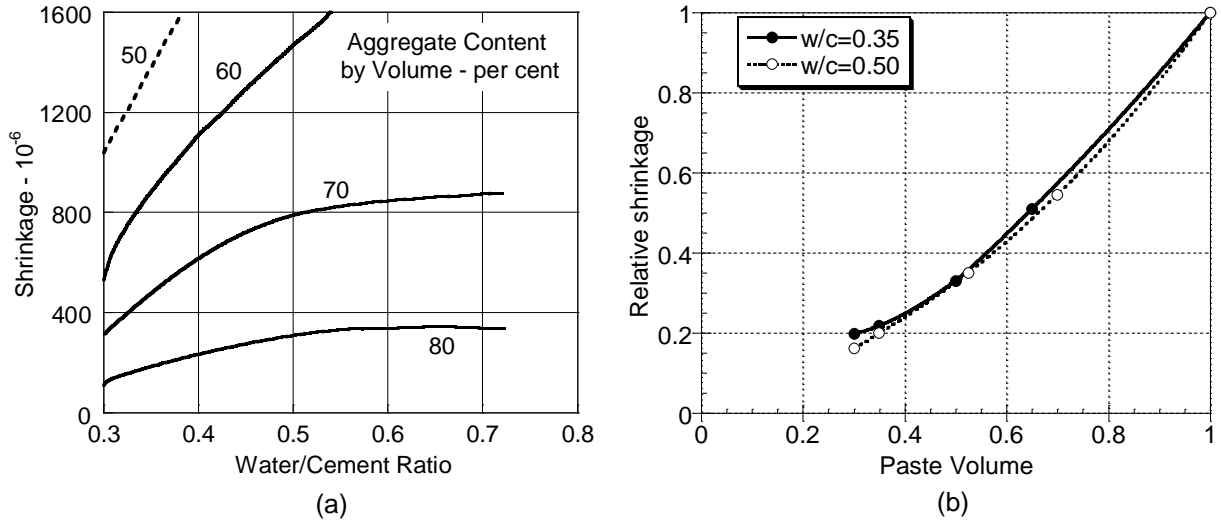
Fig. 1.4 (a) Influence of water-cement ratio and aggregate content on total shrinkage [17]; (b) effect of paste content on shrinkage [36]
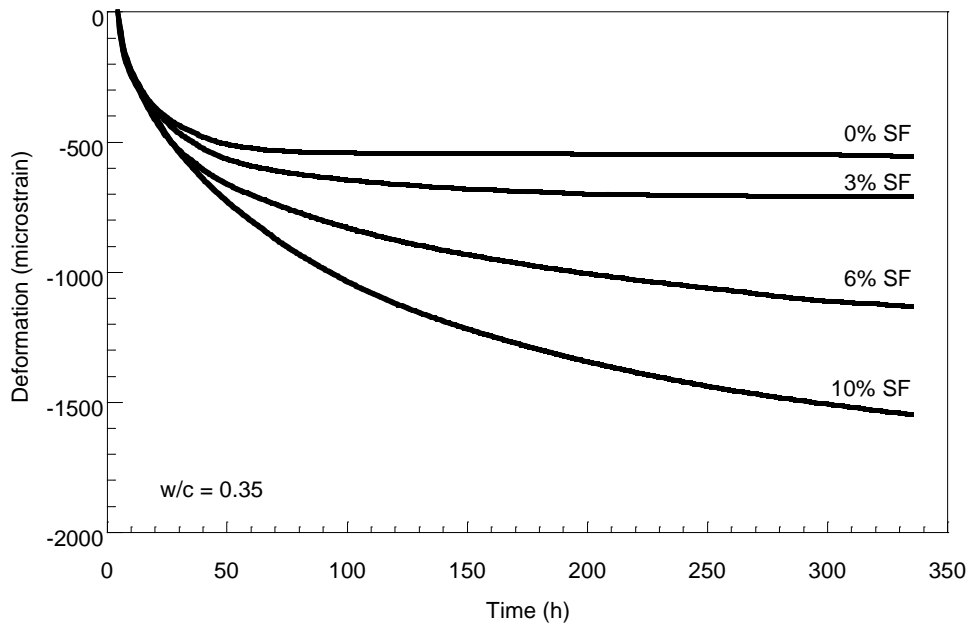
Fig. 1.5 Influence of silica fume addition on autogenous shrinkage [45]

1.3.6 Recent Advances and Trends to Minimize Shrinkage Effects

There are different mitigation strategies to minimize the effect of shrinkage. The recent trend in concrete technology towards such strategies include controlling, compensating or reducing shrinkage. The following sections provide a brief summary.

1.3.6.1 Curing of Cement-based Materials

The most obvious method of limiting the negative effects of shrinkage is by ensuring adequate and proper *curing* techniques. Proper curing conditions delay the advent of shrinkage by preventing drying via moisture loss. Prolonged moist curing will delay the onset of drying shrinkage [. Proper curing also ensures that concrete would reach adequate strength to resist tensile stresses induced by shrinkage. It is generally recommended that surfaces of fresh shotcrete be kept continuously wet for at least 3 to 7 days. Alternatively, a curing compound that complies with ASTM C309, ASTM C131, or AASHTO M 148 can be applied. However, it is often difficult to ensure proper curing to vertical and overhead shotcrete applications.

1.3.6.2 Mixture Proportioning

Another approach of controlling shrinkage is by maximizing the aggregate-cement paste ratio which has a profound effect on the w/cm ratio. This can be achieved by using paste volume fraction with the highest possible volume fraction of good quality aggregate and maximum possible aggregate size, which consequently minimizes the water content. Bear in mind that high w/cm ratio will lead to higher drying shrinkage while very low w/cm ratio will also lead to high autogenous shrinkage.

1.3.6.3 Expansive Cements

A viable approach to counteract the negative effects of shrinkage is by compensating the contraction through the use of expansive cements [17, 31]. These expansive cements significantly increase in volume during the early stages of hydration. If the expansion is properly restrained, compressive stresses develop in the concrete, which is then progressively offset by shrinkage. Hence, with adequate mix proportions, the early expansion compensates the shrinkage occurring simultaneously and subsequently. Such a concrete is then referred to as shrinkage-compensating concrete (ShCC). There exist different types of expansive binders (Type K) or compounds (Type K, Type G) [ACI 223, 2010]. With type K cement, the expansion is mostly achieved via a controlled ettringite formation, which generally requires large amount of water through moist curing.

1.3.6.4 Shrinkage and Crack Reducing Admixtures

The most effective means of reducing the magnitude of shrinkage of concrete today seem to be with *shrinkage-reducing admixtures* (SRAs). The use of SRAs can offer significant reduction in the overall shrinkage depending on the dosage. As for the principle of action, SRAs reduce the surface tension of the water in the pores of concrete [28, 46]. With a reduction in the capillary tension, the force that pulls in on the walls of the pores is decreased, resulting macroscopically in a reduction in shrinkage. The performance of SRAs in ordinary concretes are well documented [23, 28, 46, 47]. Data available in the literature also show that SRA can reduce shrinkage of shotcrete mixtures [25]. Recently, a new innovative *crack-reducing admixture* (CRA) by BASF Corporation appeared in concrete engineering. Similar to conventional SRAs, CRAs are reported to reduce the surface tension of water [48].

1.4 Estimating Cracking Sensitivity of Concrete

As previously discussed, shrinkage cracking has a detrimental effect on the service life of concrete structures, repairs, and rehabilitation works. As such, it is important to understand how it occurs and how to predict or evaluate the sensitivity to cracking of a repair material. Different test methods have been developed over the years to estimate free shrinkage as well as the cracking tendency of concrete under restrained shrinkage conditions. In the following sections, the most widely used tests will be discussed briefly.

1.4.1 Free Shrinkage Test Methods

The unrestrained or the so-called *free* shrinkage test is a term associated with the methods used to evaluate the shrinkage characteristics of cementitious materials. In these methods, the specimens are allowed to *shrink* in a controlled environment, without any external restraint. The changes in length are measured at regular intervals for a specified period. Free shrinkage is typically measured uniaxially on prismatic test specimens, but it may also be measured on test specimens with a different geometry, such as the free shrinkage ring test developed as a complementary test procedure for the restrained shrinkage ring test. Although the shrinkage cracking sensitivity of cement-based materials cannot be evaluated based solely of free shrinkage tests, a good relationship is often found between free shrinkage and the cracking sensitivity of concrete under restrained conditions. For example, if a given mixture has a high free shrinkage potential, it will generally tend to crack earlier in restrained shrinkage than a comparable mixture with lower free shrinkage potential. Still, it is difficult to discriminate between materials based on the latter. In practice, there has been an increasing tendency lately to carry out both free and restrained shrinkage tests to evaluate the potential for shrinkage cracking.

1.4.1.1 Free Uniaxial Shrinkage Test

The most common approved free uniaxial shrinkage test method is the ASTM C157 [49]. The test method involves measuring the length change of concrete or mortar on 75×75×285 mm prismatic specimens. The length change is measured with the aid of a comparator and is expressed as a function of the initial specimen length. The specimens are fabricated in accordance with ASTM C192. All specimens are left in the moulds and covered with wet burlap and a polyethylene sheet for the first 23 ±½ hours after casting. After demolding, the initial measurements using a comparator with a gauge length of 250 mm are taken on each specimen. The bars are kept in lime-saturated water maintained at 23 ±½ °C up to the time they are exposed to drying. At 28 days (or another age, as specified), specimens are stored under standard conditions of 23 ±2 °C and 50 ±4% R.H. for the remainder of the test. Length change measurement is performed at the time of retrieving the specimens from water and then regularly at specified times (initially daily, then weekly and at some point monthly), up to the age of 64 weeks.

In practice, the curing conditions and the duration of the test as well as the exposure conditions during drying and length change readings might differ from the standard depending on the project needs and requirements, but it must be reported.

1.4.1.2 Free Ring Shrinkage Test

Free shrinkage deformation can also be measured on ring specimens to extend the interpretation of the restrained shrinkage ring test results. The procedure consists of replacing the steel ring in the restrained shrinkage specimen with a white polystyrene insert with a very low stiffness. For instance, in the case of the AASHTO T 334 ring test procedure, 152 mm high and 76 mm thick ring of concrete is cast around a polystyrene ring having a diameter of 305 mm. DEMEC gauges are positioned on top of the specimens to measure the changes in length. The specimen configuration is shown in Fig. 1.6. Any ring specimen geometry may be used to perform the test.
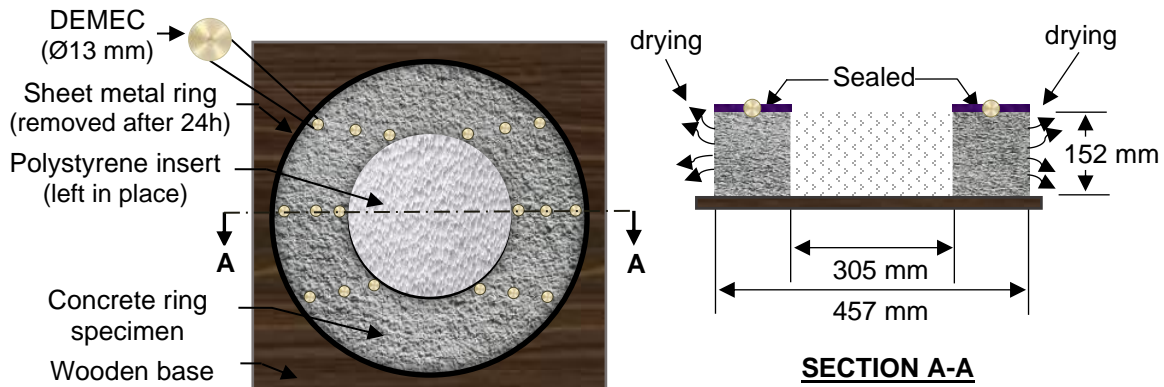
Fig. 1.6 Test specimen configuration for free shrinkage ring test based on the AAHTO ring test setup

1.4.2 Restrained Shrinkage Test Methods

Restrained shrinkage test is a terminology associated with methods used to assess the shrinkage cracking sensitivity of cementitious materials. In these methods, the *risk for shrinkage cracking* of specimens is evaluated under *restrained conditions* in a controlled environment. Due to the imposed restraint on movements, tensile stresses develop and, if they become high enough at some point, lead to cracking. The restraining device is often instrumented with strain gauges, allowing to monitor the average strain and stress development in the test specimen until cracking.

The cracking tendency of concrete or mortar can be evaluated through a range of relatively simple restrained test procedures, such as the linear bar test (e.g. German angle test), plate/slab tests (e.g. SPS plate test), and the ring test [50]. In the linear test, restraint to movement is provided either internally by axially embedded bars or tubes, or externally by a large steel mould or frame. In the plate type tests, the

restraint is provided only at the bottom of the prismatic specimens [51]. In the ring type tests, the restraint is provided by the inner stiff steel ring around which the concrete is cast. The ring test is the most popular and widely used restrained tests method due to its simplicity, effectiveness, relatively low cost, and a uniform restraint without connections and the related stress concentrations. The ring test is discussed in detail in the following sub-sections.

1.4.2.1 Shrinkage Ring Test Method

The ring test is a simple practical tool for the evaluation of a material's potential for cracking due to restrained volume changes. Although an elliptical ring geometry can also be used [50, 52], the circular ring type geometry is the most widely used for ring test. The most commonly used circular ring test procedures are the AASHTO T334-08 [4] (formerly AASHTO PP 34-99) and the ASTM C1581 [53]. These tests consist in casting a ring of concrete or mortar around a steel ring. When exposed to drying, specimens tend to shrink, but the steel ring partially counteracts the contraction. Thus, the steel ring provides a uniform restriction to the concrete volume change. This leads to the development of a compressive force in the steel ring, which is balanced by a tensile force induced in the concrete/mortar ring specimen. Cracking occurs when the induced tensile stresses exceeds the strength of the tested concrete or mortar. The steel ring is generally instrumented with strain gauges to monitor the strain development in the setup. The higher the steel thickness, the higher the degree of restraint and consequently the interface pressure will be, hence cracking will tend to occur earlier. It is worth mentioning that based upon recent development at Université Laval [3], an adapted ring test procedure is now available for evaluating the cracking of shotcrete mixtures.

In the AASHTO T 334 ring test procedure, a 152 mm high and 76 mm thick ring of concrete is cast around a steel ring having a diameter of 305 mm and a wall thickness of 12.7 mm. Details of the test specimen configuration is shown in Fig. 1.7. Upon casting, the freshly placed concrete is consolidated in the mould. All specimens are left in the moulds for the first 24 hours after casting and covered with wet burlap and plastic sheets. After curing, the exterior wall of the mould is removed, the specimens are sealed on the top and bottom sides. Specimens are then stored under the standard conditions (21±1.7 °C and 50 ± 4% R.H.) for the specified duration of the test. Drying then occurs radially from the lateral side (circumferential) of the concrete ring specimen. The inside of the steel ring is instrumented with four strain gauges connected to a data acquisition system. The rings are usually monitored for evidence of cracking which is revealed by a sudden decrease in deformation recorded from one or more gauges.

The ASTM 1581 ring test procedure is very similar to the AASHTO T 334 test procedure described above. The main difference between the two standards is the ratio of the concrete ring to steel ring thickness, which strongly influences the degree of restraint provided. ASTM uses thin concrete rings with a wall thickness of 38 mm. Hence, a 152 mm high and 38 mm thick ring of concrete is cast around a steel ring having a diameter of 330 mm and a wall thickness of 13 mm. This implies that the degree of restraint of the ASTM ring setup is much higher than that of the AASHTO ring setup. Therefore, the specimens made with

a given concrete mixture would take longer to crack in the AASHTO ring setup compared to the ASTM ring setup [34]. It is necessary to mention that the thickness of the ASTM ring is very small, making it unsuitable for shotcrete placement (see [3]).
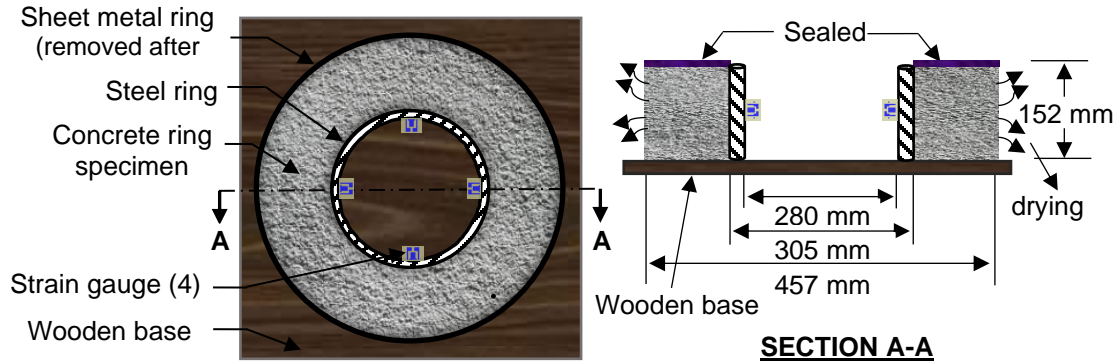
Fig. 1.7 Test specimen configuration for shrinkage cracking tendency test (AASHTO ring test setup)

1.5 Numerical Modelling of Drying Shrinkage

Numerous models derived from various approaches can be found in the literature. From a material property point of view, concrete is hierarchically structured, which means that the intrinsic material properties change with change in scale. Consequently, modelling approaches exist at different scale levels: from the nano-level (i.e., molecular size) to micro-level (i.e., microstructure and/or mixture constituents) to meso-level (i.e., mortar/concrete) to the macro-level (i.e., structure). Thus, the properties modelled at one scale becomes an input at the next higher scale of interest [54]. However, despite decades of research, no complete models have been developed and validated. In reality, it is difficult to develop realistic numerical models for predicting shrinkage alone, because several phenomena occur simultaneously, and their effects cannot be easily isolated. To be more precise in identifying the exact contribution of the different types of shrinkages to the overall total shrinkage is a huge, and yet unresolved challenge.

In general, relative humidity (R.H.) is assumed to be the main driving force when modelling of shrinkage of cementitious materials exposed to drying. As such, shrinkage is modelled as a function of moisture loss treated as a non-linear diffusion problem (example is the model by Bažant and Najjar [55]). It is also found in a number of studies that the modelling of drying shrinkage can be assimilated to the mechanical response of the material to variations in the temperature field. Thus, when simulating shrinkage of ring specimens in models such as *Ansys* FE code [50] for example, drying shrinkage of concrete can be assumed to be caused by a fictitious temperature drop. The fictitious temperature reduction is assumed to causes the same magnitude of the shrinkage strain as that induced by a given RH reduction inside the porosity.

1.6 Conclusion

The shotcrete process has undergone significant improvements since its introduction as a concrete placement method. It is clear that shotcrete is very versatile and offers numerous advantages over conventional concrete. Shotcrete has notably proven to provide tailor fit solutions in many concrete repair applications. However, the underlying issues related to shrinkage and restrained cracking have not received enough attention. It is also difficult to establish simple relationships between placement parameters, composition variables, material properties and the shrinkage cracking tendency of shotcrete based on the data available in the literature. Unfortunately, there is currently very limited information available on the key factors that lead to shrinkage cracking of shotcrete. The scarce data available on the shrinkage properties of shotcrete means it is imperative for more in-depth material characterization to be made, especially on the basis of a restrained shrinkage test. It is obvious that extensive research is needed to understand the shrinkage and cracking behaviours of shotcrete. This research project is intended to shed light on the use of the *ring test* in characterizing the shrinkage cracking sensitivity of shotcrete, to improve our understanding of the various phenomena involved, and to exploit the data generated in view in view of identifying materials levers for producing shotcrete mixtures with low cracking sensitivity.

Chapter 2 Methods and Approach

2.1 Introduction

In this chapter, the general overview of the materials used and the experimental programs carried out to address the issues of shrinkage and cracking of shotcrete are briefly described. Comprehensive laboratory studies and finite element modelling were targeted to quantify the volume characteristics and behaviour of shotcrete undergoing desiccation.

2.2 Research Approach

To achieve the proposed research objectives, the program is broken into four (4) distinct phases. The first phase deals with the evaluation and optimization of the free ring shrinkage test procedure, and the overall validation of the ring test procedure adapted for shotcrete (Chapters 3 , 4 and 7). The second phase focused on the effectiveness of a range of curing methods for preventing early water evaporation and the subsequent shrinkage in freshly applied shotcrete (Chapter 5). The third phase deals with improving the cracking resistance of dry-mix shotcrete mixtures (Chapter 6 and 7), focusing on cement paste volume, aggregate content, mineral additives, and chemical admixtures. In the final phase, a finite element analysis is carried out to study the shrinkage and cracking sensitivity of shotcrete (Appendix A).

2.2.1 Selection of Mixtures and Materials

Several different shotcrete mixture designs were investigated in this study. All the mixtures were supplied by King Shotcrete Solutions, the industrial partner involved in the NSERC CRD (cooperative research and development) project. The mixtures are grouped into two groups according to the placement method: *cast* wet-mix shotcrete mixtures (Phase I) and *spraye*d dry-mix shotcrete mixtures (Phase II and III). The cast mixtures of Phase I consist of three (3) pre-bagged wet-*mix* shotcrete mixtures with no silica fume. More details on the mixture proportions are provided in Chapters 3 and 4. In Phase I, the objective was to optimize the free ring shrinkage test procedure and to improve the interpretation of cracking behaviour in *restrained shrinkage ring specimens*. Thus, the method of placement (cast or sprayed) did not really matter, and gravitational casting was selected for simplicity.

A pre-blended and pre-bagged dry-mix shotcrete base mixture containing 10 % of silica fume (by weight of cementitious materials) and a nominal maximum aggregate size was 10 mm (⅜ in.) was used in Phase II. The mixture was used to spray shotcrete at two (2) w/cm ratios (0.31 and 0.42). The mixture proportion is provided in Chapter 5. The sprayed mixtures of Phase III consisted of fifteen (15) pre-blended and pre-bagged *dry-mix* shotcrete mixtures. An overview of the different shotcrete mixture proportions is provided in Chapter 6.

The *first series* of the Phase III mixtures were four (4) ordinary portland cement mixture without silica fume, but with varying *coarse aggregate volume* fractions and *cement content*. The objective is to exploit the possibility of improving shotcrete shrinkage cracking by use of optimized well-graded coarse aggregate content.

The *second series* of the Phase III mixtures were based on the two (2) most promising mixtures in the first series, with partial replacement of the cement content by *silica fume* (SF) and/or *fly ash* (FA). The replacement percentage of silica fume was fixed at 8% by weight of cement, while fly ash was used at a rate of 24% by weight of the total binder. The objective here is to evaluate the influence of SF and FA on shrinkage in particular, but also on the in-place shotcrete, rebound and consistency. In fact, SF was added with the primarily aim of reducing shotcrete rebound. An additional mixture, a dry-mix shotcrete incorporating 10% SF by weight of cementitious materials was also used here for comparison purposes.

The *third series* of the Phase III mixtures were intended to evaluate the influence of chemical admixtures such as *polymer*, *shrinkage-reducing admixtures* (SRA) and *crack-reducing admixtur*e (CRA). The polymer (ETONIS® 850) and SRA (Peramin® SRA 40) were powdered-based, hence pre-dosed/blended in dry form into the shotcrete mixtures before pre-bagging. Conversely, the CRA (MasterLife® CRA 007) was added in liquid form to the mixing water.

2.2.2 Mixture Constituents

2.2.2.1 Water

The water used for the shotcrete productions was ordinary tap water from Québec City's aqueduct system. The water was fit for human consumption, hence free of oil, chemical or organic impurities that may affect cement hydration reactions, such that no chemical analysis was performed.

2.2.2.2 Binders

The cement used (ordinary Portland cement with maximum 5% filler) was a binder meeting the type GU requirements of CSA A-3001 and produced from Ciment Québec in Saint-Basile, Quebec, Canada. Two (2) types of mineral additives were used in this project: silica fume (SF) and fly ash (FA). The silica fume was obtained from Silicium Québec in Bécancour (QC), Canada, while the fly ash came from Lafarge in Romeoville (IL), U.S.A. All the relevant material data and chemical analyses are presented in Appendix B.

2.2.2.3 Aggregates

All mixtures used aggregates conforming to the ACI 506 Gradation No. 2 requirements. The coarse aggregate was a crushed limestone with a nominal maximum aggregate size of 10 mm (⅜ in.). The coarse aggregates were obtained from two (2) different suppliers. The sizes of the coarse aggregates from Carrière Lafarge in Mirabel (QC), Canada ranged from 2.5 to 10 mm in diameter, while that from Carrières Laurentiennes, also in Mirabel (QC), Canada ranged from 5 to 10 mm in diameter. The sand was obtained

from Lafarge in St-Gabriel de Brandon (QC), Canada and Sables L.G. in St-Hippolyte (QC), Canada). In all cases, the fine aggregate used was a natural sand with particle sizes ranging from 0 to 5 mm. The crushed aggregates and sand from Lafarge were used for the cast wet-mix shotcrete mixtures whereas the crushed aggregates from Carrière Laurentiennes and the sand from Sables L.G. were used for the sprayed dry-mix shotcrete mixtures. The Technical data sheets can be found in Appendix B.

2.2.2.4 Admixtures

For the conventionally batched mixtures, air entraining admixture Eucon Air MAC12 and superplasticizer Eucon 37 were used where necessary (see Chapters 3, 4 and 7). Both admixtures were obtained in liquid form and were added during batching. For the mixtures that were sprayed (or shot), a shrinkage-reducing admixture (SRA), Peramin® SRA 40, a crack-reducing admixture (CRA), MasterLife® CRA 007, and/or a polymer, ETONIS® 850 were used where indicated (see Chapter 6). The polymer and SRA admixtures were powdered-based hence pre-dosed/blended in dry form into the dry mixture before being pre-bagged. The CRA, conversely, was in a liquid form and added to the mixing water.

2.2.3 Laboratory Production and Placement

All the shotcrete mixtures used were pre-blended and prebagged (30 kg per bags) prior to batching or spraying. The conventionally batched and placed mixtures were prepared in a planetary mixer and cast gravitationally at the *CRIB Concrete Laboratory* of Université Laval in Québec City (QC), Canada. The spraying activities were carried out indoors at the *CRIB Shotcrete Laboratory* of Université Laval. This shotcrete laboratory is unique as it used full size equipment and has a controlled environment suitable for this research. The shotcreting operations took place in a rebound chamber and normal spraying techniques were carried out unless otherwise specified [10, 56]. The laboratory temperature during all spraying operations was in the range of about 22 ±1.7 °C. The equipment used for the shotcreting activities is briefly present below.

2.2.3.1 Spraying Equipment

The dry-mix gun used for the dry spraying process is an industrial shotcreting ALIVA® 246 electric rotating barrel machine (shown in Fig. 2.1a). A 25 m long delivery hose with an inside diameter of about 38.1 mm (1.5 in.) and a "double-bubble" hydromix nozzle with an exit diameter of about 32 mm (Fig. 2.1b and c) is connected to the spraying machine. The nozzle is fitted with a water ring which is located about 3 m (10 ft) upstream from the exit. The dry-mix material is fed into the hopper and the airflow is adjusted via the air valves. To start spraying, the electric rotor is turned on. Once the machine is started, the dry materials pass from the hopper into the rotor chambers. The revolving rotor then drops the dry materials in a continuous process into the air outlet chamber. The materials are conveyed by air through the delivery hose into the nozzle where water is added via the water ring. The mixture is then sprayed through the nozzle. Materials flow rate can be adjusted by means of the materials valve.
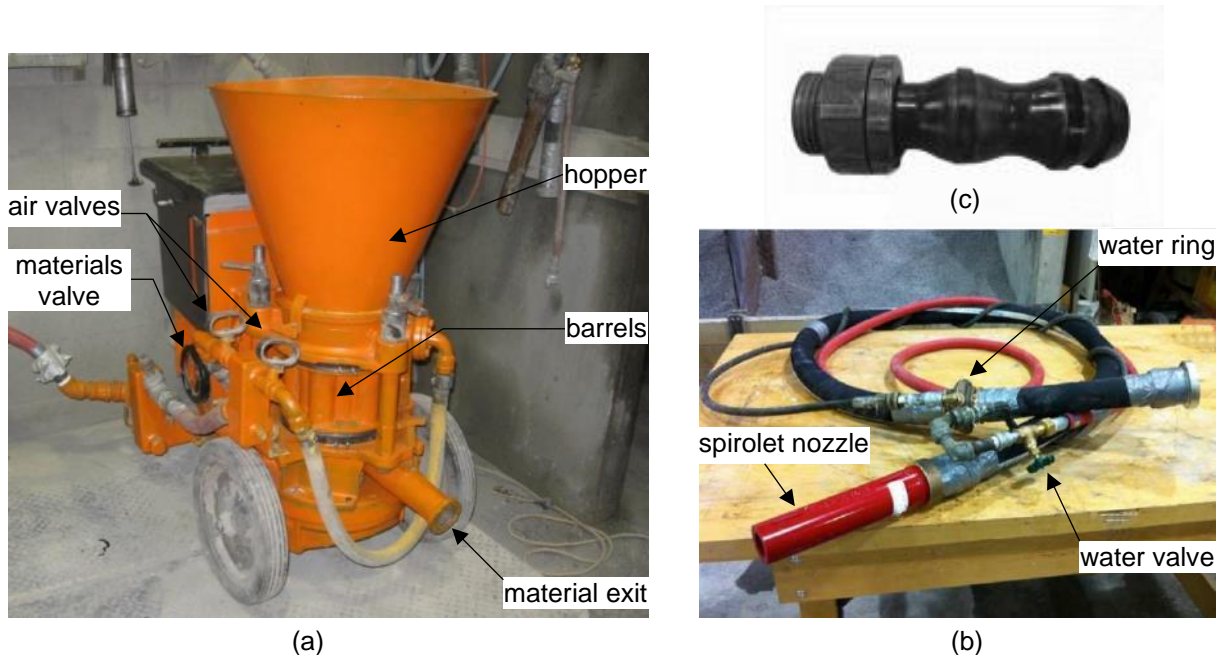
Fig. 2.1 (a) Aliva® 246 dry-mix shotcreting machine, (b) spirolet nozzle mounted on pre-wetting lance and (c) double bubble nozzle tip used in this study

2.2.3.2 Spraying technique

Proper spraying technique is critical to obtain high-quality in-place shotcrete. In this study, the mixtures were sprayed using the nozzling technique outlined in the ACI Craftsman Workbook [10], ACI-506R-16 [9], and by Crom [56].

2.3 Experimental Test Program

2.3.1 Tests on Fresh Concrete

Three common standard tests (slump test, ASTM C143; air content test, ASTM C231; and test for density, ASTM C138) were carried out to characterize the fresh properties of the conventionally batched wet-mix shotcretes. These tests were done merely to determine compliance with the mix designs. Tests were also carried out to characterize the consistency, rebound, and total in-place binder content of the sprayed dry-mix shotcretes, in accordance with procedures developed at the CRIB-Laval *Shotcrete Laboratory*. Additionally, the w/cm ratios were also determined for the sprayed dry-mix shotcretes mixtures. The properties of the freshly placed shotcrete mixtures are reported in the various articles. Additional data (on the fresh properties of the wet-mix cast shotcretes) not presented in the various articles can be found in Appendix C.

2.3.1.1 Rebound Measurement of Shotcrete

The rebound measurements were made using a vertical steel panel instrumented with load cells, as shown in Fig. 2.2. The instrumented test panel is connected to a real-time data acquisition system that records the water flow rate and the mass of total material that accumulates on the he rebound panel. The delivery rate of the dry material is also recorded since the dry-mix shotcrete machine is itself mounted on a scale connected to the data acquisition system. The latter measurement is necessary to determine the quantity of material sprayed. Based on these measurements, the rebound percentage is calculated as follows:

$$\text{Rebound (\%)} = \left[1 - \frac{\text{Mass of total material in the rebound panel} \left(\frac{kg}{s}\right)}{\text{Material delivery rate} \left(\frac{kg}{s}\right) + \text{Water flow rate} \left(\frac{kg}{s}\right)}\right] x100 \tag{2.1}$$

(a)   (b)
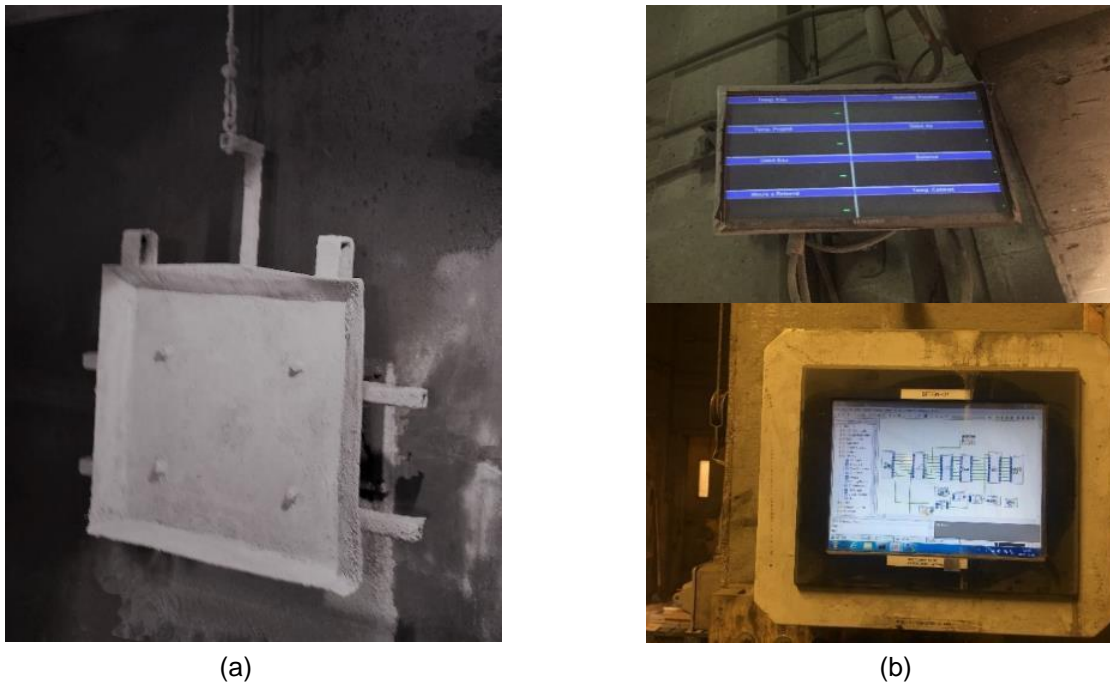
Fig. 2.2 Typical setup for rebound measurement: (a) instrumented vertical shotcrete test panel; (b) data acquisition system linked to a computer for display, controls and logging

2.3.2 Mechanical Property Tests

Standard tests were performed to characterize the mechanical properties of the different shotcrete mixtures investigated. In all cases, 100×200 mm cylindrical samples were used. Whereas the cylinders were hand cast for the batched wet-mix shotcretes, the core samples were extracted from a 600×600×125 mm test panels for the sprayed dry-mix shotcretes. An example of the cast and sprayed cylinder tests samples is shown in Fig. 2.3 a) and b), respectively. Sets of three (3) specimens were used in each case to determine the compressive strength (ASTM C39 for cast mixtures; ASTM C1604 for sprayed mixtures), splitting tensile

29

strength (ASTM C496), and elastic modulus (ASTM C469) of the mixtures at 3, 7 and 28 days. Poisson's ratio tests were also performed following ASTM C469 at the age of 3, 7 and 28 days for the cast mixtures. In each series, the specimens were stored in the 100% R.H. conditioning room until the testing age (unless otherwise specified). An example of a specimen tested in compression is shown in Fig. 2.3 c). Using the ASTM C642 procedure, the boiled water absorption (BWA) and volume of permeable voids (VPV) of the sprayed dry-mix shotcrete mixtures were determined on sets of three (3) cored samples at age of 28 days.

<div align="center">(a)</div>

<div align="center">(b)</div>

<div align="center">(c)</div>

Fig. 2.3 Specimen for the characterization of mechanical properties: (a) cast cylinder samples, (b) sprayed test panel and cored samples, and (c) test specimen in compression

2.3.3 Free Uniaxial Shrinkage Test (ASTM C157 Modified)

The ASTM C157 [49] test method was used to determine length change of shotcrete prisms (75×75×285 mm). The ASTM C157 tests were only performed where it is deemed necessary due the difficult nature of performing this test in shotcrete (the specimen can be shot into the small mold and therefore must be sawed from a test panel). After placement, the specimens were cured at 20 °C and about 100% R.H. for the first 24 hours. The test procedure was modified such that, at the end of the curing period, the specimens were

moved to an environmental chamber maintained at 50 ±4% R.H. and 23 ±2 °C. Prior to exposing the specimen to the testing environment, some were either fully sealed to prevent drying (measurement of self-desiccation) or partially sealed such that they have the same S/V ratio as the ring specimens. The sealing was achieved by using a double layer of adhesive aluminum tape.

Typical ASTM C157 test specimens for cast and sprayed mixtures are shown in Fig. 2.4 a) and b), respectively. Notice that in the case of the sprayed specimens, DEMEC (DEmountable MEChanical) gauge studs (glued brass discs) were installed on two opposite side faces of the specimens for length change measurements immediately after demolding (Fig. 2.4 b)). Installation of the gauges was performed at that stage to avoid damaging the DEMEC gauge studs during the spraying process. The unsealed and partially sealed specimens were used to measure drying shrinkage, while slef-desiccation shrinkage was measured on the sealed specimens. During the conditioning process, the length change and weight loss of each test specimen was recorded regularly.

(a)   (b)
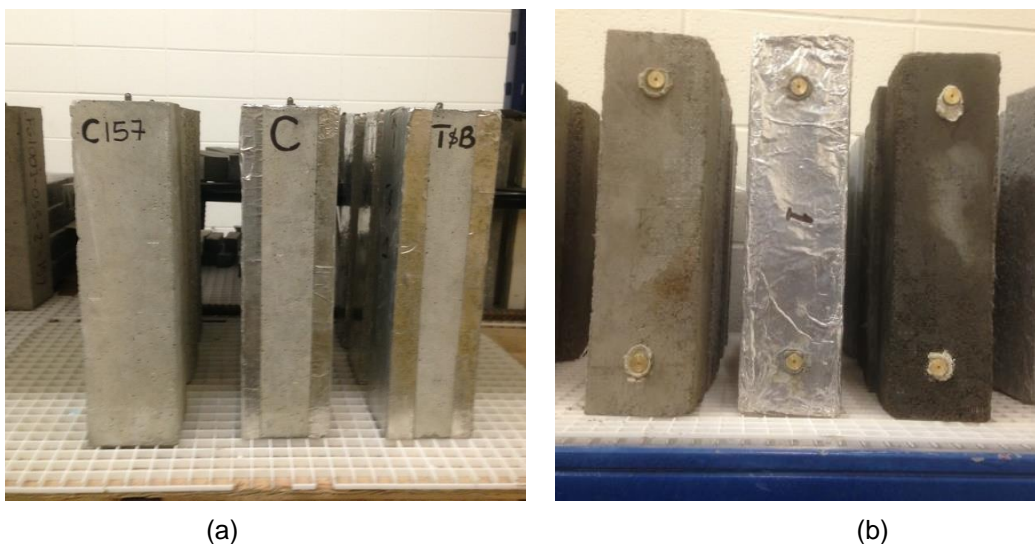
Fig. 2.4 ASTM C157 test specimens: (a) *gravity-cast* specimens and (b) *spray-cast* specimens

2.3.4 Free Ring Shrinkage Test

As previously said, in order to feed and extend the analysis of the restrained shrinkage data, free shrinkage is measured using a ring-shape specimen identical in size to that used in the AASHTO T 334 procedure, with the exception of the steel ring being replaced by an expanded polystyrene insert (described in detail in [57]). For each tested mixture, two specimens were prepared and moist cured for 24 hours under wet burlap and plastic sheets. The free ring setup and a test specimen are shown in Fig. 2.5 a) and b), respectively. After demolding, DEMEC gauge studs are installed on the top surface for length change measurements. Immediately after installation of the DEMEC gauges, the initial measurements were taken.

The ring specimens are then partially sealed with aluminum foil tape to allow drying only from the unsealed surfaces. The specimens were sealed in accordance with two configurations, such that they could dry either along their *radial* direction - also referred to as "*circumferential drying*" (as shown in Fig. 2.6 a)), or along their *axial* direction - also referred to as "*top and bottom drying*" (as shown in Fig. 2.6 b)). The specimens were exposed to drying in a temperature and humidity-controlled room at 23 ±1.7 °C and 50 ±4%. Subsequent readings were taken at regular intervals for the duration of the test (sequence inspirer by the ASTM C157 procedure).

(a)   (b)

Fig. 2.5 Free ring shrinkage test: a) mold prior to casting; and b) test specimen with outer steel ring and inner polystyrene insert, immediately after spray-casting
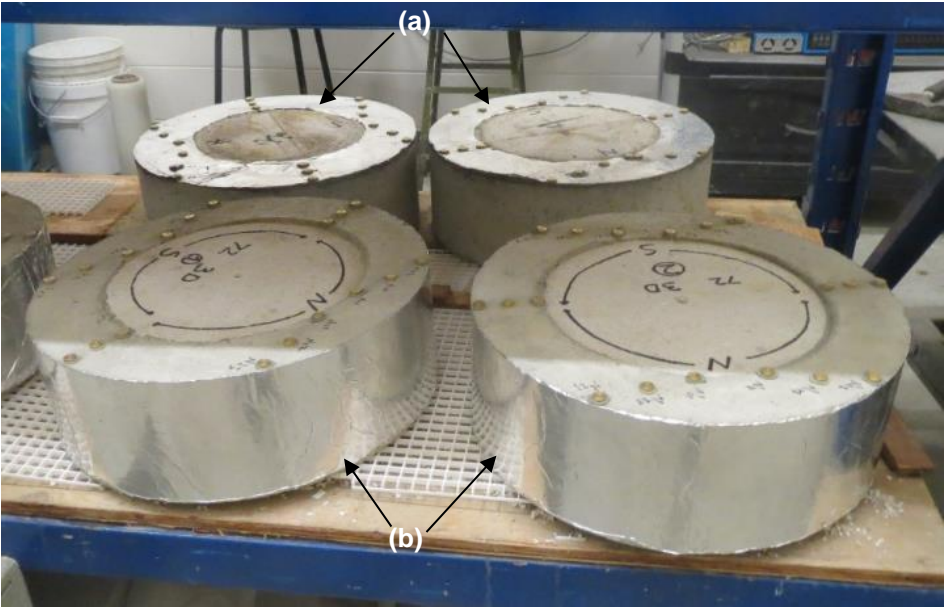
Fig. 2.6 Free ring specimen with DEMEC gauges: a) sealed on top (and bottom) for radial drying; and b) sealed on the outer circumferential surface for axial drying

2.3.5 Restrained Ring Shrinkage Test (AASHTO T 334 Modified)

The research focuses primarily on the cracking tendency test based on the AASHTO T 334 [4] test procedure. The steel rings used are instrumented with four strain gauges located at equidistant mid-height locations on their inner face to monitor the strains during the experiment and determine the average stresses generated in both the steel and concrete. Two ring specimens were prepared for each mixture (gravity-cast or spray-cast) investigated. The rings were moist cured for 24 hours under wet burlap, after what the outer mould (PVC or steel) of the specimen was removed. The ring specimen after placement and demolding are shown in Fig. 2.7 and Fig. 2.8 a) and b). The ring setup and specimen of the spray-cast rings can be found in Chapters 6 and 7. Immediately following demolding, the rings are sealed with aluminum foil tape to restrict drying to only the unsealed surfaces. As previously mentioned, the specimens were sealed in such a way that they could dry either along their *radial* direction - also referred to as "*circumferential drying*" (Fig. 2.9 a)), or along their *axial* direction - also referred to as "*top and bottom drying*" (Fig. 2.9 b)). The restrained ring specimens were exposed to drying in a temperature and humidity-controlled room at 23 ±1.7 °C and 50 ±4% until cracking occurred in the specimens.

In addition to recording the signal from the strain gauges, daily visual inspections were performed to detect and record the occurrence of cracking. Cracking of the restrained test specimen is typically indicated by a sudden drop in the strain of at least one of the strain gauges on the steel ring. Crack widths were then measured at various locations. The time to cracking was used as an index to evaluate cracking risk in addition to the quantitative information generated from the analytical calculations performed with the test data (i.e., average stress, stress rate, creep and relaxation estimations). A picture of a typical crack that developed in the restrained ring specimen is provided in Chapter 4. Additional pictures are provided in Appendix C.

(a)   (b)

Fig. 2.7 Ring specimen with inner steel ring and outer PVC, immediately after gravity-casting; and b) after removal of the outer PVC form

(a)	(b)

Fig. 2.8 Sprayed specimen with: (a) inner and outer steel ring, immediately after spraying; and (b) after removal of the steel ring
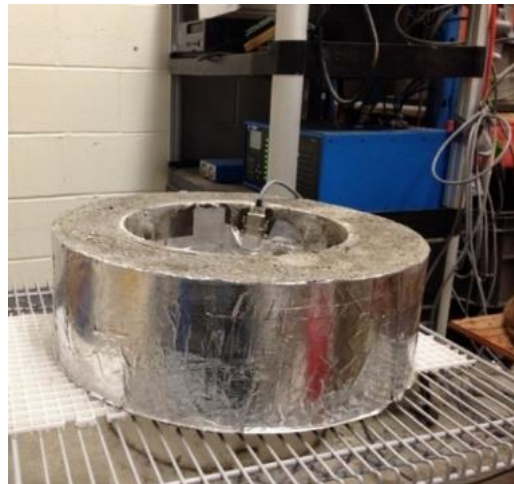
(a)	(b)

Fig. 2.9 Restrained ring specimen: a) sealed on top and bottom for radial drying; and b) sealed on the outer circumferential surface for axial drying

2.3.6 Weight loss

Since relative humidity within the mixtures could not be directly measured, weight loss caused by drying of the test specimens were monitored instead. For the conventionally cast shotcrete mixtures, the weight loss and length change measurements were taken simultaneously using the typical ASTM C157 prismatic test specimens. For the sprayed mixtures, the weight loss tests were carried out on 100 mm cylindrical cores taken from test panels. After curing (same as the test specimens), the cylinders were partially sealed with

a double layer of aluminum foil tape such that they had the same exposed surface to volume ratios as those of the ring test specimens. The cylinders were also exposed to the same drying exposed to drying in the same conditioning room as the other test series. The weight losses were recorded at the same rate as the free ring shrinkage measurements.

2.4 Finite Element (FE) Modelling of Drying Shrinkage

In addition to the comprehensive experimental programs, shrinkage and cracking were assessed numerically, with the aim of complementing the experimental tests and extending the analysis

In this study, the numerical simulation of shrinkage tests of concrete was conducted using the CEA Cast3m FE code. Drying of the material was modelled using non-linear diffusion law and the development of cracks was based on an isotropic elastic-damage model. The material properties and mass loss curves determined experimentally were used as input data. Model parameters have further been adjusted based upon the experimental results generated in the ring test experiments.

The model used is presented in Appendix A. Further information on the numerical model can be found in Appendix D.

Chapter 3 *Article 1* - Studies on the Influence of Drying Shrinkage Test Procedure, Specimen Geometry and Boundary Conditions on Free Shrinkage

Bruce MENU, Marc JOLIN, and Benoît BISSONNETTE

Department of Civil and Water Engineering, Université Laval, Quebec City, QC, Canada G1V 0A6

3.1 Résumé

Dans ce premier article, l'essai de retrait libre annulaire basé sur la norme AASHTO a été réalisé dans le but d'améliorer l'interprétation de l'essai de retrait restreint. L'étude met en évidence pour la première fois l'importance de la méthode d'essai de retrait libre annulaire sur le retrait de séchage mesuré. Elle met aussi en évidence l'influence de la géométrie, du rapport surface/volume exposé au séchage et des conditions de séchage sur le retrait de séchage mesuré. L'amélioration de la méthode d'essai de retrait libre annulaire est nécessaire à des fins pratiques, puisque des études récentes ont démontré l'utilisation croissante des déformations restreintes et libres pour évaluer le fluage et la relaxation des contraintes des bétons.

3.2 Abstract

Although considerable progress has been made in enhancing the use and interpretation of free ring shrinkage test, little is known about the impact of the test procedure, the specimen geometry, the surface area-to-volume (S/V) ratio exposed to drying, and the boundary conditions (sealing configuration) on the measured shrinkage. This paper highlights recent findings illustrating the influence of the test procedure, the S/V ratio exposed to drying, the geometry of specimen and the boundary conditions. A series of experimental results are presented from free shrinkage on ring test specimens to illustrate that the test procedure can significantly influence the measured free shrinkage. A second series of experimental results are presented from specimens with different geometries and S/V ratio exposed to drying to illustrate that drying shrinkage is both dependent on the specimen geometry and the surface exposed to drying. Test

results further shows that even for the same S/V ratio exposed to drying, shrinkage is strongly dependent on the specimen's geometry and boundary conditions.

Keywords: concrete, free, shrinkage, surface area-to-volume, drying directions, geometry, ring specimen

3.3 Introduction

Concrete undergoes significant volume changes due to the evolution of the moisture or water content within its porosity. Concrete swells when exposed to moisture, while it shrinks when exposed to relatively lower relative humidity. The net relative humidity reduction inside the pores changes the local thermodynamic equilibrium, which in turn affects the mechanical equilibrium, translating into a macroscopical contraction of the cement paste referred to as shrinkage. Concrete is very sensitive to shrinkage cracking at the early ages [58] particularly due to the rapid development of drying shrinkage. Early-age cracking can occur in concrete if the free shrinkage is *prevented* by the surrounding structure [59]. This is because concrete has low tensile strain capacity and is most sensitive to internal stresses during early-ages immediately after casting [60]. Degradation of concrete structural elements due to shrinkage of concrete, during its drying stage usually leads to significant costs of repairing [61]. The magnitude of shrinkage is dependent on many factors particularly the water content of the fresh concrete. Free or unrestrained shrinkage test methods are used to evaluate the shrinkage potential of concrete. In these methods, concrete specimens are *unrestrained* hence allowed to change volume and *shrink freely* in an environmental-controlled chamber with a constant temperature and relative humidity (R.H.). The change in length is measured at regular intervals for a specified period. Free shrinkage is typically measured uniaxially on prismatic test specimens (ASTM C157 [49]) due to the simplicity of data interpretation.

However, it may also be measured on test specimens with different geometries such as the free ring test developed as a complementary test procedure for the restrained ring test. Regardless, to directly use prismatic shrinkage results in ring test analysis, a generally accepted idea is to prepare prismatic specimen with the same S/V ratio as the restrained ring specimen. However, in reality, ring shrinkage may not always correspond to prismatic shrinkage with the equal S/V ratio. Researchers have published a great quantity of scientific literature and technical reports on the ring test in the past few decades [38, 62-64]. However, little work is focused on the impact of the *free ring* test procedure, S/V exposed to drying, and boundary conditions (i.e. drying direction) on the measured shrinkage.

The present study is part of on-going research on the durability of concrete and shotcrete mixtures. In this paper, the free ring test is used to extend the interpretation of the restrained shrinkage ring test experiment. The free ring specimen used in this studies is based on the AASHTO [5] restrained ring test specimen configuration shown in Fig. 3.1. This paper highlights the influence of the free ring test procedure on the measured drying shrinkage which is important because free shrinkage is mostly used to estimate creep

and stress relaxation [34, 65, 66] of concrete. The influence of geometry, surface area to volume (S/V) ratio exposed to drying and drying direction on the measured drying shrinkage is discussed.
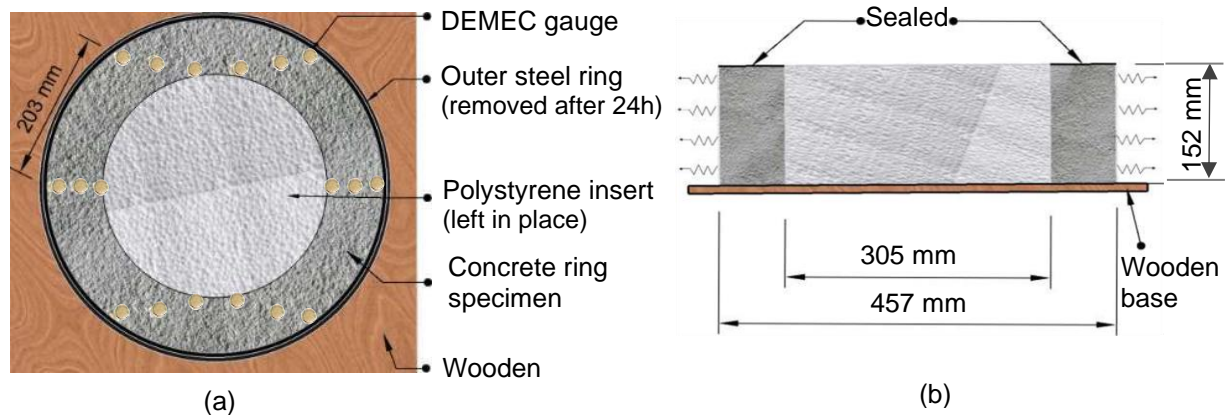
Fig. 3.1 Dimensions of free ring setup (radial drying condition illustrated). (a) Top view. (b) Front view

3.3.1 Research Significance

The research was undertaken to investigate the influence of the ring test procedure on the measured shrinkage. In addition to the need for evaluating the shrinkage vs. time curve in the most consistent fashion for analytical calculations, such validation is made necessary for practical purposes, as the ASTM C157 procedure is ill-suited for unconventional placement method such as shotcrete. More importantly, improving the free ring test method is necessary as recent studies have demonstrated the increasing use of free drying shrinkage in combination with restrained shrinkage to evaluate creep and stress relaxation of concrete.

3.4 Experimental Program

To investigate the influence of specimen geometry, of surface-to-volume (S/V) ratio expose to drying, of the ring test procedure (i.e. DEMEC (DEmountable MEChanical) gauge point locations) and surface sealing (axial vs. radial drying) on free shrinkage, both prismatic (linear) and ring specimens were prepared. The overall project evolves around shotcrete durability and performance; a shotcrete mixture (maximum coarse aggregates size of 10 mm) was used for producing concrete mixtures. The concrete mixture used was selected to resemble that of dry-mix shotcrete design (ACI 506 Guide to Shotcrete [9]). The research was aimed at optimizing the free ring shrinkage test procedure and correlating the results with the restrained ring test results. Hence, the method of placement (cast or sprayed) did not really matter, and gravitational casting was selected for simplicity (the reader can refer to [67] for a procedure developed to evaluate restrained and free shrinkage of *sprayed* ring test specimens).

No admixture was added to the w/cm=0.60 mixture; but a naphthalene-based superplasticizer and air entraining agent were added to w/cm=0.45 mixture to obtain the desired workability due to the low water to cement (w/cm) ratio. The concrete mixture proportions used in the study are provided in Table 3.1. The compressive strength, splitting tensile strength and modulus of elasticity were also determined in accordance with ASTM C39, C496 and C469 test methods. Contrary to *restrained ring* test where shrinkage of concrete is not permitted, in the *free ring* test, however, the concrete specimen is not internally restrained and hence can shrink *"freely"*. DEMEC gauges are installed on top of the ring specimens for length change measurements. The following sections briefly describe the implemented free shrinkage test methods in this study.

Table 3.1 Composition of the investigated concrete mixtures

w/cm	OPC cement (kg/m^3)	2.5-10 mm crushed limestone (kg/m^3)	0.08-5 mm natural sand (kg/m^3)	Water (kg/m^3)	Superplasticizer (kg/m^3)	Air-entraining agent (kg/m^3)
0.45	445	736	1054	197	5	0.16
0.60	417	689	988	247	-	-

3.4.1 Free Uniaxial Test Specimens

Acknowledging that drying shrinkage is dependent on the S/V ratio exposed to drying [37, 52], the first step was basically to measure free shrinkage using prismatic specimens with different S/V ratios. The S/V ratios are summarized in Table 3.2. The aim was to investigate the influence of different exposure conditions on drying shrinkage and to simulate the same exposed S/V ratios as for the ring specimens. Free uniaxial shrinkage was evaluated using a modified version of the ASTM C157 test method. Nine prismatic 75×75×285 mm prismatic concrete specimens were cast for each mixture. The specimens were moist cured for 23½±½ h and then demolded.

The test procedure was modified such that after demolding, the specimens were moist cured for 2 more days (i.e. age 3-days). The specimens were placed in an environmental chamber with a constant R.H. (50%) and temperature (21±1.7 °C). The length change was monitored with the aid of a comparator upon exposure to drying to imitate the free rings specimen procedure. Three specimens were unsealed while six specimens were sealed such that in each case three specimens have equal S/V ratio as the ring test specimens drying from the radial direction and axial direction as shown in Fig. 3.2. Drying is thus permitted only from the exposed sides of the concrete specimens. It should be mentioned that although the linear specimens were sealed to have the same S/V exposed as the radial and axial drying in the ring specimens, they can in fact only mimic the axial drying direction conditions. Three supplemental specimens were cast and completely sealed on all surfaces (S/V=0) after 24 h of moist curing.

39

Table 3.2 Dimensions and S/V ratios of specimens

Specimen	Dimensions (mm)	Drying condition	S/V (m^{-1})
Prismatic	75 x 75 x 285	All surfaces	60.4
	$H = 152.0$	No surface	0
Ring	R_{ic} = 152.5	Radial	15.8
	R_{oc} = 228.5	Axial	13.2

H = height; R_{ic}= inner radius; R_{oc} = inner radius
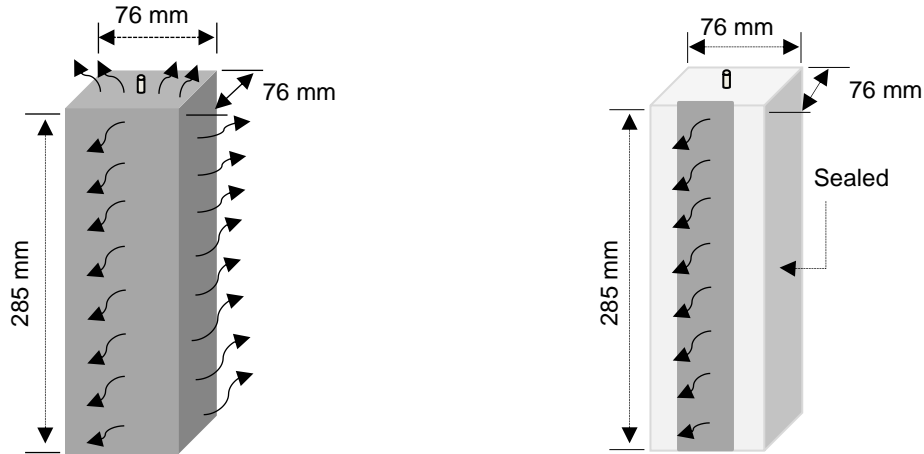
Fig. 3.2 ASTM C157 specimens

3.4.2 Free Ring Test Specimens

The goal of the free ring test was to investigate the influence of the DEMEC gauge points location and the sealing configuration (radial vs. axial drying) on the measured shrinkage. It should be mentioned that the dependence of drying conditions on shrinkage of concrete has been previously shown by Moon et el [68]. These papers, however, point toward the importance of drying conditions in shrinkage and cracking studies, while this paper focuses on the influence on free shrinkage tests. Three different DEMEC gauge points locations were investigated. The locations were chosen such that, it would cover the range of possibilities, with measurements near the inner radius, at mid-width of the concrete ring specimen, and at the outer edge of the concrete ring.

A template was designed for ensuring accurate positioning of the gauges (as illustrated in Fig. 3.3). The free ring test procedure consists of replacing the steel ring in the restrained shrinkage test (AASHTO T334-08, *formerly AASHTO PP 34-99*) with a material having a very low stiffness with respect to the concrete ring (such as white polystyrene). The choice of a polystyrene ring was basically to facilitate the test method and to mimic the companion restrained test specimen as much as possible. The aim was also to reduce the time necessary for testing (casting, demolding, placing DEMECs, etc.) and to also limit manipulation of the rings at early age. Moreover, the restraint due to the polystyrene ring is negligible as it has an elastic

modulus of about 2.2 MPa compared to steel ring used in the restrained shrinkage which is about 200 MPa. Needless to say, the choice of a removable center ring was also considered at the initial stages. In this test, a 152-mm high and 76-mm thick ring of concrete is then cast around the polystyrene ring having a diameter of 305 mm. Details of the specimen configuration is shown in Fig. 3.1.

At least four concrete ring specimens were cast for each concrete mixture to measure the free drying shrinkage. Upon casting, the freshly placed concrete was consolidated in the mould. All specimens were left in their mould for the first 24 hours after casting and covered with wet burlap and plastic sheets. After 24 hours curing, the exterior wall of the mould is removed and the specimens are cured for 2 more days (age 3-days). After curing, DEMEC gauges are installed on top of the specimens for length change measurements. The ring specimens are sealed with an adhesive aluminum tape to restrict drying to only the unsealed surfaces. At least two specimens each were sealed on the top (and bottom) and the outer circumference. The test specimens drying from the outer radial surface or so-called "circumferential drying" (a) and the axial sides or so-called "top and bottom drying" (b) are shown in Fig. 3.4. The specimens were exposed to drying under standard conditions (21±1.7°C and 50 ± 4% R.H.)

The initial zero measurement was taken immediately after curing and sealing (age 3-days), and the length change was monitored during the entire drying period. A digital DEMEC (DEmountable MEChanical digital strain gauge secured on a reference Invar bar) was used for measuring the length change between the DEMEC points. In general, the shrinkage recorded on each ring specimen is the average recorded on the three DEMEC gauge points location (inner, mid-width and outer). The free drying shrinkage strain was calculated using the following expression:

$$\varepsilon_{sh} = \Delta L / G \tag{3.1}$$

where ε_{sh} is the free shrinkage, ΔL is the change in length, and G is the gauge length.
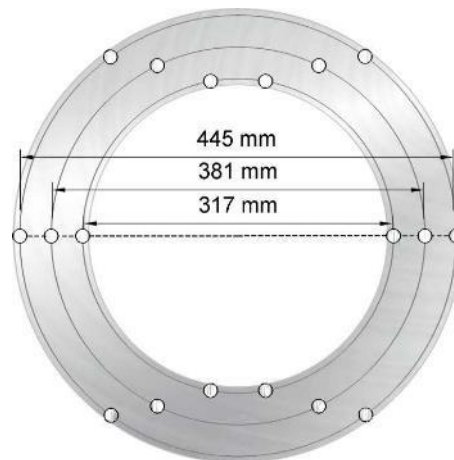
Fig. 3.3 Template for positioning of the DEMEC point discs on the free ring-shape specimens
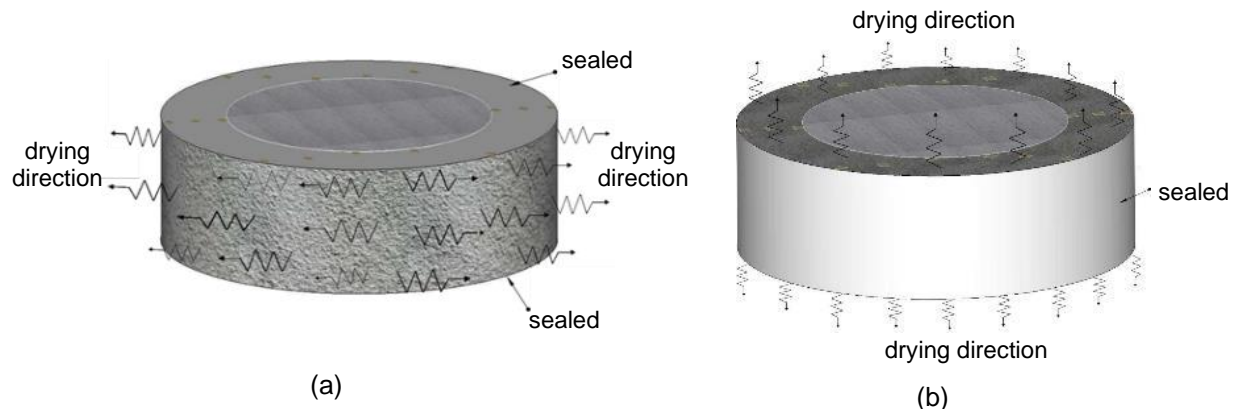
Fig. 3.4 Free ring specimen with DEMEC: (a) Sealed on top (and bottom) and (b) sealed on the outer circumferential surface

3.4.3 Characterization Test Specimens

Twenty-one 100 x 200 mm (4 x 8 in.) cylinders were also prepared for each tested concrete mixture. Four cylinders per mixtures were tested in compression at 3, 7, and 28 days after casting to determine compressive strength following ASTM C39, two of which were also used to determine the modulus of elasticity and Poisson's ratio in accordance with ASTM C469. Three supplemental cylinders were used to determine the splitting tensile strength at 3, 7, and 28 days after casting in accordance with ASTM C496. After casting of specimens, they were kept in the mould and covered with wet burlaps and a 0.15-mm polyethylene sheet for 23½ ± ½ hours, and subsequently stored under standard conditions (23±1.7 °C and 100 % R.H.) until testing age.

3.5 Test Results and Discussion

3.5.1 Mechanical properties of concrete

The mechanical properties were measured at ages of 3, 7, and 28 days using the cylindrical specimens with the same w/cm of 0.45 and 0.60 mixtures. The compressive strength result is shown in Fig. 3.5 while the splitting tensile strength elastic modulus and Poisson's ratio are summarized in Table 3.3. In general, the compressive strength, elastic modulus and splitting tensile strength show an overall steady increase with increase in curing age but a decrease with increase in w/cm ratio. The determined Poisson's ratio values in this study, however, appear to decrease with increase in strength and maturity of concrete but a slight increase with increase in w/cm ratio. Interestingly, similar results were reported in other studies [69]. Poisson's ratio of concrete must therefore not be a constant value as commonly used. Admittedly, the Poisson's ratio is a little difficult to quantify and even more so to interpret. However, it is needed for the evaluation of elastic stress and stress relaxation properties of concrete.

Table 3.3 Mechanical properties

| Age (days) | f_t (MPa) | w/cm 0.45 | | | f_t (MPa) | w/cm 0.60 | |
		E_c (GPa)	μ			E_c (GPa)	μ
3	2.4	25.8	0.18±0.012	2.4	25.4	0.19±0.014
7	2.6	26.8	0.17±0.009	2.5	26.3	0.18±0.009
28	3.2	30.0	0.16±0.007	2.7	28.8	0.17±0.011
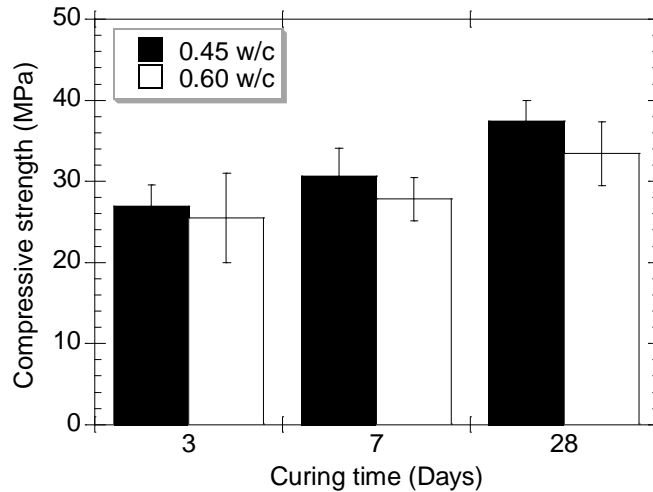
Fig. 3.5 Compressive strength of concrete (error bars represent the coefficient of variation)

3.5.2 Free Linear Shrinkage of Concrete

The average free shrinkage recorded on prismatic specimens with different S/V ratios is presented in the two graphs of Fig. 3.6, corresponding respectively the 0.45 w/cm and 0.60 w/cm mixtures. On each graph, the X-axis is the time elapsed since drying initiation, which started in all cases at the age of 3 days. In the case of the sealed specimens, they were covered and monitored for length change starting at the age of one day. Hence, the curves plotted for these specimens in Fig. 3.6 omit the strains recorded between one and three days. It should be noted that the length change curves of the sealed specimens correspond to self-desiccation shrinkage, while the test results of the drying specimens (non-sealed and partially sealed) include the effect of both autogenous shrinkage and drying shrinkage, referred to hereafter as the total free shrinkage.

The results obtained in drying conditions are quite similar for both concretes (very little differences actually observed, within experimental variations). We would actually have expected the 0.60 w/cm mixture to exhibit more total shrinkage, especially considering its larger paste content. It was also observed that for both w/cm=0.45 and 0.60 mixtures, the amount of total free shrinkage appears to be dependent on the surface area exposed to drying. In general, the higher surface-to-volume ratio resulted in the highest magnitude of shrinkage recorded due to faster drying in higher S/V ratio specimen. These observations are

consistent with those of some previous studies [52] although the specimens in the latter were moist cured for 1-day and the shrinkage was monitored up to only 28 days. In fact, this was to be expected since drying is a diffusion-based process and drying shrinkage depends on the internal relative humidity change and hence on the S/V ratio exposed to drying. As expected, Fig. 3.6 show that *sealed* shrinkage is higher in mixtures with w/cm=0.45 than w/cm=0.60. The sealed strain values for the w/cm=0.45 were similar those reported by Mors [70] for mixtures with w/cm≈0.45.
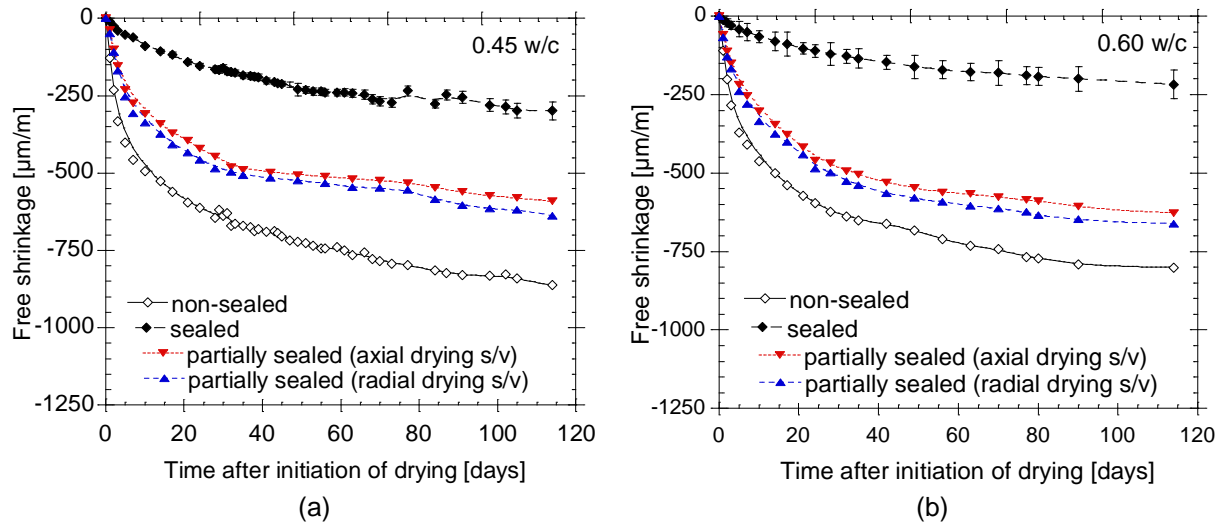
Fig. 3.6 ASTM C157 modified shrinkage strain results obtained under various drying exposure conditions. (a) w/cm 0.45 mixture, (b) w/cm 0.60 mixture

3.5.3 Free Ring Shrinkage of Concrete

The first objective of this work is to investigate the influence of the free ring test procedure on the shrinkage measured on the specimen. Three different DEMEC gauge points locations were investigated. The locations were chosen such that it would cover the range of possibilities, with measurements near the inner radius, at mid-width of the concrete ring specimen, and at the outer edge of the concrete ring. A template was designed for ensuring accurate positioning of the gauges (as illustrated Fig. 3.3). The shrinkage recorded for each ring is an average of measurements performed for four sets of DEMEC points around the circumference. At least two sets of ring specimens are cast for each mixture. The ring specimens could dry either from the radial or the axial directions. A comparison of the free ring shrinkage strain measurements at the different locations is presented in Fig. 3.7.

Overall, the results indicate that moisture gradient within the concrete ring thickness affects the recorded shrinkage strains. Implying that the location at which the shrinkage is measured on the ring specimen will influence the magnitude of free shrinkage measured. Indeed, it was observed that for both w/cm=0.45 and

w/cm=0.60 mixtures the total free shrinkage differs to a certain degree depending on the DEMEC point location (inner, mid-width and outer). In general, higher shrinkage rates were recorded at the outer location on the concrete ring specimen for both drying directions. This is attributed to the fact that the ring specimens do not shrink at the same rate at all three locations in the ring since moisture varies across the thick concrete ring wall.
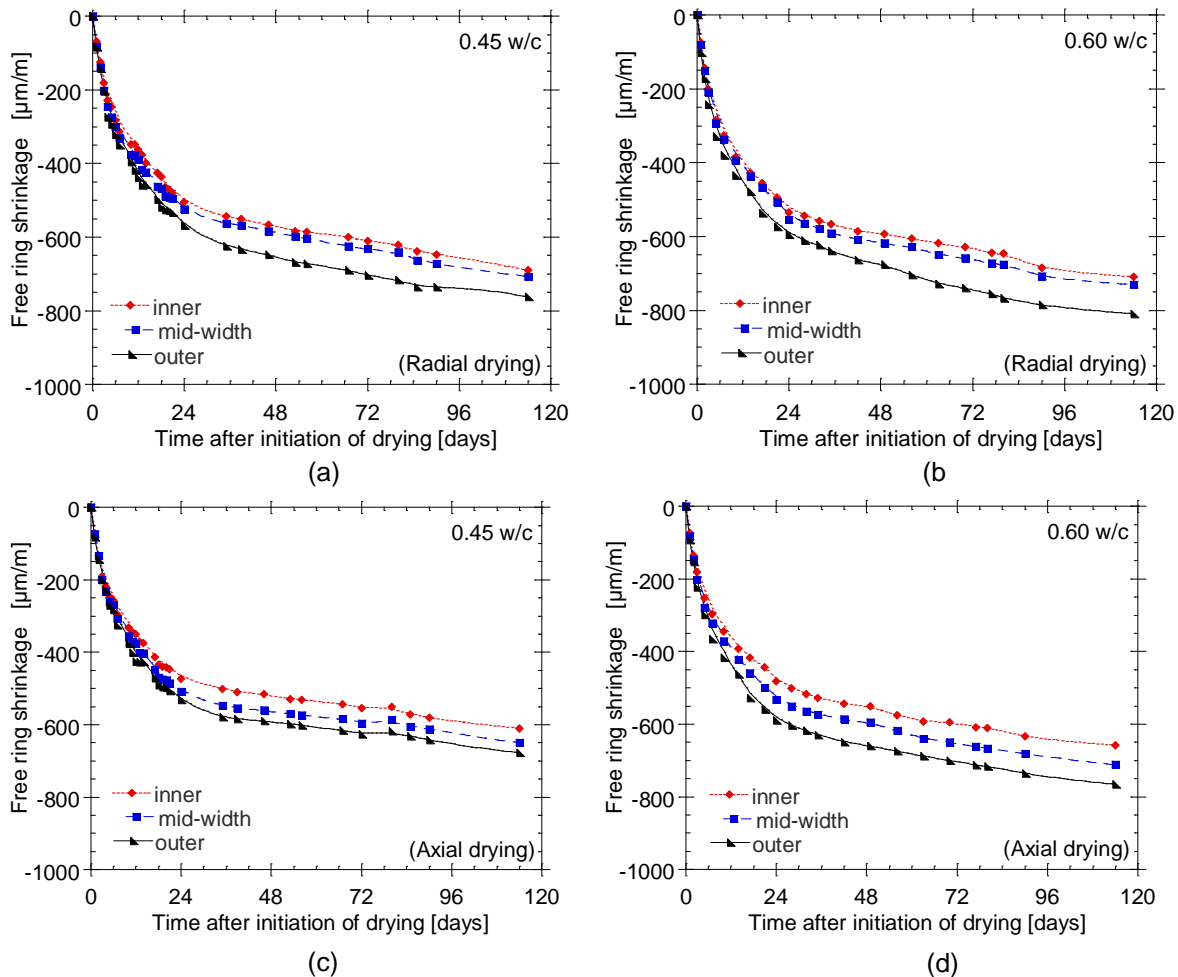
Fig. 3.7 The influence of DEMEC gauge positioning on the measured free ring shrinkage strain: (a) w/cm 0.45 radial drying specimen, (b) w/cm 0.60 radial drying specimen, (c) w/cm 0.45 axial drying specimen, (d) w/cm 0.60 axial drying specimen

The results further indicate that the drying direction (i.e. boundary condition) in the ring specimen significantly influenced the free shrinkage recorded at the different locations on the ring specimens (inner, mid-width and outer). Fundamentally, this is to be expected since the boundary conditions imposed on the ring specimen will affect the nature of moisture loss (uniform or non-uniform) along the radius of the ring.

Naturally, drying shrinkage is related to moisture loss from the concrete specimen, hence the rate of shrinkage strain will consequently be dictated by the nature of moisture loss.

It can be observed that for specimens drying from axial direction, shrinkage strain increases linearly from the inner to the outer radius. This is likely because, in specimen drying from the axial direction, moisture loss is uniform along the radial direction but not along the height direction [62]. As such, due to the geometry of the ring specimen the three DEMEC point locations on top of the specimen will not have equal drying rate. Hence they naturally will shrink at different rates, linearly from the inner to the outer radius. However, in specimens drying from the radial direction, there was no significant difference in the recorded shrinkage strain for the inner and mid-width locations compared to the outer location. This is attributed to the fact that in specimen dried from the radial direction, moisture loss is uniform along the height direction of the specimen but not along the radial direction.

In fact, the relative humidity at the outer circumferential surface is slightly higher than the ambient humidity of 50% [52]. As a result, the ring specimen shrink faster at the outer drying surface where more rapid drying occurs. However, the internal core (inner radius up to mid-width) drying at a slower pace. Consequently, the shrinkage at these DEMEC point locations did not vary significantly. Indeed similar results were reported by Lim et al., [71] although in their studies the specimen were drying from all surfaces.

3.5.4 Effects of Specimen Geometry, Size and Drying Condition on Free Shrinkage

The main objectives for the free ring and linear tests were to: (i) study the influence of surface-to-volume ratio and drying direction on drying shrinkage using different geometries, and (ii) investigate the common assumption that the magnitude of shrinkage is the same for concrete with equal S/V ratio regardless of the geometry and boundary conditions of concrete specimens. The geometrical characteristics and S/V ratios of the prismatic and the ring specimens are summarized in Table 3.2. The comparison of the shrinkage recorded on the prismatic and ring specimens of unequal S/V ratio is shown in Fig. 3.8. The free shrinkage is the average of the 3 location measurements on two ring specimens. While Fig. 3.9 shows the recorded on prismatic and rings specimen with equal S/V ratios. The results in Fig. 3.8 indicate that the geometry of specimens influences the evolution of drying shrinkage for both the w/cm=0.45 and 0.60 mixtures. As expected for both mixtures, higher shrinkage values were recorded on prismatic specimens with all surfaces exposed compared to ring specimens. This is partly because the prismatic specimen with all surfaces exposed (non-sealed) have higher S/V exposed to drying than the ring specimens.

Also, amongst the ring test specimens, drying from the radial direction leads to higher shrinkage than drying from the axial direction. This again is attributed partly to the fact that the ring specimens drying from the radial direction have higher S/V than specimen drying from the axial direction. In fact, this not surprising since at a constant R.H, size, shape, geometry and S/V of concrete elements exposed to drying dictate the magnitude of shrinkage. This is mainly because water transport from the interior of concrete to the

atmosphere (i.e. rate of water loss) is controlled by the length of the path travelled by the water, which is being expelled during drying shrinkage and/or creep [31].
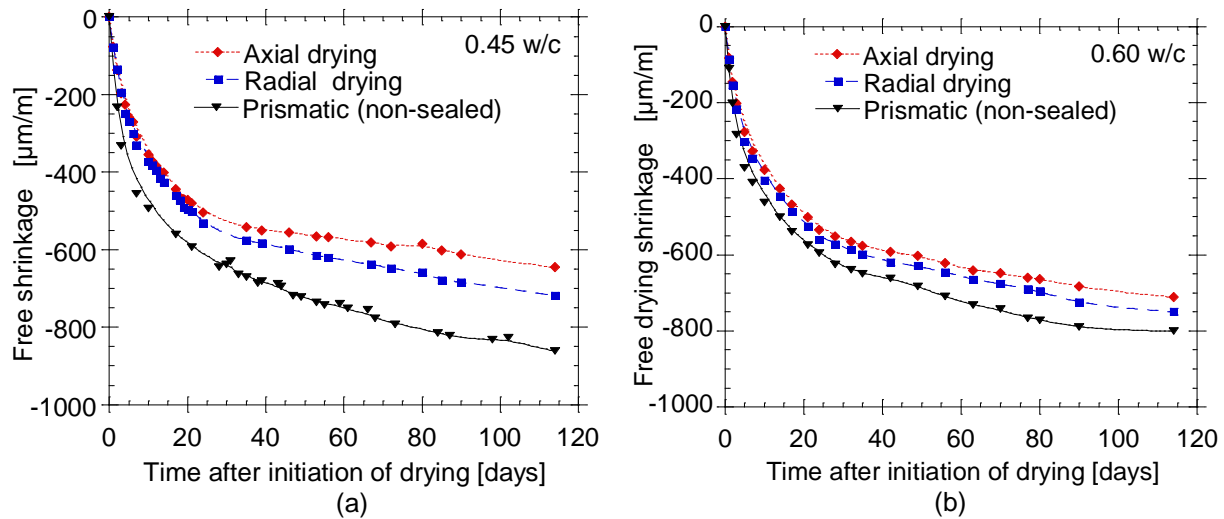
Fig. 3.8 Influence of specimen geometry, S/V and drying direction on free shrinkage recorded: (a) w/cm 0.45 mixture, (b) w/cm 0.60

Indeed, research has shown that drying direction can significantly influence the moisture profile and consequently the distribution of residual stresses inside the concrete ring [68]. Furthermore, the results in Fig. 3.9 reveal that the general consensus implying that the magnitude of shrinkage recorded on concrete specimen with the same S/V ratios is equal regardless of the geometry and drying direction of concrete specimens is not entirely true.

It was observed that for both mixtures the average shrinkage measured on free ring specimen is higher than that of the prismatic specimens although having the same S/V ratio. This is true for both drying directions. The difference is more significant for the w/cm=0.60 mixture. Interestingly, the lowest shrinkage recorded in this study at the inner radius of the ring (Fig. 3.9) is actually very close to the values recorded for the prismatic specimen with the same S/V ratio (especially for specimen drying from the axial). In previous studies by Hossain and Weiss [38] however, it was found that prismatic specimens with equal S/V ratio as ring specimens drying from the axial demonstrated similar shrinkage to measurement taken at mid-width on the ring specimen.

It should be noted that the specimen used in the present study is twice the height of the specimen used by Hossain and Weiss [38]. In a nutshell, the discrepancies between the two tests might probably be due to the specimen height. Overall, the results from this study reveal that measurements made on prismatic specimens with same S/V as the AASHTO ring specimen in most cases will underestimate the actual magnitude of the average shrinkage. Particularly if the test is intended to estimate the creep properties of

the concrete, since the results from free and restrained ring shrinkage test are often combined to estimate creep and relaxation properties of concrete.
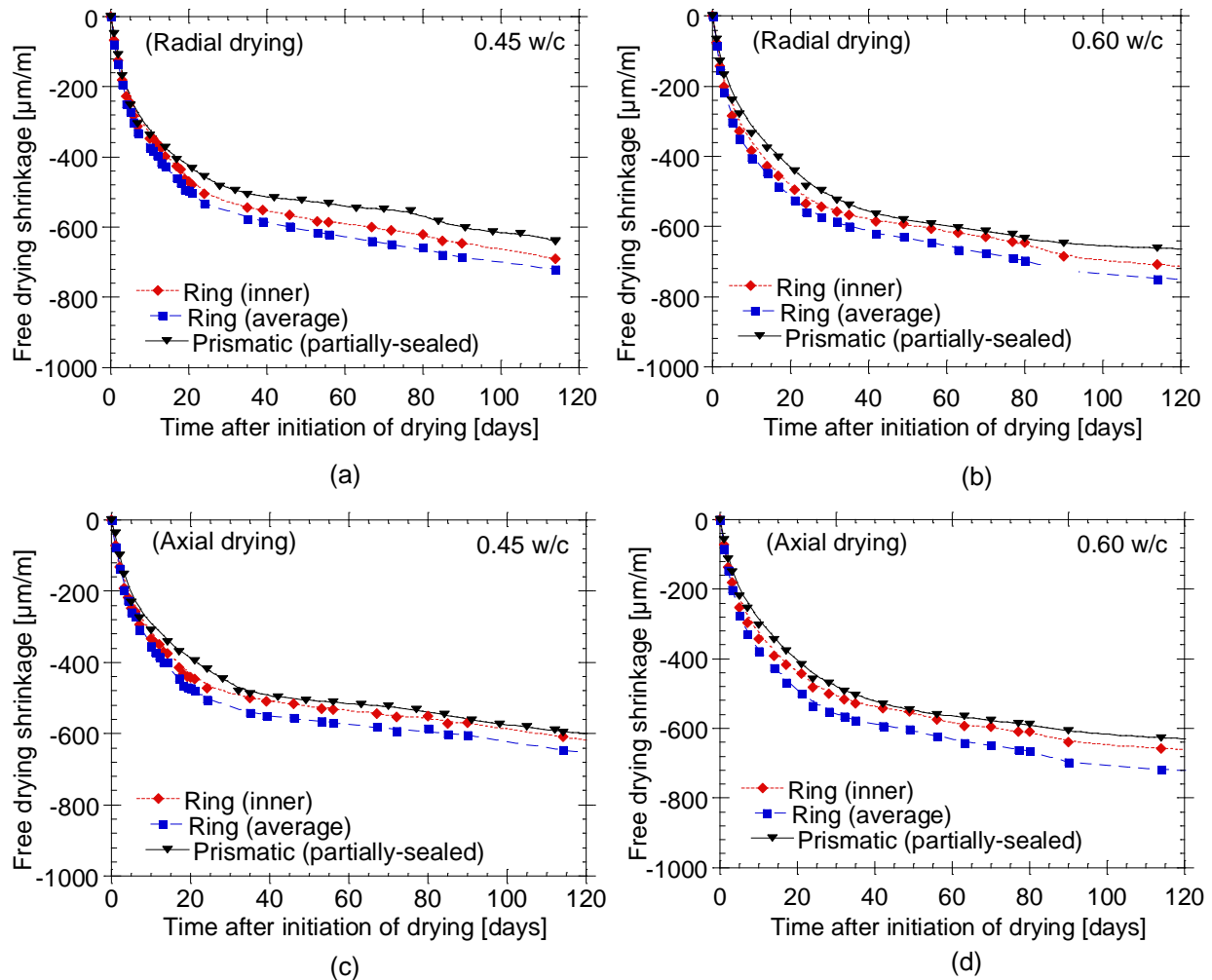
Fig. 3.9 Free shrinkage recorded on prismatic and ring specimens with equal S/V ratio: (a) w/cm 0.45 radial drying specimen, (b) w/cm 0.60 radial drying specimen, (c) w/cm 0.45 axial drying specimen, (d) w/cm 0.60 axial drying specimen

3.6 Conclusion

This paper focused on the study of the influence of free ring shrinkage test procedure, specimen geometry and drying direction upon drying shrinkage. The experimental results first showed that the location at which the deformation is measured on the concrete ring has a significant influence on the recorded drying shrinkage. This study has shown that specimen geometry and drying direction also has a significant influence on the drying shrinkage. In addition, it has been observed that the drying shrinkage increases

with an increasing surface to volume ratio. It has been found that the ring test specimens drying from the radial leads to higher recorded shrinkage than those drying from the axial sides. This can be explained by the fact that the specimens that dry from the outer radial have a higher surface-to-volume ratio. The widespread assumption that free shrinkage is the same for concrete with equal S/V ratio regardless of the geometry and drying direction of concrete specimens was found not to be satisfactory for the purpose of this study, i.e. using the ASTM C157 specimens in conjunction with ring specimens.

In fact, it was observed that even though the tested specimens had the same S/V ratio, the shrinkage recorded on the free ring specimen were not similar to that measured the corresponding prismatic specimens. Using the average ring deformation is likely to improve the reliability of the free drying shrinkage evaluation and, in turn, of the calculated creep properties. It should be further added that experiments are under way at Laval to evaluate the alternative use of prismatic specimens with the exact same cross-sections as that of the ring specimens. Although, ideally, it is recommended that similar geometry be used for both free and restrained shrinkage measurements, a complimentary test method using similar cross section of a linear prismatic and AASHTO ring specimen is also necessary due to its simplicity. Furthermore, the actual influence of using either free ring or prism (with same S/V) shrinkage data upon the calculated creep parameters needs to be investigated.

3.7 Acknowledgements

Chapter 4 *Article 2* - Assessing the Early-Age Shrinkage Cracking Potential of Concrete using Ring Specimens under Different Boundary Conditions

Bruce MENU, Marc JOLIN, and Benoît BISSONNETTE

Department of Civil and Water Engineering, Université Laval, Quebec City, QC, Canada G1V 0A6

4.1 Résumé

Étude expérimentale caractérisant la fissuration des bétons soumis à un chargement hygrothermique. La présente étude vise à mieux caractériser le potentiel de fissuration due au retrait de séchage grâce à une meilleure interprétation des résultats des essais de retrait restreint. Cet article décrit comment quantifier les contraintes induites par retrait empêché du béton. Une méthode d'analyse sur les bases de l'équilibre mécanique permettant d'évaluer l'évolution de la contrainte moyenne à travers l'ensemble du dispositif annulaire est présentée. De plus, d'autres facteurs influençant la fissuration du béton tel que les conditions de séchage, le rapport surface/volume exposé au séchage, le taux de déformation et le temps de fissuration sont également abordés.

4.2 Abstract

Early age cracking due to restrained shrinkage affects the performance and service life of concrete structures. Recent studies are successfully making use of the *free ring shrinkage test* in conjunction with *restrained shrinkage measurements* for the evaluation of the cracking potential of concrete. This study provides information to improve the interpretation of cracking in ring specimens and a theoretical approach for predicting the stress rate of thick ring specimens. Results show that the rate of strain development and the age-at-cracking vary with specimen drying direction and the exchange surface-to-volume ratio. The results further revealed that early-age shrinkage cracking depends more on the *shrinkage rate* than the *magnitude* of the shrinkage itself. Also, it was found that although the restrained ring specimens attained

approximately similar strain levels, the cracking age varies significantly, suggesting that elastic stress-strength analysis alone may be inadequate for predicting early-age cracking due to the contribution of creep-relaxation phenomena.

Keywords: cracking; restrained shrinkage; ring test; surface-to-volume ratio; shrinkage rate, stress rate.

4.3 Introduction

Shrinkage of cementitious materials is inevitable when the material is exposed to an environment with lower relative humidity (R.H.) and undergoes drying. If shrinkage is restrained, internal tensile stresses are progressively induced in the element and can eventually exceed the material's strength, leading to cracking. Drying shrinkage cracking is a major problem in concrete technology [36, 37, 72-74]. In particular, early cracking due to restrained shrinkage is a key issue in the long-term durability performance and service life of concrete elements. Indeed, many concrete structures worldwide require repair and rehabilitation, sometimes repeatedly, due to problems triggered by restrained shrinkage cracking. Many studies relating to shrinkage cracking have focused on the free shrinkage deformations. However, free drying shrinkage alone does not necessarily give a reliable indication of the risk of premature cracking.

In fact, in addition to the magnitude of the shrinkage deformation, the risk for shrinkage cracking depends on a combination of phenomena and parameters, most importantly the concrete's tensile strength, elastic modulus, creep, and the effective degree of restraint. In recent years, the *ring test* (e.g. AASHTO T334-08 [4], ASTM C1581 [53]) has become the most widely used test method to evaluate and quantify the restrained shrinkage cracking sensitivity of cement-based materials. The test consists of casting a ring of concrete around an inner steel ring, which provides a uniform restriction to the concrete contraction when it is exposed to drying. The restriction to movement results in the development of compressive strain in the steel ring when the concrete ring shrinks.

The steel ring is generally equipped with strain gauges for monitoring the strain variation as the concrete specimen shrinks against it. A sudden decrease in one or more of the strain gauges indicates the concrete specimen has cracked. Moreover, by continuously monitoring the strain development in the steel ring, it is possible to calculate a corresponding stress and, from mechanical equilibrium considerations, the average stress in the concrete ring [2, 68, 75, 76]. Thus, the ring test is not intended to only measure the time to cracking but also to provide comparative *restrained* shrinkage data on mixtures.

The ring test method is well established for evaluating the shrinkage cracking sensitivity of ordinary cast concrete [68, 75-77], but its use to assess shrinkage cracking of shotcrete has hardly been studied. The reader must understand that shotcrete is distinctly different from cast concrete due to its unique mix designs, placement techniques, compaction dynamics, strength gain mechanisms, and internal structure [78]. The shotcrete process is complex in many aspects as the final in-place quality relies upon the

interaction of a chain of phenomena (such as the nozzle manipulation, air flow, material flow, shooting consistency, rebound, etc.) during spraying. Thus, our conventional understanding of the shrinkage cracking behaviour of cast concrete under restrained conditions can be applied to shotcrete only with caution. For the proper evaluation of cracking potential of shotcrete, the specific material proportions and properties and, most importantly, the *placement technique* needs to be considered [67].

The orientation of the ring test mould, in particular, must be taken into consideration due to material rebound (i.e. particles ricocheting off the target during spraying). Rebound particles, if entrapped into the fresh shotcrete, can create defects that would negatively influence the ring test results [67]. The shotcrete techniques also make spraying a shotcrete ring specimen difficult because of the geometry and the limited available space in the ring mould. This makes the AASHTO ring test setup more preferable to the ASTM C1581 ring test setup because it offers more room to accommodate the shotcrete spray, thus enabling easier achievement of homogeneity inside the specimen [67]. For this reason, an earlier study was conducted at the Laval University Shotcrete Laboratory (Quebec City, Canada) to adapt the AASHTO ring test for *sprayed* concrete focused primarily on the interpretation of data.

This paper presents a data analysis method on the basis of average stress and stress rate at cracking for shotcrete in accordance with the AASHTO T334-08 procedure [4]. A simple approach based on the mechanical equilibrium between the inner steel ring and the outer concrete ring was implemented for determining the average stress developed in the concrete. Many approaches [2, 65, 75, 76] have been proposed for estimating the maximum stress development in the thick concrete ring. A common simplifying assumption in these approaches is the applicability of the theory of elasticity to concrete, which is, in fact, a viscoelastic material. The approach proposed in this study is independent of the elastic or viscoelastic nature of the material.

Additionally, a data analysis method on the basis of stress rate at cracking ring has been developed for the thick AASHTO ring in this study. It should be noted that a similar solution has been recently proposed for thin ASTM ring [77]. However, the proposed analysis is inadequate for thick concrete rings (as used in this study) which show different cracking behaviour compared to thin concrete rings. For example, specimens made with thicker AASHTO ring would take longer to crack compared to the thinner ASTM ring. Moreover, as previously stated, the AASHTO ring is preferable for shotcrete because it offers more room to accommodate the shotcrete spray.

It should be emphasized that the size (thickness, height) and drying configuration (exposed surface(s)) of a ring test specimen significantly influence the drying process and, thereby, the resulting shrinkage and cracking behaviour. Nevertheless, only few studies (such as ref. [38]) have examined the influence of boundary conditions on cracking of mortars using '*non-standardized*' thick ring specimens. In the present study, the AASHTO T 334-08 [4] ring procedure was used to appraise the influence of the boundary conditions (i.e. drying direction) and the exchange surface to volume ratio (S_e/V) on shrinkage and the

52

associated cracking of thick AASHTO ring specimens. The findings are expected to provide guidance towards the implementation of a suitable drying method for shotcrete ring tests to ensure cracking would occur in a reasonable amount of time.

It is expected that the experimental investigations presented here will help to better understand the cracking behaviour of shotcrete. The ring test procedure recently developed for *sprayed* concrete [67] is increasingly being adopted or used extensively by the shotcrete industry to assess the cracking behaviour of shotcrete mix designs. The data analysis methods presented here will help to better interpret the data thus obtained from the ring test procedure recently developed for *sprayed* concrete [67]. Overall, the present study is part of ongoing research on the durability of concrete and shotcrete mixtures and is aimed at better characterizing the drying shrinkage cracking potential of shotcrete, through improved interpretation of the ring test results. The AASHTO T 334-08 ring procedure was modified to quantify both the restrained and free shrinkage behaviour of shotcrete mixtures.

4.3.1 Research Significance

The *restrained shrinkage ring test* is the most widespread test for characterizing the shrinkage cracking potential of concrete. The paper indicates how it can be used to *quantify* stress development in concrete undergoing restrained shrinkage. The paper provides useful information on the influence of drying direction (boundary conditions) upon stress development and age at cracking in the restrained ring specimen. An analytical equation based on mechanical equilibrium is presented for estimating the average stress developing in the concrete ring. Additionally, the influence of water to cement ratio (w/cm) and exchange surface to volume ratio is discussed. This study is of interest to engineers and materials specifiers in view of better assessing and/or predicting the drying shrinkage sensitivity of concrete.

4.4 Experimental Program

To obtain a better understanding of the restrained shrinkage phenomenon in concrete and the influence of boundary conditions on shrinkage and stress development, free and restrained shrinkage tests were conducted. Series of test specimens were cast using the same prepackaged repair concrete mixture with nominal maximum aggregate size of 10 mm, prepared with different water to cement (w/cm) ratios (0.42, 0.45 and 0.60) intended to cover fairly well the range from moderate to high water content mixtures. Except for the 0.60 w/cm mixture, a naphthalene-based superplasticizer was used to reach the desired workability, with a slump in the range of 100 to 140 mm. The effective concrete mixture proportions used are provided in Table 4.1. Note that for the 0.42 w/cm mixture only restrained ring tests were performed to validate the proposed model and extend the interpretation of the restrained ring tests.

The implemented test procedures are described in the following sections.

Table 4.1 Concrete mixtures investigated

w/cm	OPC cement (kg/m^3)	2.5-10 mm crushed limestone (kg/m^3)	0.08-5 mm natural sand (kg/m^3)	Water (kg/m^3)
0.42	451	746	1068	186
0.45	445	736	1054	197
0.60	417	689	988	247

4.4.1 Mechanical Characterization

Compressive strength, splitting tensile strength and modulus of elasticity were determined in accordance with ASTM C39, C496, and C469 test methods respectively. Twenty-one 100×200 mm cylinders were prepared for each of the three investigated concrete mixtures to carry out mechanical characterization tests. Sets of four cylinders were tested in compression at 3, 7, and 28 days to determine the modulus of elasticity, while sets of three cylinders were used to determine splitting tensile strength at 3, 7, and 28 days.

4.4.2 Restrained Shrinkage

The research work reported herein is part of a project intended to better understand and prevent cracking of shotcrete. Although a ring test procedure was developed especially for *sprayed* concrete in recent years [67], this paper focuses primarily on the interpretation of data, by assessing the early age cracking potential of wet-mix shotcrete mixtures cast conventionally in accordance with the AASHTO T334-08 procedure [4] (*formerly AASHTO PP 34-99* [5]). As illustrated schematically in Fig. 4.1, the inner diameter of the concrete ring is 305 mm, its outer diameter is 457 mm (thickness of 76 mm), and its height is 152 mm. The restraining inner steel ring has the same height as that of the concrete, but the inner diameter and outer diameters of 280 mm and 305 mm respectively (thickness of 12.7 mm).

The degree of restraint with this particular geometry is of the order of 53 to 60 %, depending on the actual modulus of elasticity and creep of concrete (based on an analytical formula proposed by Moon et al., [68]). In comparison, the degree of restraint for the ASTM ring setup is higher (about 70 to 75 %) because of its smaller concrete wall thickness. During the experiment, compressive strain develops in the inner steel ring as the outer concrete ring dries and shrinks against it. Four resistive strain gauges installed on the interior face of the steel ring at mid-height, equidistant from each other, allows real-time monitoring of the deformation and, ultimately, detection of the cracking occurrence.

For each mixture, experiments were conducted for two different moist curing periods, 3 and 7 days respectively. In each case, two separate test batches were prepared to provide a stronger basis for the conclusions to be drawn. At least four concrete ring specimens were cast per mixture in each of the replicate batches. On each occasion, the rings were divided into two, representing the two drying configurations investigated. After casting, the specimens were covered with wet burlap and plastic sheets and left in their mould for the first 24 hours. The exterior wall of the mould was removed after 24 hours, and the specimens

were further moist cured for either 2 or 6 more days. The burlaps were wetted every day during the curing periods to ensure proper curing.

After curing, the specimens were sealed with adhesive aluminum tape in such a way that they could dry either along their *radial* direction - also referred to as "*circumferential drying*", or along their *axial* direction – also referred to as "*top and bottom drying*" from the side faces. The two investigated drying configurations are shown in Fig. 4.2. The specimens were exposed to drying at 21 ± 2 °C and 50 ± 4 % R.H. until cracking occurred in all specimens of the set. In this study, strain monitoring began immediately after placement. Thus, all deformations occurring during the moist curing periods were recorded. The strain data were recorded at 5-minute intervals. The time at cracking can be detected quite precisely by a sudden sharp change in the strain gauge readings (usually greater than 30 microstrains).
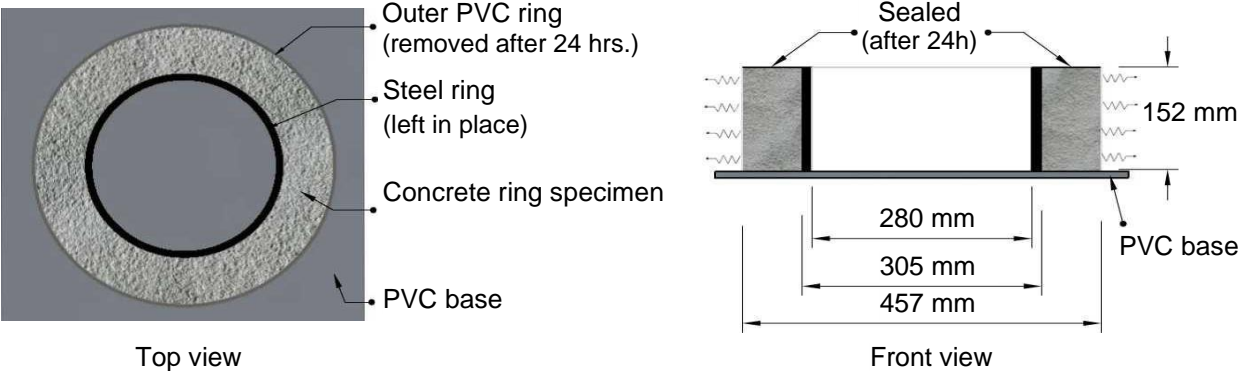
Fig. 4.1 Ring test setup used in the AASHTO T334-08 ring test
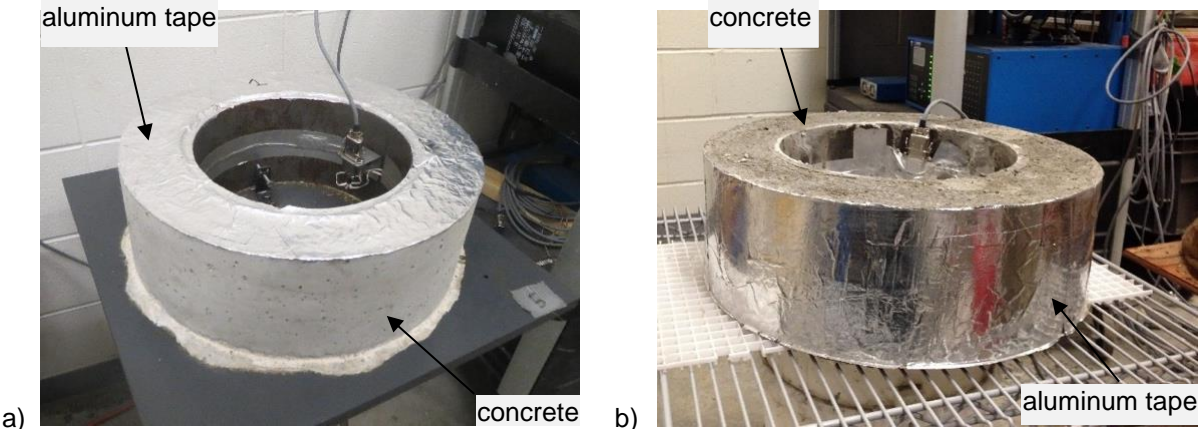
Fig. 4.2 AASHTO T334-08 ring test specimens sealed a) on top and bottom faces (i.e. *radial drying*), and b) on the outer circumferential face (i.e. *axial drying*)

4.4.3 Free Shrinkage

The AASHTO T 334-08 method comes without provisions or means for comparing restrained and free shrinkage. For free drying shrinkage measurements, ring specimens identical in size to the AASTHO rings were cast, but with the inner steel ring replaced with a core made of a very low stiffness material with respect to that of concrete. The objective was to measure *free shrinkage* on specimens having the same geometry, size and exposed surface to volume ratio such that they undergo the same drying conditions as the restrained rings. In the free ring test, the concrete specimen is not restrained and hence can shrink *"freely"*. DEMEC gauges are installed on top of the free ring specimens for length change measurements (4 chord lengths distributed over the circumference).

For each set of AASHTO ring specimens (0.45 and 0.60 w/cm mixtures), the same number of free companion rings was cast in accordance with the same protocol, except for the inner steel ring, replaced with an expanded polystyrene (EPS) core (very low stiffness). The detailed method is described elsewhere [57]. The free ring specimens underwent the curing and drying regimens described in the previous section. Free shrinkage measurements were taken regularly throughout the AASHTO ring monitoring period, from the time of demolding ($\pm$ 24 hours).

4.5 Analysis of Restrained ring Shrinkage Test

In the restrained ring test, the strain measured in the steel ring can be used to estimate the tensile stress that develops in the concrete ring [2, 68, 75]. In general, the stress distribution is analyzed based on the assumption of a frictionless relative movement between the two rings, with the steel ring being subjected to an external pressure P_s and the concrete ring being subjected to a reciprocal internal pressure P_c, as shown in Fig. 4.3 (typical for specimens drying from the radial direction). See *et al.* [77] proposed expressions that are applicable to thin concrete rings. The approach is based on the classical approach of thin-walled cylinders and is derived from an equilibrium calculation of the same kind as that considered in this study.

For thick-walled concrete rings, Weiss and co-workers [65, 75, 76] proposed a general expression for determining the maximum residual tensile stress that develops at the interface and Mojabi-Sangnier [2] proposed a similar solution for determining the average tensile stress. A common simplifying assumption in both approaches is the applicability of the theory of elasticity to concrete, which is, in fact, a viscoelastic material. Moreover, it was found by Moon and Weiss [68] that these equations were only suitable for uniform drying along the radial direction.

In this paper, a simplified approach based on the mechanical equilibrium between the steel and concrete rings for determining the *average* stress development in thick concrete ring specimens is proposed. In this approach, the theory of elasticity is applied to steel ring. Since steel behaves elastically in the ring test, the average forces in the steel ring due to the pressure at the interface can be determined based on the elastic

theory. By equilibrium of forces, the resulting force in the concrete ring must equal that calculated in the steel ring. The solution is valid independent of the nature of the material (elastic or viscoelastic).

(a)

pressure on steel ring   pressure on concrete ring

drying from axial direction   drying from radial direction

(b)   (c)
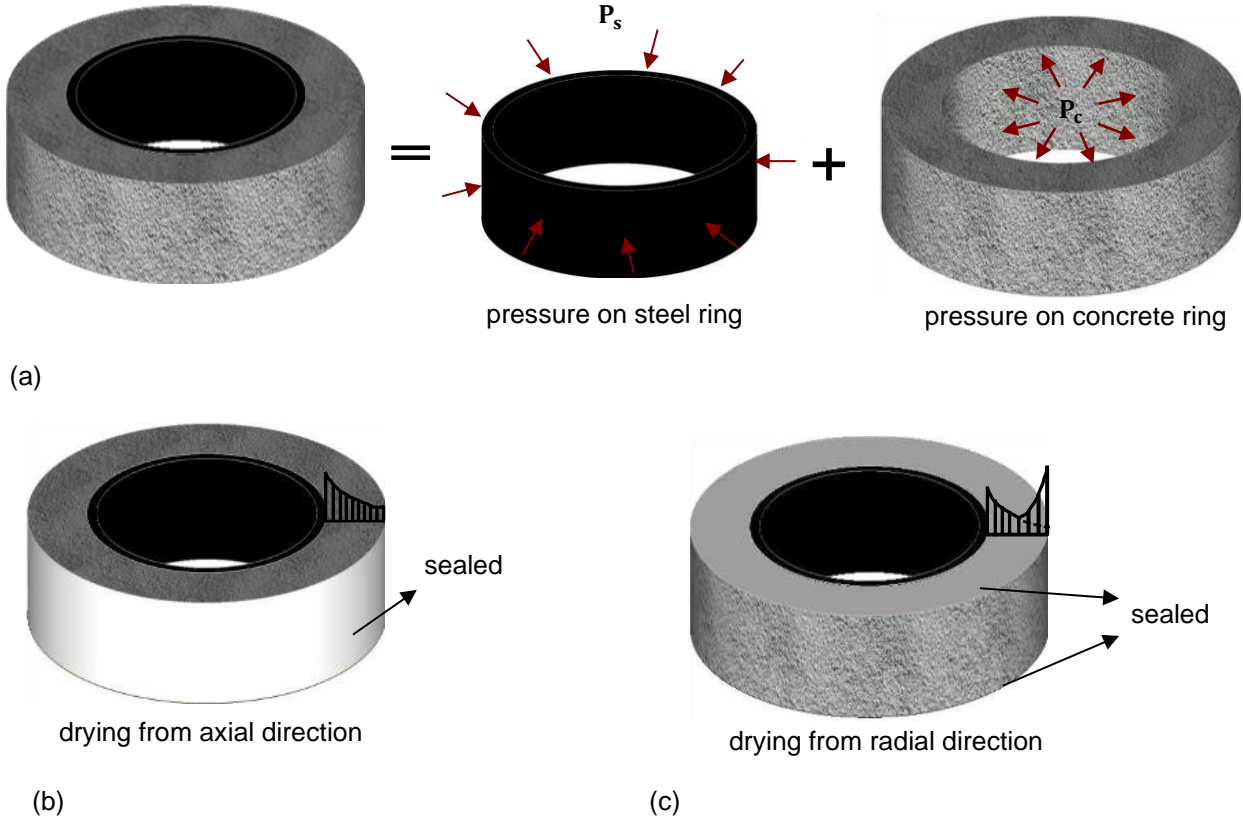
Fig. 4.3 Schematical illustration of (a) contact pressure acting in the steel ring and the concrete ring, (b) stress profile when drying from axial direction, and (c) stress profile when drying from radial direction

4.5.1 Determination of Average Tensile Stress

Mechanical equilibrium requires that irrespective of the drying conditions imposed on the concrete ring specimen, as contact pressure builds up at the interface between the two rings, the resulting internal forces in the inner and outer rings balance out, as shown in Fig. 4.4. The overall equilibrium can simply be described as follows:

$$F_s + F_c = 0 \Rightarrow F_s = -F_c \tag{4.1}$$

where, F_s and F_c are the internal resulting forces induced in the steel and concrete rings, respectively. Irrespective of the fact that the contact pressure may vary across the width of the rings, the relationship between the average stresses in the steel and concrete ring can thus be described as follows:

$$F_s = -F_c \Rightarrow \sigma_{s_{avg}}(t)\, A_s = -\sigma_{c_{avg}}(t)\, A_c \tag{4.2}$$

where, $\sigma_{s_{avg}}$, $\sigma_{c_{avg}}$ are the average stresses at a time, t, in the steel ring and concrete ring, respectively, while A_s, and A_c are the corresponding cross-sectional areas.

fc   fc

$F_c = 2*f_c \mid F_s = 2*f_s$

fs   fs
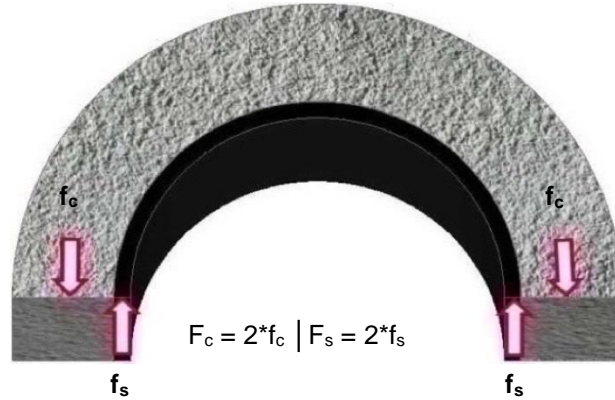
Fig. 4.4 Schematical illustration of the internal forces developing in the rings

From the classical thick-walled cylinder solution, the elastic stress distribution in the steel ring (as shown Fig. 4.3) at a radius is obtained as follows:

$$\sigma_s(r) = -\,{}^1\!/_{r^2} \cdot \left(\left[\, R_{os}{}^2 (r^2 + R_{is}{}^2)\right]/(R_{os}{}^2 - R_{is}{}^2)\right) \cdot P_s \tag{4.3}$$

where P_s is the external pressure exerted on the steel ring, r is the radial distance, R_{is} is the inner steel ring radius, and R_{os} is the outer steel ring radius. The strain in the steel ring can then be obtained as:

$$\varepsilon_s(r) = \delta_s(r)/r \tag{4.4}$$

where δ_s is the displacement of the outer surface of the steel ring which can be calculated as follows:

$$\delta_s(r) = -\,{}^1\!/_{E_s} \cdot \left[R_{os}{}^2 / r(R_{os}{}^2 - R_{is}{}^2)\right] \cdot \left[(r^2 + R_{is}{}^2) + v_s(r^2 - R_{is}{}^2)\right] \cdot P_s \tag{4.5}$$

where E_s is the modulus of elasticity of the steel [200 GPa (29 ×10^6 psi)], v_s is the Poisson's ratio of steel ring (≈ 0.30). Combining Eqs. (4.4) and (4.5), the strain in the steel ring can be determined with the following expression:

$$\varepsilon_s(r) = -\,{}^1\!/_{E_s} \cdot \left[R_{os}{}^2 / r^2(R_{os}{}^2 - R_{is}{}^2)\right] \cdot \left[(r^2 + R_{is}{}^2) + v_s(r^2 - R_{is}{}^2)\right] \cdot P_s \tag{4.6}$$

The strain measured on the inner face of the steel ring at any time can then be obtained as follows:

$$\varepsilon_s(t)|_{r=R_{is}} = \varepsilon_s(t) = -\,2/E_s \cdot \left[R_{os}{}^2 / (R_{os}{}^2 - R_{is}{}^2)\right] \cdot P_s \tag{4.7}$$

Combining Eqs. (4.3) and (4.7), to remove P_s, the elastic stress distribution in the steel ring can be obtained from the following expression:

$$\sigma_s(r) = {}^1\!/_2 . E_s . \varepsilon_s(t) . \left[(r^2 + R_{is}{}^2)/r^2\right] \tag{4.8}$$

The average steel ring elastic stress can then be determined by integrating $\sigma_s(r)$ over the thickness of the concrete section:

$$\sigma_{s_{avg}}(r) = \int_{r=R_{is}}^{r=R_{os}} \sigma_s(r)dr / \int_{r=R_{is}}^{r=R_{os}} dr = {}^1\!/_2 . E_s . \varepsilon_s(t) . \left(\left[r - (R_{is}{}^2/r)\right]_{R_{is}}^{R_{os}} / [r]_{R_{is}}^{R_{os}} \right) \tag{4.9}$$

The average stress in the steel at any given time t can be determined with the following expression:

$$\sigma_{s_{avg}}(t) = {}^1\!/_2 . E_s . \varepsilon_s(t) . \left[(R_{os} + R_{is})/R_{os}\right] \tag{4.10}$$

Considering Eqs. (4.2) and (4.10), the average tensile stress in the concrete ring is obtained as follows:

$$\sigma_{c_{avg}}(t) = - {}^1\!/_2 . {}^{A_s}\!/_{A_c} . E_s . \varepsilon_s(t) . \left[(R_{os} + R_{is})/R_{os}\right] \tag{4.11}$$

The geometrical and material properties are constant for a given ring setup, hence the tensile stress induced in the concrete ring can simply be written as:

$$\sigma_{c_{avg}}(t) = - G . \varepsilon_s(t) \tag{4.12}$$

where G is a constant for the ring setup and is obtained as follows:

$$G = \left[(R_{os} + R_{is})/2R_{os}\right] . (A_s E_s / A_c) \tag{4.13}$$

For the ring setup used in this study G= 31.6 GPa (4.58 ×10^{6} psi). The G here is synonymous with the term G derived by See *et al.* [77] for stress rate analysis in a thin ring specimen.

4.5.2 Determination of Stress at Cracking

Although the cracking age and the average tensile stress analysis are an interesting benchmark, analyzing ring test results can be further extended by developing a practical method for evaluating the test results based on the *stress rate*. The stress rate proposed in this study for thick rings is based on a similar analysis carried out by See *et al.* [77] for thin concrete rings. It should be noted that the average tensile stress analysis does not directly use the moisture gradient for calculating the stress developments. Although attempts have been made in the past to consider the stress induced by the moisture gradient [68], a direct application of the suggested solution in reference [68] is not as straightforward since it is difficult to validate and calibrate the parameters needed for the procedure. The stress rate method is thus a more practical approach to quantifying the cracking potential of mixtures. Indeed, a recent study has shown that the

average residual stress at cracking considering moisture gradient is inversely proportional to the square root of time-to-cracking [79].

For small changes in t, the stress rate after initiation of drying in the ring can be expressed as:

$$S(t) = d\sigma_{c_{avg}}(t)/dt = G|(d\varepsilon_s/dt)| \qquad (4.14)$$

where $d\varepsilon_s/dt$ is the net steel strain rate at time t. Attiogbe *et al.* [79] found that the steel strain (ε_s) is proportional to the square root of drying time up to the time to cracking. It can therefore be fitted using a linear regression as follows:

$$\varepsilon_s(t) = \alpha\sqrt{t} + c \qquad (4.15)$$

where α is the slope of the linear function, or the *strain rate* (μm/day$^{1/2}$), and c is a regression constant. Thus, from Eqs (4.14) and (4.15), the stress rate during drying is given by:

$$S(t) = G\,|\alpha|/2\sqrt{t} \qquad (4.16)$$

The stress rate at cracking for each test mixture is determined from Eq (4.16) by substituting the time to cracking, t_{cr}, in place of time, t. This stress rate will be used to complement the usual "*time to cracking*" used in analyzing the ring test data. It should be noted that Eq (4.16) is a general solution applicable to both thin and thick ring specimens, (where G=72.2 GPa (10.47 × 10^6 psi) for thin ring specimens [77, 79] while G= 31.55 GPa (4.58 ×10^6 psi) for ring specimens).

4.6 Test Results and Discussion

4.6.1 Mechanical Properties

The compressive strength (f_c), splitting tensile strength (f_{st}), and modulus of elasticity (E_c) tests performed at 3, 7, and 28 days for the w/cm of 0.45 and 0.60 mixtures are presented in Table 4.2. Each mechanical property test data reported is the average of three test specimens. The results show that strength is a function of the w/cm ratio, as expected. An increase in compressive strength with age was also noted. The tensile strength and modulus of elasticity values unsurprisingly follow the same trend as the compressive strength.

Table 4.2 *Compressive strength, tensile strength, and modulus of elasticity data*

Time after casting, days	0.45			0.60		
	f_c, MPa	f_{st},	E_c, GPa	f_c, MPa	f_{st}, MPa	E_c,
3	26.9	2.5	25.8	25.5	2.4	25.4
7	30.6	2.8	26.8	27.8	2.5	26.3
28	37.5	3.4	30.0	33.4	2.7	28.8

4.6.2 Free Shrinkage of Concrete

The free drying shrinkage strains recorded for the 0.45 w/cm and 0.60 w/cm concrete mixtures are presented in Fig. 4.5. On each graph, the shrinkage as a function of time is shown for the two drying conditions (radial and axial drying) with the corresponding curing regimes investigated. Each data point is an average of values recorded for at least two companion ring specimens. As previously stated, only restrained shrinkage tests were performed with the 0.42 w/cm mixture to validate equation Eq. (4.12) develop in this study and to extend the interpretation of the restrained shrinkage ring test experiment. It is interesting to observe from Fig. 4.5 that the moist curing duration of concrete before exposure to drying influences the rate of drying shrinkage. It can be seen that prolonged moist curing results in an early reduction in drying shrinkage, which is found to somehow stabilize after some time.

It is further observed that prolonged moist curing had a slightly larger influence in concrete with a lower w/cm (0.45). The test results also indicate that drying shrinkage is slightly higher for specimens dried from the radial direction than for specimens dried from the axial direction. This is attributed to the slightly higher S_e/V when dried from the radial direction (0.0158 mm^{-1} *vs.* 0.0132 mm^{-1}). Overall, shrinkage occurs at a rapid rate in the days following the initiation of drying and, beyond a period of the order of 28 days, the rate of shrinkage decreases quite significantly.
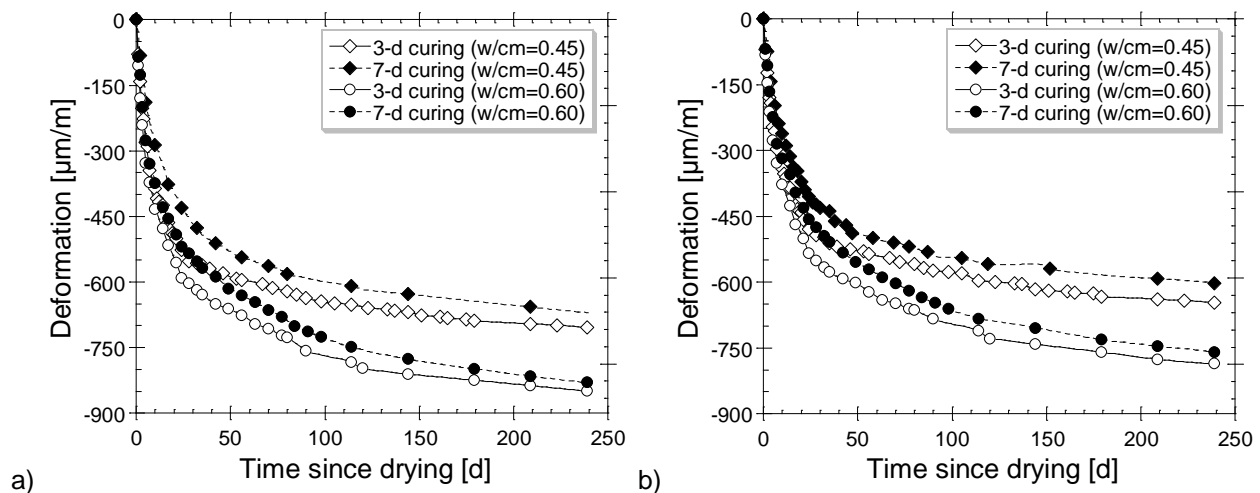
Fig. 4.5 Free shrinkage test results from companion ring specimens subjected to a) radial drying; b) axial drying

The free drying shrinkage rate factor of the 0.45 w/cm and 0.60 w/cm concrete mixtures were evaluated using equation Eq. (4.15), where the steel strain (ε_s) has been replaced with , (free shrinkage strain). The strain rate values determined for the 0.45 and 0.60 w/cm mixtures are presented in Fig. 4.6. Overall, the test results show that the strain rate increases with the S_e/V ratio. Indeed, this has to be expected since

drying is strongly influenced by the surface area where the exchanges take place [37, 38]. The impact of a longer curing period is found to be more pronounced as the w/cm decreases. Irrespective of the specimen drying configuration, extending the moist curing period from 3 to 7 days did not affect the strain rate of the 0.60 w/cm mixture. On the contrary, for the 0.45 w/cm mixture, extending the moist curing period resulted in a significantly lower strain rate factor.

a) Radial drying   b) Axial drying
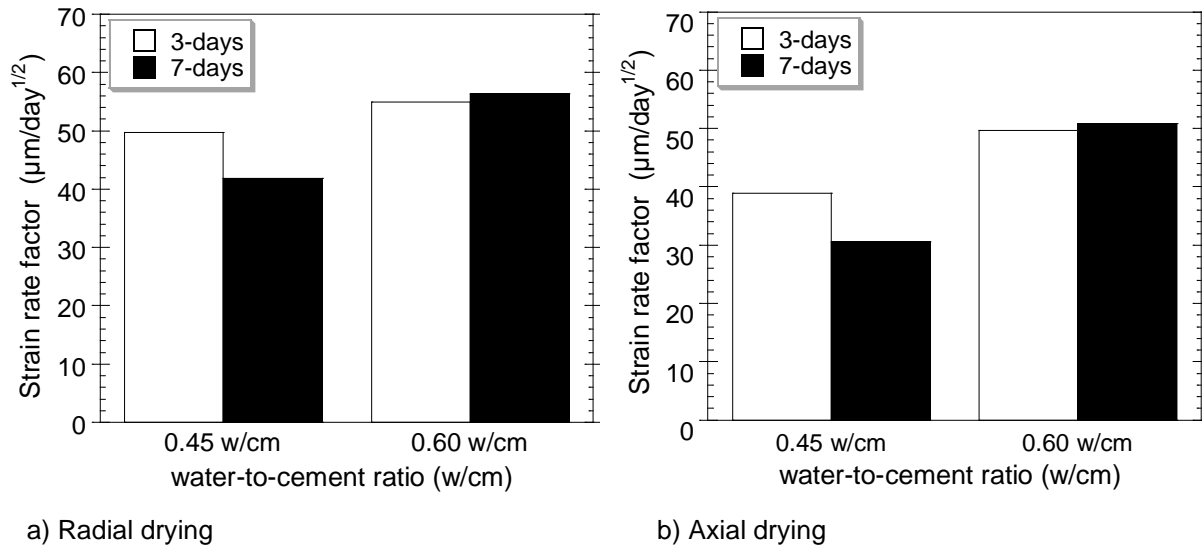
Fig. 4.6 Free shrinkage test results from companion ring specimens – strain rate factors

4.6.3 Cracking of Restrained Concrete

Typical results of the evolution of the average tensile stress developing in the restrained concrete specimen, as estimated based on the data from the strain gauges located on the inner face of the steel ring and Eq. (4.12), are shown in Fig. 4.7. The graph shows the shrinkage induced stress curves of three ring test specimens made from the same batch of the 0.42 w/cm concrete mixture and drying from the radial direction. The age at cracking refers to the age at which cracking initiates in the ring specimen. Overall, the results in Fig. 4.7 show that immediately upon exposure to drying, concrete starts shrinking, inducing in the steel ring a compressive stress that increases at a decreasing rate until failure, at which time a sudden change is recorded from the strain gauges and a visible crack has developed in the restrained ring specimens.

Thus, stress development in the ring specimen ultimately results in cracking of the restrained specimen. It can be observed from the experimental results in Fig. 4.7 that specimens cast from the same batch (and stored in the same environmental conditions) do not necessarily crack at the same time. This phenomenon is quite usual in restrained ring tests [74]. This can be partly attributed to the intrinsic concrete variability

which is influenced by a number of factors, notably the heterogeneous character of concrete and the placement process.

Indeed, the properties of concrete (particularly strength, elastic modulus, and tensile creep) are inherently characterized by some spatial variability, but the properties are not random as such. In general, the stress induced in the ring increases progressively, getting closer to the tensile strength. Failure will, therefore, occur at the location of a defect or weakness, thereby explaining the potentially significant differences in time to cracking between individual specimens. Nevertheless, it can be seen that the actual maximum recorded stress values are close at the age of cracking in the ring specimen.
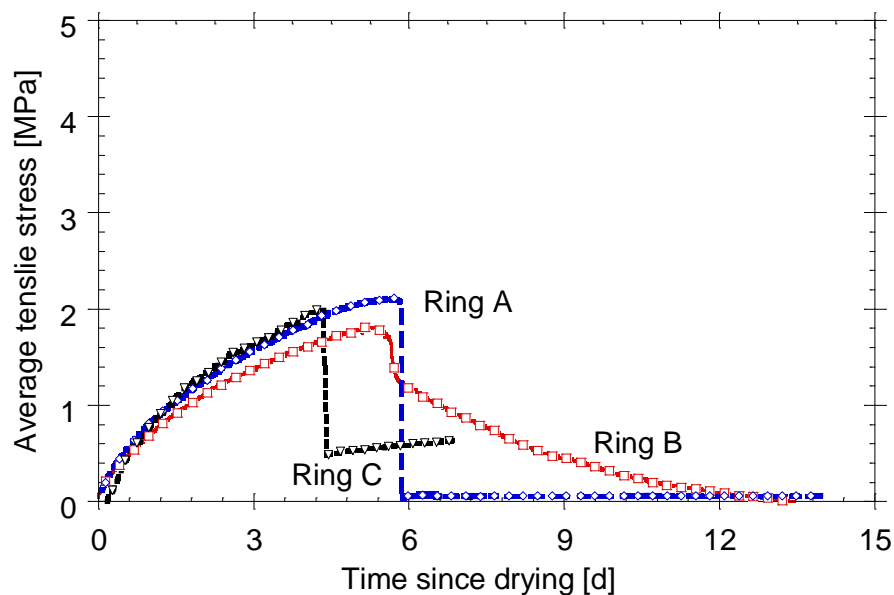
Fig. 4.7 AASHTO T334 restrained shrinkage test results – 0.42 w/cm mixture

4.6.4 Influence of boundary conditions on the age of cracking

There has been some debate over the years regarding the drying conditions in ring tests designed for evaluating the restrained shrinkage behaviour of cementitious materials. In the program reported herein, the influence of the drying direction was studied. The ring specimens were sealed in such a way to undergo one directional drying, either axially or radially. Each of these conditions implies a certain S_e/V ratio, which necessarily influences the drying process and, in turn, the shrinkage and self-stress rates. The results obtained in both drying conditions are summarized in Fig. 4.8 for the 0.45 w/cm and 0.60 w/cm concrete mixtures. On each graph, the average stress as a function of drying time is shown. Each data point is the average of values recorded on at least two test specimens. Overall, a sudden drop in the steel ring

compressive strain was recorded in all tests, except for the 0.45 w/cm specimens drying from the axial direction and cured for 7 days where a gradual loss of strain was encountered instead.

As expected, the results show that the drying direction has a significant influence on the age of cracking in the ring specimen. It was observed that the rate of drying is more rapid in specimens where the moisture exchange occurs in the radial direction in comparison to those exposed axially, for both the 0.45 and 0.60 w/cm concrete mixtures. Furthermore, a larger variation in time to cracking was observed when ring specimens are drying along the axial direction. Also, the test specimens drying from the radial direction cracked at an earlier age (*8 to 14 days*) than the specimens dried from the axial direction surfaces (*39 to 95 days*). A comparison of the age at which crack is detected by a sudden drop in the strain gauge is shown in Fig. 4.9 for the two boundary conditions studied.

The more severe consequences observed in specimens dried from the radial direction can be attributed, at least in part, to the coupled effects of a higher S_e/V and more unfavourable drying gradients. It is well known that shrinkage is highly sensitive to the exchange surface to volume ratio [37, 38, 57, 80]. Therefore, the slightly higher S_e/V of specimens drying along the radial direction implies that they will obviously shrink at a more rapid rate and therefore are likely to crack at an earlier age when concrete has a lower tensile strength. In specimens drying along the axial direction, the rate of moisture loss is slower, and it takes a longer time to reach a comparable magnitude of shrinkage. This allows for further strength gain and relaxation due to creep, overall resulting in an extended time to cracking.

The effect of S_e/V upon drying reflects the fact that drying does not occur uniformly inside the material, obeying to highly non-linear transport processes (diffusion driven). The non-uniform drying results in moisture gradients and, thereby, in differential shrinkage strains over the cross-section of the concrete specimen. In turn, because of the non-linearity of the strain profile, internal stresses are induced (self-restraint). In particular, areas where drying and shrinkage occur first, i.e. next to the exchange surfaces, can thus be subjected to important tensile stresses, as a significant portion of the free contraction is restrained by the inner part of the element, which has not undergone significant drying yet. Hence, non-linear drying shrinkage causes *per se* the development of an internal restraint (or self-restraint) and the resulting stresses add up to those caused by external restraints.

The two drying conditions investigated in the present study, referred to as radial and axial, thus result in transient moisture distributions, shrinkage gradients and stress profiles that are quite different. In the case of axial drying, the transient moisture profile is uniform along the radial direction and non-uniform along the axial direction. For radial drying, it is exactly the opposite. As a consequence, the self-restraining effect is more pronounced in the radial drying layout. Considering the steel ring restrained is constant for the ring setup, it can be argued that in the ring specimens drying from the radial direction, shrinkage cracking is mainly due to self-restraint.
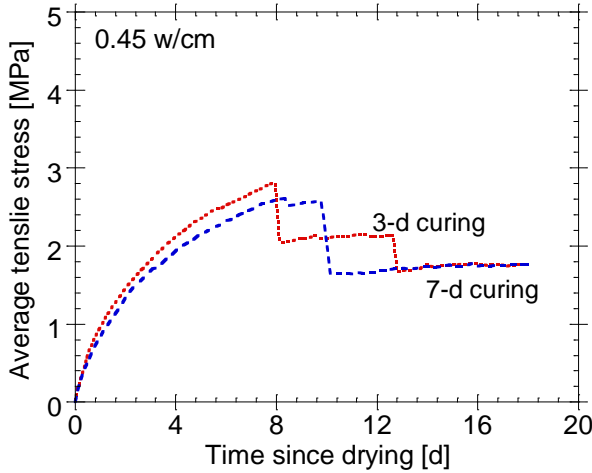
a) 0.45 w/cm mixture – radial drying
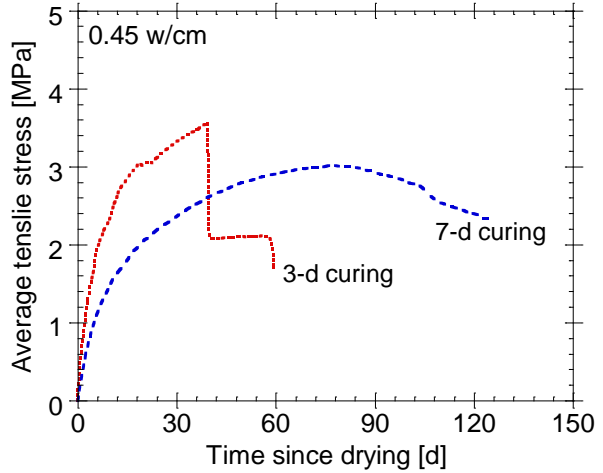
b) 0.45 w/cm mixture – axial drying
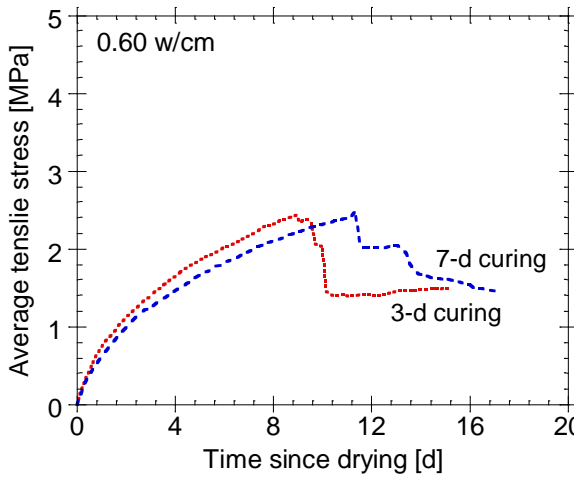
c) 0.60 w/cm mixture – radial drying
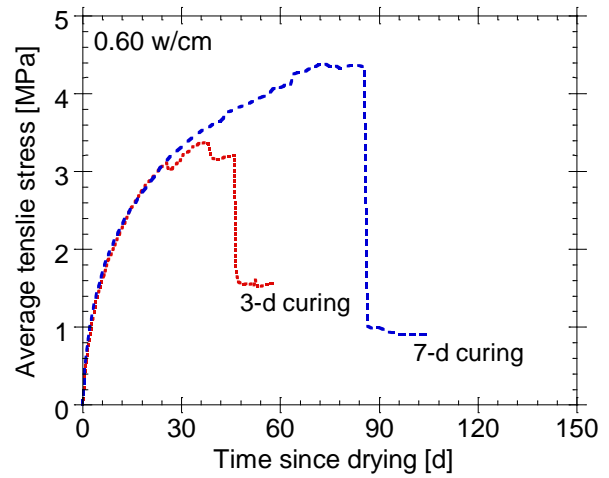
d) 0.60 w/cm mixture – axial drying

Fig. 4.8 AASHTO T334 ring test results – influence of drying conditions
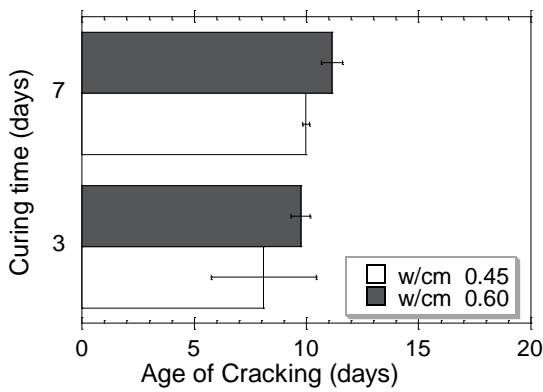
a) Radial drying
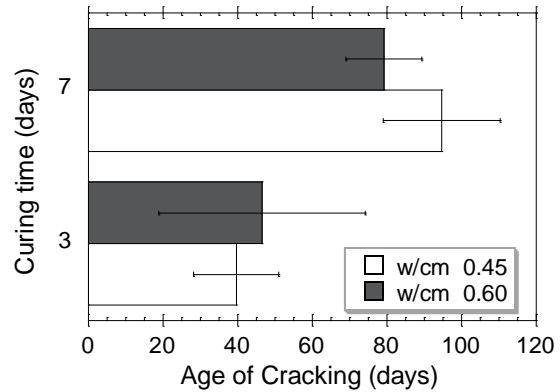
b) Axial drying

Fig. 4.9 Age at (visible) cracking of restrained ring specimens

4.6.5 Effect of Strain rate and Stress Rate on the Age of Cracking

Test results in Figs. 4.8 and 4.9 show that cracking occurs earlier when drying from the radial direction, regardless of the w/cm ratio. This behaviour is primarily due to the higher stress rate which is directly dependent on the shrinkage rate. In fact, by comparing in Fig. 4.8 and Fig. 4.10, it can be seen that higher strain rates actually lead to a shorter time to cracking in both tested mixtures. It can be noticed in Fig. 4.8 that in specimens dried along the radial direction, cracking occurred at a systematically lower average stress than in specimens dried along the axial direction. As already stated, it also occurred much earlier, at a moment when the magnitude of the free shrinkage was much lower. It appears that the risk of cracking depends more on the shrinkage rate than on the actual magnitude of shrinkage. Similar observations were reported by Wei and Hansen [52] and Attiogbe *et al.*, [79].

It is believed that high shrinkage rates induce tensile stresses early in the life of the material, too rapidly to yield enough relaxation and avoid the low early age strength to be overcome. Besides, the presumably more pronounced shrinkage gradients in the radial drying configuration result in larger self-restraint stresses (and thus larger stress concentrations), which can also explain to some extent why failure occurs earlier, under lower average stress. Further analysis of the relationship between cracking age and the corresponding stress rate reveals a strong correlation between stress rate and the cracking occurrence, with higher stress rates leading to a shorter time to cracking. The result in Fig. 4.10(b) indicates a strong power law relationship between the age of cracking and stress rate, with a coefficient of determination (R^2) of 0.94.

The results agree well with the findings from earlier investigations [74, 77, 79, 81] that the higher the stress rate, the shorter the time it takes to crack under restrained shrinkage. In the present study, it can be seen that higher stress rates are recorded in the radial drying layout compared to the axial drying layout. Consequently, the specimen drying along the radial direction cracked much earlier than the companion specimen dried from the axial side. This is somewhat in view of the fact that the lower stress rate allows for stresses to be relaxed over a longer period of time and to develop further strength. Overall, the stress rate approach was found to better quantify the stress of the concrete and thus provides a more fundamental way of evaluating the cracking potential of mixtures in the ring test experiment.

Also, a comparison of the results presented herein with data available in the literature [74, 77] suggests that the AASHTO ring test yields lower stress rates than those recorded with the ASTM C1581 ring test [53], which can essentially be attributed to the lower effective degree of restraint and lower S_e/V in the test setup of the former. Thus, the stress rate limits established in past studies [53, 77] for a performance classification of thin-walled ASTM rings as shown in Table 4.3 is not appropriate for thick AASHTO rings. Similar four performance zones, albeit slightly different stress rate limits identified for the AASHTO ring setup used in this study, are shown in Table 4.3. This table can be used to evaluate the relative cracking performance of materials when using the AASHTO ring test.

a) Strain rate factor (steel ring deformation)   b) Stress rate vs. time to cracking
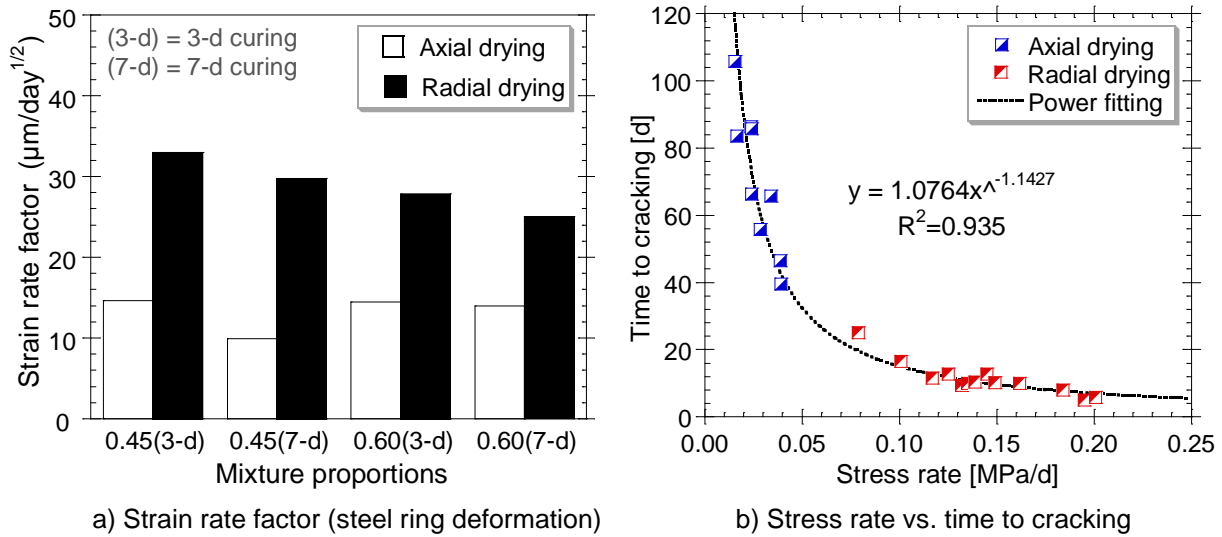
Fig. 4.10 AASHTO T334 ring test results – strain and stress rates

Table 4.3 Suggested cracking potential classification (Based on stress rate at cracking)

Net Time-to-Cracking, t_{cr}, (days)	ASTM Stress Rate, S, (MPa/day) [53]	Suggested Stress Rate, S, (MPa/day) [a]	Potential for Cracking Classification
$0 < t_{cr} \leq 7$	$S \geq 0.34$	$S \geq 0.17$	High
$7 < t_{cr} \leq 14$	$0.17 \leq S \leq 0.34$	$0.11 \leq S \leq 0.17$	Moderate-High
$14 < t_{cr} \leq 28$	$0.10 \leq S \leq 0.17$	$0.05 \leq S \leq 0.11$	Moderate-Low
$t_{cr} > 28$	$S < 0.10$	$S < 0.05$	Low

[a] suggested values for the AASHTO ring setup

4.6.6 Effect of w/cm Ratio on the Age at Cracking

Test results in Figs. 4.7, 4.8 and 4.10 clearly show that early age cracking is more likely when the w/cm of the mixture is low. For example, shrinkage cracks occurred as early as 4 to 5 days for the mixture with the lowest w/cm ratio exposed to drying from the radial direction. This tendency, very well documented in the literature [38, 73, 82], is primarily due to the manifestation of autogenous shrinkage, which increases as the w/cm decreases. Autogenous shrinkage causes the early strain and stress rates to increase, thereby increasing the potential to the shrinkage cracking in low w/cm mixtures, due to the lower tensile strength and strain capacity at an early age.

4.6.7 Crack Initiation and Pattern of Ring Specimen

Typical visible cracks that develop in restrained ring specimens drying from the radial and axial direction are shown in Fig. 4.11 (0.45 w/cm mixture). Crack growth and width were monitored by visual inspection at time intervals of not more than 2 weeks after crack initiation. It could be assessed by visual

inspection/survey that in specimens dried along the radial direction (Fig. 4.11a), cracking initiated from the outer circumference and then propagated inside the ring, while in the case of specimens dried along the axial direction (Fig. 4.11b), cracking occurred at the inner circumference and propagated towards the outer edge in the rings. Using acoustic emission to monitor crack initiation and propagation, Hossain and Weiss observed the same trend [38].

As already discussed, the higher shrinkage gradients seemingly occurring in the axial drying configuration generates larger self-restraint stresses. As a result, the maximum stress occurs at the outer face of the ring specimen, where moisture loss occurs. In this study, somewhat larger cracks were observed in specimens dried from the radial direction than in those dried from the axial direction. The average crack width for the 0.45 w/cm specimens drying along the axial direction was about 0.18 mm, while that of specimens dried along the radial direction was approximately 0.35 mm. Similarly, the average width of the crack of the 0.60 w/cm specimen was approximately 0.13 mm and 0.29 mm in the axial and radial direction of drying, respectively.
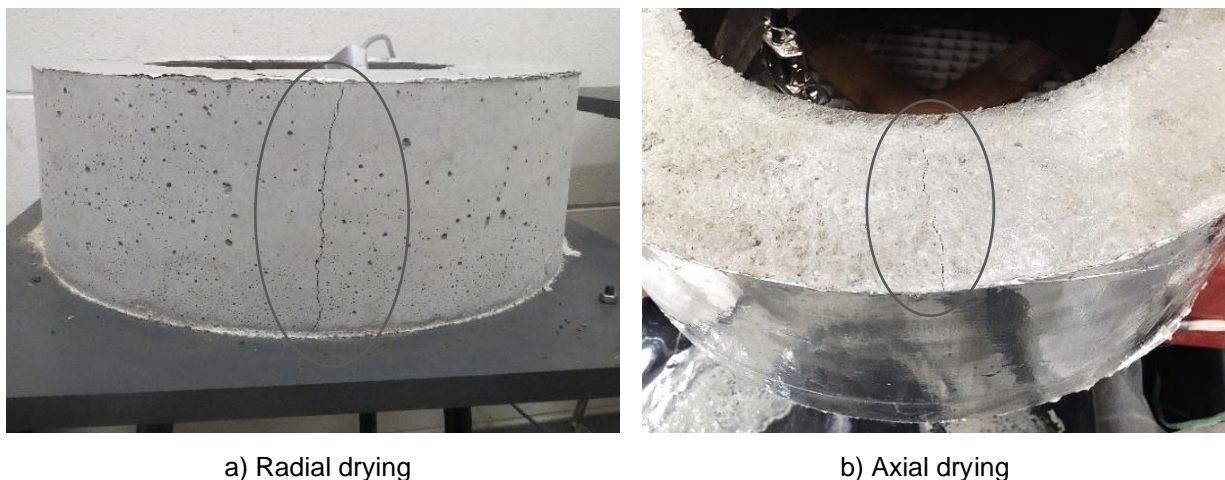
a) Radial drying   b) Axial drying
Fig. 4.11 Cracking observed in restrained ring specimen (0.45 w/cm mixture)

4.7 Summary

This research focused on the influence of drying conditions, S_e/V and moist curing on the stress development and age at cracking in the restrained shrinkage ring experiments. The study has shown that drying condition of the concrete ring specimen has a significant impact on the shrinkage and stress rates, and thus the cracking age.

It was found that the ring specimens allowed to dry along the radial direction experience higher stress rate than those allowed to dry along the axial direction. As a result, specimens drying from the radial direction were observed to be more prone to early-age cracking than to those drying from the axial direction. This

can be attributed to the fact that the specimens that dry from the radial direction has a higher exchange surface to volume ratio (S_e/V) and also experience less uniform drying which increases the stress rate.

It was also found that the risk for early age cracking increases as the w/cm of the mixture is reduced, due to the increasing contribution of autogenous shrinkage, which occurs as soon as hydration kicks in. Hence, in low w/cm materials, the self-desiccation must be considered in evaluating the risk for restrained shrinkage cracking. It has been observed that the risk for shrinkage cracking is more influenced by the *shrinkage rate* than the magnitude of shrinkage. To avoid or limit early cracking, it is, therefore, advisable to protect the surface of concrete in order to reduce shrinkage rate.

It was found that stress rate in the ring specimen can be a better way to evaluate the potential of shrinkage cracking of mixtures due to the intrinsic material variability of concrete, which may influence considerably the age at cracking. The results further show that proper moist curing can effectively delay cracking of a concrete element under restrained shrinkage conditions. Furthermore, it has been found that the gradual and prolonged evolution of stresses in the case of specimens drying from axial direction allows studying the behaviour of concrete mixtures over a longer period before cracking occurs. However, drying along the radial direction is recommended for faster assessment of cracking potential of shotcrete, owing to the longer test duration when drying from the axial direction.

Finally, a comparison of the free shrinkage and the corresponding strain measured in the restraining steel ring for both mixtures show that free shrinkage does not necessarily provide a reliable indication regarding the actual restrained shrinkage cracking potential of concrete. In conclusion, it should be mentioned that the study is still ongoing to quantify the influence of other important parameters on shrinkage cracking, such as the degree of restraint, the self-induced stress profile due to differential shrinkage (i.e. self-restraint), and the curing method.

4.8 Acknowledgments

Chapter 5 *Article 3* - The Role of Curing Methods in Early Age Moisture Loss and Drying Shrinkage

Bruce MENU, Thomas Jacob VAILLANCOURT, Marc JOLIN, and Benoît BISSONNETTE

Department of Civil and Water Engineering, Université Laval, Quebec City, QC, Canada G1V 0A6

5.1 Résumé

Cet article s'intéresse à l'importance des méthodes de cure, en particulier les durées de cure humides sur la migration de l'humidité et le retrait du béton. L'objectif est de fournir de l'information sur les bonnes pratiques de cure du béton afin de contribuer à l'élaboration de guides pratiques pour les applications des bétons projetés. Une cure appropriée est importante pour que le béton atteigne une résistance suffisante pour résister à la fissuration due au retrait.

5.2 Abstract

The experimental program reported in this paper seeked to evaluate the efficiency of a range of curing methods in view of minimizing the evaporation rate at the surface of freshly placed shotcrete and preventing the detrimental consequences of early-age shrinkage. The CSA-A23.1-14 states that severe drying conditions should be considered to exist when the surface moisture evaporation rate exceeds $0.50\ kg/m^2/h$ (0.1 lb/ft²/h). In fact, the environmental conditions that lead to such evaporation rates are regularly experienced on construction sites, requiring that adequate protection of the concrete surface be carried out in a timely manner after placement. The research effort aimed at quantifying the influence of selected curing methods upon the early-age moisture loss and resulting shrinkage. The results show that early-age volume change of freshly sprayed shotcrete can be significantly reduced by adequate surface protection. Amongst the investigated methods, moist curing is found to be the most effective.

Keywords: curing; cracking; drying; evaporation; moisture loss; shotcrete; shrinkage; surface protection

5.3 Introduction

Cement-based materials may undergo significant early-age shrinkage as a result of a decrease in relative humidity inside their porosity. It is a major concern, as the tensile strength of the material is still very low, making it vulnerable to the internal stresses induced by the volume changes [22, 60]. Many factors affect the shrinkage of concrete, notably the exposure conditions, the aggregate nature and size, the cement content, the water to binder ratio, and the curing conditions [36, 83]. Shotcrete (or sprayed concretes) mixtures, in particular, are prone to shrinkage since they are generally designed with smaller-size aggregates (10-12 mm [⅜-½ in.]), higher cement contents and also often include set accelerators. One main advantage of shotcrete is the capacity to cover large surfaces without the use of formwork. However, in field conditions, this often translates into areas of unprotected fresh concrete that may result in hasty surface water evaporation.

Surface drying of freshly sprayed concrete leads to differential shrinkage through the relatively thin concrete layers, which can lead to cracking. The most common solution to reduce early-age volume changes and the associated cracking is to minimize or delay drying by enforcing proper curing procedures after placement [22, 60]. In practice, curing is often being considered as one of the most important consideration for controlling or delaying shrinkage, and ultimately counteracting the risk of early-age cracking. Curing is particularly important for shotcrete applications, because the mixtures often contain silica fume and fly ash, which tends to make them more prone to early-age shrinkage. It is generally recommended to start curing immediately after placement under favourable moisture and temperature conditions.

Curing must be carried out to provide sufficient water not only to minimize the impact of self-desiccation, but also to promote binder hydration and yield the expected properties of the concrete [84]. The choice of an appropriate curing regime will depend on the type of concrete and on the conditions in which concrete will be placed and cured [85]. The current paper focuses on the effectiveness of a range of curing methods for preventing early water evaporation and the subsequent shrinkage in freshly applied shotcrete. This study is part of an on-going research program devoted to the improvement of shotcrete durability, especially with respect to its sensitivity to cracking.

5.3.1 Research Significance

Shrinkage is the cause of significant distress and high repairs and maintenance costs in many concrete structures. The need for mitigating shrinkage is therefore real and cannot be overstated. Many studies have investigated mitigation strategies, but the effect of curing methods upon early-age shrinkage in shotcrete has hardly been addressed yet. For successful shotcreting works, curing operations are essential to ensure the desired performance is achieved and the specific project needs are satisfied. The findings of this study are expected to provide guidance towards the implementation of suitable curing methods which prevent or at least minimize shrinkage cracking in shotcrete.

5.4 Experimental Program

A range of curing methods most commonly used in the field for concrete and shotcrete, namely *air (or dry) curing*, *sealed curing*, *application of a curing compound*, and *moist curing* (with wet burlap and polyethylene sheet), was selected for investigation.

In the *air curing* series, the most extreme case investigated, the test specimens were left untouched in open air and cured at room temperature for 24 hours. The specimens were then demoulded and exposed to drying in a conditioning room at 23 ± 1.7 °C (73 ± 3 °F) and a relative humidity (R.H.) of 50 ± 4 %.

In the case of *sealed curing*, immediately after spraying, the specimens were sealed in the moulds with three layers of plastic wrap. They were demolded after 24 hours and completely sealed again on all faces, using double layers of adhesive aluminum foil, for the remainder of testing in order to prevent drying. After sealing, the specimens were stored in the same conditioning room as the other test series. Under such sealed-curing conditions, no moisture exchange is in principle possible, leading to self-desiccation and, consequently, autogenous shrinkage.

Regarding the *curing compound* series, right after the finishing operation, the specimens were treated on their top face with a thin layer of water-based acrylic polymer curing compound using an atomizer, at a rate of 5 m^2/L (200 ft^2/gallon) and left in the mould for approximately 24 hours. Immediately after demolding, the specimens were coated over all the other faces and then exposed to drying in the conditioning room.

For *moist-curing*, durations of 1, 3 and 7 days were investigated. All specimens were wrapped in wet burlap and plastic sheets after finishing for 24 hours. After demolding, the 1-day cured specimens were immediately exposed to drying, while the 3-days and 7-days moist-cured specimens were covered with wet burlaps and plastic sheets for additional periods of 2 and 6 days, respectively. At the end of their curing regime, all test specimens were stored in the conditioning room (23 ± 1.7 °C [73.4 ± 3 °F]) and 50 ± 4 % R.H.).

5.4.1 Shotcrete Mixtures

A certified pre-blended and pre-bagged dry-mix shotcrete base mixture containing 10 % silica fume and a nominal maximum aggregate size was 10 mm (⅜ in.) was used in the study. The aggregate size distribution met the ACI 506 Gradation No. 2 requirements. The shotcrete operations were conducted as prescribed in the ACI 506 Guide to Shotcrete for the equipment, air velocity, and projection techniques. The two investigated water-to-cementitious materials (w/cm) ratios (0.31 and 0.42) are considered to cover fairly well the range from low to normal water content for dry-mix shotcrete. The lowest w/cm (0.31) mixture was shot dryer than the so-called "wettest stable consistency" [86], which is often recommended for dry-mix shotcrete placements. The highest w/cm (0.42) mixture, however, was shot at its "wettest stable consistency" (thus the consistency at which the water content is the maximum to ensure adequate rebar

encapsulation and to minimize rebound of material from the receiving surface). The test program was carried out entirely at Laval University's shotcrete laboratory.

5.4.2 Free Shrinkage and Weight Loss Measurements

To investigate the influence of curing on early-age drying, length change experiments were carried out using 75×75×285 mm (3×3×11¼ in.) prismatic specimens prepared by means of shotcreting (i.e. spraying). The specimens were tested in accordance with ASTM C157, except that the curing methods, including the moist curing period was modified. The specimens were tested monitored for both length change and weight change. At least eighteen prismatic specimens were shotcreted for each investigated mixture. The test specimen preparation and testing layout are shown in Fig. 5.1. Within the first 15 minutes after shotcreting, all prisms were finished with a wood float, in accordance with ACI CP-10 recommendations. Care was taken to ensure that the specimens were never allowed to dry (except for dry-curing prisms). After finishing, the specimens were divided into four main groups representing the different curing methods regimes consisting of *dry curing*, *sealed curing*, *curing compound*, and *moist curing*.

The specimens intended for moist curing were further divided into three subgroups that underwent curing durations of 1, 3, and 7 d respectively. The specimens were cured in the mould using their respective curing methods for the first 24 hours at an ambient temperature of 23 °C (73.4 ± 3 °F). The specimens were then demoulded and DEMEC gauges were installed on two opposite side faces of the specimens for length change measurements (Fig. 5.1b). Immediately after installation of the DEMEC gauges, zero readings were taken. With the exception of the specimens cured for 1 day, curing of the specimens continued for the intended period, depending on the curing method. The specimens were then exposed to drying under standard conditions of 23 ± 1.7 °C (73.4 ± 3 °F) and 50 ± 4 % R.H. The drying condition was identical for all tested specimens. The length change and mass loss of the specimens were measured at regular time intervals, up to 28 days.

a)   b)
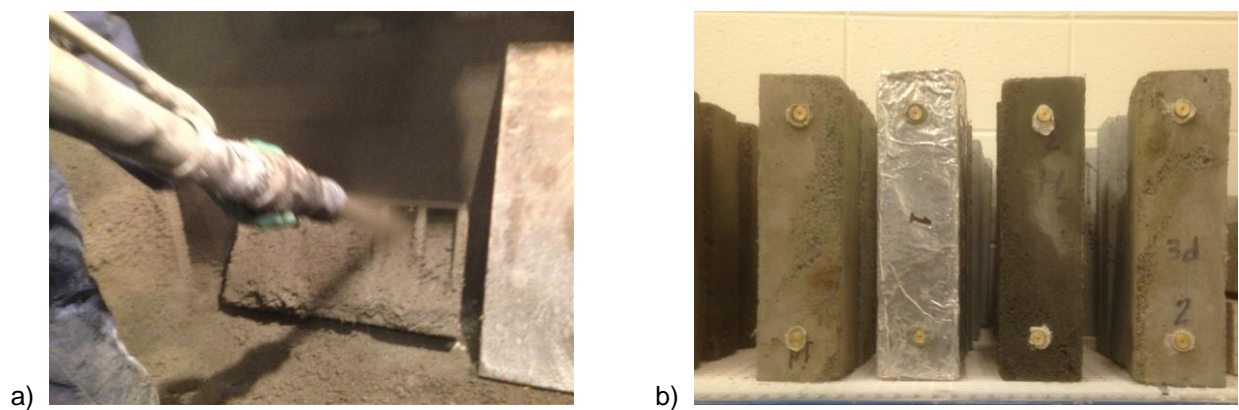
Fig. 5.1 Shrinkage test specimens: a) spraying process; b) testing layout

5.4.3 Characterization of Test Specimens

Other properties such as absorption, voids and compressive strength were evaluated on cores taken from a 300×400×100 mm (12×16×4 in.) slabs. Three test panels were shotcreted for specimen coring, as shown in Fig. 5.2. Cores were extracted from the test panels following the procedure recommended by ASTM C42. Three specimens were used to determine the 28-day compressive strength of the investigated mixture/curing combination. In each series, the specimens were stored in the 50 % R.H. conditioning room at the end of the given curing regime and then tested at the age of 28 days, in accordance with the ASTM C39. For comparison purposes, three cores were used to determine the compressive strength for specimens moist cured for 28 days.

Using the ASTM C642 procedure, the boiled water absorption (BWA) and volume of permeable voids (VPV) of both shotcrete mixtures were determined on sets of three cored samples. In addition, the ASTM C642 procedure standard test procedure was modified to evaluate the properties inside the "*skin*" of the concrete, i.e. the top 25-30 mm (1-1$\frac{1}{16}$ in.) layer [87], where the material characteristics are the most likely to be influenced by the curing medium, water, air or curing compound. In preparing the samples for the standard test procedure, the top of the cores is often removed. This mostly results in the "*skin*" not being taken into account. As part of the modified procedure followed in this study, two 10 mm (⅜ in.) thick slices sawcut from the finished end of the concrete cores were analyzed, slice A corresponding to the 0-10 mm (0-⅜ in.) layer and slice B to the 10-20 mm (⅜-¼ in.) layer. It is important to note that the property tests were not conducted for the 1-day moist curing test condition.

a)   b)
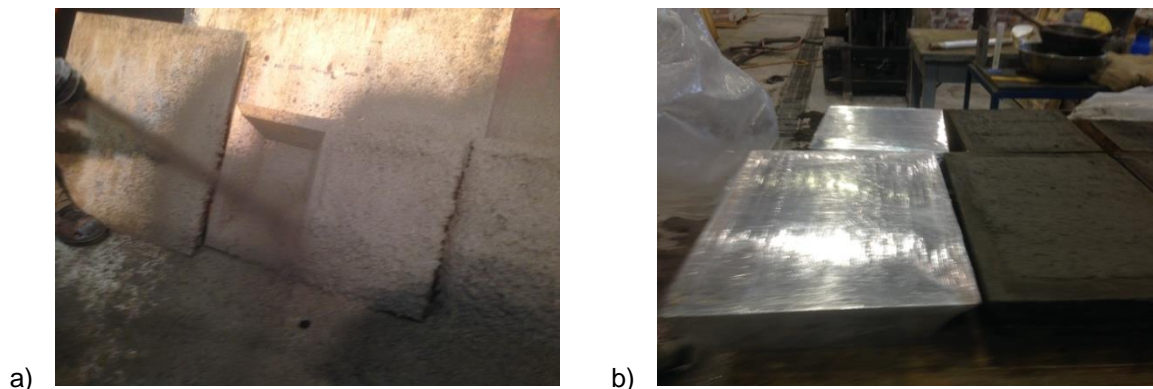
Fig. 5.2 Shotcrete test panels a) during shotcreting; b) subjected to air and sealed curing

5.5 Test results and discussion

5.5.1 Compressive strength

The 28-day compressive strength test results for the two tested mixtures are summarized in Table 5.1 for the different curing regimes. Each value represents the average result from three test specimens. Overall,

it is observed that strength development depends on the curing method used. For both mixtures, the moist-cured specimens reached the highest strengths, whereas the air-cured specimens had the lowest. This is consistent with the findings reported by Austin et al. [85]. In brief, the following conclusions can be drawn from the testing data: (1) lower w/cm mixtures reached higher compressive strength; (2) among the curing approaches investigate, moist curing produced the highest strength results; (3) increasing moist curing duration improves strength gain of concrete up to a certain age, beyond which a small reduction is recorded. These conclusions are in agreement with those reported by Nassif et al. [88].

The lower strength values obtained with the dry-cured specimens are most likely due to reduced hydration, as a result of the early moisture content reduction inside the porosity. Consequently, the concrete may not reach its full potential strength. On the contrary, moist curing ensures sufficient water is available to promote continued hydration leading to a finer pore structure, a lower pore volume and consequently the development of higher compressive strength. Note that while the use of a curing compound has little seemingly effect in a low w/cm concrete, its use can be beneficial in a mixture with a moderate w/cm. Also, the 28-d strength recorded for specimen moist cured for the entire period is found to be lower than that of specimens moist-cured for 7 days and exposed to drying thereafter, with differences of about 4 % for the 0.31 w/cm mixture and 11 % for the 0.42 w/cm mixture.

Table 5.1 28-day compressive strength test results

Curing method	w/cm = 0.31 mixture	w/cm = 0.42 mixture
	Compressive strength MPa (psi)	
Dry curing	41.1 (5961)	26.5 (3844)
Sealed curing	47.5 (6889)	31.4 (4554)
Curing compound	41.8 (6063)	31.2 (4525)
1-day moist curing	n/a	n/a
3-day moist curing	n/a	40.2 (5831)
7-day moist curing	50.0 (7252)	40.5 (5874)
28-day moist curing	48.1 (6976)	36.2 (5250)

5.5.2 Boiled Water Absorption (BWA) and Volume of Permeable Voids (VPV)

The standard and modified BWA test results from cores tested at 28 days are presented in Table 5.2. The test results of the 28-day standard and modified VPV test results are plotted in Figs 5.3 and 5.4. Each reported value is the average result of three specimens cored from the same test panel. Overall, the test results show a decrease of the BWA and VPV values as the w/cm ratio decreases. Clearly, it is evident in Table 5.2 that regardless of the curing method used, the specimens tested produced BWA values of less than 7 % in the 0.31 w/cm mixture, which is well within the acceptable range of 6 to 9 % set out in ACI 506R [9]. However, for the 0.42 w/cm mixture, only the values obtained with sealed curing, as well as 3-d and 7-d moist curing (about 9 %) fell within the acceptable range.

Similarly, the test results in Fig. 5.3 show that the standard VPV test values obtained for the 0.31 w/cm mixture were well within the acceptable range of 14 to 17 % found in ACI 506R [9]. Irrespective of the curing method used, the specimens from the 0.31 w/cm mixture has VPV values of the order of 14.8 %. On the contrary, none of the VPV values recorded for the 0.42 w/cm mixture are within the acceptable range; the dry-cured specimens and those treated with the curing compound had VPV values exceeding 22 %, while all moist curing regimes and sealed curing resulted in values of the order of 18 %.

VPV and BWA test procedures are widely used to evaluate shotcrete quality and durability. The quality indicators used are often based on the basic guidelines set out by Morgan et al. [89] for classifying the quality of in-place shotcrete. Analysis of the test results yielded in the present study shows that the quality of the in-place shotcrete shifts from good to fair and even marginal in some cases when the water content is increased from 0.31 to 0.42.

Regarding the modified BWA and VPV test results, the data from Table 5.2 and Fig. 5.4 show that the porosity of the "*skin*" of 0.31 w/cm mixture is more sensitive to curing than the core of the specimen. This has to be explained, at least in part, by the lower degree of hydration close to the surface of the 0.31 w/cm mixture which results in higher porosity. The data, however, vary more depending on the curing method for the 0.42 w/cm mixture. The BWA and VPV values of the "skin" were found to be more sensitive than the core in specimens sealed and moist cured. By contrast, the BWA and VPV values of the core were higher than the that of "*skin*" in specimens dry-cured and those treated with a curing compound. The only exception was the BWA of slice A samples submitted to 28-day moist curing which was higher than the standard value.

Overall, this sensitive of "*skin*" could be expected, as pointed out in the preceding discussion, since the "*skin*" is the boundary of the specimen where water can be gained or lost, or stand still, depending on the curing conditions. Consequently, the latter may considerably affect the top layer of concrete specimens compared to the core. In most cases, the first 10 mm (⅜ in.) layer (slice A) was slightly more porous than the second 10 mm (⅜ in.) layer (slice B), with a few exceptions.

Table 5.2 28-day boiled water absorption test results

Curing method	0.31 w/cm mixture			0.42 w/cm mixture		
	Standard	Slice A	Slice B	Standard	Slice A	Slice B
	Boiled water absorption (%)					
Dry curing	6.6	7.4	7.4	10.7	8.9	9.5
Sealed curing	6.8	7.5	7.2	8.9	9.9	9.6
Curing compound	6.8	7.5	7.3	10.7	10.0	9.8
1-d moist curing	n/a	n/a	n/a	n/a	n/a	n/a
3-d moist curing	n/a	n/a	n/a	8.7	10.0	9.0
7-d moist curing	6.7	6.9	7.3	8.9	9.8	9.7
28-d moist curing	6.9	7.3	7.7	9.8	8.5	10.4

a) 0.31 w/cm shotcrete mixture　　　b) 0.42 w/cm shotcrete mixture
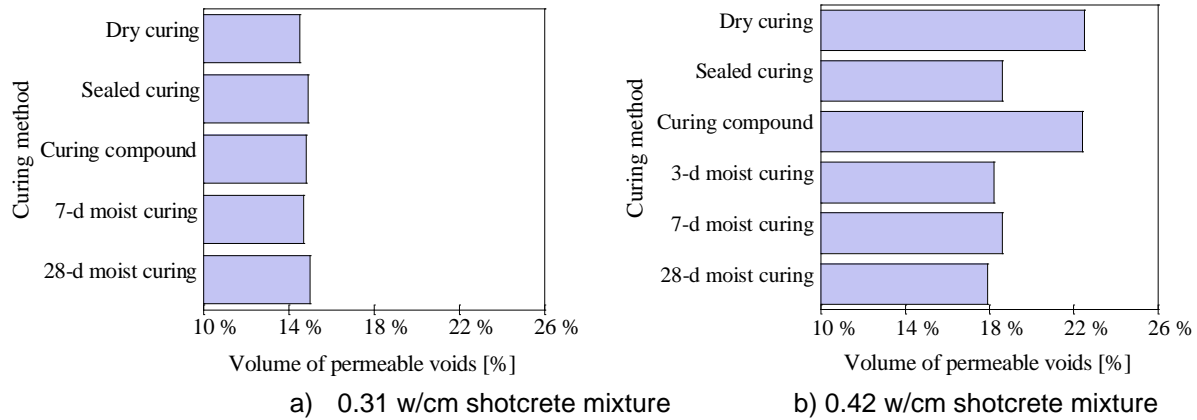
Fig. 5.3 ASTM C642 volume of permeable void results – standard VPV test

a) 0.31 w/cm shotcrete mixture　　　b) 0.42 w/cm shotcrete mixture
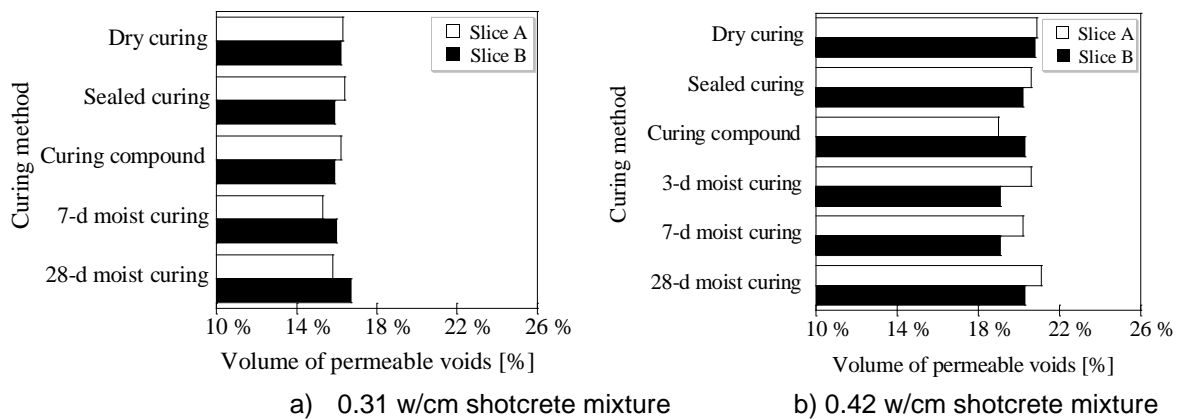
Fig. 5.4 ASTM C642 volume of permeable void results – modified VPV test for the two slices A and B

5.5.3 Shrinkage Test Results

The length change results obtained with the different curing methods investigated are presented in Fig. 5.5. On each graph, the *x*-axis is the time since the initial length change measurement, which took place in all cases at the age of 1 day. Each point on the graph is the average result from three specimens. A positive strain reading indicates swelling, which occurs as a result of water absorption during moist curing, while a negative strain reading indicates shrinkage due to drying. From the results in Fig. 5.5, it is obvious that among the investigated curing methods, sealed curing yielded the lowest shrinkage for both mixtures compared. This was expected since only self-desiccation contributes to the total shrinkage of completely sealed concrete. Also, the shrinkage of the completely sealed 0.31 w/cm mixture is higher than that of the 0.42 w/cm mixture, which is consistent with the fact that self-desiccation increases as the w/cm ratio decreases [22, 90].

After exposure to drying at the end of the various curing regimes, the total length change of the specimens was recorded to allow referencing the subsequent deformations to the beginning of the drying process in

each case. The data recorded for each curing is shown in Fig. 5.6. The *x*-axis corresponds to the time elapsed since drying, specific to each curing regime. In reality, separating the drying shrinkage and autogenous shrinkage deformations is not really possible.

It should first be noted that the total shrinkage deformations recorded for the 0.31 w/cm mixture are overall a little larger than those recorded for the 0.42 w/cm mixture in otherwise equal conditions. This has to be explained, at least in part, by the more significant contribution of autogenous shrinkage of the 0.31 w/cm mixture since autogenous shrinkage is higher when the w/cm ratio is low as previously stated. Conflicting results can be found in the literature in that regard, some consistent with the trend observed here [22, 88], others showing instead a very little influence of the w/cm ratio [36]. Another parameter that may play a significant role in the results obtained for the two shotcrete mixtures is the effective paste content, which can differ based on many factors, notably rebound [6], and cannot easily be determined.

Clearly, both Fig. 5.5 and Fig. 5.6 show that specimens continuously moist curing for 7 days exhibited the lowest shrinkage in both mixtures, followed by the 3-d moist curing. A longer moist curing also allows concrete to absorb free water, which delays the onset of drying shrinkage by replacing some of the pore water used by the hydration process. Hence, extending the moist curing period allows further development in concrete rigidity (larger elastic module, lower creep) and strength before significant drying occurs, which would enhance the capacity of the material to resist shrinkage deformations because the continuous capillary pore system through which water flows is reduced by the process of hydration [91]. Moreover, the resulting volume reduction and refinement in the pore structure, especially in the early days of hydration, leads to a reduction in the total amount of water loss and shrinkage [17]. It can actually be noted from the figures that an increase in moist curing duration from 1 day to 7 days quite significant decreased shrinkage. Based upon the data shown in Fig. 5.5 and 5.6, it can be argued that a longer curing period contributes to reducing the total shrinkage deformation undergone since the time of placement, as well as the contraction occurring from the time of drying.

At the other end of the spectrum of results, the series of specimens submitted to dry-curing and those treated with a curing compound exhibited much higher shrinkage, for both shotcrete mixtures. In fact, the reality is even worse, since in those two types of curing, significant drying occurs readily from the time of placement and the information could not be captured, the initial length and weight measurements occurring only after 24 hours. Hence, the actual difference between moist curing is significantly larger.

In comparison with the dry-curing regime, the investigated curing compound was found to be ineffective in the 0.31 w/cm mixture, while reducing very slightly shrinkage in the 0.42 w/cm mixture. The influence of the water-based acrylic polymer upon shrinkage of the two mixtures is consistent with the trends observed for compressive strength and the VPV determined in the surface layer (slice A). The shrinkage data also indicate a more significant influence of the curing compound used on the more porous concrete, but overall benefits appear to be limited. It should not be inferred from the results of the present study that using the

product at a higher rate would have yielded better results. It should also be emphasized that only one product was tested. Overall, the test results in Fig. 5.5 and Fig. 5.6 tend to show quite clearly that the curing conditions have a very significant effect on the desiccation shrinkage (both due to self-desiccation and drying) occurring in a thin concrete element.

a)   0.31 w/cm shotcrete mixture   b) 0.42 w/cm shotcrete mixture
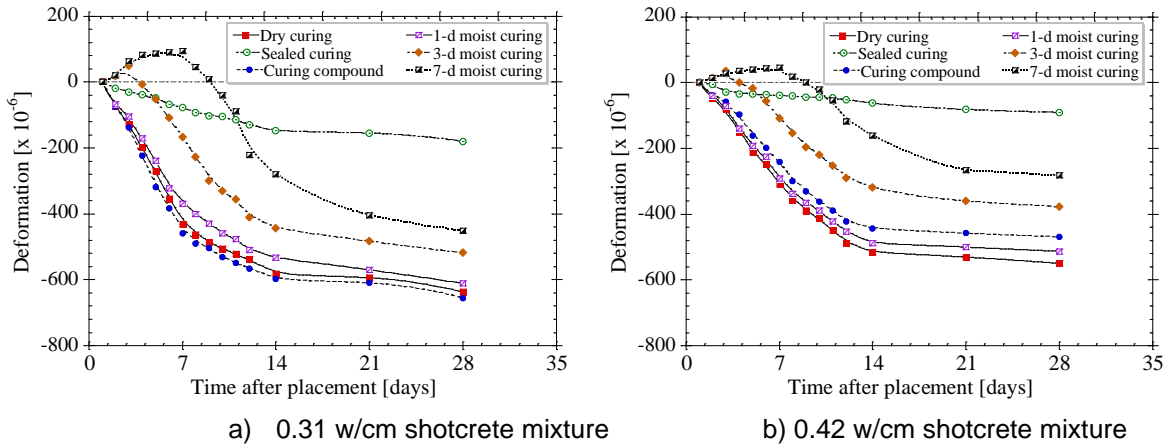
Fig. 5.5 ASTM C157 test results of the tested shotcrete mixtures submitted to different curing regimes

a)   0.31 w/cm shotcrete mixture   b) 0.42 w/cm shotcrete mixture
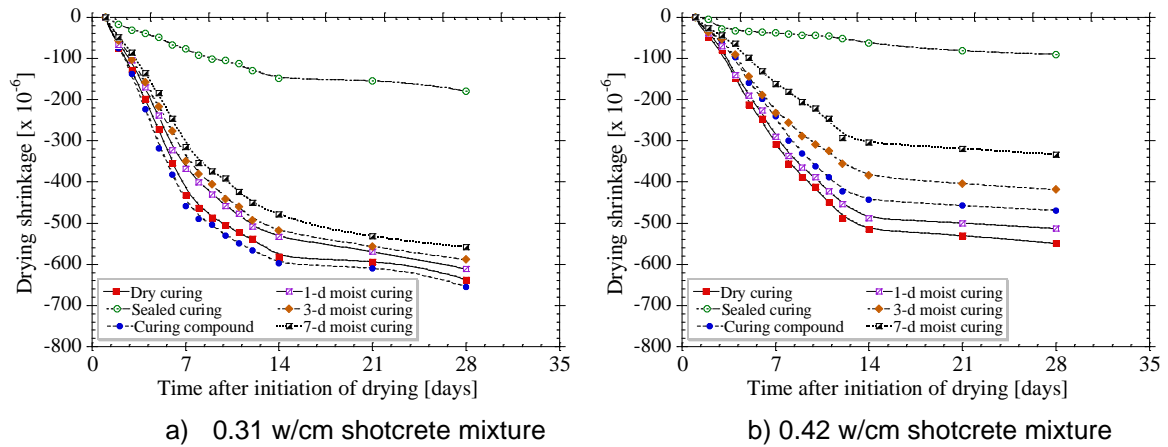
Fig. 5.6 Drying shrinkage of the tested concrete submitted to different curing regimes

Another possible approach to appraise the influence of the curing method upon drying shrinkage is to calculate the shrinkage rate [53] from the time concrete has been exposed to drying. The shrinkage strain rate factor is obtained by plotting the shrinkage deformation against the square root of elapsed time and then using linear regression analysis to fit a straight line through the data. The strain rate factor is the slope of the line:

$$\varepsilon_{dsh}(t) = \alpha\sqrt{t} + c \tag{5.1}$$

where ε_{dsh} is the free shrinkage ($\times 10^{-6}$), α is the strain rate factor ($\times 10^{-6}$/day$^{1/2}$), t is the time since drying (day) and c is a regression constant. The comparison of the drying shrinkage rates yielded with the different

curing regimes investigated is presented in the graph of Fig. 5.7, where the strain rate factor of the sealed specimens is also shown for comparison purposes. In the absence of significant drying, the sealed specimens exhibit much lower strain rate factors than that recorded with the other curing methods. The strain rate factor is observed to increases with the decreasing of w/cm ratio, essentially due to an increase in autogenous shrinkage as previously stated.

Besides, extending the moist curing period leads to a lower strain rate factor. The test results in Fig. 5.7 also confirm that the use of a curing compound provided some benefits over dry curing and 1-day moist curing for the 0.42 w/cm mixture. However, with the lower w/cm mixture, it can be seen that the strain rate experienced with dry-curing and curing compound is virtually the same. Again, curing compounds are apparently ineffective in low w/cm ratio concretes, which can be explained by the fact that it has no effect upon self-desiccation.
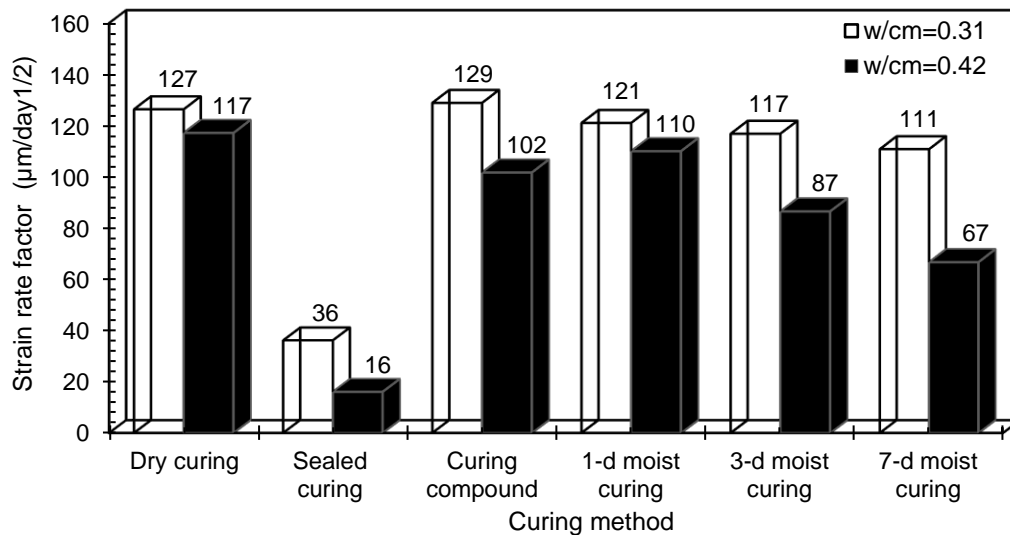
Fig. 5.7 Strain rate factors determined from ASTM C157 length change data of concrete submitted to different curing regimes, after the specimens were exposed to drying

5.5.4 Weight Change During Curing and Subsequent Drying

The weight change data recorded during the ASTM C157 experiments are presented in Fig. 5.8. The initial weight of the specimens was taken in all cases at the age of 1 day (i.e. 24 h of initial curing), right after demolding and taking the initial length reading. Here, a positive reading indicates a weight gain due to swelling during moist curing. Only moist cured specimens recorded weight gain. Overall, as intended, sealed specimens underwent practically no weight loss. Interestingly, the data in Fig. 5.8 shows that weight gain of the moist cured specimens is somewhat larger in the 0.31 w/cm mixture than in the 0.42 w/cm mixture. This may in part be attributed to the more important self-desiccation taking place in the lower w/cm mixture and, to some degree, the influence of the paste content raised previously in the discussion.

The data recorded from the time of drying for each curing is shown in Fig. 5.9. The *x*-axis corresponds to the time elapsed since drying, specific to each curing regime. Overall, the results do not show pronounced differences between the two shotcrete mixtures in terms of weight loss upon drying. Generally, the more mixing water is added to a concrete mixture, the more water is lost when exposed to drying since the resulting capillary pore volume and size both increased. In the present case, it could not be verified, but it may have been counteracted by a potentially larger effective paste fraction in the 0.31 w/cm shotcrete mixture.

At first sight, it can be readily observed that the moist cured specimens experienced higher weight loss when exposed to drying compared to those dry-cured or treated with a curing compound. Again, this can be explained to a large extent by the fact the mass loss taking place during the first 24 hours in the latter is not recorded, since the initial weight measurements are made at 24 hours and do not show in the graphs. In addition, part of the difference is related to the intake of free water absorbed during moist curing, which keeps the porosity closer to saturation until the drying process is initiated.

Besides, it can be seen that while all the 0.31 w/cm shotcrete mixture submitted to moist curing exhibit very similar weight loss curves, irrespective of the duration, the corresponding curves for the 0.42 w/cm mixture show instead of a decrease with extended moist curing. In a higher w/cm system at such an early age, it seems that prolonged moist curing benefits the hydration process more significantly, with less free water released thereafter during drying. For both shotcrete mixtures, the weight loss curves recorded from the dry-cured specimens and the specimens treated with curing compound are almost superimposed Fig. 5.8 and Fig. 5.9. If moisture loss is indicative of the performance of curing methods, it can be argued that the investigated curing compound is not much effective in creating a protective film to retain enough water inside the concrete porosity.

a) 0.31 w/cm shotcrete mixture   b) 0.42 w/cm shotcrete mixture
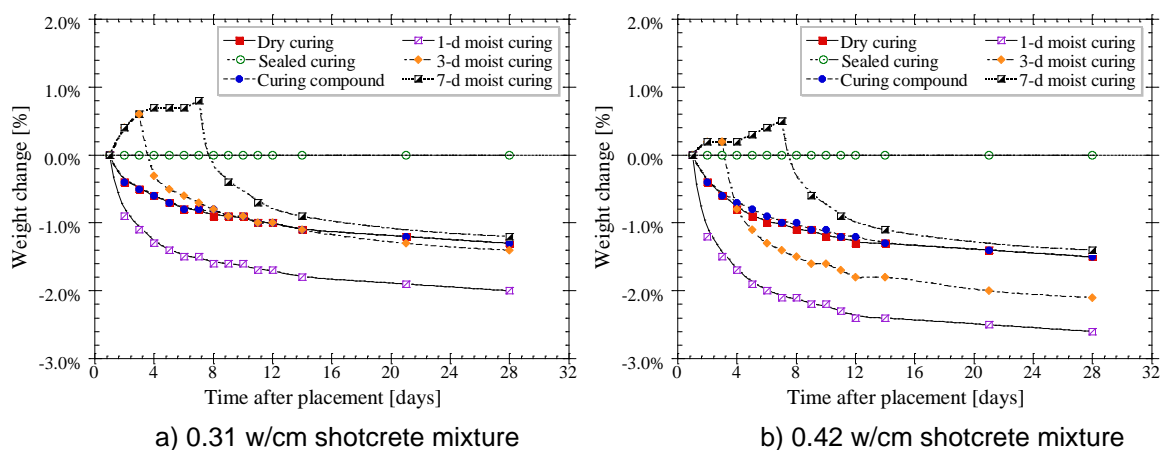
Fig. 5.8 Weight change of recorded in the ASTM C157 test specimens submitted to different curing regimes, from the time of demolding

a) 0.31 w/cm shotcrete mixture   b) 0.42 w/cm shotcrete mixture
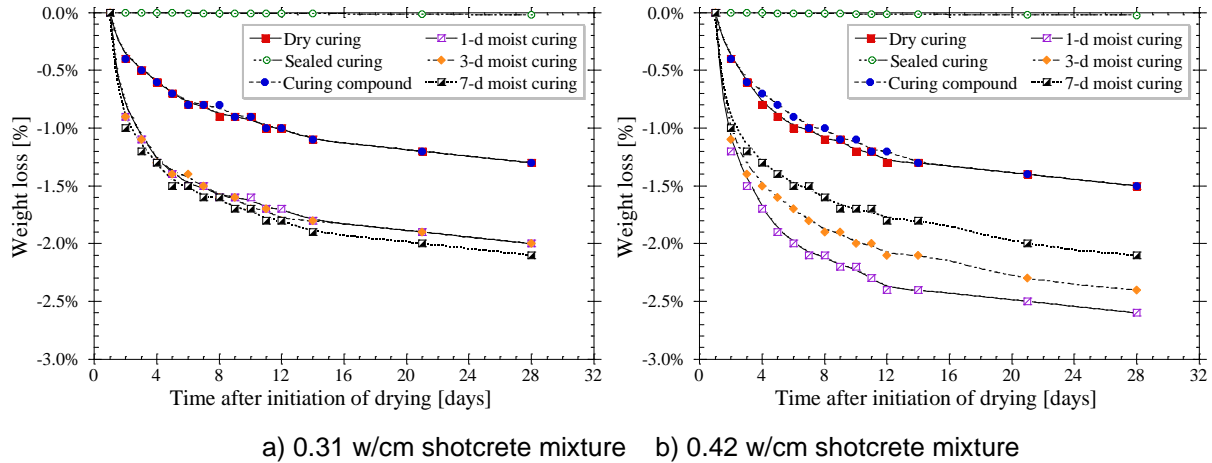
Fig. 5.9 Weight change of recorded in the ASTM C157 test specimens submitted to different curing regimes, from the time of drying

5.6 Conclusion

This research focused on the efficiency of selected curing methods in delaying weight loss and shrinkage in freshly placed shotcrete. The main findings can be summarized as follows:

1. Early-age surface protection significantly affects weight loss and volume changes of shotcrete.
2. Moist curing method is found to be the most effective amongst the range of curing methods investigated. Longer moist curing times produced higher compressive strength and lower shrinkage rates. Furthermore, specimen cured in air after 7 days of moist curing shows better strength than specimens continuously moist cured for 28 days.
3. Dry curing is found to be the least effective and most detrimental of all the curing methods, and should thus be avoided in all shotcreting works. It yielded the lowest compressive strength and fastest shrinkage rates.
4. The effectiveness of the water-based acrylic polymer curing compound is observed to be dependent on the w/cm ratio, being less efficient in low 0.31 w/cm ratio mixture, but beneficial in the 0.42 w/cm ratio concrete.
5. The "*skin*" of the low w/cm ratio concrete is found to be more sensitive to curing method than the moderate w/cm ratio mixture. This is explained, by the lower degree of hydration close to the surface of the 0.31 w/cm mixture which results in higher porosity.

Chapter 6 *Article 4* - Experimental Study on the Effect of Mixture Parameters on Shrinkage and Cracking Resistance of Dry-mix Shotcrete

Bruce MENU, Pepin-Beauset, ALEXANDRE, Marc JOLIN, and Benoît BISSONNETTE

Department of Civil and Water Engineering, Université Laval, Quebec City, QC, Canada G1V 0A6

6.1 Résumé

Le béton projeté a l'avantage d'être applicable dans les réparations minces avec capacité à couvrir de grandes surfaces. Ce grand rapport surface/volume de béton projeté frais non protégé peut entraîner un gradient d'humidité transitoire qui peuvent conduire à un retrait différentiel à travers la couche de béton projeté relativement mince lorsqu'il est soumis aux effets du séchage. Le retrait et le potentielle de fissuration dépendant des compositions des mélanges et de la cure précoce. Cet article s'intéresse dans un premier temps à l'effet de la teneur en ciment et de la fraction granulométrie sur le comportement volumique du béton projeté par voie sèche. L'étude fournit également une analyse sur l'effet des ajout cimentaire (fumées de silice et cendres volantes) sur la résistance à la fissuration des bétons projetés par voie sèche exposés au séchage. Cet article met également en lumière l'influence du polymère, de l'adjuvant réducteur de retrait (SRA) et de l'adjuvant réducteur de fissure (CRA) sur le retrait et la fissuration du béton projeté par voie sèche à l'aide d'un essai à anneau modifié. Globalement, les résultats obtenus démontrent que la résistance au retrait et à la fissuration du béton projeté est étroitement liée aux paramètres du mélange.

6.2 Abstract

Shotcrete is used in a wide variety of repair applications that usually results in concrete elements having a large surface area. After curing, this large *exposed surface area-to-volume ratio* can lead to a non-uniform

moisture distribution in the in-place shotcrete which will create differential drying shrinkage. The shrinkage and potential subsequent cracking depend on the selected material proportions and the curing regime. The three-fold focus of this study is to investigate (i) the possibility of improving the shrinkage performance of dry-mix shotcrete by optimizing the *coarse aggregate* and *cement* content, (ii) the influence of silica fume (*SF*) and a combined *SF* and fly ash (*FA*), (iii) and the influence of polymer, shrinkage-reducing admixture (SRA) and crack-reducing admixture (CRA) on shrinkage and cracking resistance of dry-mix shotcrete using a modified *restrained shrinkage ring test*. The results indicate that shrinkage and cracking resistance of shotcrete are closely related to mixture parameters.

Keywords: shrinkage cracking, ring test, silica fume, fly ash, shrinkage-reducing admixtures, crack-reducing admixtures

6.3 Introduction

Shotcrete (or sprayed concrete) is a *method* of placing cementitious materials. The application technique involves pneumatically projecting mortar or concrete at high velocity onto a surface. The two basic methods of producing shotcrete are the *dry-mix* and the *wet-mix* processes. While there is a clear distinction between the two methods, they are best suited for tunneling, slope stabilization, swimming pools, dams, and other activities for which traditional placing methods would be inefficient or economically unviable [6, 12]. A major attribute of the shotcrete method of placing concrete is flexibility and usually an excellent bond to substrate. The dry-mix process is particularly effective for repairs and rehabilitations, in vertical and overhead applications. Many new advances in shotcrete equipment and materials technology in recent years have greatly enhanced shotcreting capabilities. These new developments coupled with proven field performances have further increased the acceptance and use of shotcrete as a viable construction method.

One main advantage of shotcrete is the capacity to cover large surfaces (e.g., a wall or abutment repair) without the use of formwork. However, once finishers have completed their work on the shotcrete surface, we often find ourselves with a large area of unprotected fresh concrete. Unless protective measures are rapidly implemented, surface water evaporation will quickly lead to differential shrinkage through the relatively thin (typically 100-200 mm) repair shotcrete layer. In parallel, shotcrete mixtures generally exhibit higher shrinkage compared to conventional *cast* concrete mixtures [6, 25, 92]. The higher shrinkage of shotcretes compared to *cast* concrete is attributed to the higher cementitious content and lower coarse aggregate volume. Another parameter that can significantly exacerbate the shrinkage problem is a shotcrete-specific phenomenon known as *rebound* (i.e. materials lost during spraying) that can modify the expected *in-place* composition of fresh shotcrete.

Shrinkage of Portland cement-based materials is an inevitable phenomenon that results from changes in moisture content, temperature or chemical reactions. The major concern with regard to the shrinkage is the

potential for *cracking* and any subsequent adverse impact on concrete durability or serviceability [28]. Cracks may occur mainly because of (internal and/or external) *restraint* [36, 80, 82], which is inherent in many concreting and shotcreting works. If shrinkage is restrained, internal tensile stresses are progressively induced in the element. Over time, these stresses may eventually exceed the material's maximum tensile strength, and thus cause cracking.

Most cracks occur within the first 10 days after placing concrete. Depending on the specific application and exposure severity, cracking can lead to premature corrosion of reinforcing steel and subsequent deterioration of concrete/shotcrete in service. In addition to compromising the aesthetic appeal, cracking can also greatly increase the cost of repair and maintenance. It is thus desirable to minimize shrinkage cracking potential to harness the full benefits of shotcrete.

While mix-design parameters (e.g. cement content, aggregate volume, silica fume, fly ash, admixtures, etc.) are known to influence shrinkage and cracking of cast concrete(s) [28, 36, 43], it is not clear how and to what extent these variables are important with regards to shotcrete. This is because reliable material data on their influence on shotcrete based on *restrained ring shrinkage tests* are difficult, if not impossible to find. The reader must understand that the shotcrete *placement* process is complex in many aspects as the final *in-place* quality is dependent upon the interaction of a chain of phenomena (such as nozzle manipulation, air flow, material flow, shooting consistency, rebound, etc.) that interact with each other during spraying. This makes it is difficult to control and study one specific mixture parameter of shotcrete at a time. Thus, to properly assess the influence of targeted mixture characteristics, several concrete mixtures need to be sprayed and compared.

In the present study, we first try to describe the influence of *cement paste* and *aggregate content* on early-age shrinkage and the associated cracking of shotcrete using a modified AASHTO *ring* test. This was done primarily because, despite varying opinions on shrinkage, it is a commonly accepted that the most prevalent cause of shrinkage of concrete is the cement paste content [36, 93, 94]. Experimental tests have shown that aggregates can offer internal restraint to shrinkage of the cement paste [28, 93]. From a shotcrete viewpoint, this is critical as it must be understood that cement paste and coarse aggregate content will influence *rebound* and *placement*. Therefore, the proportions studied must serve both the ability to spray and the desired properties of the mixtures.

Additionally, we try to examine the relationship between rebound reduction, shrinkage and the likelihood of restrained shrinkage cracking occurrence in dry-mix shotcretes exposed to drying. In practice, mineral additives such as *silica fume* (SF) and *fly ash* (FA) are successfully used to reduce material rebound of shotcrete. The rebound reduction can amount up to about 10 to 30% [8, 95, 96]. Besides rebound reduction, SF is also used in shotcrete to facilitate spraying of the mixtures by providing improved cohesion and adhesion [6, 8, 95]. This leads to the production of superior quality shotcrete with reduced permeability and greater bonding strength. SF also increases the maximum build-up thickness of freshly sprayed concrete

as well its long-term strength. Similarly, FA is added to improve pumpability and finishability. In some cases, FA is combined with SF to reduce rebound and cement content, thereby improving material cost-effectiveness.

Existing literature, however, shows that replacement of cement with SF can significantly increase shrinkage of cementitious materials while FA is said to minimize shrinkage [41-43]. Data available in the literature also show that SF can drastically increase shrinkage cracking potential at early age [41, 82]. Conflicting results can be found with regard to FA, some showing a reduction in cracking potential [41, 42, 82], others showing instead a significant reduction in early age cracking performance [44]. Thus, attempts to reduce shotcrete material rebound and cement content with SF and/or FA may, on the other hand, involuntarily result in an increase in their shrinkage cracking propensity. Yet, knowledge about the adverse effects linked to the use of SF and/or FA in dry-mix shotcrete is very limited. Specifically, no research has prospectively examined the link between the reduction of rebound and the subsequent impact on shrinkage cracking of shotcrete. With this in mind, different dry-mix shotcrete mixtures were shot, and a relative comparison of the performance in terms of rebound reduction, shrinkage and cracking resistance is provided.

To confront the early age shrinkage problem of cementitious materials, *shrinkage-reducing admixtures* (SRAs) are often recommended [28, 46, 47]. The use of *crack-reducing admixtur*e (CRA) [48] and *polymers* in conventional cast concrete has also been tested. It has been claimed that these admixtures can mitigate the detrimental effect of shrinkage of cement-based materials and thus improve their cracking resistance. According to some researchers, the reductions in shrinkage can be as high as 40 to 60% when SRA is used depending on the dosage [28, 46], whereas CRA is said to provide similar reductions as SRAs at equal dosages [48]. There is, however, very little consistency in the testing and very little data available to compare the use of polymers to minimize shrinkage of concrete. Insofar as shotcrete is concerned, the use of these admixtures to reduce shrinkage and the associated potential risk of cracking has not been properly investigated. In this context, the recently modified AASHTO *ring* test method was again used to evaluate the potential of using a polymer, SRA, and CRA to mitigate shrinkage cracking of dry-mix shotcrete.

It is worth mentioning that the *ring test* procedure was adapted especially for *shotcrete* in recent years [67]. At present, the ring test is the most accurate laboratory method for measuring shrinkage cracking performance of cement-based materials [41, 42, 77, 79, 97]. This so-called *ring test* considers all the necessary material properties (such as restraint, shrinkage, elastic modulus, tensile capacity, and creep) involved in evaluating the cracking potential of concrete materials. The ring test method was also adapted for evaluating the *free* shrinkage of shotcrete. This overall study is part of a series of a comprehensive research project on the early-age cracking of shotcrete at the Centre de recherche sur les infrastructures en béton (CRIB), at Université Laval.

6.3.1 Research Significance

Shotcrete technology has seen significant mix design developments over the past decade with regards to chemical admixtures, silica fume, and fly ash. a diversity of mixture designs are used in a wide variety of projects ranging from repairs and rehabilitation to new constructions. The addition of these materials through the complex process of pneumatic placement affects the early-age shrinkage and the associated cracking potential. Yet, the state of knowledge regarding the influence of mixture parameters on shrinkage performance of shotcrete is currently scarce or undocumented. The aim of this project is, therefore, to provide knowledge on shrinkage and the potential for cracking of dry-mix shotcrete. Overall, the paper shows that there are no simple answers to changing one mixture parameter to improve the shrinkage performance of dry-mix shotcrete as the whole placement process needs to be taken into account.

6.4 Experimental Program

This paper presents the results of a research program on the effect of key mixture parameters on the free shrinkage and restrained shrinkage cracking potential of dry-mix shotcrete. The project is divided into three (3) phases. In the first phase, the role of *cement paste* and *aggregate* content was investigated. In the second phase, the effect of *SF* and *FA* on dry-mix shotcrete was investigated. In the third phase, the potential of using a *polymer*, *SRA* or *CRA* to mitigate the shrinkage and subsequent cracking of dry-mix shotcrete was tested. The main tests performed to quantify the shrinkage and cracking potential of the mixtures were the *free* and *restrained* shrinkage ring test based on the AASHTO T 334-08 procedure. Other properties such as rebound, absorption, voids, compressive strength, splitting tensile strength, and elastic modulus were also evaluated. The test program was carried out entirely at Université Laval's CRIB Shotcrete Laboratory. In the following sections, the detailed experimental program and the methods used are briefly described.

6.4.1 Materials and Mixture Proportions

Fifteen (15) dry process shotcrete mixtures were designed for this project. Several key mix parameters were investigated to compare their effects on shrinkage as well as other properties of shotcrete. These were: the *cement paste* content, *coarse aggregates* volume, the presence of *mineral additive*s (*SF* and *FA*), and *chemical admixtures* (*polymer*, *SRA,* and *CRA*). Two aggregate size gradations were used in this project. They are called *Gradation curve A* and *Gradation curve B* as detailed in Fig. 6.1 along with the ACI Committee 506 recommended limits for Gradation No 2. The same Ordinary Portland cement (OPC) was used in all the mixtures. The fine aggregate used was a natural sand while the coarse aggregate was a crushed limestone with a nominal maximum aggregate size of 10 mm (⅜ in). The coarse aggregate had a bulk loose density of 1561 kg/m^3, a bulk specific gravity (SSD) of 2.802, and absorption of 0.56 %. The sand also had a bulk loose density of 1696 kg/m^3, a bulk specific gravity (SSD) of 2.737, and absorption of 0.71 %. In all cases, the mixture proportions are specified by the percentage of dry constituents along with

the corresponding *theoretical sprayed* composition of a cubic metre of the same mixtures having a *water-to-cementitious* materials (w/cm) ratio of 0.40 and an air content of 3.0 %.

The *phase I* mixtures were four (4) simple OPC based dry process shotcretes. Three (3) of the mixtures were designed from the Gradation curve A with 16%, 21%, and 25% cement content (by weight of the total dry ingredients) and a fixed fine-to-coarse-aggregate ratio. These mixtures will be called herein 15-16%, 15-21%, and 15-25%. The first number identifies the proportion of coarse aggregate by weight of the total dry ingredients. Following the results obtained, one additional mixture was tested using the Gradation curve B by increasing the coarse aggregate of the mixture with 21% cement content from 15.0% to 23.7%. This mixture will be referred to as 24-21%. The objective of the later mixture 24-21% is to verify the possibility of optimizing the coarse aggregate content of the in-place mixture. The *phase I* mixture proportions are detailed in Table 6.1.

The *phase II* mixtures were based on two (2) most revealing mixtures selected from phase I (i.e. 15-21% and 24-21%). Both mixtures contained 21% cement by weight of the total dry ingredients. Four (4) dry-mix shotcretes were designed from the two selected mixtures. These included a mixture incorporating SF alone as a partial cement replacement, and a mixture combining both SF and class C FA as partial cement replacement. The percentage replacement of the SF and FA was fixed at 8% and 24% by weight of cementitious materials. This corresponds to about 1.6% and 5% by weight of the total dry ingredients, respectively. These mixtures will be called 15SF, 24SF, 15SF/FA and 24SF/FA. An additional mixture incorporating 10% SF by weight of cementitious materials (i.e. 2.1% SF by weight of total mixture) was prepared for comparison purposes. This mixture will be called 15SF-C. The different mixtures produced in this series are presented in Table 6.2.

The *phase III* mixtures were also based on two (2) mixtures chosen from phase II for further investigation (i.e. 15SF and 24SF). Those mixtures had the best performance in terms of materials rebound. The binder (cement + SF) content of both mixtures is 21%. Six (6) dry-mix shotcretes were designed from the two selected mixtures. These included a mixture containing a polymer(POL), a shrinkage-reducing admixture (SRA) and a crack-reducing admixture (CRA). The polymer treated mixtures will be referred to as polymer-modified shotcrete (PMS). The mixture proportions are summarized in Table 6.3. The polymer and SRA were added at 2% and 5% by mass of cement to the shotcrete mixtures, respectively. Note that the polymer and SRA used were powdered-based hence pre-dosed/blended in dry form into the shotcrete mixtures before pre-bagging. However, the CRA was added in liquid form to the mixing water. It should be note that the in-place water content was unknown prior to spraying, therefore, the dosage of the CRA was determined based on the average water content of the control SF mixtures. This explains the difference in dosage between the two CRA-mixtures; the 24-21% CRA mixture required approximately 5 ml/L more water to achieve the same desired consistency as the corresponding 15-21% CRA mixture.

All the shotcrete mixtures investigated were pre-bagged (by King Packaged Materials). The mixtures were sprayed in controlled testing conditions at the Université Laval's well-equipped *CRIB Shotcrete Laboratory*. The shotcrete mixtures were sprayed using a rotating barrel ALIVA 246 machine (Fig. 6.2a) equipped with a 38.1 mm (1.5 in.) interior diameter hose (Fig. 6.2b) and a water ring placed 1.5 m (5 ft) before the exit of the nozzle. The nozzle tip was the double-bubble hard rubber type (Fig. 6.2c). Shooting operations took place in a rebound chamber and normal gunning techniques were observed [10, 56]. The average laboratory temperature during all spraying operations was in the range of 22 ± 1.7 °C.
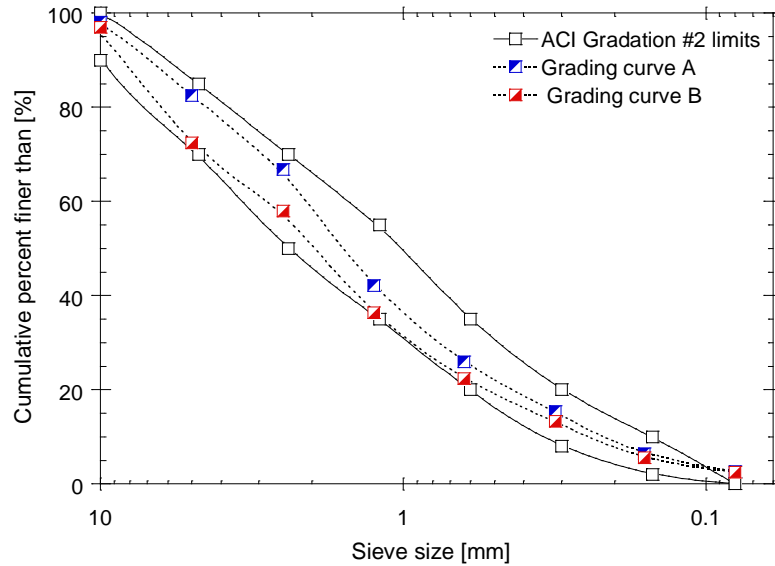
Fig. 6.1 Aggregate size distribution for the combined aggregates used in this study
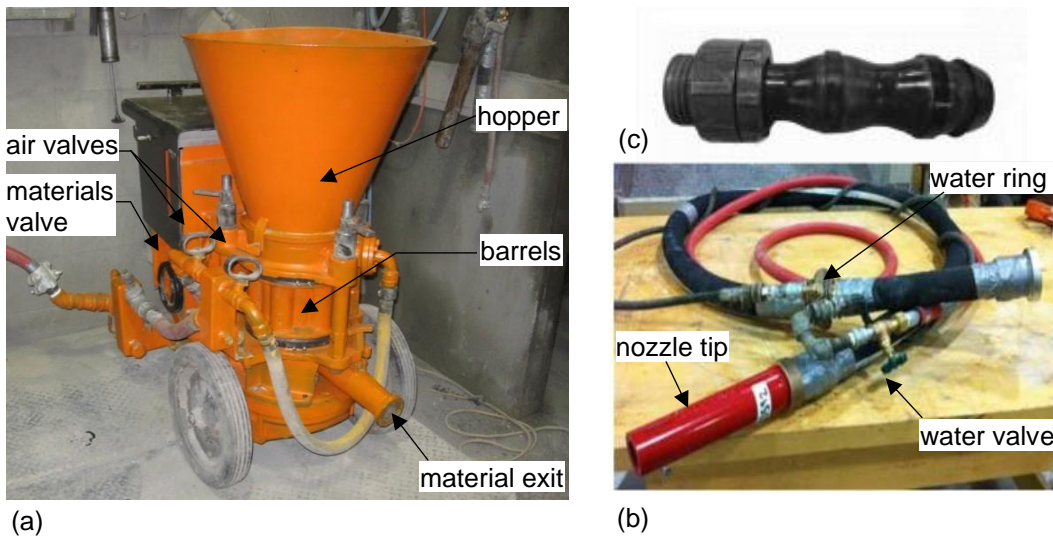
Fig. 6.2 (a) Aliva®-246 dry-mix shotcrete machine, (b) typical hydomix nozzle assembly with water ring 1.5 m before exit and (c) double bubble nozzle tip used in this study

Table 6.1 Compositions of shotcrete mixtures investigated - Phase I

Mix no.	Mix description	OPC cement wt.%[†]	kg/m³[‡]	Sand (0-5 mm) wt.%[†]	kg/m³[‡]	Stone (2.5-10 mm) wt.%[†]	kg/m³[‡]
M1	15-16%	16.0	378	68.0	1608	15.9	377
M2	15-21%[†]	21.0	476	63.9	1452	15.0	341
M3	24-21%[†]	21.0	477	55.3	1257	23.7	539
M4	15-25%	25.0	549	60.8	1335	14.3	313

[†] values by weight of the total dry mixture constituents; [‡] assuming w/cm = 0.40; * mixtures used in Phase II

Table 6.2 Compositions of shotcrete mixtures investigated - Phase II

Mix no.	Mix description	OPC cement wt.%[†]	kg/m³[‡]	Sand (0-5 mm) wt.%[†]	kg/m³[‡]	Stone (2.5-10 mm) wt.%[†]	kg/m³[‡]	Silica fume wt.%[†]	kg/m³[‡]	Fly ash wt.%[†]	kg/m³[‡]
M5	15SF-C	18.9	426	64.0	1443	15.0	338	2.1	47.4	-	-
M6	15SF[†]	19.4	438	64.0	1445	15.0	339	1.6	36.1	-	-
M7	24SF[†]	19.4	439	55.3	1251	24.0	536	1.6	36.2	-	-
M8	15SF/FA	14.4	323	64.0	1437	15.0	337	1.6	35.9	5.0	112.3
M9	24SF/FA	14.4	324	55.3	1244	23.7	533	1.6	36.0	5.0	112.5

[†] values by weight of the total dry mixture constituents; [‡] assuming w/cm = 0.40; * mixtures used in Phase III

Table 6.3 Compositions of shotcrete mixtures investigated - Phase III

Mix no.	Mix description	OPC cement wt.%[†]	kg/m³[‡]	Sand (0-5 mm) wt.%[†]	kg/m³[‡]	Stone (2.5-10 mm) wt.%[†]	kg/m³[‡]	Silica fume wt.%[†]	kg/m³[‡]	Admixtures Type	Dosage
M10	15SF-PMS	19.4	430	64.0	1418	15.0	333	1.6	35.5	Polymer	20g/kg of binder
M11	24SF-PMS	19.4	431	55.3	1227	23.7	526	1.6	35.5		
M12	15SF-SRA	19.4	428	64.0	1411	15.0	331	1.6	35.3	SRA	50g/kg of binder
M13	24SF-SRA	19.4	429	55.3	1222	23.7	524	1.6	35.4		
M14	15SF-CRA	19.4	438	64.0	1445	15.0	339	1.6	36.1	CRA	40ml/L of water
M15	24SF-CRA	19.4	438	55.3	1251	23.7	536	1.6	36.2		45ml/L of water

[†] values by weight of the total dry mixture constituents; [‡] assuming w/cm = 0.40

6.4.2 Restrained Shrinkage Ring Test

The restrained ring test involves placing concrete around a rigid steel ring. As the ring specimen dries, it shrinks but the internal rigid steel ring prevents movement, leading to tensile stresses in the concrete. As drying progresses, the induced tensile stresses inside the concrete specimen increase progressively at a decreasing rate. Cracks will initiate in the concrete ring when the shrinkage-induced stresses eventually exceed the material strength of the concrete. A sudden decline in the strain (i.e. 30 microstrain or more) in one or more gauges placed inside the steel ring indicates crack in the concrete ring specimens. There are currently no specific standard procedures for testing restrained shrinkage of shotcrete. So, the restrained shrinkage ring tests were carried out using the AASHTO T334-08 ring geometry, which consists of a concrete ring with a wall thickness of 76 mm (inner and outer diameter of 305 mm and 457 mm) and height

of 152 mm, with a 12.7 mm thick restraining inner steel ring (inner and outer diameter of 280 mm and 305 mm). The adaptation of the ring test fabrication method and its validation on shotcrete are described in detail elsewhere [67]. In brief, the ring setup is placed overhead at an angle of 30˚ from the horizontal position to facilitate rebound evacuation and homogenous placement during shotcreting operations (as shown in Fig. 6.3a and Fig. 6.3b).

For each shotcrete mixture tested, at least two ring specimens were shot. After spraying, the shotcrete rings were covered with wet burlap followed with plastic sheets to prevent moisture loss from specimens for the first 24 hours. After this initial curing, the exterior wall of the shotcrete specimen was removed and the specimens were additionally moist cured for 2 days. After the final curing, the top surface was coated with a thin layer of paraffin wax and sealed with self-adhesive aluminum foil as quickly as possible to limit drying to the *radial direction only* (see Fig. 6.3c). The rings were then exposed to drying in a controlled environment at 21±1.7°C and 50 ± 4% R.H. (relative humidity) until cracking occurred. The inner steel ring of each specimen is instrumented with four strain gauges at equidistant mid-height locations. This was done primarily to monitor strain development and to facilitate the detection of cracking in the concrete ring. The strain data were automatically recorded at 5-minute intervals. The rings were monitored daily for strain development in the steel ring and crack detection. Once cracking occurs, the specimens were visually inspected for crack locations and the crack widths were measured and recorded.

Fig. 6.3 Inclined overhead setup used to spray the shotcrete ring test specimens; (a) setup before spraying, (b) setup after spraying, (c) sealed instrumented restrained ring specimens, and (d) free ring specimens

6.4.3 Free Shrinkage Ring Test

In parallel with the restrained ring tests, free shrinkage ring tests were also performed to compare the shrinkage properties of the dry-mix shotcrete mixtures investigated. Two free shrinkage ring specimens were prepared for each mixture (Fig. 6.3d). The *free rings* were prepared to mimic the restrained specimens in terms of geometry, size, finishing, curing method, and drying conditions. The only exception for free ring specimens is replacing the steel ring with a white polystyrene core with a very low stiffness (described in [57]). After curing and sealing (same as the restrained specimen), DEMEC (DEmountable MEChanical) gauges are installed on top of the specimens to allow for length change measurements. Zero readings were taken immediately after DEMEC gauges are installed at the age of 1 day. Subsequent length changes were measured at different time intervals. The free ring specimens were exposed to the same drying environment as the restrained shrinkage ring test specimens.

6.4.4 Weight Loss

Since the relative humidity within the mixtures could not be directly measured, loss of mass due to drying of the test specimen was measured instead. The measurements were carried out on 100 mm cylindrical cores taken from a 600×600×125 mm test panels. The cylinders underwent the same curing as the ring test specimens. After curing, the cylinders were partially sealed with a double layer of self-adhesive aluminum foil such that they have the same exposed surface area-to-volume ratio as their corresponding ring test specimens. The cylinders were also exposed to the same drying conditions as those of the ring test specimens. The weight losses were recorded at the same rate as the free ring shrinkage measurements.

6.4.5 Characterization of the Shotcrete

The properties of the shotcrete mixtures were evaluated on cores drilled from a 600×600×125 mm test panels. Three (3) test panels per mixture were shotcreted for specimen coring, as shown in Fig. 6.4. These test panels were covered with wet burlap and plastic sheets immediately after spraying for the first 24 hours in their forms at an ambient temperature of 23°C. Core samples, 100 mm diameter × 200 mm long, were extracted from the test panels according to the procedure recommended in ASTM C1604. Three (3) specimens each were used to determine compressive strength (ASTM C1604), splitting tensile strength (ASTM C496), and elastic modulus (ASTM C469) of the investigated mixtures at 3, 7 and 28 days. In each series, the specimens were stored in the 100% R.H. conditioning room until the testing age. Using the ASTM C642 procedure, the boiled water absorption (BWA) and volume of permeable voids (VPV) of the shotcrete mixtures were determined on sets of three cored samples at age of 28-days. Additionally, the material rebound rate, the total in-place binder content and the w/cm ratio were also determined.

Fig. 6.4 Shotcrete test panel (left) and cored samples (right)

6.5 Test results and discussion

6.5.1 Fresh Properties of Dry-mix Shotcrete

6.5.1.1 Rebound

The application of shotcrete entails rebound - which is the bulk of materials (mainly large aggregates) that ricochets off the receiving surface during spraying and falls on the ground. Rebound can have severe implications on the in-place composition of fresh dry-mix shotcrete and, by extension, on both the long-term durability and mechanical performance of shotcrete elements. Therefore, measuring rebound is critical in this study. The rebound measurements were made using a vertical steel panel instrumented with load cells that is mounted on the wall. The total material rebound, reported as a percentage of the total sprayed materials, is shown in Fig. 6.5. Notice that the material rebound rates seem to depend more on the particle size distribution (i.e. consistently higher for mixtures made from Gradation curve A). Fundamentally, one would have expected the mixtures from Gradation curve B with higher coarse aggregate content to exhibit higher rebound rates since most of the rebounding particles are the larger aggregates. However, it is the shape of the particle-size distribution curve that is important not necessarily the absolute value of one aggregate size or another, as demonstrated by Jolin and Beaupre [13]. With this in mind, the lower rebound rates could be attributed to the higher w/cm ratios attained.

Further, Fig. 6.5 show that the rebound obtained for the plain OPC mixtures were excessive, but the overall rebound rates do not appear to be affected much by the cement content. This is explained by the counteracting effect of lowering w/cm ratio. In contrast, the addition of mineral additives significantly reduced the amount of shotcrete rebound. This is attributed to the marked improvement in adhesion and cohesion of the mixtures and the higher water content allowed. The shotcrete rebound was reduced by about 24% to 37% when compared to the control OPC mixtures. The largest decrease in shotcrete rebound came from increasing the SF content from 8% to 10% (by wt. of cement). In general, these reductions were expected and are in good agreement with values reported in the literature [6, 8, 95, 96].

93

Also, it can be seen that the addition of polymer did not improve the rebound performance of the control dry-mix SF shotcretes. The addition of SRA and CRA, on the other hand, appears to reduce the material rebound of the same control dry-mix SF shotcrete mixtures. Overall, SRA seems to be more effective in reducing dry-mix shotcrete rebound than CRA. A reduction of approximately 20 to 24% was observed when SRA was used compared to the reduction of about 5 to 15% when CRA was used.

Rebound in shotcrete has major financial consequences. But in reality, it is still unclear how much rebound is acceptable for shotcreting works. Based on decades of research on dry-process shotcrete, it is fair to say that the rebound values obtained for the OPC mixtures were unsatisfactory. In contrast, the values obtained for the mixtures with mineral additives and/or chemical admixture fall within the acceptable range of 20% to 30% rebound values reported for modern SF-based dry-mix shotcretes [6, 8, 9, 12, 95]. The reader must keep in mind that the laboratory set-up for rebound evaluation is more severe than may be encountered during actual field operations. Taken globally, the results indicate that the mineral additives and chemical admixtures used can be considered as an excellent mean to control rebound.
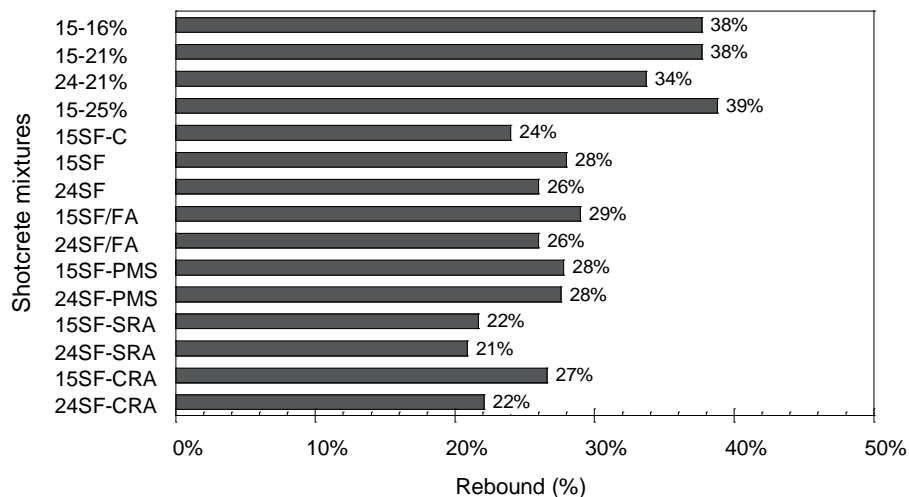
Fig. 6.5 Rebound calculated for the tested mixtures

6.5.1.2 Water-to-Cementitious Materials (w/cm) Ratio

Naturally, the w/cm ratio is important when it comes to comparing and ensuring the quality of cement-based materials. Since the exact w/cm ratios of the dry shotcrete mixtures were unknown prior to spraying, it needed to be experimentally evaluated. The w/cm ratios were determined using a rapid drying technique (or the microwave method) within 30 min after the spraying. The test results of the w/cm ratios are presented in Table 6.4. The results suggest that the w/cm ratios of the OPC mixtures decreased as the cement content increased to achieve comparable spraying consistency. The trend suggests that a shotcrete mixture can

be sprayed drier by increasing the cement content and vice versa. It is also observed that an increase in the coarse aggregate volume increases the w/cm ratio.

Further, it is clear that the w/cm ratios of the mixtures with mineral additives have significantly increased compared to the control OPC mixtures. This was to be expected since SF and FA normally increase water requirements due to their high surface areas. In dry-mix shotcrete, this allows shooting at the *wettest consistency* for a given shooting position. In contrast, the w/cm ratios of mixtures with polymer, SRA or CRA have decreased relative to their respective control SF mixtures. The decrease is particularly remarkable for the mixtures treated with CRA (nearly 30% decrease). This may be because the CRA was used in a liquid form whereas the polymer and SRA were used in the powdered form. Indeed, the w/cm ratios of the polymer and SRA treated mixtures were practically identical. It must be pointed out that the difference in w/cm ratios between the 15-SF and 15-SF/FA can be explained by the slightly drier consistency of the 15SF mixture during spraying rather than its lower water demand.

The overall results seems to indicate that the w/cm ratios vary linearly with the materials rebound rate. This would be consistent with previous studies [8]. It is worth noting that the w/cm ratios obtained for the OPC mixtures, the CRA treated mixtures, and the 15SF-PMS mixture fall within the typical range of 0.30 to 0.45 reported in the literature for dry-mix shotcrete [6, 9]. In contrast, the w/cm ratios of the mixtures with mineral additives, the SRA treated mixtures and the 24SF-PMS mixture were all higher than the typical values (ranging from 0.48 to 0.55).

6.5.1.3 In-Place Binder Content

The total *in-place* binder content was evaluated using a decantation and sieving test (within 30 min after spraying). The results obtained for the different mixtures tested are presented in Table 6.4. Clearly, the results show that the binder contents of all the mixture tested have increased post spraying. This is attributed to the loss of material through rebound during spraying. It is, however, worth noting that the addition of mineral additives decreased the total in-place binder content when compared to the OPC mixtures. This is attributed primarily to the reduction in overall rebound rates when SF and/or FA are used, suggesting that a direct relationship exists between the in-place binder content and rebound. Indeed, a study by Jolin [8] has demonstrated that for a constant binder content in the original mixture, the in-place binder content is directly related to the overall rebound rate, implying that if the initial binder content is fixed, decreasing rebound will decrease the in-place binder content and the overall aggregate content will increase.

Of course, one must bear in mind that the dry shotcrete process is somehow self-adjusting, so a reduction in rebound may not necessarily translate into a reduction in post-spraying binder content. For example, there was a reduction in material rebound when the mixtures were treated with SRA and CRA, but this did not translate into a reduction in in-place binder content. The increase in the *in-place* binder may also be

related to the amount of coarse aggregates in the mixture. It can be seen that the increase in the in-place binder content is consistently higher for the mixtures with higher coarse aggregates.

6.5.1.4 Effective Paste Volume

The post-spraying paste volume expressed as the cumulative percentage of cementitious materials, water, air of 3.0 %, and admixtures (where applicable) is also shown in Table 6.4. It may strike as odd that there was no significant difference in the in-place paste volume. Again, this is because the dry shotcrete process is somehow self-adjusting on the receiving surface. At the start of the shotcreting process, the aggregates bounced off the receiving surface until there is enough paste on the surface to absorb the incoming aggregates. Different mixture designs may lead to very different self-adjusting behaviours during spraying to achieve a minimum paste content. For example, an increase in cement content reduces the w/cm ratio and increase the rebound rate; as a result, the coarser aggregates bounce off the surface until there is enough paste to capture the particles [98]. Conversely, a mixture with low cement content (i.e. high aggregate content) is subject to high rebound, until the water content is sufficiently increased to facilitate paste buildup to absorb aggregates.

Similarly, an increase in coarse aggregate will increase the w/cm ratio, the rebound rate decreases leading to higher in-place paste content. This last case illustrates the importance of aggregate size distribution on the rebound rate and final *in-place* composition of dry process shotcrete. A general conclusion that can be drawn from these observations is that any admixture used in dry-mix shotcrete would have a distinct effect on the in-place paste volume due to how the nozzleman adapts to maintain a certain desired consistency.

Table 6.4 Characterization of fresh dry-mix shotcrete mixtures investigated

Mix no.	Mix description	w/cm	In-place Binder		Water content	Aggregate content	Density	Paste volume*
			%	kg/m^3	kg/m^3	kg/m^3	kg/m^3	%
M1	16-16%	0.45	19.7	459.0	218.3	1647.9	2325.2	39.7
M2	15-21%	0.35	25.0	590.1	208.3	1560.4	2358.7	42.9
M3	24-21%	0.39	26.7	607.9	222.4	1506.0	2336.3	44.9
M4	14-25%	0.30	28.8	689.7	194.3	1511.1	2395.1	44.7
M5	15SF-C	0.51	22.1	455.9	232.9	1608.1	2296.9	41.1
M6	15SF	0.48	21.6	453.9	218.0	1651.3	2323.2	39.5
M7	24SF	0.55	25.1	493.9	270.9	1471.2	2236.0	46.1
M8	15SF/FA	0.53	19.7	379.5	197.5	1762.3	2339.3	35.5
M9	24SF/FA	0.55	20.7	378.2	207.4	1736.3	2321.9	36.4
M10	15SF-PMS	0.44	28.0	579.4	253.8	1488.0	2321.2	45.5
M11	24SF-PMS	0.51	26.3	530.9	269.2	1484.2	2284.3	45.7
M12	15SF-SRA	0.45	28.8	483.6	232.3	1759.2	2475.1	35.6
M13	24SF-SRA	0.51	22.0	529.2	290.3	1576.5	2396.0	42.3
M14	15SF-CRA	0.34	28.8	479.6	230.4	1744.7	2454.7	36.1
M15	24SF-CRA	0.39	26.6	489.6	268.5	1458.3	2216.4	46.6

* The paste volumes include 3% air.

6.5.2 Hardened Properties of Dry-mix Shotcrete

6.5.2.1 Boiled Water Absorption (BWA) and Volume of Permeable Voids (VPV)

The BWA and VPV were measured on cores after immersion and boiling according to ASTM C 642 test procedures at age 28 days. The average data are summarized in Table 6.5. The test results show a small decrease in the BWA and VPV values as the cement content increased. But when the coarse aggregate content rose from 15% to 24% percent, no noticeable change in the value of the BWA value is noted while a slight increase in VPV value is noted. In this test, the addition of SF alone as partial cement replacement increased the BWA and VPV values. Whereas, a decrease in the BWA and VPV values is observed when SF is combined with FA. Also, the addition of SRA and CRA significantly decreased both the BWA and VPV values. But the polymer did not appear to affect the BWA and VPV values.

On the practical side, BWA and VPV tests are commonly used in specifications (and quality control testing) to quantify the quality of the shotcrete placement based on the quality indicators out in ref. [89]. All the OPC mixtures, the SF-only mixtures, and the PMS mixtures have BWA and VPV test results that can be rated as "good". The addition of FA in the presence of SF enhanced the overall quality by shifting from "good" to "excellent". Similarly, the addition of SRA and CRA also improved the overall placement quality of the control SF mixtures from "good" to "excellent". Of course, the reader must keep in mind that these indicators may not necessarily give a complete picture of the sprayability of the mixtures. For example, it was easier to spray the admixtures in a powdered form (polymer and SRA) than in a liquid form (CRA).

Table 6.5 Shotcrete quality control indicators

Mix no.	Mix description	BWA (%)	VPV (%)	Rating
M1	16-16%	6.7%	14.8%	Good
M2	15-21%	6.5%	13.7%	Good
M3	24-21%	6.6%	14.4%	Good
M4	14-25%	5.8%	13.2%	Good
M5	15SF-C	7.4%	15.6%	Good
M6	15SF	7.7%	17.0%	Good
M7	24SF	6.6%	14.9%	Good
M8	15SF/FA	4.9%	10.9%	Excellent
M9	24SF/FA	4.6%	10.4%	Excellent
M10	15SF-PMS	7.7%	16.6%	Good
M11	24SF-PMS	6.3%	14.4%	Good
M12	15SF-SRA	5.0%	10.8%	Excellent
M13	24SF-SRA	3.8%	8.5%	Excellent
M14	15SF-CRA	4.2%	9.4%	Excellent
M15	24SF-CRA	4.8%	11.0%	Excellent

6.5.2.2 Compressive Strength

The compressive strength tests were performed on cores at age 3, 7, and 28 days and the average results are given in Table 6.6. The coefficient of variation (COV) are also presented such as to appreciate the level

of homogeneity achieved. The overall trends observed from the test results in Table 6.6 are consistent with the current prevailing concepts that strength is a function mainly of w/cm ratio [23, 40, 99]. It can also be seen that the strength developments of the OPC mixtures appear to be dependent on the initial cement content. This is partly because an increase in cement content requires a reduction in the w/cm ratio for a constant consistency and therefore produces a stronger and stiffer matrix [99]. In shotcrete applications, this translates into increased shooting stiffness.

Generally speaking, all the mixtures with mineral additives experienced slower early strength development. But notice that the SF-only mixtures either gained more strength (M7) than or reached very close (M5 and M6) to, the control shotcrete's strength at age 28 days. The overall slow strength gains were expected and correlate well with previously published reports [43, 44, 96] that these mineral additives often result in slower early strength gain. It should also be mentioned that the pozzolanic effect of FA is much slower than that of SF, hence it is not surprising that the FA/SF-based mixtures had the lowest strength gain.

Observing Table 6.6, one can also see that the use of SRA negatively affected the compressive strength developments. The addition of SRA reduced the compressive strengths of the control SF dry-mix shotcretes by about 17 to 30% (depending on the percentage of coarse aggregate). A study by Morgan et al., [25] also found that the addition of SRA (4% by mass of cement) to dry-mix SF shotcrete reduced the compressive strength by about 16 to 18%. Similar trends have been reported in published studies on cast concrete(s) [23, 46, 47]. A study by Folliard and Berke [46] showed a reduction in the range of about 8% to 10% with SRA addition. While Shah, Karaguler, and Sarigaphuti [47] observed a reduction of compressive strength in the order of 10 to 30% when SRA is used. However, some studies [28] also found that SRA only had minimal effect on compressive strength. Generally, the strength loss at early age can be attributed primarily to the effects of SRA on early cement hydration [46]. Thus, the use of SRA may have reduced the cement hydration reaction speed at early age which consequently delays the development strength.

By contrast, the addition of CRA produced results that are not entirely clear. The 15SF-CRA blend showed a strength increase of about 10% at all ages, whereas the 24SF-CRA blend recorded a strength decrease of about 20% at all ages. This is likely due to the difference in dosage between the two mixtures and the w/cm ratio. Previous studies by Nmai et al., [48] reported tendencies contrary to the results in this study. According to the study by Nmai et al., [48], the effect of CRA on the strength of concrete is similar to the effects of SRA. In the present case, it could not be verified, but it may have been because SRA was powdered-based hence pre-dosed/blended in dry form into the dry mixture before pre-bagged whereas the CRA was added to the mixing water in a liquid form. As a result, the CRA-treated mixtures had lower w/cm ratios compared to the SRA-treated mixtures.

The use of polymer also negatively affected strength gain. The addition of polymer resulted in a reduction in compressive strength in the order of 7% to 16% depending on the mixture. Data available in the literature [100] also shows a decrease in compressive strength when polymer (polyvinyl acetate) was used in the dry

98

shotcrete process. The recommended curing procedure for polymer treated concrete in the laboratory is wet curing at 100% R.H. followed by dry curing at 50% R.H. The strength data obtained by wet and air curing of the PMS blends at the age of 7 and 28 days was about 32.6 MPa and 48.8 MPa for 15SF-PMS mixture and about 30.8 MPa and 40.2 MPa for the 24SF-PMS mixture, respectively. Compared to the data in Table 6.6, it is seems that incorporation of polymer into dry-mix shotcrete would allow for a simple dry curing without any adverse effect on the compressive strength.

Table 6.6 Compressive strength of the mixtures tested (unit: MPa)

Mix no.	Mix description	3-days		7-days		28-days	
		$\int_{c\ avg.}$	COV	$\int_{c\ avg.}$	COV	$\int_{c\ avg.}$	COV
M1	15-16%	20.5	9%	26.4	5%	35.6	
M2	15-21%	35.3	10%	41.2	7%	45.0	10%
M3	24-21%	35.8	6%	42.1	5%	48.8	5%
M4	15-25%	48.6	5%	52.2	9%	54.4	1%
M5	15SF-C	19.4	4%	25.4	3%	32.5	9%
M6	15SF	27.4	8%	32.1	4%	43.5	6%
M7	24SF	32.0	9%	35.1	6%	50.9	8%
M8	15SF/FA	20.5	6%	27.5	8%	29.1	7%
M9	24SF/FA	23.0	3%	28.1	5%	34.2	8%
M10	15SF-PMS	25.6	9%	28.0	2%	41.2	9%
M11	24SF-PMS	27.6	6%	31.9	5%	41.4	6%
M12	15SF-SRA	21.5	10%	26.5	10%	34.6	5%
M13	24SF-SRA	22.2	9%	26.1	10%	35.4	3%
M14	15SF-CRA	30.1	8%	34.9	8%	47.9	9%
M15	24SF-CRA	25.5	7%	29.5	4%	40.8	3%

6.5.2.3 Splitting Tensile Strength

The average splitting tensile strength test results and the associated standard deviations are reported in Fig. 6.6. It unsurprisingly follows the same trend as the compressive strength with few exceptions. Again, increasing the initial cement content increased the splitting tensile strength because of a reduction in the w/cm ratio. Furthermore, an increase in coarse aggregate content slightly improved the splitting tensile strength. Also, a reduction in splitting tensile strength is observed at all ages for the FA/SF mixtures. In comparison, a reduction in splitting tensile strength is observed only at the ages of 3 and 7-days in the SF only mixtures (M8 and M9). The results also indicate that the use of SRA greatly decreased splitting tensile strength development. Again, the CRA-treated mixtures produced results that are not entirely clear. A 10% increase in splitting tensile strength was observed for the 15SF-CRA mixture whereas a reduction of about 10% was recorded for the 24SF-CRA mixture. As aforementioned, this may be due to the differences in CRA dosage between the 15SF-CRA and 24SF-CRA mixtures. Interestingly, the PMS mixtures had the highest tensile strength values among the mixtures with chemical admixtures. Overall, the splitting tensile strength values were found to be in the range of about 6% to 11% of the compressive strength values.
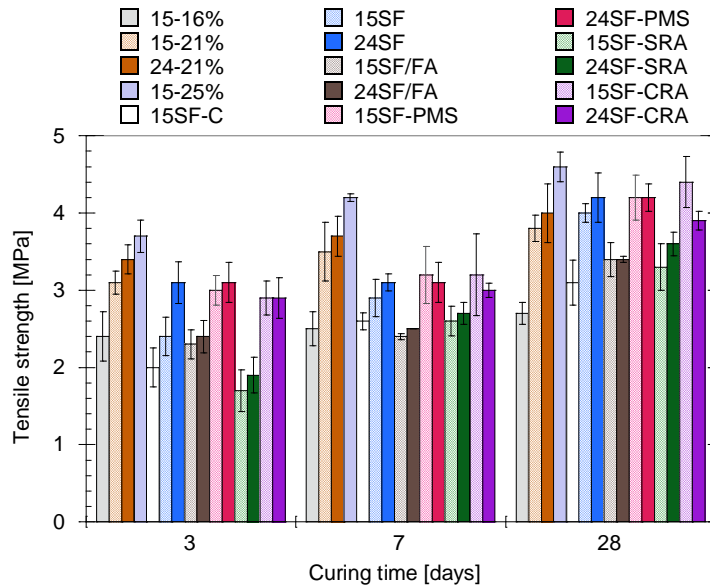
Fig. 6.6 Effect of chemical admixtures on the splitting tensile strength

6.5.2.4 Elastic Modulus

The average result of the elastic modulus of the different mixtures investigated is shown in Fig. 6.7. The data obtained agree with previously published studies [23, 99] that reducing the w/cm ratio increases the elastic modulus due to a stronger and stiffer matrix. The elastic modulus of the OPC mixtures follow the same trend as the compressive strength. However, the overall trends observed for the other mixtures differ significantly from both the compressive and tensile strength tests. For example, all the mixtures with mineral additives exhibited lower elastic modulus at the ages of 3 and 7-days. But all the FA-inclusive mixtures reached the same elastic modulus values as the control mixtures; whereas only the 24SF mixture among the SF-only mixtures reached very close to the control shotcrete's elastic modulus at age 28 days. This suggests that long-term elastic modulus is not affected by the addition of FA. Indeed, a previous study also reported that the elastic modulus of FA/SF-based mixtures are comparable to the control mixtures at the age of 28 days [42].

Furthermore, the results indicate that the use of polymer did not affect the rigidity of the mixtures when compared to the control SF mixture. By contrast, the addition of SRA significantly reduced the elastic modulus. Again, CRA produced results that are difficult to explain. While the 15SF-CRA mixture had about a 15% decrease in elastic modulus at the ages of 3 and 7 days but an increase of about 24% at the age of 28 days; the 24SF-CRA mixture recorded a reduction of about 7% at all ages.

100
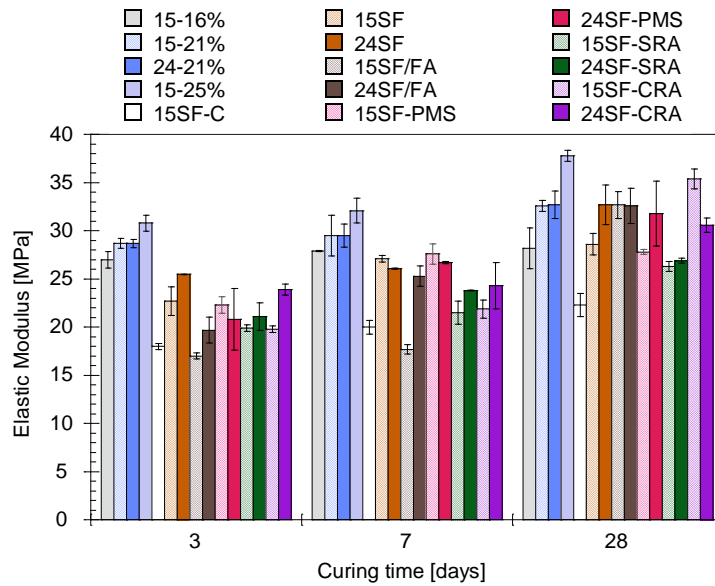
Fig. 6.7 Results of the elastic modulus test

6.5.3 Shrinkage Test Results

The "total" free shrinkage response of the drying shotcrete ring specimens (3 days after spraying) is presented in Fig. 6.8. Each curve in Fig. 6.8 represents the average result of at least two ring specimens. Note that for ease of interpretation, the curves for the OPC mixtures and that of the mixtures with additives and/or admixtures are shown on separate graphs. As is evident from the experimental results, the overall expected effect of increasing cement content on total shrinkage is rather smaller than expected in otherwise equal conditions (Fig. 6.8a). This coincides with the findings of a previous study [40] that found the overall effect of cement content on shrinkage to be also rather small. From a shotcrete point of view, this is somewhat related to the self-adjusting nature of the dry shotcrete process raised previously in the discussion. Accordingly, an increase or decrease in the initial cement content affects how the nozzleman adapts to maintain a certain desired consistency, which in turn affects the effective paste content and the resulting shrinkage.

The minor differences in the shrinkage curves of the OPC mixtures lie in the variations in aggregate volumes, and thus the restraining effect of aggregates. Normal aggregates tend to restrict paste movement provided the aggregates are stiffer than the paste. Implying that the more aggregate a mixture can accommodate, the lower the overall shrinkage will likely be [94]. This is consistent with the current prevailing concept that the dominant cause of shrinkage of cement-based materials is the shrinkage of cement paste [36, 93, 94]. Further, the trends observed here suggest that the overall effect of w/cm on the total shrinkage is rather small. It is possible, that some of the several factors that are dependent on the w/cm ratio and that affect shrinkage (pore size distribution, total porosity, modulus of elasticity, creep, water diffusion, etc.) might have opposite individual effects in such a way that the overall effect is rather small [36]. Conflicting

results can be found in the literature in that regard, some consistent with the trend observed here [36, 40], others showing instead a strong influence of the w/cm ratio [23, 82]. Strict comparisons are, of course, difficult due to miscellaneous variations in materials, experimental procedures and methods of placement.

It is quite evident from Fig. 6.8b that partial replacement of OPC with only SF increased the overall total shrinkage (by about 10% to 38%) when compared to the control OPC mixtures. On the other hand, the presence of FA reduced the total shrinkage by about 8% to 15%. The overall trends observed here are consistent with the data reported in the literature [41-44, 82] which showed when FA is present, shrinkage decreases but increases with the use of only SF. Suggesting that FA can fairly reduce the negative influence of SF on the shrinkage [43]. This is attributed to the refinement in the pore structure by pozzolanic reaction, especially in the early days of hydration, which leads to a reduction in the total amount of water loss and shrinkage. It can further be seen in Fig. 6.8b that all the admixtures tested minimized the shrinkage of the dry-mix shotcretes investigated (although their effectiveness varied). SRA and CRA, for example, were more effective in reducing shrinkage of dry-mix shotcrete than polymer.

The addition of SRA yielded a reduction in free shrinkage of the control dry-mix SF shotcrete in the range of about 40% to 60% at early age. An earlier study by Morgan et al., [25] also found that adding SRA to dry-mix SF shotcrete can reduce free shrinkage by about 20% to 70% at early age. The overall trend also corroborates with some published studies on cast concrete which also found that adding SRA to concrete decreases the shrinkage considerably [28, 46, 47]. For instance, Folliard and Berke [46] reported that the addition of SRA to SF concrete reduced free shrinkage in the order of 43% to 52% whereas the addition of SRA to the concrete without SF yielded a shrinkage reduction of about 29% to 35%. A study by Nmai et al., [28] also found a reduction in shrinkage of about 40% to 50% with the addition of SRA to concrete without SF. It is claimed that the mechanism that reduces the free shrinkage when SRA is used may be related to the reduction of the pore water surface tension [28, 46], leading to lower capillary stresses and consequently reduced shrinkage.

Similarly, a comparative evaluation shows that CRA also markedly reduced total free shrinkage in the order of about 30% to 50%. According to Nmai et al., [48], CRA-treated mixtures should provide similar reductions in shrinkage as SRAs at equal dosages because they also reduce the surface tension of pore water. Again, in the present case, it could not be verified because SRA and CRA were not added at equal dosages. Moreover, SRA was powdered-based hence pre-blended and pre-dosed into the mixture before pre-bagged while the CRA was added to the mixing water in a liquid form during spraying. Also, the addition of polymer reduced the shrinkage of dry-mix shotcrete. The reduction in shrinkage varied from about 20% to 30% for the 15SF-PMS mixture but about 13% to 21% for the 24SF-PMS mixture. Data reported in the literature [6, 100] also show that the use of polymer can reduce shrinkage of shotcrete.

It is worth noting in Fig. 6.8a that the shrinkage deformations of the control OPC mixtures developed at a very high rate at the beginning of the drying process but evolved slowly as drying progressed. Meanwhile,

Fig. 6.8b shows that the shrinkage of the mixtures incorporating mineral additives developed slowly at the beginning of the drying (in reality the shrinkage values are comparable at early ages). However, a clear distinction can be observed as drying progressed (after about 10 days); the shrinkage of the SF-only mixtures increased rapidly while that of the FA/SF-based mixtures evolved slowly. Gesoğlu et al. [43] also reported similar trends for mixtures incorporating mineral additives. The shrinkage of the mixtures incorporating chemical admixtures evolved slowly throughout the drying process.
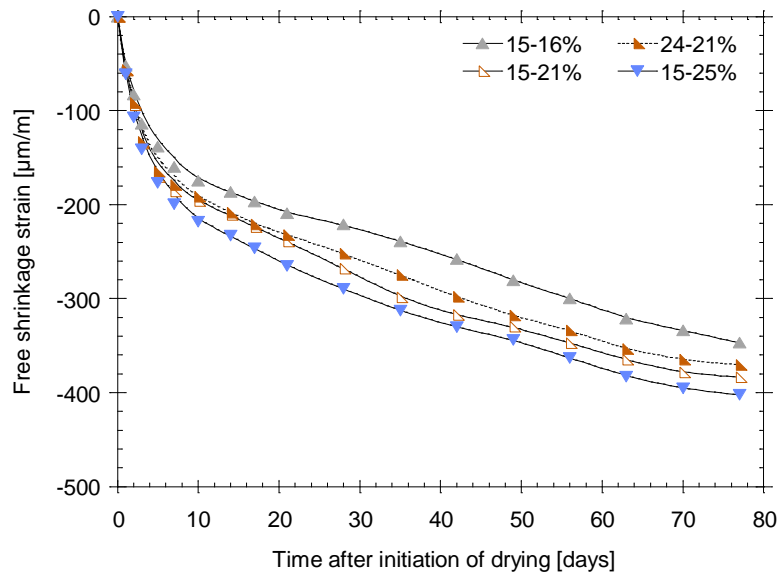
(a) Effect of cement content on shrinkage - OPC mixtures
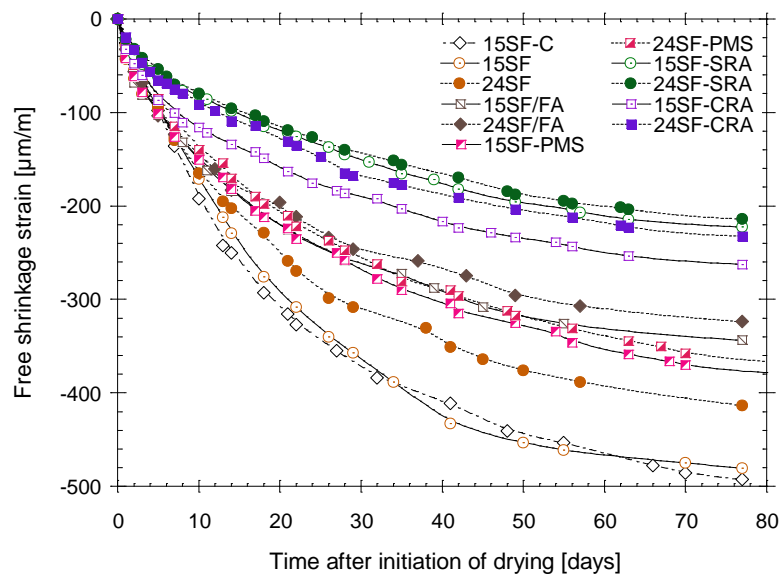
(b) Effect of mineral additives and chemical admixtures on shrinkage

Fig. 6.8 Total free shrinkage of the tested dry-mix shotcrete mixtures

6.5.3.1 Shrinkage Strain Rate Factor

Another possible approach to appraise the influence of mix-design parameters on shrinkage is to evaluate the *shrinkage rate* [53, 82] from the time the free shrinkage ring specimen has been exposed to drying. Generally, the higher the *shrinkage* strain rate factor is, the faster the overall free drying shrinkage of the mixture develops. The strain rate factor is obtained by plotting the shrinkage deformation against the square root of elapsed time and then using linear regression analysis to fit a straight line through the data. The strain rate factor is the slope of the line:

$$\varepsilon_{sh}(t) = |\alpha|\sqrt{t} + c \tag{6.1}$$

where ε_{dsh} is the free shrinkage (µm/m), α is the (free shrinkage) strain rate factor (µm/m /day$^{1/2}$), t is the time since drying (day) and c is a regression constant.

The comparison of the shrinkage strain rate factors obtained for the different mixtures investigated is presented in the graph of Fig. 6.9. First, the *shrinkage* strain rate factor results indicate that shrinkage of shotcrete does not seem to be affected much by the cement content, and the small differences may be related to the w/cm ratio. Second, the SF-only mixtures had higher strain rates compared to the FA/SF-based mixtures. The inherent effect of dry-mix spraying did not allow us to validate a difference between the two mixtures with 8% and 10% SF as the strain rate factors were almost identical. Third, the test results show that the mixtures with SRA had the lowest strain rate. The strain rate of the mixtures containing CRA was equally very low compared to the control SF mixtures. It is also evident that the use of polymer did not significantly lower the strain rate. The strain rate data also confirm that shrinkage is slightly higher in the mixtures with lower coarse aggregate contents.
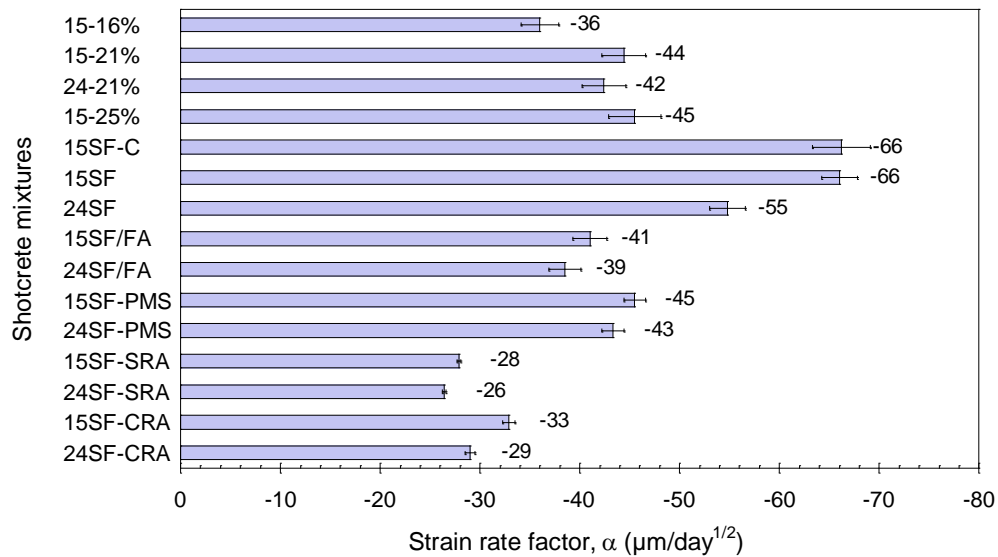
Fig. 6.9 Free shrinkage strain rate factors determined from free ring specimen length change data

6.5.4 Weight Loss

The results of the average weight loss over time for the different dry-mix shotcretes investigated can be seen from Fig. 6.10. The trend observed for the weight loss is quite different from the trend observed for the total shrinkage as no systematic trend could be seen. For the OPC mixtures, weight loss is inversely proportional to the w/cm. In fact, the mixture with the lowest w/cm (15-25%) exhibited the lowest weight loss during drying among all mixtures tested. By contrast, the weight loss of the mixtures with additives and/or admixtures is independent of the w/cm ratio. The mixture containing SF/FA mixture exhibited the highest weight loss. The SF only mixtures also showed a high weight loss except for the 24SF mixture. All the chemical admixtures used reduced the weight loss during drying. However, the PMS mixtures exhibited slightly higher weight loss compared to the mixtures treated with SRA and CRA.

It is interesting to note that the addition of SRA and CRA reduced shrinkage considerably without any significant weight loss. Some previous studies also found that the SRA reduced shrinkage considerably without any noticeable difference in weight loss [47]. Overall, the results of this experiment support the fact that polymer, SRA, and CRA can reduce the water evaporation from concrete when exposed to unsaturated air.
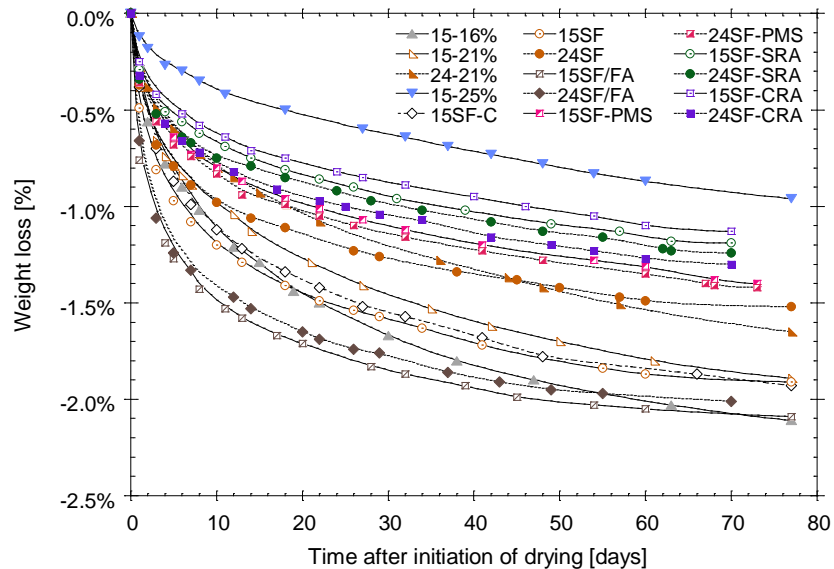
Fig. 6.10 Total percentage of weight loss of the tested dry-mix shotcretes

6.5.5 Shrinkage-induced Stress Development in the Restrained Ring Specimens

In this study, the strains measured in the restraining steel rings were used to calculate the *average shrinkage-induced stresses* in the concrete using Eq. (6.2), [97].

$$\sigma_t(t) = -\frac{1}{2}\frac{A_s}{A_c} E_s \varepsilon_s(t)\frac{R_{os}+R_{is}}{R_{os}} = -G \varepsilon_s(t) \tag{6.2}$$

where A_s and A_c are the cross-sectional areas of the steel and concrete, R_{is} and R_{os} are the internal radii of the steel and concrete, respectively, E_s is the elastic modulus of the steel ring, ε_s is the strain recorded in the steel ring, and G is a constant (31.55 GPa [4.58 ×10^6 psi] for the ring setup used).

Typical curves showing the average computed shrinkage-induced stress developed during drying of the restrained ring specimen is shown in Fig. 6.11. In Fig. 6.11, zero indicates the initiation of the drying process which is 3 days after spraying. Again, for easy analysis, the curves for the OPC mixtures, the mixtures with additives, and the mixtures treated with admixtures are shown on separate graphs. Also note the different horizontal axis scales as the curves were plotted close to time of cracking of the mixtures.

In general, cracking resistance seems to decrease for a given mixture group as the w/cm ratio decreased (with few exceptions). This is explained by the more significant contribution of autogenous shrinkage as the w/cm ratio decreased. Recent studies have also shown that the potential for early-age cracking tends to increase with lowering w/cm ratio [23, 80, 82]. In higher w/cm ratio mixtures, drying is likely to take a longer time to reach a comparable magnitude, due to excess water available for evaporation in a coarser pore structure; which allows for some strength gain and relaxation due to creep, overall resulting in potentially extended time-to-cracking [80]. Further, the data in Fig. 6.11a shows that among the OPC mixtures, the lowest cement content mixture (15-16%) had the lowest shrinkage stress while the higher cement mixtures had higher shrinkage stresses. Consequently, shrinkage cracks occurred earlier in the mixtures with higher cement contents (which could be explained by the lower w/cm ratios). Also, increasing the coarse aggregate volume increased the stress build-up, but improved the cracking resistance of shotcrete.

Furthermore, it can be observed in Fig. 6.11b that the stress development at early age is higher in mixtures with mineral additives. Consequently, they exhibit inferior cracking-resistance compared to the OPC mixtures and mixtures treated with chemical admixtures. This indicates that shrinkage cracking is a major concern for dry-mix shotcretes when SF used as partial cement replacement. The risk of shrinkage cracking is even more severe when FA is added. These findings coincide with data reported in the literature for regular concrete which showed that the addition of SF leads to early-age cracking [23, 41, 42]. Conflicting results can be found in the literature with regard to the use of FA in regular concrete. Some studies [41, 42] found that the use of FA alone leads to lower stress levels hence later cracking ages; others [44] showing instead that when FA alone is used in regular concrete cracks occur earlier. In the present case, the early cracking of the FA/SF-based may be attributed to the negative influence of SF. Of course, many varying parameters can be involved in the shotcrete spraying process, notably, rebound, that may play a significant role in the results obtained for the shotcrete mixtures.

It can also be seen in Fig. 6.11c that adding polymer was not effective in reducing the early age shrinkage stress development, but the overall cracking resistance was improved. The induced stresses of the PMS

mixtures were actually higher (about 16 to 45%) than their respective control SF mixtures. In contrast, both SRA and CRA were very effective in reducing the early age shrinkage-induced stresses as well as the potential for cracking under restrained shrinkage. The addition of SRA reduced the induced-shrinkage stress in order of about 20% to 50% compared with the control SF mixtures. As a result, SRA appears to be the most effective in terms of improving the potential for cracking of shotcrete despite the mixtures with SRA recording the lowest strengths. A study by Morgan et al., also showed that SRA is very effective in reducing the restrained shrinkage cracking potential of both wet-mix and dry- mix SF shotcretes [25]. Studies performed on cast concrete mixtures have also shown that SRA is effective in reducing shrinkage stress and therefore cracking of cast concrete with SF [46] and without SF [23, 28].

The addition of CRA reduced the cracking potential, but the exact effect on stress development is not that clear. While about 35% reduction in stress development was recorded for the 24SF-CRA mixture, about 45% increase in stress was observed for the 15SF-CRA mixture. The principal benefit of CRA over SRA appear to be its post-cracking behaviour. For instance, whereas a sudden abrupt drop in compressive strain was observed in all other shotcrete specimens indicating cracking; a gradual reduction in strain was instead observed in the CRA-treated mixtures. Indeed, a visual inspection of the individual rings after cracking and a closer look at each strain gauge installed revealed that for the CRA-treated mixtures, there was a cycle of increase and decrease in the recorded strains until the experiment was ended. A similar observation was reported in a study by Nmai et al., [48] for CRA-treated concrete specimens. This phenomenon is attributed to the relaxation of tensile stress (i.e. internal stress relief) within the CRA-treated specimens [48]. At the ends of the ring tests, microcracks were detected at several positions of the CRA-treated rings.
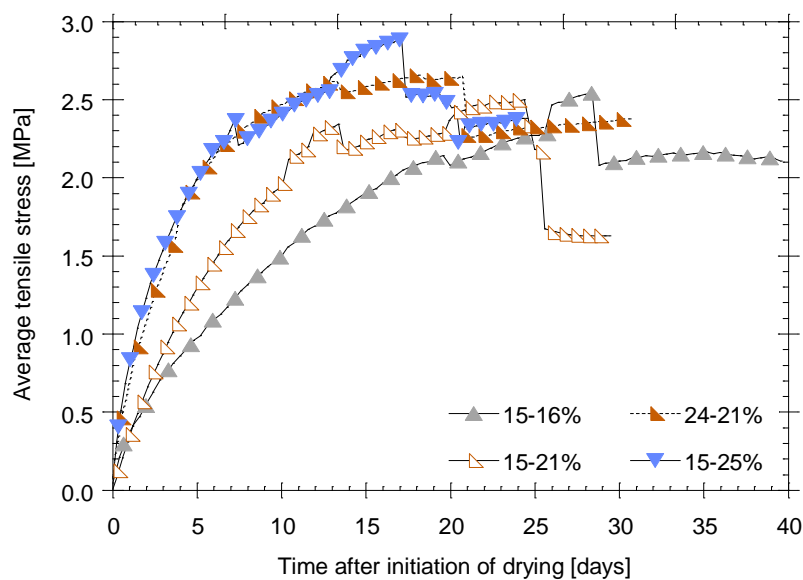
(a) Shrinkage stress development of OPC mixtures
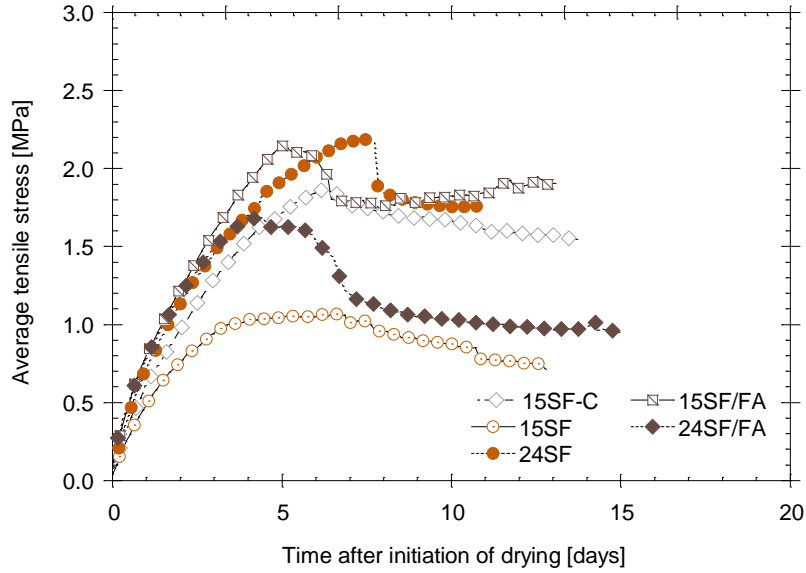
(b)   Shrinkage stress development of mixtures with mineral additives
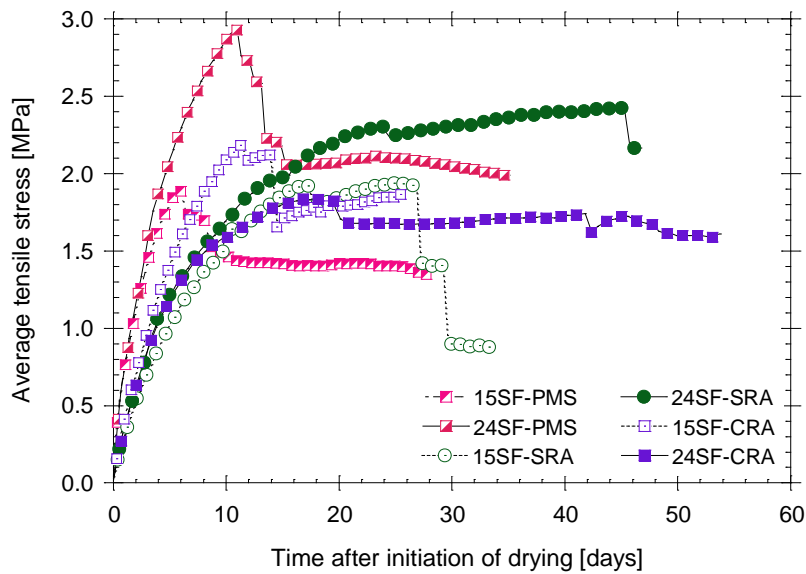
(c) Shrinkage stress development of mixtures with chemical admixtures

Fig. 6.11 Effect of mixture parameters on shrinkage cracking of the tested dry-mix shotcrete mixtures

6.5.5.1 Age of cracking of the restrained ring specimens

The cracking resistance of the dry process shotcrete mixtures was first evaluated based on the average *time-to-cracking*. The abrupt drop in stress in Fig. 6.11 corresponds to the age at which a visible crack developed in the restrained ring specimens. Note that the cracking age of the CRA-treated mixtures was

taken as the age at which the most significant drop in stress is recorded. The average cracking age of the mixtures tested along with their correspondingly standard deviations is shown in Fig. 6.12.

Among the OPC mixtures, it was found that the 16% cement rings cracked after 28 days of drying, while the 21% cement rings cracked between the ages of 20 and 28 days. On the contrary, the 25% cement rings cracked under 20 days of drying. Thus, cracking resistance seems to be affected by the cement content, the coarse aggregate volume, and the w/cm ratio. The variability in cracking ages between two rings from the same spray is indicated by the standard deviations shown in Fig. 6.12). It can be observed that the variability is just 1 day for the 15-21% rings, 2.2 days for the 15-25% rings, but about 10 days for 24-21% rings and 20 days for the 15-16% rings. The overall variability in cracking ages is related to many varying parameters that can be involved in the dry spraying process, which can differ based on many factors, notably the self-adjusting behaviours during spraying, and cannot easily be determined.

Clearly, it can be seen that the substitution of cement by mineral additives significantly decreased the cracking resistance. The FA/SF mixtures cracked below the age of 6 days while the SF-only mixtures cracked below the age of 10 days. Thus, the addition of SF-only decreased the cracking age by 67 to 75%, while the introduction of FA further decreased the cracking age by 77 to 81% when compared to control OPC mixtures (M2 and M3). Further, the data shows that all the admixtures tested improved the cracking resistance of the dry-mix SF shotcretes investigated. Overall, the addition of SRA produced the best cracking resistance. An increase in cracking age in the range of about 73% to 78% is observed with the addition of SRA when compared to their control dry-mix SF shotcrete mixtures. A previous study on shotcrete also found that SRA significantly improved the cracking resistance of SF shotcretes [25]. In the case of cast concretes, Folliard and Berke [46] reported about 88% reduction in cracking for SRA-treated rings when compared to the control SF rings without SRA.

The effect of CRA on the resistance to early-age cracking is comparable with SRA (the cracking ages are very close). The addition of CRA resulted in about 55% to 77% reduction in cracking when compared to the control dry-mix SF shotcrete mixtures. It is interesting, however, to note that 24SF-SRA and 24SF-CRA recorded a comparable improvement in cracking resistance, but a noticeable difference can be observed between 15SF-SRA and 15SF-CRA. The addition of polymer was the least effective method. A reduction in cracking of just 13% to 35 was observed with the addition of polymer. Data reported in the literature [6] also show that the use of polymer can minimize the risk of cracking of shotcrete. No data exists in the literature on cracking resistance of PMS mixtures treated with SRA; however, in unpublished data from tests done at the Université Laval, an increase in the time to cracking in the range of 40-80% have been observed.

Further analysis showed that mixtures with a higher elastic modulus at the time of initiation of drying tend to have a higher potential for cracking. On the contrary, lower elastic modulus significantly reduces the risk of shrinkage cracking due to higher tensile strain capacity which increases the ability of the mixture to

develop greater tensile stress relaxation. The average crack width observed was about 0.18 mm for the CRA-treated specimen compared to about 0.20mm to 0.25 recorded the SF, SF/FA, PMS, and CRA-treated mixtures. For the OPC mixtures, the average crack width was between 0.21 and 0.28 for the 16% cement mixture and in the range of about 0.30 to 0.40 mm for the 21% and 25% cement mixtures.
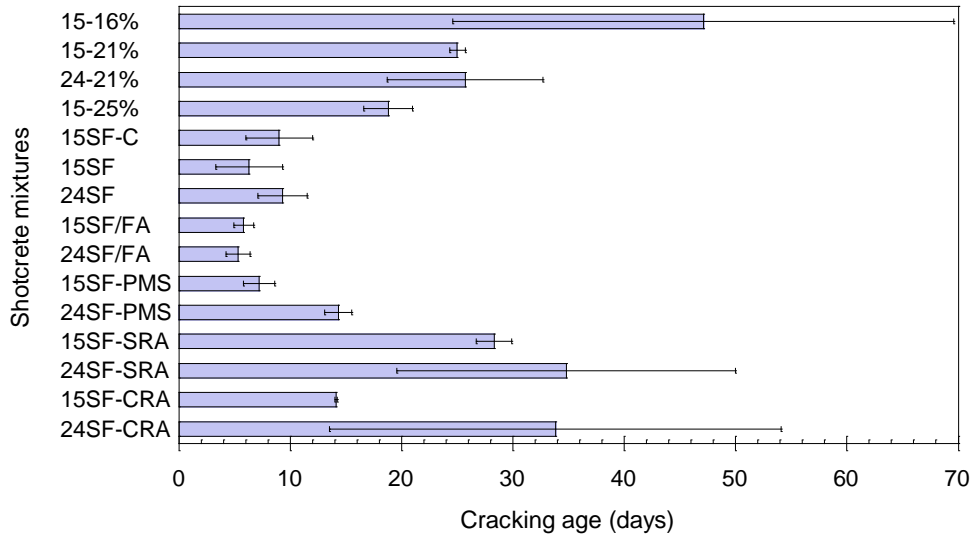
Fig. 6.12 Cracking age of restrained shotcrete

6.5.5.2 Stress Rate at Cracking

Although the cracking age is an interesting benchmark for assessing the cracking resistance of cement-based mixtures, the potential for cracking of a material can also be classified on the basis of the rate of stress development in the material (i.e. the *stress rate* at cracking. Besides, the approach can also be used to examine the stress rate at an earlier age as a basis for a preliminary assessment of cracking potential materials [77]. The *rate of stress development* in a material at time t after initiation of drying, $S(t)$, is obtained as:

$$S(t) = \frac{G \, |\alpha|}{2\sqrt{t}} \tag{6.3}$$

with S as stress rate (MPa/day), α as steel strain rate factor ($\mu\epsilon$/day$^{1/2}$), t as time-to-cracking (day) and G as a constant (35.55 GPa, from [97]). The steel strain rate factors of the shotcrete mixtures tested were computed using equation Eq. (6.3), where the free shrinkage strain (ε_{sh}) has been replaced with the steel strain (ε_s). It should be noted that the stress rate was estimated for each shotcrete ring specimen analyzed in this study.

The relationship between the stress rate parameter and the corresponding age of cracking found experimentally for the shotcrete mixtures tested are presented in Fig. 6.13. The overall trend in Fig. 6.13 shows that a good relationship exists between the time-to-cracking and stress rate as has been reported in some previous studies [77, 79, 80]. The figure clearly shows that the higher the stress rate, the shorter the time it takes to crack simply because of insufficient strength development (or inversely, too much early shrinkage). This indicates that the resistance to cracking can be significantly improved by slowing down the rate at which drying occurs [79].

For the OPC mixtures, the stress rate is lower in the 16% cement mixture compared to 21% and 25% cement mixtures. It can be observed that the stress rate more than doubled when the cement is increased from 16% to 21% and almost tripled when the cement is increased from 16% to 25%. This suggests that an increase in cement content will significantly decrease the cracking resistance of shotcrete mixtures. Further, it is noted that the stress rate at cracking rose by about 10% on average when the coarse aggregate increased from 15% to 23.7%.

Also, it is evident from the same figure that the mixtures with mineral additives demonstrate higher stress rates at cracking than the plain OPC mixtures. In fact, the stress rate more than doubled when only SF is used and almost tripled when FA was added in the presence of SF, despite the fact that the addition of FA reduced the overall free shrinkage of shotcrete. Fundamentally, this tends to confirm that the assertion that free shrinkage results are not sufficient to assess the risk for restrained shrinkage cracking [101]. This also suggests that for a given shotcrete mixture, the substitution of cement by mineral additives from the point of view of reducing shrinkage and cracking potential is not beneficial. However, the use of these mineral admixtures is interesting from an economic point of view since they can reduce the loss of material related to the rebound, which has financial implications.

A paradox therefore emerges, where the addition of mineral additives significantly reduces rebound which is desirable, but also has a very high potential for cracking which is undesirable. Alternatively, the results obtained may lead to re-evaluate the need for SF. More research is needed to evaluate the use of FA alone to reduce rebound. Considering FA was added to SF in the present study, a possible way forward to "work around" this issue may be to consider the influence of FA alone on shrinkage and cracking compared to SF alone. Also, the influence of FA and SF on thermal shrinkage need to be evaluated. Since modern shotcrete mixtures without SF and/or FA is relatively unlikely, it is recommended to extend the curing time of these mixtures (to at least 7 days) or to use an admixture such as SRA and CRA.

Indeed, the trend of the data in Fig. 6.13 demonstrates the beneficial effect of using SRA and CRA. It is clear that SRA and CRA mixtures exhibited superior cracking resistance. In fact, when SRA is used, the stress rate at cracking was reduced by about 60 to 75%. Similarly, CRA also reduced the stress rate at cracking by about 50 to 70%. This indicates that SRA and CRA are good choices for reducing the cracking potential of shotcrete under restrained shrinkage. The stress rate data from an earlier investigation [77] also

indicated that SRA is very effective in reducing restrained shrinkage cracking of concrete (without SF). The PMS mixtures also demonstrated superior results compared with those of the control SF mixtures by reducing the stress rate.

Based on stress rate at cracking, a "*cracking potential"* can be assigned to each mixture. A classification based of stress rate at cracking proposed by See et al. [77] for thin ring specimens has been adopted by ASTM C1581 [53]. The AASHTO ring test produces a lower stress rates than ASTM ring test due to a thicker concrete section [97]. Therefore, the stress rate limits established in past studies [53, 77] for a performance classification of thin-walled ASTM rings as shown in Table 6.7 is not appropriate for the thicker AASHTO rings. Similar four performance zones, identified for assessing the cracking performance of shotcrete based on the AASHTO ring setup used in this study are shown in Table 6.7. These classifications take into account all available data on shotcrete (at least 70 shotcrete ring specimens). The zones are:

(i) 'High' when cracking occurs less than 7 days with stress rates higher than 0.17 MPa/day;

(ii) 'Moderate-high' when cracking occurs between 7 and 14 days with stress rates between 0.17 and 0.11 MPa/day;

(iii) 'Moderate-low' when cracking occurs between 14 and 28 days with stress rates between 0.11 and 0.05 MPa/day; and

(iv) 'Low' when cracking occurs above 28 days (or in case of no cracking) with stress rates lower than 0.05 MPa/day.
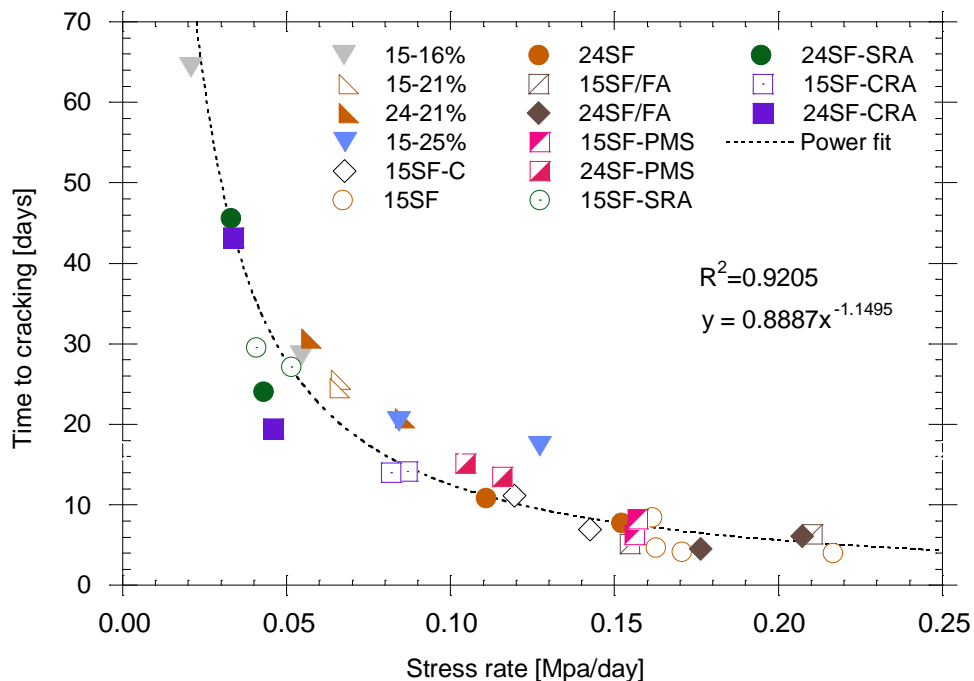
Fig. 6.13 Stress rate at age of cracking of the mixtures tested

Table 6.7 Suggested cracking potential classification. (Based on stress rate at cracking)

Net Time-to-Cracking, t_{cr}, (days)	ASTM Stress Rate, S, (MPa/day) [7]	Suggested Stress Rate, S, (MPa/day) [a]	Potential for Cracking Classification
$0 < t_{cr} \leq 7$	$S \geq 0.34$	$S \geq 0.17$	High
$7 < t_{cr} \leq 14$	$0.17 \leq S \leq 0.34$	$0.11 \leq S \leq 0.17$	Moderate-High
$14 < t_{cr} \leq 28$	$0.10 \leq S \leq 0.17$	$0.05 \leq S \leq 0.11$	Moderate-Low
$t_{cr} > 28$	$S < 0.10$	$S < 0.05$	Low

[a] suggested value for the AASHTO ring setup

Table 6.8 Suggested cracking potential classification. (Based on stress rate at 7 days after initiation of drying)

Net Time-to-Cracking, t_{cr}, (days)	Stress Rate at 7 days after initiation of drying, S, (MPa/day) [a] [77]	Suggested Stress Rate at 7 days after initiation of drying, S, (MPa/day) [b]	Potential for Cracking Classification
$0 < t_{cr} \leq 7$	$S \geq 0.41$	$S \geq 0.22$	High
$7 < t_{cr} \leq 14$	$0.28 \leq S \leq 0.41$	$0.18 \leq S \leq 0.22$	Moderate-High
$14 < t_{cr} \leq 28$	$0.17 \leq S \leq 0.28$	$0.10 \leq S \leq 0.18$	Moderate-Low
$t_{cr} > 28$	$S < 0.17$	$S < 0.10$	Low

[a] suggested value for the ASTM ring setup; [b] suggested value for the AASHTO ring setup

It is interesting to note that the stress rate approach is more consistent than the cacking age approach. For example, one ring specimen of the 24SF-SRA cracked around 24.1 days while the other ring cracked at 45.6 days. Thus, the first ring can be classified as "Moderate-Low" and the second rings as "Low" according to the net time-to-cracking criterion. However, both rings would be classified as "Low" according to the stress rate criterion (S < 0.05). Similarly, one ring specimen of the 24SF-CRA cracked around 19.5 days while the other ring cracked at 48.2 days. Again, the first ring can be classified as "Moderate-Low" and the second rings as "Low" according to the net time-to-cracking criterion. But both rings would be classified as "Low" according to the stress rate criterion (S < 0.05). Another example is the 15SF-PMS which would be classified as "High" and "Moderate-High" based on the net time-to-cracking criterion, but just "High" based on the *stress rate* criterion.

With regards to preliminary assessment of cracking potential materials, See et al. [77] determined that 7 days after initiation of drying is adequate. The stress rate limits Table 6.8 are established for classifying the cracking resistance of shotcrete when the drying shrinkage and modulus of elasticity of the test material are determined at 7 days after initiation of drying.

6.6 Conclusions

This research focused on the influence of key mixture parameters upon shrinkage, stress development, and age of cracking of dry-mix shotcrete mixtures using the ring shrinkage test. The study has produced original results which demonstrated again that there are no simple answers to changing one mixture parameter to improve the shrinkage performance of dry-mix shotcrete. Thus, unlike regular cast concrete mixtures, it is difficult to study the effect of just one parameter in the dry-mix shotcrete process, because of the auto-adjusting phenomenon that occurs during spraying. This implies that the desired result may not necessarily result from adjusting various mixture parameters because a change in any one parameter would affect the entire system. The auto-adjusting effect of dry process shotcrete has been acknowledged in a previous study by Jolin [8]. This is evident from the observed trends that the results lack consistency when one tries to explain the data in terms of any single parameter. Ultimately, the final in-place composition and properties are dependent on the cross-influence of many parameters during spraying. Overall, the following remarks can be made:

1. Strength of shotcrete is a function mainly of the w/cm ratio;

2. SF, FA, polymer, SRA or CRA have the potential of reducing shotcrete rebound as well as improve their porosity and placement quality;

3. Shotcrete containing SF and/or FA exhibited lower early strengths than companion OPC mixtures. Similarly, the addition of polymer, SRA or CRA reduces the early-age strength gain;

4. The effect of cement content on shrinkage is relatively small and no trend for higher shrinkage with increased cement content could be established. Likewise, the effect of w/cm ratio on shrinkage is also found to be relatively small;

5. Whereas cement replacement with only SF increased total shrinkage, the combined use of the FA and SF can greatly diminish the adverse effect of SF on shrinkage;

6. The addition of SF or combined SF/FA increased the cracking potential of the dry-mix shotcrete mixtures;

7. The addition of polymer had minimal effect on reducing the total free shrinkage (about 13 to 30%). However, the use of polymer can improve the cracking resistance by 13% to 35%;

8. The use of SRA and CRA significantly reduced the total free shrinkage by about 30 to 60%. The cracking resistance was also considerably improved by 55 to 78%.

9. CRA can provide internal stress relief and thus change the mode of failure detected in the instrumented ring from abrupt drop in compressive strain to a gradual release of the compressive strain in the steel ring;

10. Finally, this study demonstrates that it is possible to produce high-quality shotcrete ring specimens that comply with the AASHTO T 334 restrained ring test standard.

Based on the results presented, it is strongly recommended to extend the curing time of SF and/or FA mixtures to at least 7 days or to use an admixture such as SRA and CRA. In a subsequent phase to this research, the focus should be directed towards assessing the effect of FA and slag addition on rebound and shrinkage properties of dry-mix shotcrete in the absence of silica fume. It would be ideal to determine a dosage of SRA and CRA that would produce the highest reduction in shrinkage to minimize the potential for cracking of dry-mix shotcrete. In addition, the potential for shrinkage and restrained shrinkage cracking of blended dry-mix shotcrete mixtures under different curing regimes should also be tested experimentally. Further research will also be necessary to better evaluate the influence of fibres on reducing the effects of shrinkage, since fibre reinforced shotcrete is increasingly used for repairsf.

6.7 Acknowledgments

Chapter 7 *Article 5* - Evaluation of Early-age Viscoelastic Characteristics of Shotcrete Using Ring Specimens

Bruce MENU, Benoît BISSONNETTE, and Marc JOLIN

Department of Civil and Water Engineering, Université Laval, Quebec City, QC, Canada G1V 0A6

7.1 Résumé

Cet article a comme objectif de développer un modèle analytique pouvant prédire le fluage de traction des bétons projetés en couplant l'essai de retrait restreint et l'essai retrait libre effectué sur une éprouvette annulaire. L'étude fournit également une expression de la relaxation des contraintes de traction induites par retrait restreint. Les résultats obtenus confirment l'influence du fluage et relaxation sur le potentiel de fissuration des bétons de réparation.

7.2 Abstract

In this study, free and restrained shrinkage tests were conducted to derive the tensile creep characteristics of shotcrete mixtures using AASHTO ring specimens. A simple analysis procedure is outlined to quantify the tensile creep properties of wet-mix and dry-mix shotcretes using the results of the AASHTO ring tests and the elastic modulus tests. Analyses of the experimental results indicated that specimens with a higher level of creep or relaxation and lower shrinkage exhibited lower risk of shrinkage cracking. This indicates that higher tensile creep capacity is only useful in reducing the risk for cracking if the shrinkage is not increased in the same proportion. The results also indicated that silica fume, fly ash, polymer SRA and CRA influenced shrinkage and creep in a different manner. Overall, the analysis indicates that tensile creep is an essential component in the evaluation of the risk and sensitivity to cracking of shotcrete under restrained conditions.

Keywords: shotcrete; shrinkage cracking; ring test; tensile creep; relaxation; silica fume; fly ash; polymer; SRA; CRA

7.3 Introduction

Shotcrete (also called sprayed concrete) is a technique that consists of pneumatically projecting cement-based mixtures at high velocity onto a surface, using either the dry-mix or the wet-mix process. The technique is most suitable for shotcrete repairs, ground support in tunnels and mines, swimming pools, and other applications for which conventional placing methods would be impractical or very expensive. The benefits of using shotcrete is due to the inherent construction cost and time saving potentials since little or no formwork is required [6, 102]. Shotcrete also offer attributes such as good compaction, high strength, high durability, and low porosity and permeability. Shotcrete also has some drawbacks, notably with regards to its sensitivity to early-age shrinkage cracking [102]. In general, shotcrete mixtures have higher shrinkage rates than most conventionally cast concretes [6, 25] because they are often designed with high cementitious content and low coarse aggregate volume [78].

When cementitious materials are exposed to unsaturated ambient air after their curing, some of the water contained in the pores begins to evaporate. This phenomenon causes the material to undergo a contraction referred to as *shrinkage*. In practice, most shotcrete/concrete members are rarely, if ever, free to shrink; they are often internally or externally restrained (e.g. presence of reinforcement bars, connection with adjacent members, friction with the ground, etc.). These restraints to free shrinkage induces tensile stresses in the material that may easily reach the material's tensile strength and result in cracking if it is high enough [59, 101, 103, 104]. Shrinkage-induced phenomena can be severe and will, in most cases, lead to significant additional repair costs to prevent premature deterioration of concrete in service. It is one of the biggest challenges in the concrete construction industry due to the potential for *cracking*.

Early-age cracking characteristics of cementitious materials has been a subject of several studies over the years. Most studies on early-age cracking have focused on free shrinkage, shrinkage stress buildup, degree of restraint, and the tensile strength of concrete [36, 57, 101, 105]. However, the tensile viscoelastic behaviour (i.e. creep) of concrete also plays a significant role in the early-age cracking sensitivity of concrete [34, 72, 103, 106]. Unlike shrinkage, creep may be beneficial or detrimental depending on the situations or the type of structure. For instance, creep may be detrimental if it causes significant losses of prestress or if it results in excessive deformation and deflection, which may impair the structural integrity or behaviour of the structure. Conversely, it may be quite beneficial in reducing the cracking sensitivity of concrete, notably, most especially in repairs and in highly stressed areas of reinforced concrete elements, because it provides the material with some stress relaxation and distribution capabilities.

The ability to partially relieve the shrinkage induced tensile stress concentrations contributes to preventing or at least delay cracking. In many instances, the improved shrinkage cracking performance of concrete is due to creep-relaxation phenomena [72, 101, 103, 106]. It is therefore desirable to quantify tensile creep and relaxation of materials when studying the early-age cracking behaviour of concrete.

The ring test is widely used to qualitatively assess the sensitivity of cement-based materials to restrained-shrinkage cracking [65, 75, 101, 104, 105], but to this day, there is no standard method or approach for determining meaningful parameters or properties based upon the recorded material performance [34]. In this context, an approach was proposed in a previous study by See et al. [34] for indirectly assessing the tensile creep properties of concrete using *thin* concrete ring specimens. The model on which this approach relies, however, is not applicable to the thicker AASHTO ring setup, since shrinkage strain and the resulting stress in the latter are not uniform across the thickness. From the shotcrete technique point of view, the AASHTO test setup is preferable because it offers more room to accommodate the shotcrete spray, thus enabling easier achievement of homogeneity inside the specimen [67]. Besides, the previous model focused on conventional cast-in-place concrete which provides little insight on the cracking behaviour of shotcrete under restrained shrinkage conditions.

Otherwise, shotcrete significantly differs from conventionally cast concrete due to its unique mix designs, placement techniques, compaction dynamics, strength gain mechanisms, internal structure, and transport properties [78]. Therefore, our knowledge and understanding of the shrinkage cracking behaviour of cast concrete under restrained conditions must be applied to shotcrete with great caution. For example, many factors related to the shotcrete placement technique such as the orientation of the ring test set-up may affect the overall quality the sprayed specimens due to the risk of entrapping rebounding particles into the fresh shotcrete and creating defects that would negatively influence the homogeneity of the specimen and alter the test result [67].

To be able to select the mixtures that are best suited for thin repairs, information on the tensile creep capacity of concrete is necessary [35, 103]. However, literature regarding the tensile creep of shotcrete is rather scarce. The essential objective of this study is, therefore, to develop a protocol for indirectly quantifying tensile creep properties of shotcrete mixtures using an AASHTO ring specimen, using simple mathematical expressions. The study is also aimed at extending the interpretation of the ring test experiments performed on shotcretes. In essence, wet-mix shotcretes were cast following the AASHTO standard to validate the protocol developed. Then the AASHTO T 344 standard ring test method recently adapted to the shotcrete process (see [67]) was used to extract quantitative data on the tensile creep behaviour of different dry-mix shotcrete (i.e. ordinary portland shotcrete, shotcrete containing mineral additives (silica fume, fly ash) and chemical additives (polymer, shrinkage-reducing admixture, crack-reducing admixture). The overall study is part of an on-going research program devoted to the improvement of shotcrete robustness and durability, especially concerning its sensitivity to cracking.

7.3.1 Research Significance

Shrinkage cracking has a detrimental effect on the service life of shotcrete works. It is therefore essential to understand how the sensitivity to cracking of shotcrete mixtures can be effectively evaluated. To assess the risk for shrinkage cracking in shotcrete, a calculation approach based on the use of the AASHTO ring

test and the principle of superposition of deformations is proposed. This paper shows how the AASHTO ring can be used to obtain data on the tensile creep and relaxation behaviour of shotcrete. The model provides useful data for the shotcrete practice by helping engineers design cement-based materials that are more robust against cracking.

7.4 Determining Tensile Creep and Relaxation from Ring Specimen Measurements

It was shown in a previous study that cracking in restrained ring test specimens is strongly linked to the difference between free shrinkage and creep [102, 104]. In this context, it is imperative to evaluate the tensile creep that develops simultaneously when the shotcrete ring shrinks under restrained conditions. In this study, a model is proposed to indirectly extract quantitative data on the tensile creep properties by running in parallel free and restrained shrinkage tests (based on the AASHTO T334-08).

7.4.1 Quantifying Tensile Creep of Concrete Using Ring Specimen

From the principle of superposition of strains, the total average strain ($\varepsilon_c{}^T$) of a concrete element such as the ring test specimen subjected to both mechanical and environmental loads (temperature and relative humidity (R.H.)) can be expressed as the algebraic sum of all strain components given as follows:

$$\varepsilon_c{}^T(t) = \varepsilon_{sh}(t) + \varepsilon_e(t) + \varepsilon_{cr}(t) + \varepsilon_T(t) \tag{7.1}$$

where t, is the age at which the different strains are evaluated, ε_{sh} is the free shrinkage strain, ε_e is the instantaneous elastic strain, ε_{cr} is the creep strain, and ε_T is the thermal strain component. Since the temperature of a drying concrete ring specimen is kept constant during the experiments, the thermal strain can be neglected (i.e. $\varepsilon_T(t) \approx 0$). Therefore, the net concrete ring deformation is the sum of the elastic strain, creep strain, and drying shrinkage strain, which is balanced by the gradual increase of elastic contraction strain in the steel ring. This can be expressed algebraically as follows:

$$\varepsilon_c{}^T(t) = \varepsilon_{sh}(t) + \varepsilon_e(t) + \varepsilon_{cr}(t) \tag{7.2}$$

In the restrained shrinkage ring test, the total average strain, $\varepsilon_c{}^T$ is usually approximated as the strain recorded on the inner face of the steel ring with strain gauges, $\varepsilon_s(t)$. Thus, Eq. (7.2) can be rewritten algebraically as:

$$\varepsilon_s(t) = \varepsilon_{sh}(t) + \varepsilon_e(t) + \varepsilon_{cr}(t) \tag{7.3}$$

While Eq. (7.3) is valid for thin concrete ring specimens, in the case of thick cylinders, it is not valid to assume that the average total strain in the concrete is equal to the inner steel strain value. An alternate approach proposed in this study is to determine creep as the difference between the experimental average

strain (ε_e) and the theoretical average elastic strain ($\varepsilon_{e,theo}$), as depicted in Fig. 7.1. This can be expressed as follows:

$$\varepsilon_{cr}(t) = \varepsilon_{e,theo} - \varepsilon_e = \frac{\sigma_{c\_elas}(t)}{E_c(t)} - \frac{\sigma_{c\_avg}(t)}{E_c(t)} \tag{7.4}$$

where, E_c is the elastic modulus of concrete, σ_{c_elas} is the theoretical average elastic stress, and σ_{c_avg} is the experimental average stress. Considering the mechanical equilibrium between the steel and shotcrete rings, the experimental average tensile stress in the thick shotcrete ring can be expressed as follows [97]:

$$\sigma_{c\_avg}(t) = -\frac{R_{is}+R_{os}}{2R_{os}} \frac{A_s E_s}{A_c} \varepsilon_s(t) = -G\,\varepsilon_s(t) \tag{7.5}$$

where R_{is} and R_{os} are the inner and outer radius of steel ring, A_s and A_c are the corresponding cross-sectional areas, v_s is the *Poisson's* ratio of steel, E_s is the elastic modulus of the steel ring. G is a constant for a given ring setup ($G = 31.55$ GPa for the AASHTO ring used in this study). Based upon the work by Hossain and Weiss [75], the theoretical average elastic stress that would be expected to be induced by shrinkage in the absence of creep and relaxation at any given time, t can be determined using the following expression:

$$\sigma_{c\_elas}(t) = -\frac{\frac{\left(R_{oc}^2+R_{os}^2\right)}{R_{oc}^2-R_{os}^2}}{\frac{1}{E_s}\left(\frac{R_{os}^2+R_{is}^2}{R_{os}^2-R_{is}^2}-v_s\right)+\frac{1}{E_c(t)}\left(\frac{R_{oc}^2+R_{os}^2}{R_{oc}^2-R_{os}^2}+v_c(t)\right)}\,\varepsilon_{sh}(t) = -G'(t)\,\varepsilon_{sh}(t) \tag{7.6}$$

where R_{oc} is the outer radius of the shotcrete ring, v_c is the *Poisson's* ratio of shotcrete. $G'(t)$ for the selected ring setup can be expressed as:

$$G'(t) = \frac{2.6063\,E_c(t)}{0.0000571\,E_c(t)+2.6063+v_c(t)} \tag{7.7}$$

The tensile creep coefficient, ϕ_c can then be expressed in terms of tensile creep and elastic strains as:

$$\varepsilon_e(t) + \varepsilon_{cr}(t) = \varepsilon_e(t)[1+\phi_c(t)] \tag{7.8}$$

where $\phi_c(t) = \varepsilon_{cr}(t)/\varepsilon_e(t)$ (7.9)

Combining Eqs. (7.4), (7.6) and (7.9) leads to the expression for tensile creep coefficient summarized in Eq. (7.10):

$$\phi_c(t) = \left[\frac{G'(t)}{G}\frac{\varepsilon_{sh}(t)}{\varepsilon_s(t)}\right] - 1 \tag{7.10}$$

Note that equation (7.10) is only applicable provided the thickness of the concrete ring is sufficiently high enough to assume a thick cylinder behaviour.
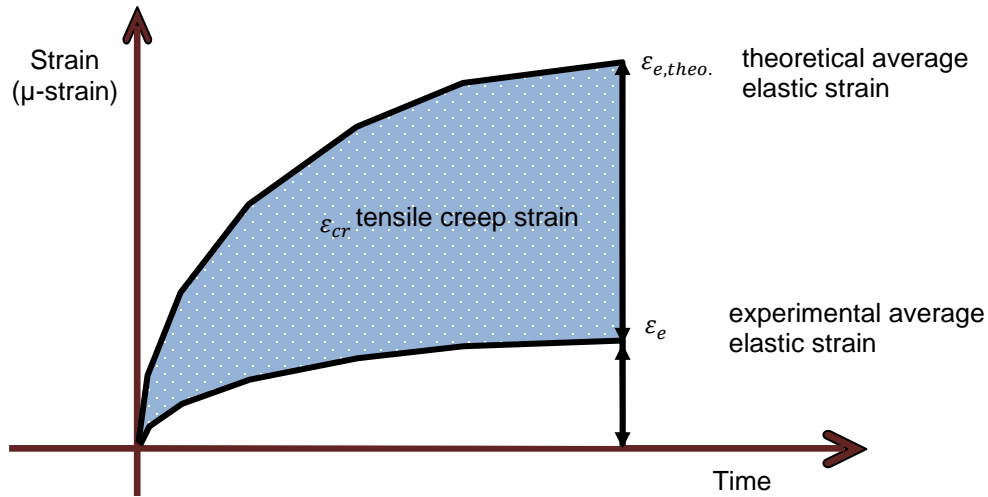
Fig. 7.1 Conceptual illustration of concrete strain components

7.4.2 Quantifying Stress Relaxation Using Ring Specimen

The theoretical average elastic stress and the average experimental stress can be compared to quantify the stress relaxation of shotcrete due to creep in the ring experiments. Thus, stress relaxation in ring specimens can be computed as the difference between Eqs. (7.4) and (7.6) (7.9) :

$$\Delta\sigma_{relax}(t) = G'(t)\ \varepsilon_{sh}(t) - G\ \varepsilon_s(t) \tag{7.11}$$

A similar approach has been previously adopted by other researchers [75, 107] to evaluate stress relaxation in concrete ring specimens. In the present article, the stress relaxation data are expressed in terms of the percentage ratio of the theoretical average elastic stress.

7.5 Experimental Program

Restrained and free shrinkage ring tests were performed to extract quantitative data on the tensile creep behaviour of shotcrete. Basic mechanical properties were also determined, namely: compressive strength, tensile strength, elastic modulus, and Poisson's ratio. From these measured properties, the theoretical average elastic strains, experimental average elastic strains, and the tensile creep properties were calculated. The main objective is to evaluate the effect of drying scenarios (i.e. radial and axial drying configurations), curing durations (i.e. 3 and 7 days), coarse aggregate content, silica fume, fly ash, polymer, shrinkage reducing admixture (SRA), and crack reducing admixture (CRA) on early age viscoelastic behaviour of shotcrete. The effect of drying scenarios (i.e. radial and axial drying configurations) and curing durations (i.e. 3 and 7 days) on early age viscoelastic behaviour of shotcrete was performed using wet-mix shotcretes while the effect of coarse aggregate content, silica fume, fly ash, polymer, SRA and CRA were performed using dry-mix shotcretes. The details of the experimental program are described in the following sections.

7.5.1 Materials and Mixture Proportions

The tests were performed using wet-mix and dry-mix shotcrete mixtures with a nominal maximum aggregate size of 10-mm. The aggregate size distributions used met the ACI 506 Gradation No. 2 requirements. All the mixtures were made with the same ordinary portland cement (OPC). The tested shotcrete mixtures were pre-blended and prepackaged. The wet-mix shotcretes were cast-in-place while the dry-mix shotcretes were sprayed. The wet-mix shotcretes were cast because the aim was to validate the model proposed to indirectly extract quantitative data on the tensile creep properties, study the influence drying layout, curing duration, and correlating the results with the literature. Hence, the method of placement (cast or sprayed) did not really matter, and gravitational casting was selected for simplicity. Two water-to-cementitious materials (w/cm) ratios of 0.45 and 0.60 were investigated. For the w/cm=0.45 mixture, about 5 kg/m^3 of naphthalene-based superplasticizer was used to obtain a satisfactory workability. No admixture was used in the w/cm=0.60 mixture. The wet-mix mixture proportions are presented in Table 7.1.

The dry-mix shotcretes consist of thirteen mixtures: two plain control shotcretes; three silica fume (SF) shotcretes; two combined silica fume and (class C) fly ash (FA) shotcretes; two silica fume shotcretes treated with a polymer (POL); two silica fume shotcretes including shrinkage reducing admixture (SRA); and two silica fume shotcretes including crack reducing admixture (CRA). The mixtures were divided into two groups representing the proportion of coarse aggregate by weight of the total dry ingredients: *15%* or *24% (23.7%)*. The mixture proportions of the dry constituents along with the corresponding *theoretical sprayed* composition of a cubic metre of the dry-mix shotcretes having a w/cm of 0.40 are presented in Table 7.2. It should be noted that the actual w/cm of sprayed shotcrete mixtures is unknown before spraying and therefore was experimentally determined (see Table 7.4).

The total binder (cement+SF or cement+SF+FA) content of all the dry-mix shotcretes is 21%. The replacement percentages of silica were 1.6% and 2.1% by weight of the total dry ingredients (i.e. about 8% and 10% by weight of cementitious materials). The replacement percentage of fly ash was 5% by weight of the total dry ingredients (i.e. about 24% by weight of cementitious materials). It should be mentioned that the polymer and SRA admixtures were pre-dosed/blended in dry form into the shotcrete mixtures before pre-bagging while the CRA was added in liquid form to the mixing water. Since the water content was unknown prior to spraying, the CRA dosages were determined based on the average water content of the corresponding reference silica fume only shotcrete.

Table 7.1 Composition of the wet-mix shotcretes mixtures investigated

Mix. description	w/cm	OPC cement (kg/m^3)	2.5-10 mm crushed limestone (kg/m^3)	0.08-5 mm natural sand (kg/m^3)	Water (kg/m^3)
W-045	0.45	445	736	1054	197
W-060	0.60	417	689	988	247

W denotes wet-mix

Table 7.2 Composition of the dry-mix shotcretes mixtures investigated

Mix. description	OPC cement		Sand (0-5 mm)		Stone (2.5-10 mm)		Silica fume (SF)		Fly ash (FA)		Admixtures	
	kg/m³*	wt.%**	kg/m³*	wt.%**	kg/m³*	wt.%**	kg/m³*	wt.%**	kg/m³*	wt.%**	Type	Dosage
D-15CA-Control	476	21.0	1452	63.9	341	15.0	-	-	-	-	-	-
D-24CA-Control	477	21.0	1257	55.3	539	23.7	-	-	-	-	-	-
D-15CA-2.1SF	426	18.9	1443	64.0	338	15.0	47.4	2.1	-	-	-	-
D-15CA-1.6SF	438	19.4	1445	64.0	339	15.0	36.1	1.6	-	-	-	-
D-24CA-1.6SF	439	19.4	1251	55.3	536	24.0	36.2	1.6	-	-	-	-
D-15CA-1.6SF-5FA	323	14.4	1437	64.0	337	15.0	35.9	1.6	112.3	5.0	-	-
D-24CA-1.6SF-5FA	324	14.4	1244	55.3	533	23.7	36.0	1.6	112.5	5.0	-	-
D-15CA-1.6SF-POL	430	19.4	1418	64.0	333	15.0	35.5	1.6	-	-	Polymer	20g/kg of binder
D-24CA-1.6SF-POL	431	19.4	1227	55.3	526	23.7	35.5	1.6	-	-		
D-15CA-1.6SF-SRA	428	19.4	1411	64.0	331	15.0	35.3	1.6	-	-	SRA	50g/kg of binder
D-24CA-1.6SF-SRA	429	19.4	1222	55.3	524	23.7	35.4	1.6	-	-		
D-15CA-1.6SF-CRA	438	19.4	1445	64.0	339	15.0	36.1	1.6	-	-	CRA	40ml/L of water
D-24CA-1.6SF-CRA	438	19.4	1251	55.3	536	23.7	36.2	1.6	-	-		

D denotes dry-mix; * values assuming w/cm=0.40; ** values by weight of total dry mixture constituents.

7.5.2 Placement methods

The conventionally batched and placed wet-mix shotcretes were prepared in a planetary mixer and cast gravitationally following the same sequence. The dry constituents were first introduced into the mixer. The water (including the water containing the superplasticizer where necessary) was then progressively added and mixing continued for 10 minutes. The springs activities were carried out indoors at the Université Laval's well-equipped *CRIB Shotcrete Laboratory*. The shotcreting operations took place in a rebound chamber and all the usually recommended spraying practices were followed [10].

7.5.3 Restrained Ring Test Specimens

The potential for shrinkage cracking was determined using the AASHTO T334-08 ring test geometry, which consists of a concrete ring with a wall thickness of 76 mm (inner and outer diameter of 305 mm and 457 mm) and height of 152 mm, with a 12.7 mm thick restraining inner steel ring (inner and outer diameter of 280 mm and 305 mm). As said before, the wet-mix shotcretes were cast while the dry-mix shotcretes were sprayed. The wet-mix shotcrete rings were cast-in-place following protocol as per AASHTO T334-08 (*formerly AASHTO PP 34-99*) whereas the dry-mix shotcrete rings were prepared using a modified AASHTO ring test method. As shown in Fig. 7.2c, the ring setup is placed overhead at an angle of 30˚ from

the horizontal position to facilitate rebound evacuation during spraying. The adaptation of the ring test method for shotcrete and its validation on shotcrete are described in detail elsewhere [67].

For each wet-mix shotcrete/test condition (i.e. drying scenarios and curing periods), at least two ring test samples were cast. In each case, two separate test batches were prepared to yield reliable data. Two ring specimens were also sprayed for the dry-mix shotcretes (in a single spraying session for each mixture). In all cases, the rings were kept under a wet burlap and a plastic sheet and kept at an ambient temperature of 23°C ± 2°C for the first 24 h after casting or spraying. Then, the outer wall of the ring forms was removed and the specimens were moist-cured for additional periods of 2 and 6 days with wet burlaps. A freshly cast and sprayed ring specimen (with an outer PVC or steel ring used temporarily for casting purposes) and a demolded test specimen are shown in Fig. 7.2.

a)   b)

c)   d)
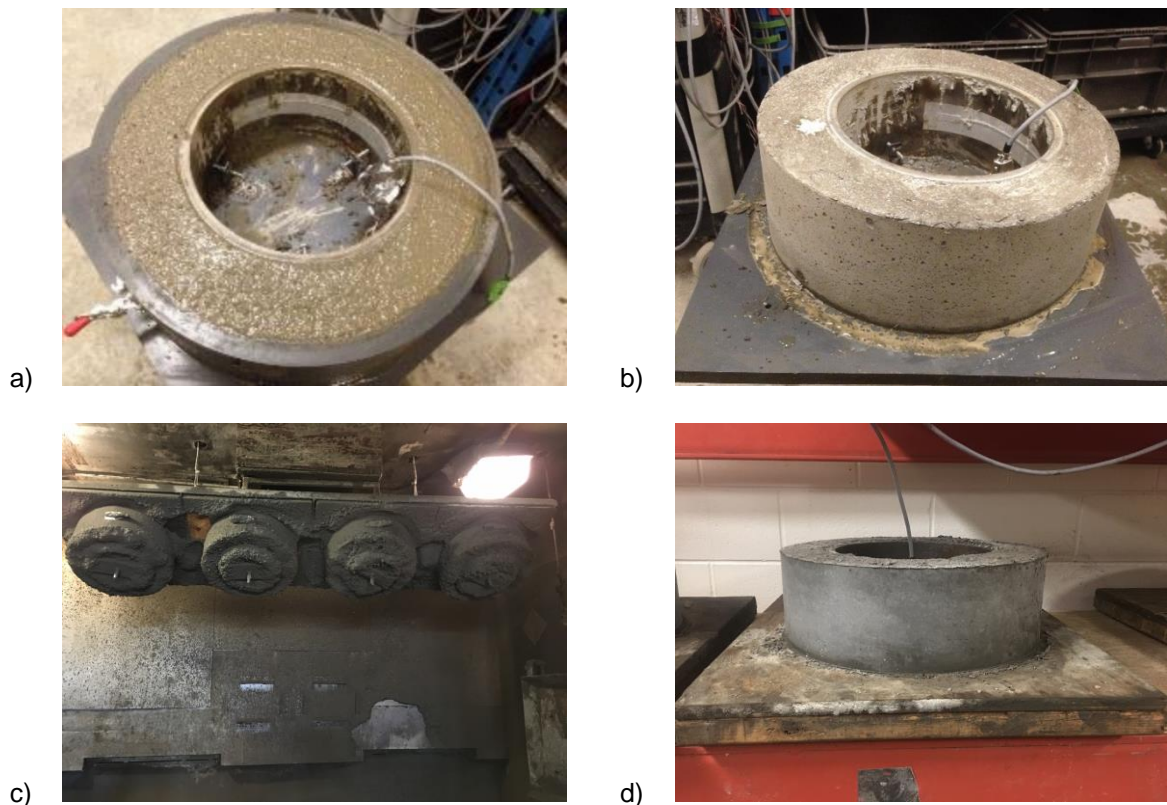
Fig. 7.2 AASHTO T334-08 ring test specimens: a) cast ring specimen with outer PVC wall (before demolding); b) demolded cast ring specimen at 24 h; c) inclined overhead sprayed ring specimen with outer steel wall (before demolding); and d) sprayed demolded ring specimen at 24 h

At the end of each moist curing period, two separate sets of the cast (wet-mix) ring specimens were subjected to different drying configurations: in the radial direction ("*circumferential drying*") or in the axial direction ("*top and bottom drying*"). Conversely, the sprayed (dry-mix) ring specimens were all subjected to

drying only in the radial direction, owing to the longer test duration when drying along the axial direction. The drying configurations were achieved by sealing with an adhesive aluminum tape such that drying is restricted only to the unsealed surfaces. All the ring specimens were exposed to drying in the same temperature- and relative humidity-controlled room at 21 ± 1.7°C (72 ± 3°F) and 50 ± 4% R.H. until cracking occurred. During the test, the shotcrete ring specimen dries and shrinks, but the inner steel ring opposes the shrinkage. This leads to a compressive stress buildup in the steel ring, which in turn induces increasing tensile stresses in the shotcrete ring. If the tensile stresses eventually exceed the tensile strength of the material in some location of the shotcrete ring, cracks will initiate.

The inner steel ring is instrumented with four (4) strain gauges to monitor the compressive strain development in the steel ring and to detect the occurrence of cracking in the shotcrete rings. The steel strain is monitored continuously from the time of shotcrete placement until cracking occurs in the ring. Cracking of the restrained specimen is revealed by a sudden and sharp decrease in the steel ring compressive strain (as seen in Figs. 7.3 to 7.6, (b)).

7.5.4 Free Ring Test Specimens

Free shrinkage tests were also performed on ring specimens using the AASHTO ring protocol except for the inner steel ring, which was replaced with an expanded polystyrene disc insert (details reported elsewhere [57]). Instead of using a free prismatic specimen, the approach is intended to measure both free and restrained shrinkage on specimens with identical geometry and boundary conditions to facilitate analysis and interpretation of the results. Again, the free wet-mix shotcrete ring specimens were cast while the free dry-mix shotcrete ring specimens were sprayed using the modified AASHTO ring test method. For each restrained specimen cast, a companion free ring specimen was cast or sprayed. The rings were demolded 24 h after casting and moist cured for an additional period of either 2 or 6 days under wet burlaps. Immediately after moist curing, DEMEC gauges were installed on top of the specimens for length change measurements. The free rings were then sealed with adhesive aluminum tape.

The rings were sealed such that they mimic the drying conditions of the corresponding restrained ring specimen (radial or axial drying conditions). The free ring specimens were stored in the same room as the restrained rings (21 ± 2°C and 50 ± 4% R.H.). Zero readings were taken immediately after sealing and upon exposure to drying. The length change of the specimens was monitored regularly throughout the drying period.

7.5.5 Mechanical characterization

Cylindrical specimens, 100×200 mm, were cast for the two wet-mix shotcrete mixtures. For the dry-mix shotcrete mixtures, a 600×600×200 mm test panels were sprayed for specimen coring. Core samples, 100×200 mm, were then extracted from the test panels according to the procedure recommended in ASTM C1604. In all cases, two specimens each were tested in compression at 3, 7, and 28 days after casting to

determine the modulus of elasticity and Poisson's Ratio of each mixture following ASTM C 469. Sets of three cylinders were used to determine splitting tensile strength at 3, 7, and 28 days. After curing in the cylindrical moulds in a normal laboratory environment for 24 h, the specimens were demoulded and moved into an environment chamber with 23 ± 2°C and 100% R.H. for curing until testing age. It is worth mentioning that the w/cm ratios of the sprayed mixtures were experimentally determined using a rapid drying technique within 30 min after the spraying.

7.6 Test Results

The evolution of the splitting tensile strength, modulus of elasticity, Poisson's ratio, and the 28-day compressive strength data of the tested wet-mix shotcretes are presented in Table 7.3. The experimentally determined w/cm ratios, splitting-tensile strength, modulus of elasticity, and 28-day compressive strength of the dry-mix shotcretes are also summarized in Table 7.4. The elastic modulus and Poisson's ratio values correspond to the average of two results, while the splitting-tensile strength and compressive strength values correspond to the average three results. Globally, the results are normal for such shotcrete mixtures. An important observation from these tests is that the utilization of polymer had no obvious effect.

Table 7.3 Mechanical properties of the hardened wet-mix shotcretes

Mixtures	Tensile strength, MPa			Modulus of elasticity, GPa			Poisson's ratio			Compressive strength, MPa
	3-days	7-days	28-days	3-days	7-days	28-days	3-days	7-days	28-days	28-days
W-045	2.4	2.6	3.2	25.8	26.8	30.0	0.18	0.17	0.16	37.2
W-060	2.4	2.5	2.7	25.4	26.3	28.8	0.19	0.18	0.17	33.2

Table 7.4 W/cm ratio and mechanical properties of the hardened dry-mix shotcretes

Mixtures	w/cm*	Tensile strength, MPa			Modulus of elasticity, GPa			Compressive strength, MPa
	-	3-days	7-days	28-days	3-days	7-days	28-days	28-days
D-15CA-Control	0.35	3.1	3.5	3.8	28.7	29.5	32.6	46.6
D-24CA-Control	0.39	3.4	3.7	4.0	28.7	29.5	32.7	48.8
D-15CA-2.1SF	0.51	2.0	2.6	3.1	18.0	20.0	22.3	33.3
D-15CA-1.6SF	0.48	2.4	2.9	4.0	22.7	27.1	28.6	43.9
D-24CA-1.6SF	0.55	3.1	3.1	4.2	25.5	26.1	32.7	50.8
D-15CA-1.6SF-5FA	0.53	2.3	2.4	3.4	17.0	17.7	32.7	29.8
D-24CA-1.6SF-5FA	0.55	2.4	2.5	3.4	19.7	25.3	32.6	34.2
D-15CA-1.6SF-POL	0.44	3.0	3.2	4.2	22.3	27.6	27.8	41.2
D-24CA-1.6SF-POL	0.51	3.1	3.1	4.2	20.8	26.7	31.8	41.4
D-15CA-1.6SF-SRA	0.45	1.7	2.6	3.3	19.9	21.5	26.3	34.6
D-24CA-1.6SF-SRA	0.51	1.9	2.7	3.6	21.1	23.8	26.9	35.4
D-15CA-1.6SF-CRA	0.34	2.9	3.2	4.4	19.8	21.9	35.4	47.9
D-24CA-1.6SF-CRA	0.39	2.9	3.0	3.9	23.9	24.3	30.6	40.8

* experimentally determined

The average free and restrained shrinkage test results obtained in radial drying condition for the two tested wet-mix shotcretes are presented in Fig. 7.3, while those obtained in axial drying are presented in Fig. 7.4. Similarly, the average free and restrained shrinkage test results obtained in radial drying condition for the dry-mix shotcretes containing 15% and 24% coarse aggregates are presented in Fig. 7.5, and Fig. 7.6, respectively. On each graph, the *x*-axis is the time elapsed since drying. As expected, a comparison of the free shrinkage strains and the corresponding strains measured in the restraining steel ring shows that the steel ring contraction is much less than the free shrinkage strain, irrespective of the mixture design.

Furthermore, Figs. 7.3 and 7.4(a) show that the higher the water content is in a freshly cast shotcrete, the greater the free shrinkage magnitude gets. However, the trends in Figs. 7.5 and 7.6(a) suggest that the overall effect of the water content on free shrinkage of sprayed shotcretes is rather small. Strict comparisons are difficult due to different methods of placement, but conflicting results can also be found in the literature, some indicating a strong influence of w/cm ratio on shrinkage [23, 44, 82], while others show instead a smaller impact of w/cm [36, 40]. By contrast, a very clear influence of the w/cm ratio on cracking resistance can be observed from Figs. 7.3 to 7.6(b), as it seems that a sharp drop in the steel strains occurs earlier in mixtures with lower w/cm ratio in otherwise equal conditions.

Also, it is found that the specimens moist cured for 7 days exhibited relatively smaller shrinkage strain after the same period and crack at later ages than those moist cured for 3 days. This suggests that prolonged moist curing, at least in that range (3 to 7 days), can improve the early-age shrinkage cracking performance of shotcrete in practice [102]. It can also be seen from Figs. 7.5 and 7.6 that the influence of coarse aggregate content is more pronounced under restrained conditions than under unrestrained conditions. The test data further show that silica fume increases free shrinkage while fly ash reduced the overall negative effect of silica fume on shrinkage. It is known that silica fume increases shrinkage [43, 108-110] whiles fly ash reduces shrinkage [44, 82, 108, 109] of concrete prepared with portland cement. However, cracking (i.e. a sudden drop in the streel strains) occurred at a significantly early age when silica fume or fly ash and silica fume are at the same time as partial replacement of cement due to slower development of strength at early ages [23, 44]. The results also clearly show that SRA and CRA were more effective in reducing shrinkage and cracking resistance of dry-mix shotcrete compared to polymer. The beneficial trends SRA and CRA are consistent with numerous previous findings [23, 25, 28, 48, 58].

It is interesting to note in Figs. 7.3 to 7.6 that higher free shrinkage in shotcretes does not always translate into earlier cracking under restrained conditions. As an example, the 0.60 w/cm ring specimens moist-cured for 3-days recorded higher free shrinkage than the 0.45 w/cm specimens moist-cured for 3-days. Yet, under restrained shrinkage, the 0.45 rings crack earlier than the 0.60 w/cm rings, irrespective of the boundary condition. Also, the silica fume only rings had higher shrinkage rates than the combined silica fume and fly ash rings, but the latter rings crack earlier. This tends to confirm that free shrinkage results are not always sufficient to assess the risk for restrained shrinkage cracking as previously reported [65, 82, 101]. In

127

practice, this implies that specification of a threshold limit for free shrinkage of cement-based materials *may not* result in shrinkage cracking prevention and as such may not be a proper criterion to ensure crack-free shotcrete or concrete.

Additionally, it is observed that the age at which shrinkage cracks occur in restrained shotcrete is dependent on the boundary condition and consequently the exchange surface-to-volume ratio (S/V) exposed to drying. It can be seen that the free shrinkage rate was significantly higher, and cracking occurred much earlier, respectively, in the case where the test specimens dried along the radial direction. This has to be explained, at least in part, by the higher S/V of ring specimens drying along the radial direction (i.e. 0.0158 mm^{-1}) compared to those drying along the axial direction (i.e. 0.0132 mm^{-1}).

a) Free shrinkage   b) Restrained shrinkage
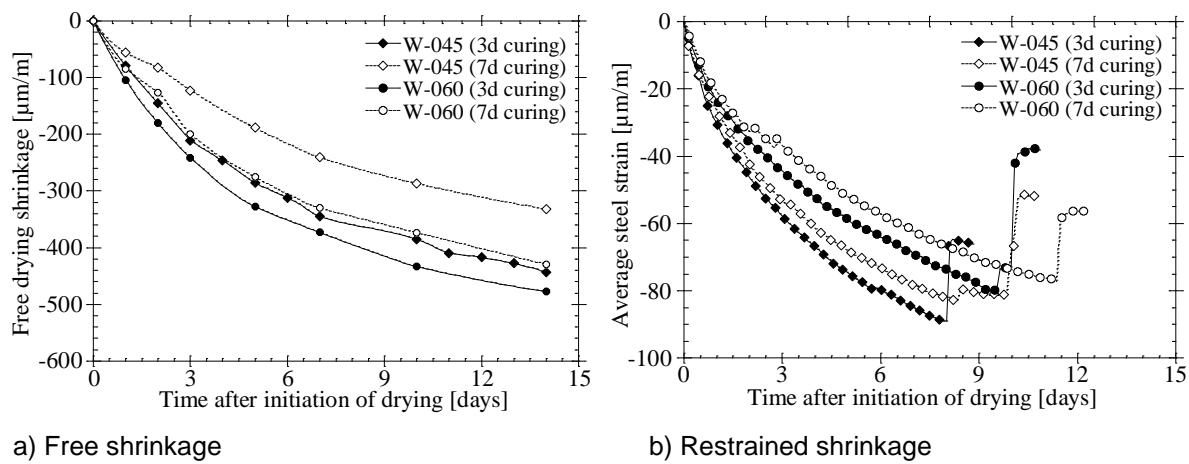
Fig. 7.3 Evolution of free and restrained ring shrinkage of the wet-*mix shotcretes* in radial drying configuration

a) Free shrinkage   b) Restrained shrinkage
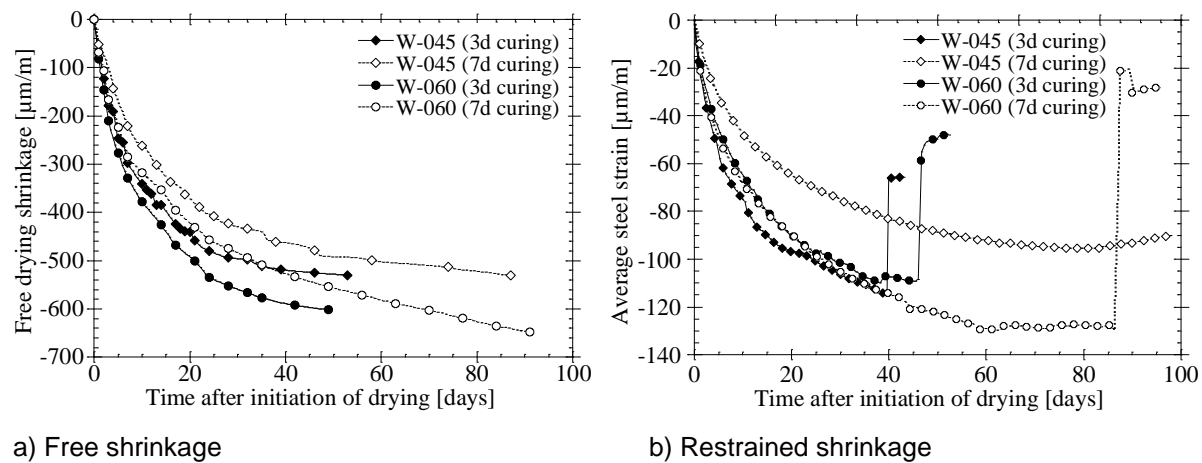
Fig. 7.4 Evolution of free and restrained ring shrinkage of the *wet-mix shotcretes* in axial drying configuration
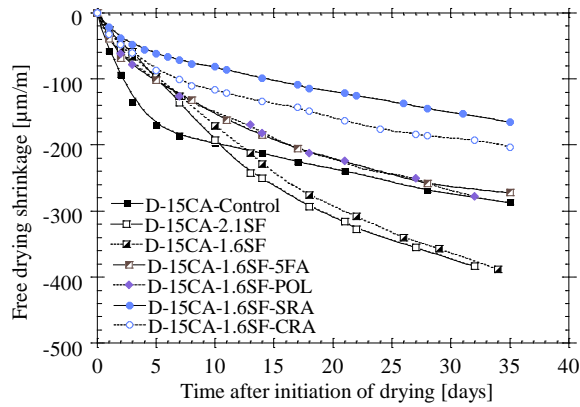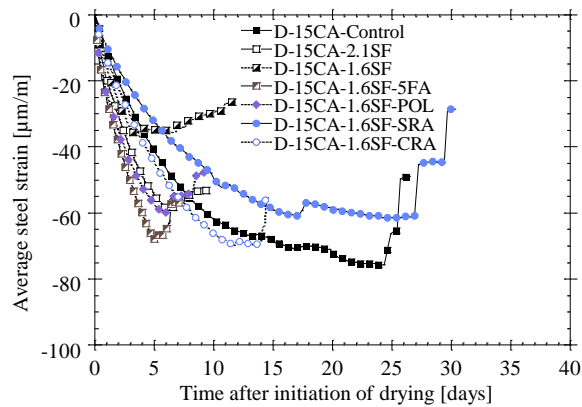
a) Free shrinkage

b) Restrained shrinkage

Fig. 7.5 Evolution of free and restrained ring shrinkage of the *dry-mix shotcretes* with 15% coarse aggregates
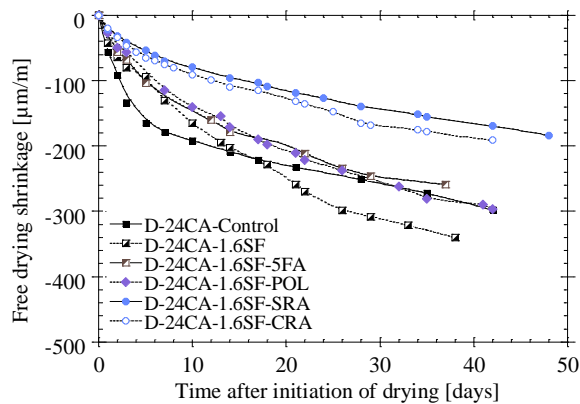
a) Free shrinkage
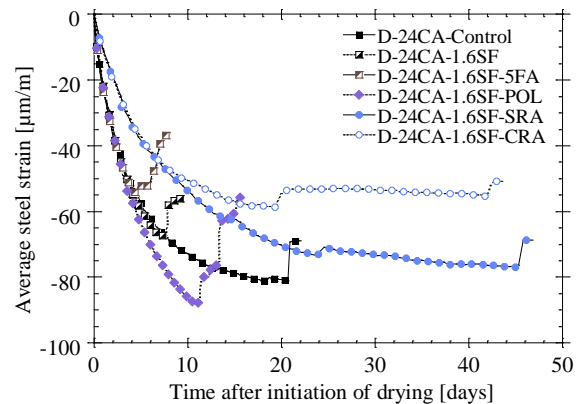
b) Restrained shrinkage

Fig. 7.6 Evolution of free and restrained ring shrinkage of the *dry-mix shotcretes* with 24% coarse aggregates

7.7 Discussion of Test Results

7.7.1 Influence of concrete creep and relaxation in the ring stress build-up and cracking outcome

In accordance with the approach presented earlier, creep underwent in the restrained shrinkage ring can be assessed based upon the evolution of the elastic modulus, Poisson's ratio, free and restrained shrinkage strains. In the process, the recorded elastic modulus and the Poisson ratio data were fitted as a function of natural-log of time, while the free and restrained shrinkage strains were fitted as a function of the square root of drying time, as has been reported in a previous study [34]. It should be mentioned that the Poisson's

129

ratio is difficult to quantify for the sprayed shotcretes, hence the values obtained for the cast shotcretes were used depending on the w/cm ratio. Also, Poisson's ratio of the steel ring is assumed not to vary with time (≈ 0.3). The tensile creep strain and coefficient values were calculated using Eq. (7.9) and Eq. (7.10), respectively. The specific tensile creep was subsequently determined as the ratio of the tensile creep strain to the corresponding tensile stress. It is worth noting that the creep parameters could be calculated up to the age of cracking in the ring specimens.

Figs. 7.7 and 7.8 present the specific tensile creep curves determined for the wet-mix and dry-mix shotcrete mixtures. In general, it can be inferred from the figures that the rings with higher specific tensile creep took a longer time to crack in otherwise equal conditions. The results in Fig. 7.7 indicate that the drying conditions had a significant influence on the calculated creep response in the ring specimens. Significantly higher specific tensile creep values were recorded for rings dried along the axial sides compared to those dried along the radial direction and cracking occurred significantly later in the former. The test results further show that the values obtained for the 7-day moist-cured rings are larger than the corresponding 3-day moist-cured specimens. Thus, an increase in curing time increases the tensile creep response that can contribute to relaxation before the occurrence of cracking.

The results in Fig. 7.8 also indicate that coarse aggregate content influenced the calculated creep response in the ring specimens. The early age specific creep response of ring specimens made with plain control mix, silica fume mix, and combined silica fume-fly ash mix decreased when the coarse aggregate content is increased from 15% to 24%. By contrast, the trend observed for the specific creep response in the rings treated with polymer, SRA, or CRA is exactly the opposite. At this stage, we do not have a satisfactory explanation for the mechanism involved. However, one could infer that higher coarse aggregate volume is more beneficial in dry-mix shotcrete when polymer, SRA, or CRA are used.

Furthermore, it can be observed that the addition of silica fume reduced the specific creep response, irrespective of the aggregate content. But as the proportion of silica fume increased, the creep response increased. The addition of fly ash in the presence of silica fume further decreased the specific creep response in the ring specimens. Generally, silica fume and fly ash improve the transition zone which could be responsible for the decrease in creep response [111]. There is conflicting data in the literature on the effects of silica fume and fly ash on creep response of cement-based materials. Some studies indicate that partial replacement of cement with silica fume or fly ash tends to reduce creep response [108, 109, 111], while others indicate instead an increase [35, 44, 110]. Some studies also found that creep response increase when silica fume is combined with fly ash [111] which is opposite to the trend observed here. As noted earlier, literature regarding tensile creep of shotcrete, in general, is rather scarce. A parameter that may play a significant role in the results obtained for the shotcrete mixtures is the effective paste content, which can differ based on many factors, notably rebound, and cannot easily be determined.

Also, it is evident in Fig. 7.8 that the use of polymer, SRA, and CRA markedly reduced the calculated specific creep response but took longer to crack. As pointed out in recent publications [34, 58, 112], the use of polymer and SRA can significantly reduce creep response. CRA is expected to have a similar influence as an SRA at equal dosages [48]. Given that fly ash, SRA and CRA also decreased shrinkage strains, and reduction in shrinkage is different from the reduction in creep [58], it can be argued that other factors besides tensile creep, such as shrinkage rate, can also significantly affect cracking behaviour [34]. As for the effect of the w/cm ratio, the results in Fig. 3.7 indicate that increasing the w/cm ratio from 0.45 to 0.60 resulted in increased specific tensile creep of cast rings. This could be expected since the creep behaviour is dependent upon the movement of pore water and pore structure [113]. The inherent effect of dry-mix spraying unfortunately did not allow us to validate the effect of w/cm ratio on the sprayed rings as it could not be strictly controlled.
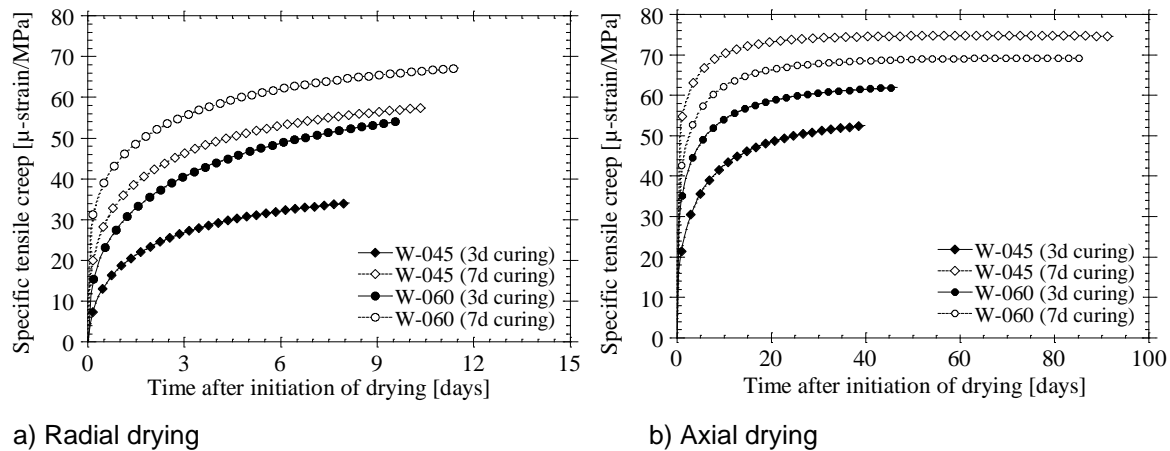
a) Radial drying   b) Axial drying

Fig. 7.7 Tensile creep data of the *wet-mix shotcretes* from the ring tests - evolution of the specific creep deformations

a) 15% coarse aggregates   b) 24% coarse aggregates
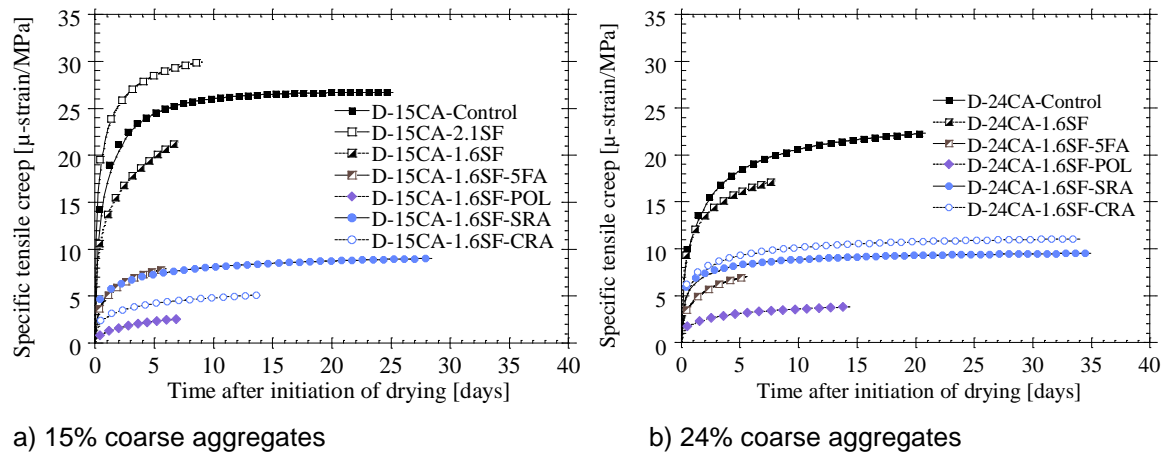
Fig. 7.8 Tensile creep data of the *dry-mix shotcretes* from the ring tests - evolution of the specific creep deformations

131

The tensile creep coefficients are presented in Fig. 7.9 and 7.10 for the wet-mix and dry-mix shotcretes, respectively. Again, it is obvious from Fig. 7.9 that the creep response of ring specimens is influenced significantly by a change in boundary conditions. Clearly, increases in creep coefficient of about 68 and 38% are observed in the case of 0.45 w/cm rings dried from the axial sides when compared to outer radial drying rings after 3- and 7-day curing, respectively. For the 0.60 w/cm rings, increases of about 24 and 15% were found, respectively. This indicates that creep played a very significant role in the long-testing periods observed in rings dried along the axial direction. This is attributed in part to the difference in the S/V ratio, the moisture and the stress profiles in the two drying layouts. The reader can refer to several interesting publications to find more information [65, 75, 97].

Similarly, it is clear from Fig. 7.10 that the creep coefficient of ring specimens is influenced by the coarse aggregate content and it follows the same trend as the calculated specific creep. The calculated creep coefficient of the plain control mix, the silica fume (only) mix, and the combined silica fume and fly ash mix decreased by 20%, 11%, and 12% when the coarse aggregate content is increased from 15% to 24%. This decrease in creep coefficient could be attributed to the higher elastic deformation in the rings containing 24% coarse aggregate so that the ratio of creep strain to elastic strain is relatively smaller. On the contrary, an increase of about 80%, 13%, and 150% is observed for the polymer, SRA and CRA treated shotcretes, respectively, when the coarse aggregate content is increased.

Concerning the effect of mineral and chemical additives, it was found that the addition of silica fume and combined silica fume-fly ash decreased the creep coefficient of the D-15CA-Control shotcrete by 38% and 75%. Comparatively, this value was about 29% and 71% for rings of the D-24CA-Control shotcrete when silica fume and combined silica fume-fly ash is added. Increasing the silica fume content (from 8% to 10% by wt. of cement) increased the creep coefficient by 12%. When treated with polymer, SRA, and CRA, the creep coefficient decreased by 88%, 40%, and 76%, relative to D-15CA-1.6SF and about 75%, 24%, and 27%, relative to D-24CA-1.6SF.
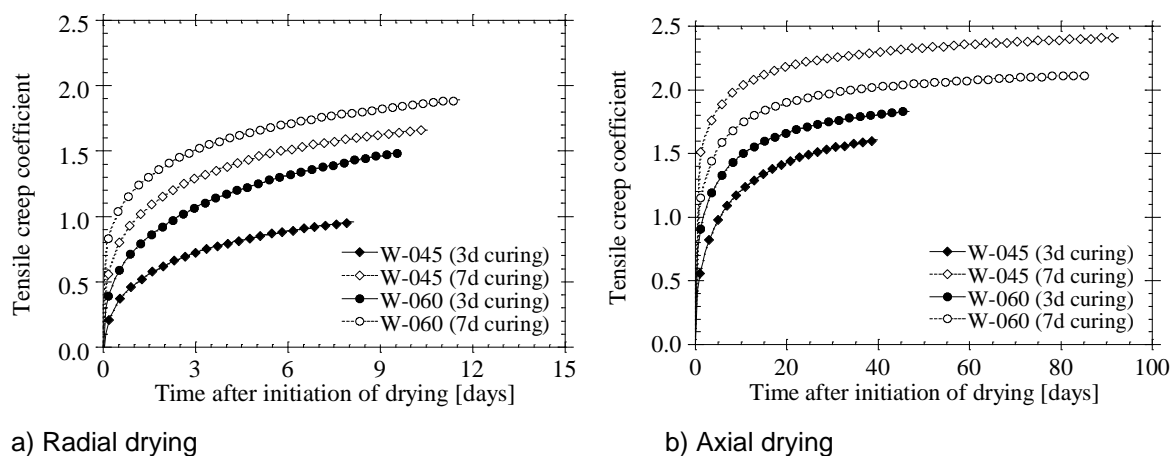
a) Radial drying   b) Axial drying

Fig. 7.9 Tensile creep data of the *wet-mix shotcretes* from the ring tests - evolution of the creep coefficients

a) 15% coarse aggregates   b) 24% coarse aggregates
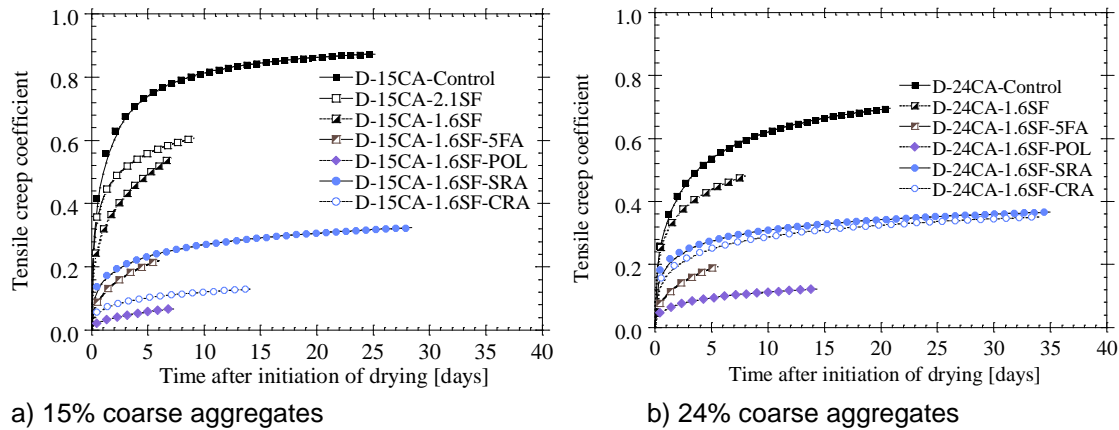
Fig. 7.10 Tensile creep data of the *dry-mix shotcretes* from the ring tests - evolution of the creep coefficients

The total tensile creep strain values of the wet-mix and dry-mix shotcretes investigated are presented in Figs. 7.11 and 7.12, respectively. The tensile creep strains at cracking for the 0.45 and 0.60 w/cm wet-mix shotcrete ring specimens moist cured for 3 days and then dried along the radial direction are about 102 and 136 microstrains. These represent 57 and 60% of the creep strains underwent in the rings dried along the axial direction, respectively. Comparatively, this value was about 62% for rings of both mixtures moist cured for 7 days. Further, it can be observed from Fig. 7.12 that the effect of coarse aggregate content on the development rate of tensile creep strains is lower than on the specific creep and creep coefficient. This is largely attributed to the different effects of coarse aggregate on tensile stress development and elastic deformation. Compared with the D-15CA-Control and D-24CA-Control shotcretes, the addition of silica decreased the tensile creep strains at cracking by about 48% and 32%. Comparatively, this value was about 75% for rings of both control shotcretes when fly ash is added in the presence of silica fume. Increasing the silica content also increased the tensile creep strains at cracking by 68%. When treated with polymer, SRA, and CRA, the tensile creep strains at cracking decreased by 83%, 43%, and 68%, relative to D-15CA-1.6SF and 70%, 42%, and 34%, relative to D-24CA-1.6SF.

a) Radial drying   b) Axial drying
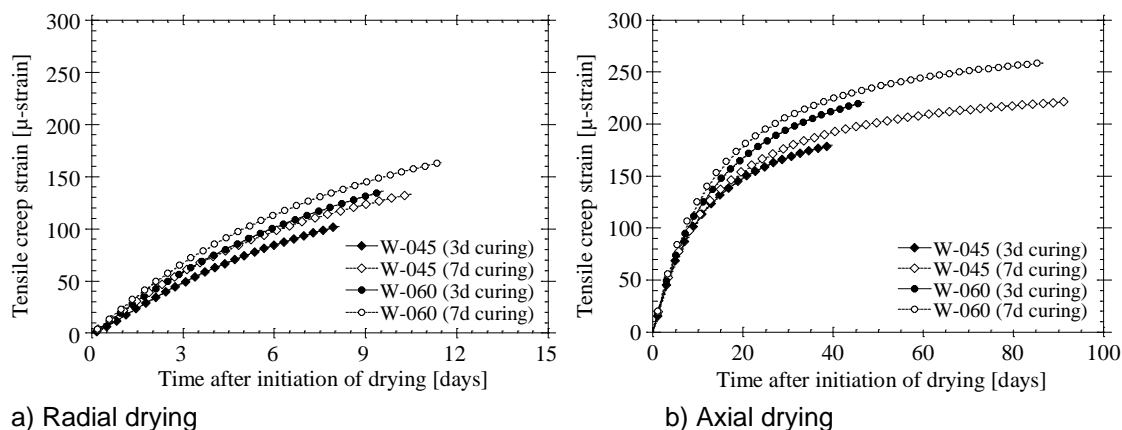
Fig. 7.11 Tensile creep data of the *wet-mix shotcretes* from the ring tests - evolution of the total creep deformations
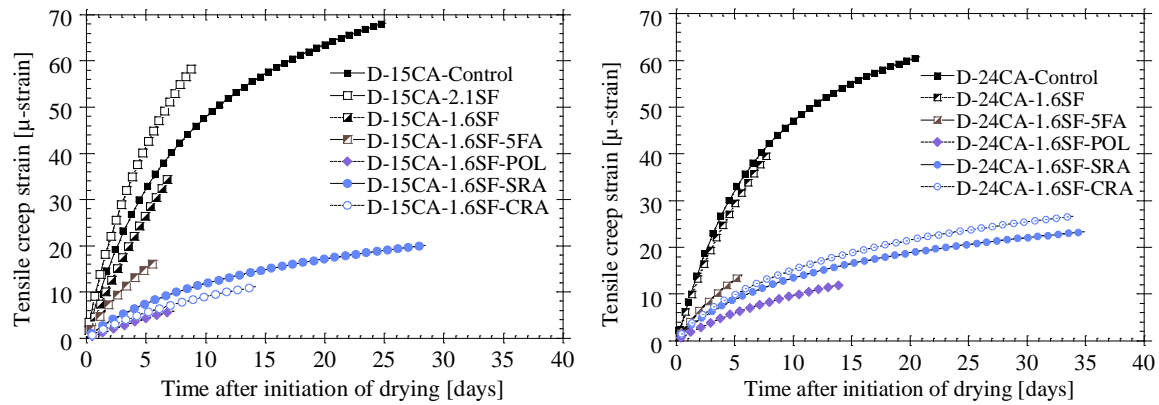
a) 15% coarse aggregates   b) 24% coarse aggregates

Fig. 7.12 Tensile creep data of the *dry-mix shotcretes* from the ring tests - evolution of the total creep deformations

The results obtained in terms of tensile creep strain to free shrinkage strain ratio which reflects reduction of tensile strain development in the restrained ring specimen is shown in Figs. 7.13 and 7.14 for the wet-mix and dry-mix shotcretes, respectively. Overall, the data in Fig. 7.13 shows that the creep/shrinkage ratio of cast shotcretes can be as high as 45% when the ring specimens are drying along the axial direction and about 40% along the radial direction. Fig. 7.14 also show that creep/shrinkage ratio of the control dry-mix shotcretes reached about 27%. This value is about 22% when silica is added and about 11% when fly ah is added to silica fume, about 7% when treated with a polymer, and 14% when treated with SRA and CRA. This indicates that tensile creep strain is a higher fraction of the free shrinkage strain for the wet-mix shotcrete, the plain dry-mix shotcretes, and the silica fume only dry-mix shotcretes than for the dry-mix shotcretes incorporating silica fume plus fly ash, polymer, SRA, or CRA. Overall, it can be inferred from the figures (especially when comparing mixtures with the same mixture proportions) that the higher the tensile creep/shrinkage ratio, the higher the resistance to cracking.

Fundamentally, the results obtained are consistent with the assertion that higher tensile creep capacity will only be useful in reducing the risk for cracking if the shrinkage is not increased in the same proportion [35]. This is particularly interesting in the case of the dry-mix shotcretes. For instance, the silica fume only shotcretes (D-15CA-1.6SF and D-24CA-1.6SF) recorded higher creep values than the same shotcretes treated SRA and CRA, but this was not useful in reducing the risk for cracking because the potential benefit was counteracted by an equally high shrinkage rate. Thus, although SRA and CRA significantly reduced creep response in ring specimens, the reduction in free shrinkage was in the same proportion or even higher, so the cracking resistance was improved. On the other hand, one could infer that the early age cracking observed in the ring specimens when fly ash or polymer is used is primarily because the reduction in tensile creep response is much greater than the reduction in shrinkage. This again shows that other

factors besides tensile creep, such as shrinkage rate, can also significantly affect cracking behaviour of shotcrete.
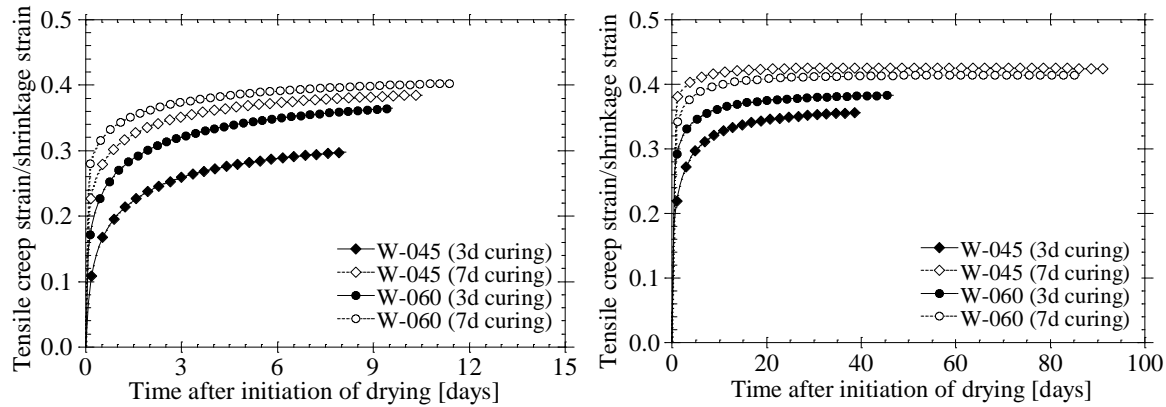
a) Radial drying   b) Axial drying

Fig. 7.13 Evolution of the tensile creep strain-to-shrinkage ratio of the *wet-mix shotcretes* in the ring experiments
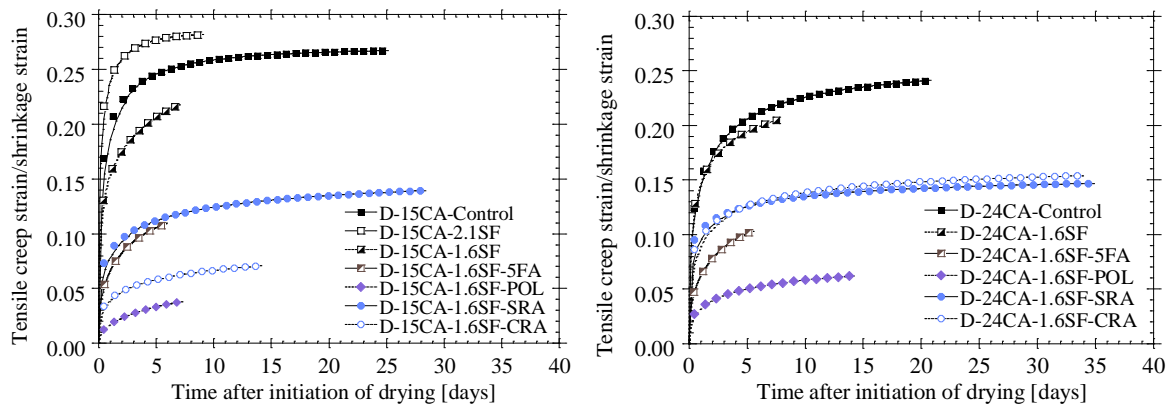
a) 15% coarse aggregates   b) 24% coarse aggregates

Fig. 7.14 Evolution of the tensile creep strain-to-shrinkage ratio of the *dry-mix shotcretes* in the ring experiments

The stress relaxation expressed as a percentage of the theoretical elastic stress for the wet-mix and dry-mix shotcretes is shown in Figs. 7.15 and 7.16. It can be seen in Fig. 7.15 that the amount of relaxation can reach as high as 70% at the time of cracking for the wet-mix shotcretes. It can also be seen in Fig. 7.16 that the amount of relaxation reaches about 45% for the control dry-mix shotcretes, 30 to 35% when silica is added, 18% when fly ah is added to silica fume, 9% when treated with a polymer, and 23% when treated with SRA and CRA. This implies that shotcretes containing blended cements do not relax as much as ordinary cement shotcretes and the potential for relaxation is even further decreased when chemical

additives (such as a polymer, SRA, or CRA) is used. It is worth noting that the amount of relaxation increased slightly when the silica content is increased. Overall, one could infer from the results that higher relaxation generally leads to greater resistance to cracking in restrained specimens. It is also apparent from the figures that rings with higher creep exhibited a higher amount of stress relaxation. Taken globally, it can be concluded that creep is beneficial to the assessment of the long-term durability of shotcrete mixtures, most especially if no chemical additive is used.

a) Radial drying   b) Axial drying
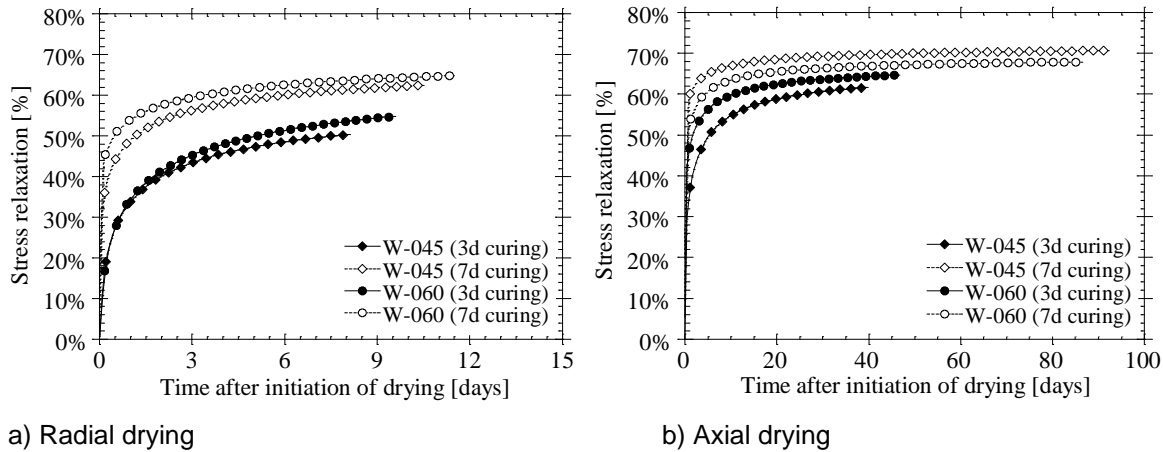
Fig. 7.15 Evolution of the tensile stress relaxation versus drying time of the *wet-mix shotcretes* in the ring tests

a) 15% coarse aggregates   b) 24% coarse aggregates
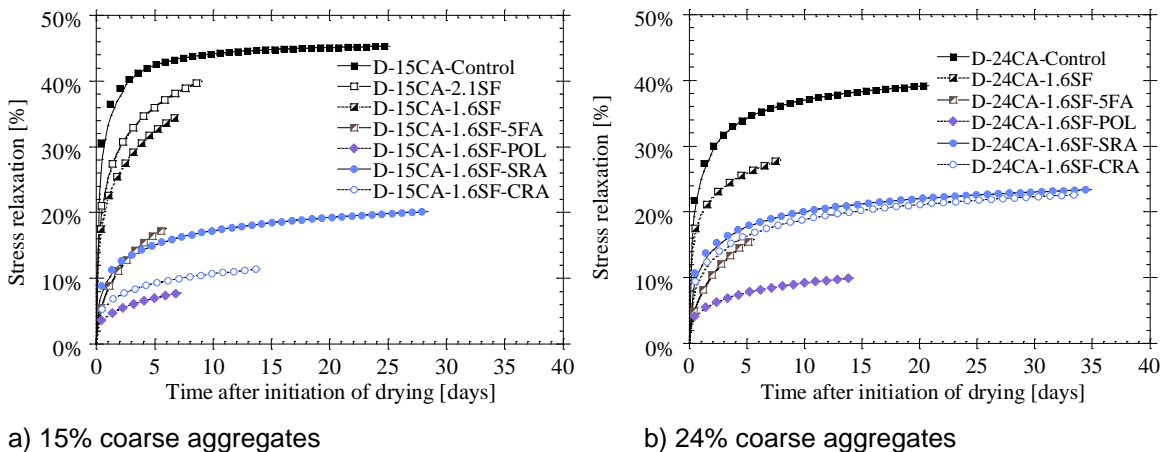
Fig. 7.16 Evolution of the tensile stress relaxation versus drying time of the *dry-mix shotcretes* in the ring tests

7.7.2 Cracking of restrained concrete

The prediction of cracking of cement-based materials in the restrained shrinkage ring test experiment is essentially based on the ratio of the experimental average shrinkage-induced stress and the tensile stress

(or the so-called *cracking potential*) [59, 75, 105, 107]. In this approach, the ring specimen is assumed to be close to failure when the shrinkage-induced stresses exceed the tensile strength of the material. Although theoretically failure is expected to occur when the ratio reaches about 1.0, experimental evidence typically shows that cracking takes place at lower values [75, 107]. Figs. 7.17 and 7.18 show the computed values of the average residual stress to tensile strength ratios obtained in the ring experiments for the wet-mix and dry-mix shotcretes.

a) Radial drying

b) Axial drying
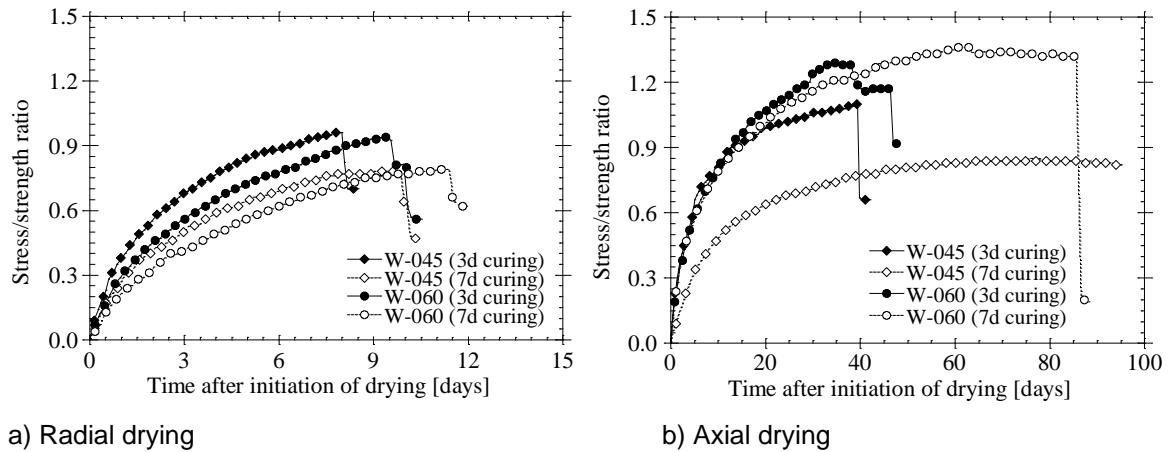
Fig. 7.17 Evolution of the stress-strength ratio of the *wet-mix shotcretes* in the ring experiments

a) 15% coarse aggregates

b) 24% coarse aggregates
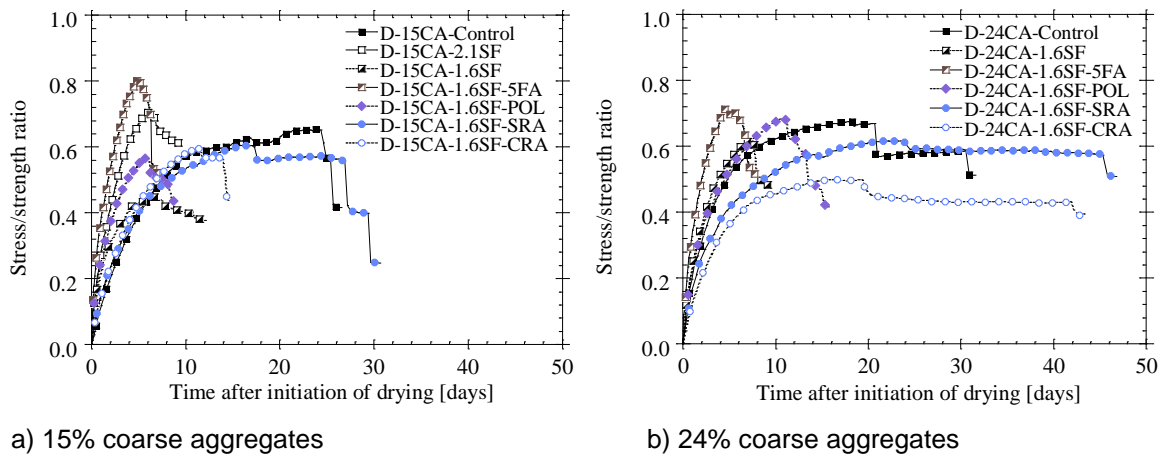
Fig. 7.18 Evolution of the stress-strength ratio of the *dry-mix shotcretes* in the ring experiments

Overall, it can be seen that failures occur at lower stress/strength ratios when rings are dried along the radial direction than along the axial direction. It has been found that failures occur at stress/strength ratios in the range of 0.70 to 1.0 when cast rings are dried along the radial direction and in the range of 0.81 to 1.22 when the same cast rings are dried along the axial direction. As mentioned earlier, the sprayed rings were subjected to drying only in the radial direction and it has been found that the failures occur at ratios of

0.50 to 0.80. In previous studies on conventional cast concrete, cracking at a stress/strength ratio in the range of 0.7 to 1.0 was also observed in ring specimens subjected to drying along the radial direction [65, 75, 107]. In an inherently more restrained ASTM ring specimen, cracking at a lower stress/strength ratios of about 0.35 to 0.51 has been reported for ring specimen dried along the radial direction [34] and approximately 0.65 for specimen dried along the axial direction [106]. This suggests that restraint is higher when shotcrete mixtures are sprayed than when cast-in-place.

Since all shotcrete rings from a given shotcrete mixture had the same tensile strength, if a tensile strength failure criterion was to be strictly applied, the rings drying along the axial direction with higher stress/strength ratios may be expected to crack earlier. However, it can be noted that despite the lower recorded stress/strength values, the rings drying along the radial direction failed at a much earlier age (≈ 8 to 12 days). Besides, comparing mixtures in Fig. 7.18(a) and Fig. 7.18(b), it can be seen that mixtures with higher stress/strength ratios did not always crack earlier. This tends to demonstrate that cracking resistance of concrete is not dependent on a single material property but the combined effect of different material properties and parameters of concrete [103]. Indeed, how long it takes for the ring specimens to crack may depend on other factors such as stress relaxation, S/V ratio, the degree of structural restraint, and the drying conditions which influence the rate of stress development [65, 72, 101, 105].
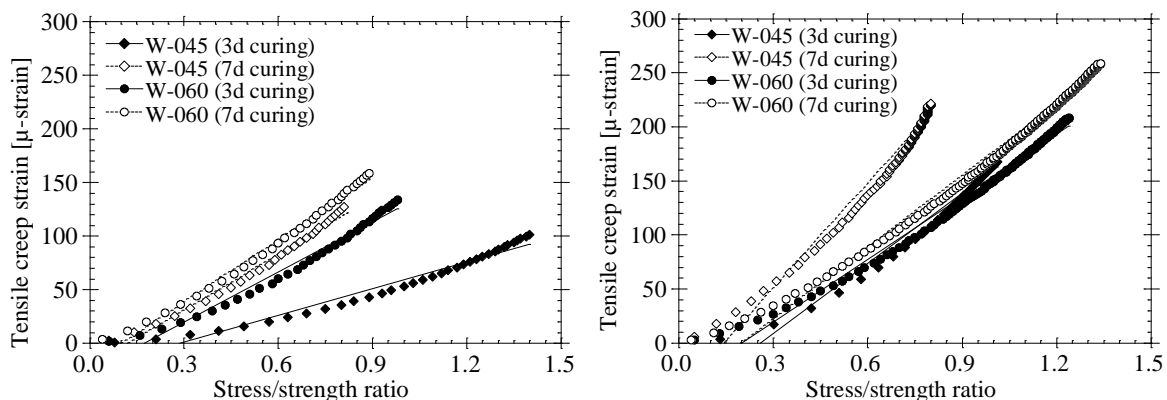
a) Radial drying

b) Axial drying

Fig. 7.19 Tensile creep data of the *wet-mix shotcretes* from the ring experiments - relationship between the creep strain and the stress-strength ratio

Further analysis showed that the relationship between tensile creep strain and stress/strength ratio departs from linearity at a stress/strength ratio of the order of 50 to 60% (Figs. 7.19 and 7.20). Beyond this limit, the ring specimen is close to failure, and microcracks may develop under restrained condition. Clearly, it can be that the stress/strength limit for failure is reached at lower creep values in rings dried from the radial sides compared to those dried from the axial direction. It may be recalled that the rings dried from the radial

direction also cracked at lower tensile stress/strength ratios (Fig. 7.17(a) and Fig. 7.18) compared to those dried from the axial direction (Fig. 7.17(b)).

a) 15% coarse aggregates   b) 24% coarse aggregates
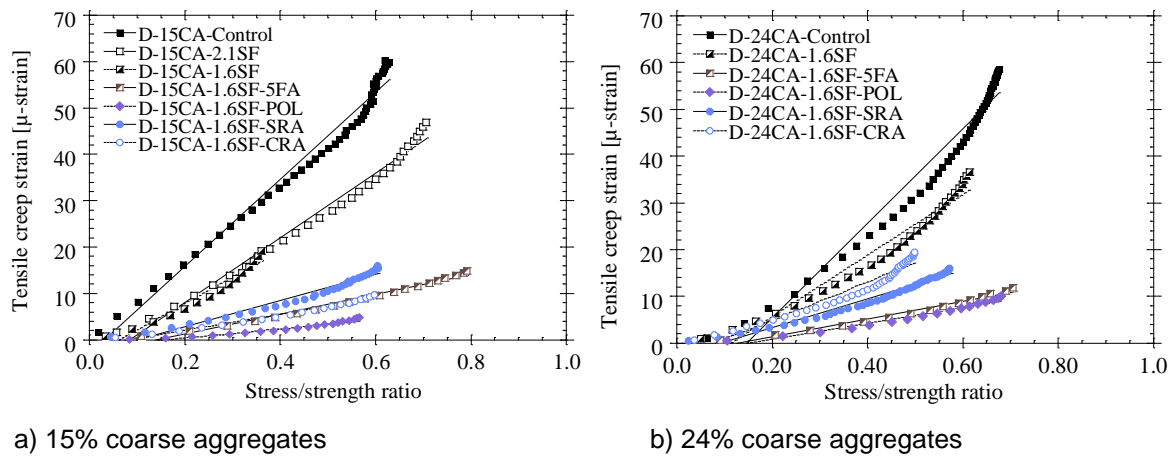
Fig. 7.20 Tensile creep data of the *dry-mix shotcretes* from the ring experiments - relationship between the creep strain and the stress-strength ratio

7.8 Conclusion

The experimental results and analytical treatment reported in this paper demonstrates how the restrained ring test can be used to extract quantitative data on tensile creep and the stress relaxation behaviour of shotcrete. Creep can be assessed provided that free shrinkage is monitored on companion specimens and material properties such as the elastic modulus, and the Poisson's ratio are known. Assuming the validity of the strain superposition principle, a simple procedure is proposed to evaluate the tensile creep behaviour of shotcrete using ring specimens. Additionally, stress relaxation was quantified by simply comparing the average stress determined experimentally in the shotcrete rings and the corresponding theoretical elastic stress.

1. The ring specimens can be used to extract quantitative data on tensile creep and stress relaxation behaviour of shotcrete. Specimens with higher tensile creep and relaxation characteristics generally took longer to crack in otherwise equal conditions.

2. The tensile creep/shrinkage ratio was found to be an important index for characterizing the role of creep in relaxing shrinkage stresses in shotcrete. The tensile creep strain determined in the ring specimen can be as high as 45% of the free shrinkage strain for the wet-mix shotcretes tested and ranged from 7% to 27% for the dry-mix shotcretes tested. The stress relaxation can also reach as high as 70% of the theoretical elastic stress for wet-mix shotcretes tested and ranged from 9% to 45% for the dry-mix shotcretes tested. This indicates that creep and relaxation must be taken into account for accurate characterization of early-age cracking of shotcrete.

3. The creep response of ring specimens is influenced significantly by a change in boundary conditions (i.e. drying conditions). Rings dried along the axial direction had higher creep and relaxation characteristics compared to those dried along the radial direction. Also, it has been found that at a similar stress/strength ratio, shotcrete deforms more when drying along the axial direction than along the radial direction.

4. The mixtures moist-cured for 3-days had a substantially lower tensile creep contribution than those moist-cured for 7-days, irrespective of the boundary conditions. This suggests that the duration of moist curing influences the balance of the various strain components involved and likely reaches an optimum at some point with regards to reducing the risk for cracking. The more favorable strain balance (shrinkage, elastic strain, and creep strain) explains the delayed cracking observed in longer moist-cured rings.

5. Coarse aggregate content affects the tensile creep of shotcrete. Increasing the coarse aggregate content of mixtures without chemical additives decreases creep response, which indicates that high coarse aggregate volume is more beneficial in dry-mix shotcrete when polymer, SRA, or CRA are used.

6. The use of silica fume, fly ash, polymer, SRA, CRA decreases tensile creep characteristics of dry-mix shotcrete. However, the reduction in creep characteristics when SRA and CRA are used does not increase the potential for early age cracking because shrinkage is also reduced in the same proportion.

To reduce the potential for shrinkage cracking of shotcrete, it may be necessary to rethink the use of silica fume and fly ash in dry-mix shotcrete. Keeping in mind that these mineral additives are used principally to reduce material rebound rate, it is recommended to use SRA or CRA to minimize their impact on the cracking potential of dry-mix shotcrete. A similar recommendation could be made when shotcrete is modified with a polymer. Overall, the creep approach presented in this paper provides an improvement to the use and interpretation of ring test results, which is much awaited in the repair industry, to assist both the development of crack-free repair materials and the issuance of improved materials performance specifications. Further work is needed to demonstrate its applicability to a wider range of shotcretes and its usefulness in applications such as concrete repair.

7.9 Acknowledgments

Chapter 8 Discussion of Test Results

8.1 Introduction

This chapter presents a discussion of the results compiled from the different papers to better summarize the influence of key parameters on rebound, shrinkage, and cracking behaviour of shotcrete. By the end of this chapter, the reader will understand that there are no simple answers to changing one mixture parameter to improve the shrinkage performance of shotcrete. Indeed, the potential for shrinkage cracking is dependent on the interaction of several factors, including the rate of shrinkage, age-dependent development of material properties, creep/stress relaxation, and degree of restraint.

8.2 Influence of Specimen Geometry and Boundary Conditions

The influence of fundamental drying parameters (specimen geometry, drying boundary conditions, and surface-to-volume ratio exposed to drying) upon shrinkage and cracking of shotcrete are studied in Chapters 3, 4, and 7. It was shown in Chapter 3 that shrinkage values recorded on prismatic specimens are higher than those recorded on ring specimens. This can be explained by the fact that the prismatic specimens have a higher surface to volume ratio exposed to drying than the ring specimens. Also, it was shown in Chapters 3, 4, and 7 that for the ring test specimens, drying from the radial direction leads to higher shrinkage than drying from the axial direction because of the higher surface-to-volume ratio of the former. Consequently, cracking occurred much earlier in the radial direction specimens than for those exposed to drying from the axial sides (as shown in Chapters 4 and 7). The early cracking of the ring specimen drying along the radial direction can also be attributed to the higher stress development along the outer circumference due moisture gradient [68, 114]. The overall influence of boundary conditions is also evident in the failure behaviour and the crack pattern. For example, crack initiates at the outer circumference and propagates towards the inside the ring for specimens dried in the radial direction, but initiates at the inner circumference and propagates towards the outer edge in the rings in the case of specimens dried in the axial direction. Proper modelling of the two drying configurations would be an exciting follow up to this project as it could help to better understand more precisely how the specimen boundary condition influences crack development and propagation in the restrained rings.

It should be noted that, due to the longer test duration when drying from the axial direction, that the radial drying configuration was used for the remainder of the research study for faster assessment of cracking potential of shotcrete in the lab (i.e. to determine the impact of the curing methods, the duration of moist curing and the effect of the key mixture parameters on shrinkage and cracking of shotcrete).

8.3 Influence of Key Mixture Parameters

8.3.1 Influence of Cement Content

The influence of cement content on the performance of shotcrete is addressed in Chapter 6. It was shown that the overall rebound rate is not affected much by the cement content. Also, it was expected that reducing the cement content (conversely, increasing the aggregate volume fraction) would decrease the shrinkage of shotcrete since shrinkage is a cement paste-related phenomenon. However, the results presented in Chapter 6 showed the overall influence of cement content on total free shrinkage is rather *small*, and no systematic trend of increase in total free shrinkage with an increase in the initial cement content could be established. It was shown that unlike regular cast concrete, the shotcrete placement process creates a somewhat "*self-adjusting*" material through the high velocity impact on the receiving surface to achieve a optimal paste content during spraying. Accordingly, an increase or decrease in the initial cement content affects how the nozzleman adapts the water content to maintain a certain desired consistency, which in turn affects the rebound and the optimal paste content (i.e., the in-place composition) and thus, the resulting shrinkage. Besides, as seen by the trend in Table 6.4, the w/cm ratio increased as the cement content decreased to achieve comparable spraying consistency, which increases the drying shrinkage, but decreases the autogenous shrinkage. The exact opposite occurs when the cement content is decreased. Since the total free shrinkage of the drying specimens included both the effect of autogenous and drying shrinkages, it is most probable that the respective variations in the two types of shrinkage somehow balance each other out, in such a way that the total shrinkage does not differ greatly.

Contrary to free shrinkage data, it was shown that reducing the cement content decreases the stress development in the ring specimen, and as a result, increases the age of cracking in the restrained specimen. This could be explained by the increase in tensile creep with a reduction in cement content (supplementary data is shown in Appendix C). However, it is necessary to mention that decreasing the cement content somewhat affects the homogeneity of the sprayed specimen, which may have altered the test results due to a potential increase in the intrinsic concrete variability. Indeed, it has been shown in Fig. 6.12 that the variability in cracking ages between two rings of the same spraying session is much higher in the lower cement content mixtures. As discussed in Chapter 4, failure in the concrete ring specimen occurs at the location of a defect or weakness. Therefore, the greater the spatial variability of the concrete, the higher is the potential differences in the time to cracking between the individual specimens. Besides, the potential benefit of the increase in cracking age when the cement content is decreased is also counteracted by the reduction in compressive strength and tensile strength.

Thus, considering the pluses and minuses, it is obvious that simply reducing the initial cement content of a dry-mix shotcrete mixture *does not* improve its overall performance.

8.3.2 Effect of Coarse Aggregate Volume Fraction

The influence of coarse aggregate volume on the performance of shotcrete is considered in Chapters 6 and 7. It was shown that an increase in the coarse aggregate volume fraction improves the strength of shotcrete. It was also shown that the overall influence of increasing coarse aggregate volume on total free shrinkage is rather small. However, the overall average age of cracking in the ring specimen was increased. This is explained by the increase in tensile creep strain with an increase in the aggregate content. But again, it is necessary to mention that the variability in cracking ages between two rings from the same spraying session is higher for the shotcrete mixtures with higher coarse aggregate contents than in the lower coarse aggregate content mixtures.

Generally, for the same cement content, the higher coarse aggregate volume should lead to a lower shrinkage. In the present study, it could not be verified, but may have been due to rebound and the self-adjusting phenomenon mentioned above. Although the overall rebound values obtained for the higher coarse aggregate mixtures were lower at similar consistency (refer to Fig. 6.5), the effective paste volume increased (refer to Table 6.4), because most of the rebounding particles are larger aggregates. This minimizes the actual expected influence of the additional coarse aggregates to restrain the shrinkage of the paste.

Taken globally, the results demonstrated again that it is difficult to study the effect of just one parameter in the shotcrete process, because of the self-adjusting phenomenon that occurs during spraying. But it is safe to say that the use of higher coarse aggregate content in shotcrete mixtures can be beneficial to both the plastic and hardened properties, especially when mineral additives and admixtures are used. The secret lies in knowing how much coarser aggregates is enough to prevent excessive rebound and unnecessary increase in the in-place paste content (i.e., finding the optimal aggregate size distribution, Jolin and Beaupré [13]).

8.3.3 Effect of Silica Fume

The influence of silica fume on the performance of shotcrete is studied in Chapters 6 and 7. It was shown that the presence of silica fume in shotcrete improve the 28-day compressive and tensile strength values, although a lower strength is observed at an early age (i.e., 3 and 7 days). The presence of silica fume, however, did not reduce the boiled water absorption (BWA) and volume of permeable voids (VPV) of shotcrete, which may be related to the higher water content of the silica fume mixtures (refer to Table 6.4). The clear advantage of using silica fume in shotcrete is the substantial reduction in rebound losses (up to a 37% reduction). The reduction is attributed to the marked improvement in adhesion and cohesion of the mixtures and the higher water content allowed when silica fume is added. Thus, silica fume in shotcrete is beneficial from an economic point of view [95, 115, 116].

Although this one reason alone may be a strong argument for its use of in shotcrete, it was shown conversely that the presence of silica fume also significantly increases the early-age shrinkage and risk for cracking. Overall, silica fume increased the total free shrinkage by up to 38% when compared to the plain mixtures. The age of cracking was also reduced by as much as 67 to 81%. An earlier study by Girard [3] also found that adding silica to dry-mix shotcrete can reduce the age of cracking by 59 to 68%. This increase in the sensitivity to cracking is attributed to higher stress at an early age coupled with the lower creep potential of silica fume shotcretes, due to their dense microstructure. It is known that silica fume increases the early-age shrinkage and cracking tendency of cement-based materials [23, 43, 108-110]. Increasing silica fume content did not affect the overall shrinkage, which again can be explained the self-adjusting phenomena.

From a practical viewpoint, this is a challenge, because silica fume significantly reduce shotcrete rebound and facilities the overall placement, which is highly desirable. One of the questions is whether extended moist curing would allow to reduce the cracking potential to an acceptable level for a silica fume shotcrete. As can be found in Chapter 5, longer moist curing periods can delay the advent of drying shrinkage and therefore can prevent cracking of silica fume shotcrete on the job site. When longer moist curing periods are not possible, it may be necessary to use admixtures such as polymer, SRA and CRA.

8.3.4 Effect of Fly Ash

The influence of fly ash on the performance of shotcrete is shown in Chapters 6 and 7. It should be noted fly ash was not used alone but added to silica fume. It was shown that the presence of fly ash in shotcrete decreased shotcrete strength and tensile strength at all age (i.e., 3, 7, and 28 days). However, the presence of fly ash improved the BWA and VPV of shotcrete, hence enhancing the overall quality of the placement by shifting it from "good" to "excellent" (refer to Table 6.5). Furthermore, fly ash reduced the rebound of shotcrete by 24% when compared to the plain mixtures but did not improve rebound when compared to the silica fume only mixtures. The addition of fly ash also reduced the total free shrinkage when compared to the OPC and silica fume only mixtures (refer to Fig. 6.8 b). This suggests that fly ash has the potential to reduce the negative influence of silica fume on the shrinkage [43]. However, it appears that fly ash in the presence of silica fume tends to significantly increase the potential for early-age cracking. The introduction of fly ash reduced the cracking age by as much as 81% when compared to plain mixtures and between 8% to 35% compared to the silica fume only mixtures. This could be associated with the increased stress rate and the reduction in creep potential of these shotcretes.

From a practical viewpoint, this is again a challenge, because fly ash can reduce rebound, improve the placement quality and free shrinkage of shotcrete, which is desirable, but it also increases the potential for cracking, which is undesirable. Once more, the question is whether extended moist curing would allow to reduce the cracking potential to an acceptable level.

8.3.5 Effect of Polymer

The influence of polymer on the performance of shotcrete is studied in Chapters 6 and 7. It was shown the addition of polymer reduced strength development at an early age, but did not significantly affect the 28-day strength. It was also shown that the used polymer did not improve the BWA and VPV of shotcrete, so the overall quality of placement is not improved (refer to Table 6.5). However, even if this is a single observation, the dust produced during the spraying process was significantly reduced. Adding polymer also reduced the rebound by up to 25% when compared to the plain shotcretes but did not further improve rebound performance when compared to the silica fume only mixtures. Further, it was shown that the addition of polymer can reduce the overall free shrinkage of shotcrete by up to 30%. It was also shown that the addition of polymer can also extend the time to cracking by 13 to 35% when compared to the silica fume only mixtures. This suggests that polymer can fairly increase cracking resistance where silica fume is included in shotcretes; it should most probably be included more generally in repair dry-mix shotcrete as it somehow improves the robustness, with regard to the potential for cracking of mixtures containing silica fume.

8.3.6 Effect of Shrinkage-Reducing Admixture (SRA)

The influence of SRA on the performance of shotcrete is studied in Chapters 6 and 7. It was shown that the addition of SRA slightly reduces the strength development of shotcretes at all ages. It was also shown that SRA significantly improves BWA and VPV of shotcrete, thereby improving the overall placement quality by shifting from "good" to "excellent" (refer to Table 6.5). Furthermore, it was shown that SRA can reduce shotcrete rebound by up to 40% compared to the plain and about 24% compared to the silica fume only mixtures. The advantage of using SRA in shotcrete is the substantial reduction in shrinkage and the associated cracking. The reduction in shrinkage is about 40-50% when compared to silica fume only shotcrete mixtures. An increase in the time to cracking of up to 78% is also observed with the addition of SRA. The weight loss measurements also indicated that SRA reduced the rate of weight loss from drying, which in part explains the associated reduction in shrinkage rate. Also, it was shown in Chapter 6 that SRA decreases the magnitude of tensile creep of shotcrete, but does not increase the potential for early-age cracking because shrinkage is also reduced in the same proportion.

Thus, with the exception of a slight decrease in strength, the SRA appears to be the best option for shrinkage and cracking control of shotcrete in addition to reducing rebound and the placement quality, especially when prolonged moist curing is not possible.

8.3.7 Effect of Crack-Reducing Admixture (CRA)

The influence of CRA on the performance of shotcrete is also addressed in Chapters 6 and 7. It was shown that the addition of CRA increased the strength of the lower coarse aggregate content mixtures by 10%, while reducing the strength of mixtures with higher coarse aggregate content by 20%. The addition of CRA

also significantly improved the BWA and VPV of shotcrete, and thus enhanced the overall placement quality by shifting it from "good" to "excellent". Furthermore, it was shown that CRA can reduce shotcrete rebound by up to 30% compared to the plain and about 5 to15% compared to the silica fume mixtures. Also, it was shown that addition of CRA can substantially decrease shrinkage of shotcrete and thus improve its cracking resistance. The reduction in shrinkage is about 30-50% when compared to that of the silica fume shotcrete. An increase in the age of cracking of up to 77% is also observed with the addition of CRA. The use of CRA also decreased tensile creep characteristics of shotcrete but similar to SRA, it does not increase the sensitivity to early age cracking because shrinkage is also reduced in the same proportion.

The overall results suggest that CRA is effective in minimizing shrinkage and cracking of shotcrete without compromising its overall performance and as such could be used in shotcrete to improve the robustness of mixtures containing silica fume. The principal benefit of CRA over SRA appears to be its post-cracking behaviour. Indeed, whereas a sudden abrupt drop in compressive strain was observed in all other shotcrete specimens upon cracking (as expected), a gradual reduction in strain was instead observed in the CRA-treated mixtures. This phenomenon is attributed to the relaxation of tensile stress (i.e. internal stress relief) within the CRA-treated specimens. It will be extremely interesting to investigate how this promising post cracking behaviour observed in restraint shrinkage rings translate in the field. With proper curing, this may well be the most robust mix design tested during this project.

8.3.8 Effect of w/cm Ratio

The influence of the w/cm ratio on the performance of shotcrete mixtures has been discussed in Chapters 3 to 7. Overall, the test results show that strength development of shotcrete is a function of the w/cm ratio. Mixtures with a lower w/cm ratio, in general, tend to produce higher strengths and vice versa. It was also shown that the relationship between w/cm ratio and shrinkage of shotcrete is not consistent. For example, while the test data in Figs. 3.7, 4.5, 7.3a, and 7.4a show that higher w/cm leads to higher free shrinkage, the results in Figs. 5.5, and 5.6 seems to suggest the exact opposite. Further, the test data in Figs. 3.6, and 6.8 also seems to suggest that the overall effect of the w/cm on free shrinkage is rather small. This is what was concluded by Bissonnette et al. [36] for concrete, mortar and cement paste between w/cm = 0,35 to 0,55. It is possible that some of the several factors that are dependent on the w/cm ratio and that affects shrinkage (pore size distribution, total porosity, modulus of elasticity, creep, water diffusion, etc.) might have opposite individual effects [36] in such a way that the overall effect of w/cm on shrinkage may vary depending on the mixture composition and the placement method. Conflicting results can also be found in the literature, some indicating a strong influence of w/cm ratio on free shrinkage [23, 44, 82], while others showing instead a smaller impact of w/cm [36, 40].

In contrast with the free shrinkage results, a very clear influence of the w/cm ratio on cracking resistance of shotcrete has been observed under restrained conditions. The test results presented in Chapters 4, 6, and 7 clearly show that cracking occurs earlier when the w/cm of the mixture is lower in otherwise equal

conditions. This behaviour is primarily due to the more significant contribution of autogenous shrinkage in the lower w/cm mixtures. Since autogenous shrinkage is higher when the w/cm is low, this increases the stress rate in the material and consequently the potential for shrinkage.

Overall, it does appear that within the limits and conditions met in this study, designing shotcrete mixtures to target a higher w/cm can increase the cracking resistance (although the free shrinkage magnitude *may not* be decreased). Incidentally this supports and 80-year-old recommendation for "gunite" (dry-mix shotcrete) which recommends to place it at its *wettest stable consistency* for best results [86].

8.4 Effect of Curing Method and Curing Periods

The influence of curing methods on shrinkage and strength development of shotcrete is discussed in Chapter 5 while the influence of moist curing duration is shown in Chapters 3, 4, 5, and 7. Overall, it was shown that curing methods and the duration of moist curing markedly affect the magnitude of shrinkage and strength of shotcrete. As expected, it was shown in Chapter 5 that the moist-cured specimens reached the highest strengths, whereas the air-cured specimens had the lowest. It was also shown that moist curing produced the lowest total free shrinkage, while dry curing produced the highest total free shrinkage. Curing compound is found to be ineffective in the lower w/cm mixture while reducing only very slightly the shrinkage in the higher w/cm mixture. Furthermore, it was shown in Chapters 3, 4, 5, and 7 that increasing the moist curing duration improves the strength gain of shotcrete. Longer moist curing duration is also found to delay the onset of shrinkage or prevent the effects of shrinkage on shotcrete. It was shown in Chapters 4 and 7 that the specimens moist cured for 7 days crack at later ages than those moist cured for 3 days. This is attributed to an increase in tensile creep response that can contribute to relaxation before the occurrence of cracking.

This suggests that prolonged moist curing, at least in that range of 3 to 7 days, can markedly improve the early-age shrinkage cracking resistance of shotcrete in practice. Thus, going back to the discussion on the need for silica fume and/or fly ash to control rebound, the questions was whether extended moist curing would allow to reduce the cracking potential to an acceptable level when these mineral additives are used in shotcrete. The answer to the question appears to be yes, proper or longer curing would allow to mitigate the cracking potential of shotcrete on the job site.

8.5 Influence of Method of Placement

This discussion would not be complete without looking at the relationship between the shotcrete placement method and the performance. The shrinkage of the sprayed dry-mix shotcretes (Chapters 5, 6, and 7) were first compared to the cast wet-mix shotcretes were (Chapters 3, 4, and 7). The mixtures compared were simple OPC based shotcretes (i.e. both groups of mixtures consisted of cement, natural sand and crushed limestone). In comparison with the "cast" shotcretes with similar mixture composition, the "sprayed" shotcretes studied exhibited better early-age strength development and shrinkage resistance in otherwise

equal conditions. Although strict comparisons are hazardous because of miscellaneous differences in experimental procedures, placement method and materials, the shrinkage of the sprayed dry-mix shotcretes (Chapters 5, 6, and 7) and shrinkage data from a previous study [3] were also compared to data extracted from the literature (mixtures with identical w/cm ratios and curing method). Considering the pluses and minuses, it is the view of the author that a properly designed and applied shotcrete can achieve higher strength with equal or lower shrinkage cracking sensitivity when compared to an equivalent cast-in-place concrete in otherwise equal conditions.

For example, the 28-day total free shrinkage value of the 0.35 w/cm cast-in-place OPC mixture extracted from a study by Tongaroonsri and Tangtermsirikul [82] is 375 microns. When compared to an identical OPC shotcrete mixture with 0.35 w/cm in Chapter 6, the shrinkage obtained at 28 days is about 270 microns. The reality is even better, since in the specimens in the study by Tongaroonsri and Tangtermsirikul were moist cured for 7 days, while the specimen in Chapter 6 were moist cured for 3 days. The cast-in-place value extracted from reference [82] is, however, comparable to the 390 microns obtained for a sprayed shotcrete mixture of 0.35 w/cm tested in a previous study [3]. Similarly, the 28-day total free shrinkage values of the 0.35 w/cm gravity-cast silica fume concrete (moist cure for 1 day before exposed to drying) extracted from studies by Altoubat et al. [58] is approximately 519 microns. These values are comparable to the 513 to 605 microns obtained at 28 days for sprayed silica fume shotcretes of 0.42 and 0.31 w/cm exposed to drying after 1-day moist curing, as reported in Chapter 5.

In another study by Hossain et al. [41] on a silica fume concrete (0.30 w/cm) moist cure for 1 day, the free shrinkage values of 740 to 800 microns recorded at 28 days were higher than the 611 microns values recorded for a silica fume shotcrete (of 0.31 w/cm) reported in Chapter 5. Subramaniam et al. [42] also performed a study on a silica fume concrete (0.40 w/cm) moist cure for 3 days before being exposed to drying and obtain total free shrinkage of about 690 microns and drying shrinkage of about 415 microns at 28 days. The total shrinkage value is higher than that recorded for an equivalent silica fume shotcrete (of 0.42 w/cm, moist cure for 3 days before exposed to drying) in Chapter 5 while the drying shrinkage values are comparable. This last case is particularly interesting because shotcrete mixtures are typically designed to achieve a *theoretical* w/cm ratio of 0.40.

It is commonly assumed that sprayed shotcrete mixtures have greater shrinkage than ordinary cast concrete because they typically have a high cementitious content and low coarse aggregate volume fraction [6, 25, 78, 92, 117]. As discussed earlier, the shotcrete process is self-adjusting, so the initial cement or coarse aggregate content does not significantly influence its shrinkage characteristics. One main advantage of shotcrete is the capacity to cover large surfaces without the use of formwork. In field conditions, this often translates into areas of unprotected fresh concrete that may result in hasty surface water evaporation. It can thus be argued based on the data presented in Chapter 5 that the high shrinkage (or severe cracking in some cases) of shotcrete experienced in field conditions is rather related to the high rate of evaporation of water from the surface of large unprotected fresh shotcrete exposed to drying immediately after spraying.

Moreover, in practice, silica fume is often used to reduce rebound losses (refer to Chapters 6, and 7) which tends to make them more prone to early age shrinkage and cracking.

It is thus recommended to keeping the surface of freshly sprayed shotcrete moist to minimize the impact of self-desiccation, promote the binder hydration and yield the expected properties of the concrete. Shotcrete mixtures can benefit from the use SRA or CRA to limit shrinkage and cracking, just like ordinary cast concrete. Although not tested in this project, the use of hybrid curing and protection methods adapted to jobsite conditions such as the use of evaporation retarder or curing compound immediately after placement (or finishing) followed later by a proper wet curing could to be explored. Results in a recent study by Blouin-Dallaire [118] could be used to establish timing guidelines.

8.6 Conclusion

The shotcrete process is complex and in itself requires further research efforts to better understand and quantify the mechanisms taking place during placement, especially with regards to the final in-place content and proportions. Nevertheless, quite interesting and significant findings were generated in the present study. Indeed, as long as silica fume is used in the shotcrete practice to reduce rebound, better curing will be needed to enhance robustness of the material with regards to shrinkage and the associated risk of cracking. In parallel, shotcrete mixtures can benefit from the use SRA or CRA to limit shrinkage and cracking on the job site. Additional research is also needed to compare sprayed wet-mix and dry-mix of similar compositions.

Summary and Conclusions

Summary

Many concrete structures are experiencing alarming deterioration rates worldwide. As a result, much of the concrete industry is now focused on extending their service life. Yet, some repairs still fail prematurely due to the use of improper repair materials or techniques. Many of these fail primarily due to dimensional incompatibility between the repair material and the existing concrete, as a result of differential shrinkage. To guarantee the quality of repaired concrete infrastructure, it is important to understand the behaviour of repair materials under restrained conditions. However, there is a significant gap in the understanding of the impact of shrinkage upon the performance of repair materials and the interpretation of restrained shrinkage tests results, particularly with shotcrete. This study was thus aimed at contributing to fill the research gap and investigating shrinkage of shotcrete based on the shrinkage ring tests.

Conclusions

Throughout this study on the cracking resistance of shotcrete, specific conclusions have been drawn at the end of each chapter and the reader can refer to those for a more detailed account. Overall, the study demonstrated that there are no simple answers to changing one mixture parameter to improve the shrinkage performance of dry-mix shotcrete. Unlike regular cast concrete mixtures, it is thus difficult to study the effect of just one parameter in the dry-mix shotcrete process, because of the self-adjusting phenomenon that occurs during spraying. This is evident in that the observations are sometimes apparently contradictory when one tries to explain the data in terms of any single parameter. Ultimately, the final in-place composition and properties are dependent on the cross-influence of many parameters during spraying. As for general conclusions to be drawn from this research program, it may be said that:

- As usual, strength is mostly a function of the w/cm and does not appear to be significantly influenced by the absolute cement content.

- Specimen geometry and drying configuration also have a significant influence on the results of the ring shrinkage tests. It has been found that shrinkage and the risk for cracking increase with an increasing surface to volume ratio. In addition, concerning the risk of cracking, it should be mentioned that the gradients induced under radial drying are much more harmful to the performance in the restrain ring than the gradients arising under axial drying.

- Free shrinkage tests are useful in comparing the shrinkage characteristics of the different mixtures, but cannot be used to accurately predict the cracking behaviour of repair materials. Cracking resistance of materials rather depends on the combined influence of shrinkage rate, stress development and tensile creep of concrete.

- A strong relationship exists between the shrinkage rate, stress rate and the time-to-cracking, where higher strain and stress rates often lead to lower time-to-cracking.

- Mixtures with lower w/cm ratios tend to show a shorter time to cracking compared to mixtures with higher w/cm ratios. In other words, mixtures with significant autogenous shrinkage strain tend to be more sensitive to early-age cracking.

- The effect of cement content on free shrinkage was relatively small and no trend for higher shrinkage with increased cement content could be established. By contrast, the effect of cement content on restrained shrinkage cracking was very pronounced, with increased cement content leading to early-age cracking. The effect of cement content on rebound was also relatively small and no trend for lower rebound with increased cement content could be established for the mixtures investigated.

- The effect of coarse aggregate content is more pronounced under restrained conditions than under free conditions. Also, increasing the coarse aggregate content did not lead to increase in shotcrete rebound.

- Silica fume, fly ash, polymer, SRA and CRA markedly reduce shotcrete rebound, reduce porosity and improve placement quality.

- Partial replacement of cement with silica fume increases free shrinkage, while the addition of fly ash reduced the overall negative effect of silica fume on shrinkage. However, both silica fume and fly ash markedly increase the risk for restrained shrinkage cracking due to slower development of strength at early-age. The current results suggest that relying solely on silica fume and fly ash to reduce rebound in shotcrete should be revisited in light of the increased risk for cracking observed in this study.

- The addition of polymer slightly reduces the magnitude of shotcrete shrinkage, but it is not effective in enhancing its cracking resistance.

- SRA and CRA were observed to be among the best options for shrinkage control in shotcrete applications. The reduction in shrinkage is about 40-60% and the increase in time-to-cracking is about 55 to 80% (depending on the dosage). The weight loss measurements also indicated that SRA and CRA reduced the rate of weight loss from drying, which in part explains the associated reduction in shrinkage.

- Moist curing method is found to be the most effective method of curing. Seven (7) days moist curing is as recommended on the job site to limit the negative effects shrinkage of shotcrete mixtures, especially if silica fume is used to reduce rebound.

- Higher level of creep or stress relaxation and lower shrinkage leads to lower risk of restrained shrinkage cracking. The tensile creep to shrinkage ratio was found to be a potentially important parameter for characterizing the role of creep in relaxing shrinkage stresses in shotcrete.

- Despite the inherent variation between shotcrete spraying sessions and the self-adjusting nature of the dry-mix shotcrete, high-quality shotcrete rings that comply with the AASHTO T 334 restrained ring test standard were produced in this research program. The results obtained allowed to build a near perfect performance classification table (Table 6.7) based on Fig. 6.13. Just as for the ASTM C1581 restrained

ring test standard, the inclusion of a cracking potential classification table based on the net time-to-cracking and the average stress rate at cracking (as shown in Table 6.7) in the AAHTO ring test standard for relative comparison of materials would be very useful for the shotcrete industry.

- Although not reported in the thesis (see Appendix A), it should be noted that the global behaviour of shotcrete under free and restrained conditions have been correctly reproduced with a numerical model used in this research. Modelling has the potential to play an important role in search of crack-resistant shotcrete.

Perspectives for Future Research

Experimental Investigation

In continuation of this research, it is strongly recommended to extend the curing time of all the dry-mix shotcrete mixtures tested to 7 days. Future research should also focus on assessing the effect of fly ash and slag addition on rebound and shrinkage properties of dry-mix shotcrete, in the absence of silica fume. The use of polymers as rebound-reducing agent should also be investigated. Also, the combined use of polymers and SRA or polymers and CRA should also be tested. It would be ideal to determine a dosage of SRA and CRA that would produce the highest reduction in shrinkage to minimize the potential for cracking of dry-mix shotcrete. In addition, the shrinkage and sensitivity to restrained-shrinkage cracking of blended dry-mix shotcrete mixtures should also be tested under different curing regimes. Further research will also be necessary to better evaluate the influence of fibres on reducing the effects of shrinkage, since fibre reinforced shotcrete is increasingly being used for repairs. The influence of expansive cements on the shrinkage properties of should also be examined. It is also of interest to study the shrinkage and cracking sensitivity of shotcrete mixtures under curing regimes that simulate specific climate conditions (i.e. temperature and humidity conditions) encountered in real field applications (e.g. tunnel environments).

It was shown in this project that the stress rate at cracking gives an accurate assessment of the potential for cracking of shotcrete. It will be extremely interesting to examine the use of the integrated criterion approach (proposed by Kovler and Bentur [119]) based on combining the criteria of time-to-cracking and stress rate at cracking for classification of sensitivity to cracking of shotcrete mixtures. It will be interesting to examine the use of the drying shrinkage limits at 7 days after initiation of drying for the various material classification levels in Table 6.8 as a basis for a preliminary assessment (following the method proposed by See et al. [77]). It would also be reasonable to investigate the relationship between the stress rate at cracking and the free shrinkage strain rate to examine the possibility of using the rate of shrinkage for a preliminary classification of the potential for cracking of shotcrete mixtures.

Numerical Modelling

The work presented in Appendix A is a contribution to the modelling of shotcrete shrinkage in restrained conditions, with explicit account for the evolution of mechanical properties, autogenous shrinkage and creep. The numerical simulations of the ring test did not take into account the moisture profile within specimens (i.e. non-uniform drying and resulting self-restraint). A further step of this study would involve improvements in the model formulation to take into consideration evolving moisture fields and the shrinkage-induced stresses they give rise to. It could subsequently be extended for aiding in the selection of repair materials with low potential for cracking for specific projects. Some on this work is currently on-going at CRIB-Laval.

References

[1] B. Bissonnette. 1996. Le fluage en traction: un aspect important de la problématique des réparations minces en béton, PhD Thesis, Université Laval, Quebec, Canada, pp. 290 pages. (in French)

[2] F. Modjabi-Sangnier. 2010. Approche Quantitative de la notion de compatibilité des bétons de réparation autoplaçants, PhD Thesis, Université Laval, Canada, pp. 240 pages.

[3] S. Girard. 2013. Etude du bilan deformationnel des bétons projetés, MSc Thesis, Université Laval, Quebec, Canada, pp. 124 pages. (in French)

[4] AASHTO-T334-08. 2012. Standard practice for estimating the crack tendency of concrete, AASHTO Provisional Standards, Washington, D.C., pp. 6 pages.

[5] AASHTO-PP-34-99. 1999. Standard Practice for Estimating the Cracking Tendency of Concrete, AASHTO Provisional Standards, Washington, DC, pp. 4 pages.

[6] S.A. Austin, P.J. Robins. 1995. Sprayed Concrete: Properties, Design and Application, Whittles Publishing, Caithness, pp. 393 pages.

[7] ACI-CP-60. 2009. Certification program for shotcrete nozzleman, Craftsman Workbook, American Concrete Institute, Farmington Hills, USA, pp. 126 pages.

[8] M. Jolin. 1999. Mechanisms of placement and stability of dry process shotcrete, PhD Thesis, University of British Columbia, Canada, pp. 157 pages.

[9] ACI-506R-16. 2016. Guide to Shotcrete, American Concrete Institute, Farmington Hills, USA, pp. 40 pages.

[10] ACI. 2000. Shotcrete for the Craftsman, Volume 4 of Concrete Craftman Series, American Concrete Institute, pp. 59 pages.

[11] M. Jolin, D. Beaupre. 2001. Effect of Shotcrete Consistency and Nozzleman Experience on Reinforcement Encasement Quality, Shotcrete Mag., (Fall), 20-23.

[12] M. Jolin, D. Beaupré, S. Mindess. 1999. Tests to characterise properties of fresh dry-mix shotcrete, Cem. Concr. Res., 29(5), 753-760.

[13] M. Jolin, D. Beaupre. 2004. Effects of particle-size distribution in dry process shotcrete, ACI Mater. J., 101(2), 131-135.

[14] D. Beaupré, C. Talbot, M. Gendreau, M. Pigeon, D.R. Morgan. 1994. Deicer Salt Scaling Resistance of Dry-and Wet-Process Shotcrete, ACI Mater. J., 91(5), 487-494.

[15] M. Jolin, D. Beaupre. 2003. Understanding wet-mix shotcrete: mix design, specifications, and placement, Shotcrete Mag., Shotcrete (Summer), 6-12.

[16] B. Bissonnette, J. Marchand, J. Charron, A. Delagrave, L. Barcelo. 2001. Early age behavior of cement-based materials, Materials Science of Concrete VI. American Ceramic Society, Inc, 735 Ceramic Place, Westerville, OH 43081, USA, (2001) 243-326.

[17] A.M. Neville. 2011. Properties of Concrete, 5th ed., Pearson, Harlow, England, pp. 846 pages.

[18] CSA-A23.1-14. 2014. Concrete materials and methods of concrete construction, Canadian Standards Association, Toronto, Ontario, Canada, pp. 268 pages.

[19] ACI-305R-10. 2010. Guide to Hot Weather Concreting, American Concrete Institute, Farmington Hills, pp. 28 pages.

[20] B. Wan, C.M. Foley, J. Komp. 2010. Concrete cracking in new bridge decks and overlays, pp. pages.

[21] J.M. Torrenti, G. Pijaudier-Cabot, J.M. Reynouard. 2010. Mechanical Behavior of Concrete, Wiley, pp. 448 pages.

[22] E.E. Holt. 2001. Early Age Autogenous Shrinkage of Concrete, Technical Research Centre of Finland, VTT Publications 446, pp. 184 pages.

[23] S.P. Shah, W.J. Weiss. 2000. High performance concrete: strength, permeability, and shrinkage cracking, Proceedings of the Proceedings of the PCI/FHWA International Symposium on High Performance Concrete, Orlando Florida, pp. 331-340.

[24] S. Ahn, V. Gopalaratnam. 1995. Restrained Shrinkage: its impact on the response of reinforced concrete members, Fracture mechanics of concrete structures, Vol. 2 1155.

[25] D. Morgan, R. Heere, C. Chan, J. Buffenbarger, R. Tomita. 2001. Evaluation of shrinkage-reducing admixtures in wet and dry-mix shotcretes, in: E.S Bernard (ed.), Shotcrete: Engineering Developments, Proceedings of the International Conference on Engineering Developments in Shotcrete, Hobart, Tasmania, Australia, pp. 185-192.

[26] W.J. Weiss. 1999. Prediction of early-age shrinkage cracking in concrete elements, PhD Thesis, Northwestern University, Evanston, IL, USA, pp. 274 pages.

[27] S.P. Shah, C. Ouyang. 1994. Fracture mechanics for failure of concrete, Annu. Rev. Mater. Sci., 24(1), 293-320.

[28] C.K. Nmai, R. Tomita, F. Hondo, J. Buffenbarger. 1998. Shrinkage-reducing admixtures, Concrete International, 20(4), 31-37.

[29] X. Hu, Z. Shi, C. Shi, Z. Wu, B. Tong, Z. Ou, G. de Schutter. 2017. Drying shrinkage and cracking resistance of concrete made with ternary cementitious components, Constr. Build. Mater., 149 406-415.

[30] A.M. Vaysburd, B. Bissonnette, K.F. von Fay During. 2017. The Challenges of Achieving Compatibility in Concrete Repair, Concrete International, 39(12), 37-43.

[31] P. Mehta, P.J.K. Mehta, P.J. Monteiro. 2006. Concrete: microstructure, properties, and materials, 3rd ed., McGraw - Hill, New York, pp. 659 pages.

[32] N.J. Carino, J.R. Clifton. 1995. Prediction of cracking in reinforced concrete structures, US Department of Commerce, National Institute of Standards and Technology, NISTIR 5634, 51.

[33] F. Benboudjema. 2002. Modélisation des déformations différées du béton sous sollicitations biaxiales. Application aux enceintes de confinement de bâtiments réacteurs des centrales nucléaires, PhD Thesis, Université de Marne la Vallée, Champs-sur-Marne, France, pp. 254 pages. (in French)

[34] H.T. See, E.K. Attiogbe, M.A. Miltenberger. 2003. Shrinkage cracking characteristics of concrete using ring specimens, ACI Mater. J., 100(3), 239-245.

[35] B. Bissonnette, M. Pigeon. 1995. Tensile creep at early ages of ordinary, silica fume and fiber reinforced concretes, Cem. Concr. Res., 25(5), 1075-1085.

[36] B. Bissonnette, P. Pierre, M. Pigeon. 1999. Influence of Key Parameters on Drying Shrinkage of Cementitious Materials, Cem. Concr. Res., 29(10), 1655-1662.

[37] J.A. Almudaiheem, W. Hansen. 1987. Effect of specimen size and shape on drying shrinkage of concrete, ACI Mater. J., 84(2), 130-135.

[38] A.B. Hossain, J. Weiss. 2006. The role of specimen geometry and boundary conditions on stress development and cracking in the restrained ring test, Cem. Concr. Res., 36(1), 189-199.

[39] M. Abou-Zeid, D.W. Fowler, E.G. Nawy, J.H. Allen, G.T. Halvorsen, R.W. Poston, J.P. Barlow, W. Hansen, R.J. Rhoads, M.E. Brander. 2001. Control of Cracking in Concrete Structures, Report, ACI Committee, 224 12-16.

[40] R. Wassermann, A. Katz, A. Bentur. 2009. Minimum cement content requirements: a must or a myth?, Mater. Struct., 42(7), 973-982.

[41] A.B. Hossain, S. Islam, K.D. Copeland. 2007. Influence of ultrafine fly ash on the shrinkage and cracking tendency of concrete and the implications for bridge decks, Proceedings of the 86th Transportation Research Board Annual Meeting, pp. 15.

[42] K.V. Subramaniam, R. Gromotka, S.P. Shah, K. Obla, R. Hill. 2005. Influence of ultrafine fly ash on the early age response and the shrinkage cracking potential of concrete, J. Mater. Civ. Eng., 17(1), 45-53.

[43] M. Gesoğlu, E. Güneyisi, E. Özbay. 2009. Properties of self-compacting concretes made with binary, ternary, and quaternary cementitious blends of fly ash, blast furnace slag, and silica fume, Constr. Build. Mater., 23(5), 1847-1854.

[44] I. Khan, A. Castel, R.I. Gilbert. 2017. Effects of fly ash on early-age properties and cracking of concrete, ACI Mater. J., 114(4).

[45] M. Jensen, P.F. Hansen. 1996. Autogenous deformation and change of the relative humidity in silica fume-modified cement paste, ACI Mater. J., 93(6), 539-543.

[46] K.J. Folliard, N.S. Berke. 1997. Properties of high-performance concrete containing shrinkage-reducing admixture, Cem. Concr. Res., 27(9), 1357-1364.

[47] S. Shah, M. Krguller, M. Sarigaphuti. 1992. Effects of shrinkage-reducing admixtures on restrained shrinkage cracking of concrete, ACI Mater. J., 89(3), 289-295.

[48] C.K. Nmai, D. Vojko, S. Schaef, E.K. Attiogbe, M.A. Bury. 2014. Crack-reducing admixture, Concrete international, 36(1), 53-57.

[49] ASTM-C157. 2014. Standard Test Method for Length Change of Hardened Hydraulic-Cement Mortar and Concrete, ASTM International, West Conshocken, PA, pp. 7 pages.

[50] X. Zhou, W. Dong, O. Oladiran. 2013. Experimental and numerical assessment of restrained shrinkage cracking of concrete using elliptical ring specimens, J. Mater. Civ. Eng., 26(11), 04014087.

[51] P.H. Emmons, A.M. Vaysburd. 1995. Performance Criteria for Concrete Repair Materials, Phase I, US Army Corps of Engineer, pp. 127 pages.

[52] W. Dong, X. Zhou, Z. Wu, G. Kastiukas. 2016. Effects of specimen size on assessment of shrinkage cracking of concrete via elliptical rings: Thin vs. thick, Computers & Structures, vol. 174 66-78.

[53] ASTM-C1581. 2009. Standard Test Method for Determining Age at Cracking and Induced Tensile Stress Characteristics of Mortar and Concrete under Restrained Shrinkage, ASTM International, West Conshohocken, PA, pp. 7 pages.

[54] D.P. Bentz, D.A. Quenard, V. Baroghel-Bouny, E.J. Garboczi, H.M. Jennings. 1995. Modelling drying shrinkage of cement paste and mortar Part 1. Structural models from nanometres to millimetres, Mater. Struct., 28(8), 450-458.

[55] Z. Bažant, L. Najjar. 1971. Drying of concrete as a nonlinear diffusion problem, Cem. Concr. Res., 1(5), 461-473.

[56] T.R. Crom. 1981. Dry mix shotcrete nozzling, Concrete International, 3(1), 80-93.

[57] B. Menu, M. Jolin, B. Bissonnette. 2017. Studies on the influence of drying shrinkage test procedure, specimen geometry, and boundary conditions on free shrinkage, Adv. Mater. Sci. Eng., 2017(Article ID 9834159), 9.

[58] S. Altoubat. 2010. Early Age Creep and Shrinkage of Concrete with Shrinkage Reducing Admixtures (SRA), Jordan J. Civ. Eng., 4(3), 281-291.

[59] W.J. Weiss, W. Yang, S.P. Shah. 2001. Using fracture to predict restrained shrinkage cracking: The importance of specimen geometry, ACI Special Publication, 201 17-34.

[60] R. Mishra, R. Tripathi, V. Dubey. 2016. Early Age Shrinkage Pattern of Concrete on Replacement of Fine Aggregate with Industrial by-product, J. Radiat. Res. Appl. Sci., vol. 9, no. 4 386-391.

[61] L. Iures, C. Badea, S. Dan, C. Bob. 2013. Assesment of cracking index and characteristic contraction due to concrete'shrinkage, International Multidisciplinary Scientific GeoConference: SGEM: Surveying Geology & mining Ecology Management, 361.

[62] B. Pease, F. Rajabipour, J.-H. Moon, J. Weiss. 2006. Quantifying the influence of specimen geometry on the results of the restrained ring test, J. ASTM Int., 3(8), 1-14.

[63] G. Lomboy, K. Wang, C. Ouyang. 2010. Shrinkage and fracture properties of semiflowable self-consolidating concrete, J. Mater. Civ. Eng., 23(11), 1514-1524.

[64] K.V. Subramaniam, A.K. Agrawal. 2009. Concrete Deck Material Properties, (C-02-03), Cornell University Research Consortium, pp. 111 pages.

[65] A. Hossain, B. Pease, J. Weiss. 2003. Quantifying early-age stress development and cracking in low water-to-cement concrete: restrained-ring test with acoustic emission, Transportation Research Record: Journal of the Transportation Research Board, (1834), 24-32.

[66] P. Van Itterbeeck, N. Cauberg, B. Parmentier, L. Vandewalle, K. Lesage. 2010. Evaluation of the cracking potential of young self-compacting concrete, Proceedings of the Proceedings of the 6th International RILEM Symposium on SCC, Montréal, pp. 991-1001.

[67] S. Girard, M. Jolin, B. Bissonnette, J.-D. Lemay. 2017. Measuring the Cracking Potential of Shotcrete, Concrete International, 39(8), 44-48.

[68] J.H. Moon, J. Weiss. 2006. Estimating residual stress in the restrained ring test under circumferential drying, Cem. Concr. Compos., 28(5), 486-496.

[69] R.N. Swamy. 1971. Dynamic Poisson's ratio of portland cement paste, mortar and concrete, Cem. Concr. Res., 1(5), 559-583.

[70] R.M. Mors. 2011. Autogenous Shrinkage of Cementitious materials containing BFS, Master Thesis, Delft University of Technology, Delft, Netherlands, pp. 63 pages.

[71] J.-S. Lim, S.-H. Kim, J.-H. Jeong. 2014. Testing and analysis of viscoelastic characteristics of solidifying concrete pavement slabs, KSCE J. Civ. Eng., 18(4), 1063-1071.

[72] S.A. Altoubat, D.A. Lange. 2001. Creep, shrinkage and cracking of restrained concrete at early age, ACI Mater. J., 98(4), 323-331.

[73] TRB. 2006. Control of Cracking in concrete: state of the art, Transportation Research E-Circulars, Transportation Research Board, pp. 56 pages.

[74] J.H. Ideker, T. Fu, T. Deboodt. 2013. Development of Shrinkage Limits and Testing Protocols for ODOT High Performance Concrete, (SPR 728), ODOT Research Section, Oregon, pp. 87 pages.

[75] A.B. Hossain, J. Weiss. 2004. Assessing residual stress development and stress relaxation in restrained concrete ring specimens, Cem. Concr. Compos., 26(5), 531-540.

[76] H. Shah, J. Weiss. 2006. Quantifying shrinkage cracking in fiber reinforced concrete using the ring test, Mater. Struct., 39(9), 887-899.

[77] H.T. See, E.K. Attiogbe, M.A. Miltenberger. 2004. Potential for restrained shrinkage cracking of concrete and mortar, Cem. Concr. Agg., 26(2), 1-8.

[78] N. Banthia. 2019. Advances in sprayed concrete (shotcrete), in: S. Mindess (Ed.), Developments in the Formulation and Reinforcement of Concrete, Woodhead Publishing, pp. 289-306 pages.

[79] E.K. Attiogbe, W. Weiss, H.T. See. 2004. A look at the stress rate versus time of cracking relationship observed in the restrained ring test, RILEM Publications SARL, Proceedings of the In International RILEM Symposium on Concrete Science and Engineering: A Tribute to Arnon Bentur, pp.

[80] B. Menu, M. Jolin, B. Bissonnette, N. Ginouse. 2017. Evaluation of early age shrinkage cracking tendency of concrete, Proceedings of the CSCE Annual Conference on Leadership in Sustainable Infrastructure, Vancouver, Canada, pp. EMM649-1-EMM649-8.

[81] Y. Wei, W. Hansen. 2013. Early-age strain-stress relationship and cracking behavior of slag cement mixtures subject to constant uniaxial restraint, Constr. Build. Mater., 49 635-642.

[82] S. Tongaroonsri, S. Tangtermsirikul. 2009. Effect of mineral admixtures and curing periods on shrinkage and cracking age under restrained condition, Constr. Build. Mater., 23(2), 1050-1056.

[83] I. Soroka. 2004. Concrete in Hot Environments, CRC Press, pp. 251 pages.

[84] G. Sant, D. Bentz, J. Weiss. 2011. Capillary Porosity Depercolation in Cement-based Materials: Measurement Techniques and Factors which Influence their Interpretation, Cem. Concr. Res., 41(8), 854-864.

[85] S. Austin, P. Robins, A. Issaad. 1992. Influence of Curing Methods on the Strength and Permeability of GGBFS Concrete in a Simulated Arid Climate, Cem. Concr. Compos., 14(3), 157-167.

[86] C.H. Studebaker. 1939. Report on Gunite at Arrowrock Dam, U.S. Bureau of Reclamation Memorandum, 10 March 66.

[87] P. Kreijger. 1984. The Skin of Concrete Composition and Properties, Matériaux et Construction, 17(4), 275-283.

[88] H. Nassif, N. Suksawang, M. Mohammed. 2003. Effect of Curing Methods on Early-age and Drying Shrinkage of High-performance Concrete, Transportation Research Record: Journal of the Transportation Research Board, (1834), 48-58.

[89] D.R. Morgan, N. McAskill, J. Neill, N.F. Duke. 1987. Evaluation of Silica Fume Shotcrete, Proceedings of the Proceedings of CANMET/ACI workshop on condensed silica fume in concrete, Montreal, Canada, pp. 34.

[90] S.H. Kosmatka, B. Kerkhoff, D. Hooton, J.R. McGrath. 2011. Design and Control of Concrete Mixtures, 8th canadian ed., Cement Association of Canada, pp. 411 pages.

[91] B.M.O.C. Elie El Hindy, A. Pierre-Claude. Drying Shrinkage of Ready-Mixed High-Performance Concrete, ACI Mater. J., 91(3).

[92] ACI-506R-05. 2005. Guide to shotcrete, American Concrete Institute, Farmington Hills, USA, pp. 40 pages.

[93] T. Fujiwara. 2008. Effect of aggregate on drying shrinkage of concrete, J. Adv. Concr. Technol., 6(1), 31-44.

[94] M.G. Alexander. 1996. Aggregates and the deformation properties of concrete, ACI Mater. J., 93 569-577.

[95] J. Wolsiefer, D.R. Morgan. 1993. Silica fume in shotcrete, Concrete International, 15(4), 34-39.

[96] V. Bindiganavile, N. Banthia. 2000. Rebound in dry-mix shotcrete: influence of type of mineral admixture, ACI Mater. J., 97(2), 115-119.

[97] B. Menu, M. Jolin, B. Bissonnette. 2020. Assessing the shrinkage cracking potential of concrete using ring specimens with different boundary conditions, Adv. Mater. Sci. Eng., 2020(Article ID 4842369), 13.

[98] M. Jolin, J.-D. Lemay, N. Ginouse, B. Bissonnette, É. Blouin-Dallaire. 2015. The Effect of Spraying on Fiber Content and Shotcrete Properties.

[99] P.J. Monteiro, P.R. Helene, S. Kang. 1993. Designing concrete mixtures for strength, elastic modulus and fracture energy, Mater. Struct., 26(8), 443-452.

[100] H. Schorn. 1985. Epoxy modified shotcrete, Polymers in Concrete, Special Publication, 89 249-260.

[101] S.P. Shah, W.J. Weiss, W. Yang. 1998. Shrinkage Cracking-Can It Be Prevented?, Concrete International, 20(4), 51-55.

[102] Z. Zhou, P. Qiao. 2019. Prediction of restrained shrinkage cracking of shotcrete rings using fracture mechanics–based approach, J. Mater. Civ. Eng., 31(10), 04019214.

[103] M. Pigeon, B. Bissonnette. 1999. Tensile creep and cracking potential, Concrete International, 21(11), 31-35.

[104] S.P. Shah, C. Ouyang, S. Marikunte, W. Yang, E. Becq-Giraudon. 1998. A method to predict shrinkage cracking of concrete, ACI Mater. J., 95(4), 339-346.

[105] W.J. Weiss, W. Yang, S.P. Shah. 2000. Influence of specimen size/geometry on shrinkage cracking of rings, J. Eng. Mech., 126(1), 93-101.

[106] I. Khan, A. Castel, R.I. Gilbert. 2017. Tensile creep and early-age concrete cracking due to restrained shrinkage, Constr. Build. Mater., 149 705-715.

[107] A.B. Hossain, A. Fonseka, H. Bullock. 2008. Early age stress development, relaxation, and cracking in restrained low W/B ultrafine fly ash mortars, Journal of Adv Concr Tech, 6(2), 261-271.

[108] B.A. Gedam, N. Bhandari, A. Upadhyay. 2016. Influence of supplementary cementitious materials on shrinkage, creep, and durability of high-performance concrete, J. Mater. Civ. Eng., 28(4), 04015173.

[109] I. Pane, W. Hansen. 2002. Early age creep and stress relaxation of concrete containing blended cements, Mater. Struct., 35(2), 92.

[110] S.-i. Igarashi, A. Bentur, K. Kovler. 2000. Autogenous shrinkage and induced restraining stresses in high-strength concretes, Cem. Concr. Res., 30(11), 1701-1707.

[111] R. Khatri, V. Sirivivatnanon, W. Gross. 1995. Effect of different supplementary cementitious materials on mechanical properties of high performance concrete, Cem. Concr. Res., 25(1), 209-220.

[112] A. Assmann, H. Reinhardt. 2014. Tensile creep and shrinkage of SAP modified concrete, Cem. Concr. Res., 58 179-185.

[113] I. Keishiro, H. Tatsuya, H. Umehara. 1999. Study on the relationship between compressive creep and tensile creep of concrete at an early age, Concrete library of JSCE, June(No. 33), 185-198.

[114] W. Weiss, S. Shah. 2002. Restrained shrinkage cracking: the role of shrinkage reducing admixtures and specimen geometry, Mater. Struct., 35(2), 85-91.

[115] A. Gagnon. 2017. Développement de mélanges de béton projeté à valeurs environnementales ajoutées, MSc Thesis, Université Laval, Quebec, Canada, pp. 116 pages. (in French)

[116] S. Austin, P. Robins, C. Peaston. 1998. Effects of silica fume on dry-process sprayed concrete, Mag. Concr. Res., 50(1), 25-36.

[117] A. Ansell. 2010. Investigation of shrinkage cracking in shotcrete on tunnel drains, Tunnelling and Underground Space Technology, 25(5), 607-613.

[118] É. Blouin-Dallaire. 2019. Les méthodes de cure et leurs impacts sur le retrait et la fissuration du béton projeté, MSc Thesis, Université Laval, Quebec, Canada, pp. 125 pages. (in French)

[119] K. Kovler, A. Bentur. 2009. Cracking sensitivity of normal-and high-strength concretes, ACI Mater. J., 106(6), 537.

Appendix A *Article 6* - Évaluation de la Sensibilité et Potentiel à la Fissuration des Bétons Projetés au Jeune Âge

Bruce MENU[A], Marc JOLIN[A], Benoît BISSONNETTE[A], and Laurent MOLEZ[B]

[A] Centre de recherche sur les infrastructures en béton, Université Laval, Québec, Canada

[B] Laboratoire de Génie civil et Génie mécanique, INSA, 1065, Rennes, France

A.1 Abstract

This article deals with the numerical modelling of shrinkage and cracking of shotcretes subjected to hygrothermal loading. The numerical tool presented in this paper takes into account the evolution of mechanical properties during hydration process and the autogenous shrinkage. The aim of the numerical model developed is to complement the experimental tests by numerical simulations of several phenomena occurring simultaneously (hydration, curing, creep, etc.) during the ring test. The results obtained agree well with experimental observations on shrinkage deformation and crack patterns observed in the restrained shrinkage ring test. Further, model highlights the importance of increasing the amount of cement content in a mixture. Also, the model demonstrated that the addition of silica fume as a partial replacement of the cement results in a decrease in the crack resistance of concrete. Overall, the model developed allows selective choice of repair materials that are less vulnerable to cracking.

A.2 Résume

Le béton projeté est une technique de mise en place largement utilisée pour la réhabilitation, la réalisation des travaux miniers et souterrains ainsi que pour les réparations. L'un des principaux avantages du béton projeté est sa capacité à couvrir de grandes surfaces sans coffrage. Cependant, cela peut entraîner une

grande surface de béton projeté frais non protégé; l'évaporation de l'eau de surface peut rapidement conduire à un retrait différentiel à travers la couche de béton projeté relativement mince qui peut mener à la fissuration au jeune âge lorsqu'il est soumis aux effets du séchage. Le potentiel de fissuration dépend en réalité du retrait, de l'évolution des contraintes de traction et de la relaxation des contraintes. L'objectif de ce projet de recherche est de développer des bétons qui auront une tendance à la fissuration significativement réduite. Le programme expérimental comporte l'étude du retrait libre et de la fissuration par retrait empêché en laboratoire et sous conditions contrôlées basée sur des essais à l'anneau. Exploitant les résultats recueillis, une approche croisée expérimentale et numérique est développée pour estimer la sensibilité à la fissuration des bétons en fonction de leurs propriétés individuelles. Ceci permettra une analyse plus poussée pour expliquer les tendances observées. Les résultats démontrent entre autres que la sensibilité à la fissuration dépend du rapport volume/surface exposé au séchage. Ainsi, les résultats démontrent que la diminution du rapport eau/ciment augmente le risque de fissuration par retrait. Ce phénomène s'explique par le fait que le retrait endogène se développe plus rapidement et est plus important pour un rapport eau/ciment plus faible.

Mots cles : béton projeté, retrait, fissuration retrait empêché, essai à l'anneau

A.3 Introduction

Le béton projeté est un moyen rapide de mise en œuvre du béton par projection à grande vitesse sur une surface au moyen d'air comprimé, sans coffrage. Il y a deux procédés utilisés pour faire du béton projeté, le procédé par voie sèche et celui par voie humide [9]. Vu les nombreux avantages que présente le béton projeté, de nombreuses constructions et réparations sont réalisées avec ce type de matériau. Le béton projeté par voie sèche est particulièrement bien adapté pour les réparations. Bien que le béton projeté soit un matériau généralement très performant, il existe encore des phénomènes de retrait et fissuration qui sont mal compris par les chercheurs et les ingénieurs en pratique. En fait, les bétons projetés ont généralement des potentiels de retrait plus importants que les bétons conventionnels. Le retrait est la principale cause de fissuration non structurale des ouvrages en béton projeté.

Le béton a tendance à subir un retrait lors de l'hydratation du ciment. Lorsque le béton se déforme en condition empêchée, ce retrait génère des contraintes internes importantes qui peuvent mener à la fissuration du matériau. Par exemple le retrait du matériau de réparation est empêché par le substrat [120]. Toutefois, peu d'informations sont disponibles dans la littérature concernant le retrait et fissuration du béton projeté. Une bonne maîtrise du comportement au jeune âge des bétons projetés est l'assurance performance à long terme de ces matériaux. Cette étude vise donc à améliorer les connaissances sur la fissuration par des études expérimentales et numériques. Ces résultats serviront à tous les domaines utilisant le béton projeté afin de produire des bétons qui fissurent moins.

A.4 Campagne expérimentale

A.4.1 Composition des mélanges

Ce travail porte sur la fissuration des bétons projetés soumis à un chargement hygrothermique. Six (6) mélanges de bétons projetés ont été testés dans le cadre de ce projet. Les proportions des différents constituants entrant dans la formulation de béton projeté sont présentées dans les Tableau A.1 et A.2. Le mélange M4 correspond au mélange M2 avec une partie du ciment remplacée par de la fumée de silice. Le ciment utilisé est de type Portland GU (utilisation générale). Les mélanges ont été mis en place grâce à deux techniques différentes. Deux mélanges ont été coulés sur place alors que quatre mélanges ont été projetés par voie sèche dans la salle de projection du CRIB de l'Université Laval, Québec, Canada. Les mélanges ont été ensachés par la compagnie King Packaged Materials à Boisbriand, au Québec. Dans le cas de mélanges projetés, les matériaux secs, pré-ensachés et livrés au laboratoire, sont introduits directement dans la benne de l'appareil de projection. L'air comprimé amène les matériaux à la lance, où l'on introduit l'eau, et le béton est projeté directement dans les moules.

Tableau A.1 Compositions des mélanges coulés en place

Mélanges	Ciment GU (%)	Pierre (%)	Sable (%)	Fumée de silice (%)	Eau/liant (kg/kg)
C1	19,9	15,0	64,0	0,0	0,45
C2	19,9	15,0	64,0	0,0	0,60

Tableau A.2 Compositions des mélanges projetés par voie sèche

Mélanges	Ciment GU (%)	Pierre (%)	Sable (%)	Fumée de silice (%)	Eau/liant (kg/kg)
M1	16,0	16,0	68,0	0,0	0,48
M2	21,0	24,0	55,0	0,0	0,40
M3	25,0	14,0	61,0	0,0	0,32
M4	19,4	24,0	55,0	1,6	0,55

A.5 Procédure des essais

Les éprouvettes destinées aux essais de résistance en compression, de résistance à la traction et de module élastique ont été carottées dans les panneaux de caractérisation. L'essai a été mené selon les normes ASTM C39, C496 et C469, respectivement à des échéances de 28 jours. La cure des éprouvettes s'est faite dans une chambre à 100% d'humidité relative (H.R.). La résistance en compression à 28 jours de ces bétons est de 37.4 MPa, 33.4 MPa, 35.6 MPa, 48.8 MPa, 54.4 MPa, 49.2 MPa, respectivement pour les mélanges C1, C2, M1, M2, M3, et M4.

A.5.1 Essais de retrait libre

Les essais de retrait libre sont réalisés au moyen de prismes et d'anneaux. L'essai de retrait sur les prismes a été réalisé conformément à la norme ASTM C157 sur des éprouvettes coulées. En revanche, l'essai de retrait libre annulaire est basé sur la norme AASHTO T334-08 à la différence que l'anneau interne a été remplacé par un cœur en polystyrène de même dimension [57]. La cure de ces éprouvettes s'est faite avec de la jute et des toiles de polyéthylène maintenues humides. Les surfaces supérieures et inférieures des anneaux ont été scellées à l'aide de papier d'aluminium autocollant afin de limiter le séchage selon l'axe circonférentiel. Aussitôt que le séchage a débuté, des plots ont été appliqués sur la surface supérieure de l'anneau du béton pour la mesure des variations volumétriques. Les retraits des éprouvettes prismatiques et annulaires ont été pris régulièrement, ce qui a permis de tracer les courbes de retrait avec une très bonne précision. Pendant toute la durée de l'essai, les éprouvettes ont été conservées dans une chambre contrôlée (température de 21±1.7 ℃ et humidité relative à 50±4 %). Les éprouvettes prismatiques et annulaires ont des rapports surface/volume (S_d/V) exposés au séchage de 0.0604 mm^{-1} et 0.0158 mm^{-1} respectivement.

A.5.2 Essais de retrait restreint

Parallèlement, les essais de retrait restreint sont effectués au moyen d'une éprouvette annulaire selon la norme AASHTO T334-08 [3]. Deux éprouvettes annulaires ont été réalisées pour chacun des mélanges testés. L'anneau a été démoulé au bout de 24 heures et recouvert de jutes humides et de toiles de polyéthylène pour 2 jours supplémentaires. Une fois leur cure humide terminée, les surfaces supérieures des anneaux des bétons sont scellées par une couche d'aluminium autocollant et la surface circonférentielle est exposée au séchage dans une chambre contrôlée (température de 21±1.7 ℃ et humidité relative à 50±4 %). La mesure du retrait a été effectuée à l'aide de jauges de déformation posées à mi-hauteur de la face intérieure de l'anneau d'acier. L'acquisition automatique des données se fait toutes les 5 minutes. L'analyse de retrait empêché conjointement celle du retrait libre permet de déduire le fluage au cours de séchage. L'extraction du fluage au cours du retrait restreint est basée sur l'hypothèse de la décomposition additive des déformations :

$$\varepsilon_{tot}(t) = \varepsilon_s(t) + \varepsilon_e(t) + \varepsilon_f(t) \tag{8.1}$$

où ε_{tot} est la déformation totale, ε_s est la déformation due au séchage, ε_e est la déformation élastique et ε_f est le fluage

A.6 Modélisation numérique

Dans le béton, plusieurs phénomènes se produisent simultanément au jeune âge. Ces phénomènes (hydratation, retrait endogène, fluage …) sont pris en compte dans le cadre de cette étude par le modèle proposé par Molez [121]. Nous avons intégré les phénomènes physiques des bétons dans un code aux

éléments finis existant (CAST3M, code du CEA). Dans ce modèle, l'évolution de la résistance en compression est liée à l'avancement de la réaction hydratation. Selon [122], le taux d'hydratation peut être déterminé à partir de l'évolution des résistances mécaniques à l'aide de la relation suivante :

$$\xi(t) = \xi_0 + (1 - \xi_0)\frac{f_c(t)}{f_c(t_\infty)} \tag{8.2}$$

où ξ_0 est le seuil de percolation tel que défini par Acker [123], $f_c(t)$ est la résistance au temps t et $f_c(t_\infty)$ est la résistance à un temps infini. L'évolution des propriétés mécaniques due à la structuration est prise en compte, par la suite, par une fonction de lissage du type proposé par Molez Molez [121]:

$$f_c(t) = f_c(t_\infty)\frac{t^{m_1}}{m_2 + t^{m_1}} \tag{8.3}$$

où m_1 et m_2 sont des paramètres de forme déterminés à partir des résultats expérimentaux en Fig. A.1.
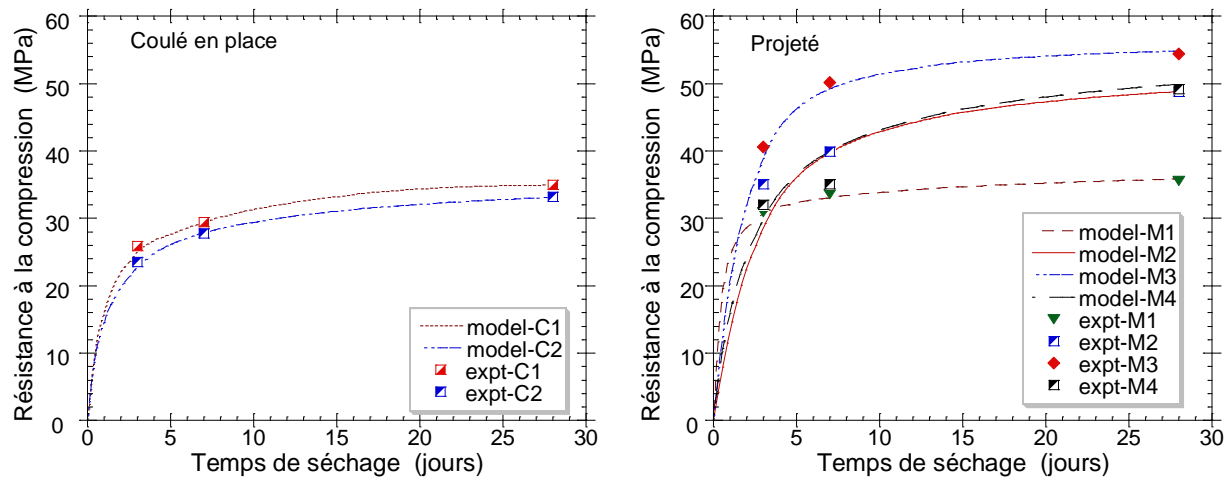
Fig. A.1 Évolution de la résistance à la compression

Le retrait causé par séchage est un phénomène donnant lieu au déséquilibre hygrométrique dans le béton et son environnement extérieur. En effet, le facteur initiant le séchage du béton est le gradient d'humidité relative existant entre l'environnement (extérieur) et le béton (intérieur) [33]. Ce déséquilibre se traduit par le transport de l'eau et la perte de masse dans le béton. La modélisation du phénomène de séchage peut être alors faite à l'aide des équations de conservation de la masse. L'équation de conservation de la masse, exprimée en fonction de la teneur en eau massique , permet d'écrire localement (voir Molez, [121]) :

$$\frac{\partial w}{\partial t} = -\text{div}(J_v + J_l) + \frac{\partial w_{ad}}{\partial t} \tag{8.4}$$

Les termes J_v et J_l représentent le flux d'eau liquide et vapeur, et le terme $\partial w_{ad}/\partial t$ représente la variation de teneur en eau due à l'auto-dessiccation lors de la progression des réactions d'hydratation. Ensuite, pour

les H.R. comprises entre 0,40 et 0,95, le séchage peut être modélisé plus simplement à l'aide d'une seule équation de diffusion :

$$\frac{\partial w}{\partial t} = -\text{div}(J_v + J_l) + \frac{\partial w_{ad}}{\partial t} \qquad (8.5)$$

où $D(h_r)$ est le coefficient de diffusion de l'eau. Nous utilisons le modèle de Bažant [55].

$$D(h_r) = D_0\left(a + \frac{1-a}{1+\left(\frac{1-h_r}{1-h_c}\right)^n}\right) \qquad (8.6)$$

où D_0, a, n et h_c sont des paramètres à déterminer par l'évolution expérimentale de la perte en masse. La variation de D_0 en fonction de la maturation du béton est prise en compte par l'inverse de l'évolution de la résistance en compression (voir Molez, [121]).

$$D_0(t) = D_0(t_\infty)\frac{m_2 + t^{m_1}}{t^{m_1}} \qquad (8.7)$$

Les coefficients m_1 et m_2 seront déterminés à partir de l'équation (8.3). Les conditions aux limites sur les surfaces séchantes sont du type convectif. Le flux d'eau à la surface d'échange J_s (en lm^{-2}s^{-1}) est déterminé alors à partir de la relation suivante:

$$J_s = \beta(h_r{}^s - h_r{}^a) \qquad (8.8)$$

où β est le coefficient d'échange par convection (fixe à 5 mm/jours), $h_r{}^s$ est la teneur en eau sur la surface, et $h_r{}^a$ est la teneur en eau à l'humidité relative environnante. Le retrait provoqué par les variations d'humidité relative est donc défini en fonction du coefficient de dilatation hydrique (α_h) comme:

$$\underline{\dot{\varepsilon_{ds}}} = \alpha_h \dot{h_r}\underline{\underline{1}} \qquad (8.9)$$

Le comportement viscoélastique est modélisé par un modèle rhéologique de Kelvin. La décomposition en série de Dirichlet permet d'éviter le stockage de l'historique de chargement (voir Molez, [121]). En ce qui concerne le comportement du béton à la fissuration, le critère en déformation de Mazars [124] sera utilisé. La relation entre la contrainte σ, la variable d'endommagement D, la déformation totale ε_{tot}, le retrait endogène ε_{end}, le retrait de séchage ε_s, la déformation élastique ε_e, et le fluage ε_f, sont alors donnés par la relation suivante:

$$[\sigma = (1-D)\bar{\sigma} = (1-D)E\dot{\varepsilon_e} = (1-D)E(\dot{\varepsilon}_{tot} - \dot{\varepsilon_f} - \dot{\varepsilon_s} - \dot{\varepsilon_{end}}) \qquad (8.10)$$

La variable d'endommagement, D, est comprise entre 0 (matériau sain) et 1 (complètement endommagé), voir Fig. A.6. Les paramètres du modèle sont calibrés par la suite sur des essais expérimentaux de caractérisation. On notera que pour des raisons de symétrie, seule le ¼ l'éprouvette a été maillé pour les

simulations pour reproduire l'essai complet. Le paramètre α_h est identifié à partir de la courbe expérimentale du retrait de séchage. Les simulations sont menées en imposant une H.R. extérieure égale à 50 %.

A.7 Résultats et discussion

A.7.1 Retrait libre: ASTM C157 et annulaire

Les comparaisons des résultats obtenus numériquement et les résultats expérimentaux sont présentées dans les Figs. A.2 et A.3. La Fig. A.2 présente le retrait mesuré sur des prismes. La Fig. A.3 présente le retrait mesure sur les anneaux. On constate une bonne concordance entre les courbes expérimentales et numériques pour les différents mélanges de béton étudiés, à la fois à court terme et à long terme. La comparaison entre les résultats expérimentaux et les simulations numériques met en évidence que les cinétiques du processus de séchage sont différents. En effet, le modèle proposé permet de reproduire l'effet de la cinétique de séchage et déformation identique aux résultats expérimentaux, quel que soit le mélange (coulé ou projeté) ou la géométrie d'éprouvette. Comme on s'y attendait, le mélange à haute teneur en ciment (M3) a subi les plus importantes déformations alors que le mélange à faible teneur en ciment (M1) a subi les plus faibles. Ensuite, on constate que le mélanges avec la fume de silice (M4) a développé des déformations nettement plus élevées que le mélange sans fumée de silice (M2). Les variations du rapport eau/liant amplifient ces variations.

En comparant les Fig. A.2 et A.3, on constate que pour un même mélange (C1 ou C2), le retrait de séchage de ces bétons dépend de la géométrie des éprouvettes et, par conséquent, le S_d/V exposé au séchage. On constate que des valeurs plus élevées de retrait étaient enregistrées sur des éprouvettes prismatiques comparées aux éprouvettes de géométrie annulaires. En fait, plus le rapport surface/volume est grand, plus le taux de séchage est important ce qui mène à un retrait important.
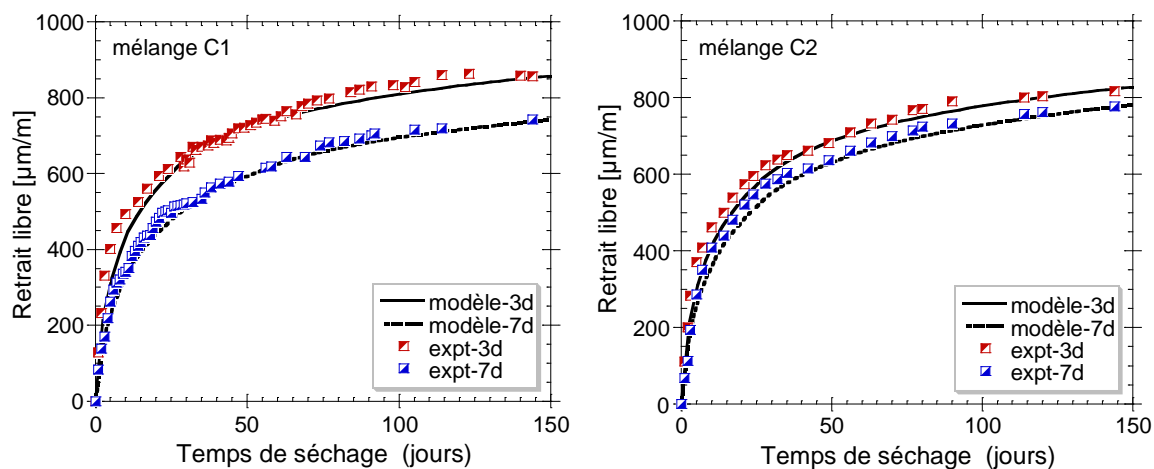
Fig. A.2 Évolution du libre retrait sur prisme après 3 et 7 jours de mûrissement à 100% H.R. (t_0= 3d et 7d): Comparaison des résultats expérimentaux et de la modélisation - Cas du béton coulé en place
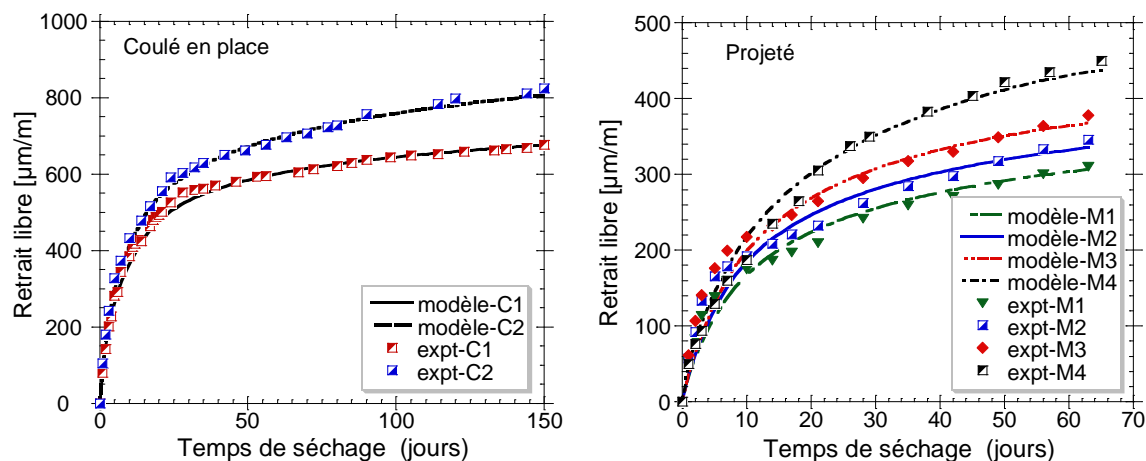
Fig. A.3 Évolution du retrait libre sur anneau après 3 jours de mûrissement à 100% H.R.: comparaison des résultats expérimentaux et de la modélisation - Cas du béton coulé en place et projeté

A.7.2 Sensibilité à la fissuration du béton projeté

Les Figs. A.4 et A.5 donnent les évolutions expérimentales et simulées de la contrainte moyenne dans le cas de l'essai de retrait restreint annulaire. La Fig. A.4 présente les graphiques pour les mélanges coulé en place et la Fig. A.5 présente les graphiques pour les mélanges projeté par voie sèche. On observe à nouveau que le modèle permet de reproduire la cinétique observée expérimentalement. On voit sur cette figure que l'évolution des contraintes circonférentielles et le temps à la fissuration sont correctement décrits, en utilisant les paramètres identifiés sur l'essai expérimental. Ainsi, le modèle est capable de reproduire correctement la dépendance à la cinétique de séchage, quel que soit le mélange, la géométrie ou la méthode de mise en place. En effet, plus la vitesse de séchage est importante, moins le matériau a de temps disponible pour développer sa résistance et fluer. Par conséquent, la sensibilité à la fissuration est plus élevée.

On peut observer que la sensibilité à la fissuration au jeune âge croît avec l'augmentation de la quantité de ciment. En fait, une diminution de la teneur en ciment réduit le taux d'évolution de contrainte moyenne. On constate également que l'ajout de fumée de silice en remplacement partiel du ciment se traduit par l'augmentation du potentiel de fissuration. Ainsi, les résultats démontrent que pour les mélanges sans fumée de silice, la diminution du rapport eau/ciment augmente le risque de fissuration par retrait. Ce phénomène s'explique par le fait que le retrait endogène se développe plus rapidement et est plus important pour un rapport eau/ciment plus faible.

La fissuration observée expérimentalement et dans le modèle sont comparés à la Fig. A.6. On peut observer, en outre, que la fissure s'initie au bord extérieur et se propage vers le bord intérieur. On voit que

la variable d'endommagement est plus importante au bord extérieur. En effet, le gradient d'humidité induit à cet endroit une concentration de contraintes de traction qui mènent à la fissuration du béton.

Le même phénomène est observé expérimentalement à l'aide d'une méthode d'émission acoustique par Hossain et Weiss [75]. Cela est conforme à l'idée que la contrainte de traction maximale se développe sur le bord extérieur dans l'anneau de béton en raison des gradients d'humidité [57]. Il apparaît clairement sur la Fig. A.6 que la fissuration de retrait présente des zones d'endommagement distinctes entre 0 (matériau sain) et 1 (matériau rompu). Ceci signifie que la distribution des contraintes dans l'anneau n'est pas uniforme.
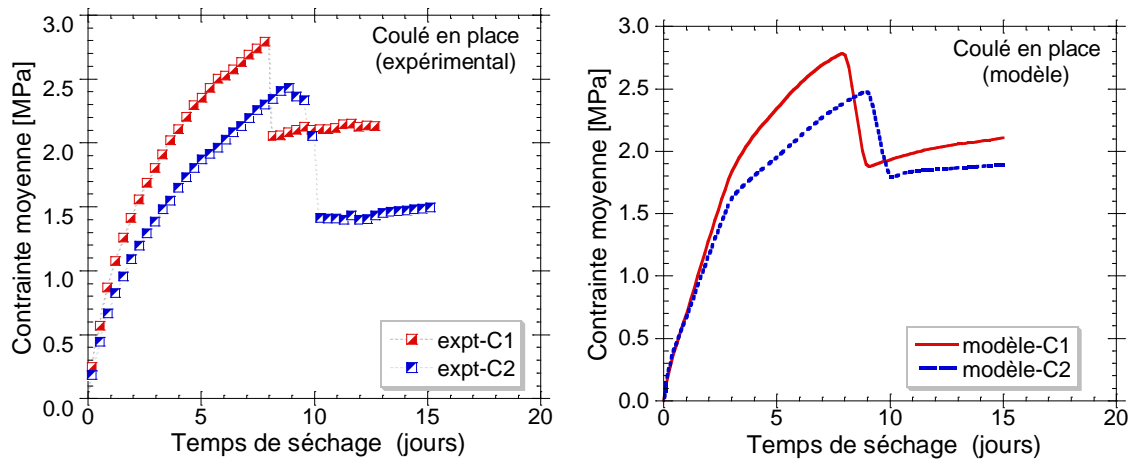
Fig. A.4 Évolution de la contrainte moyenne après 3 jours de mûrissement à 100 % H.R. : comparaison des résultats expérimentaux et de la modélisation - Cas du béton coulé en place
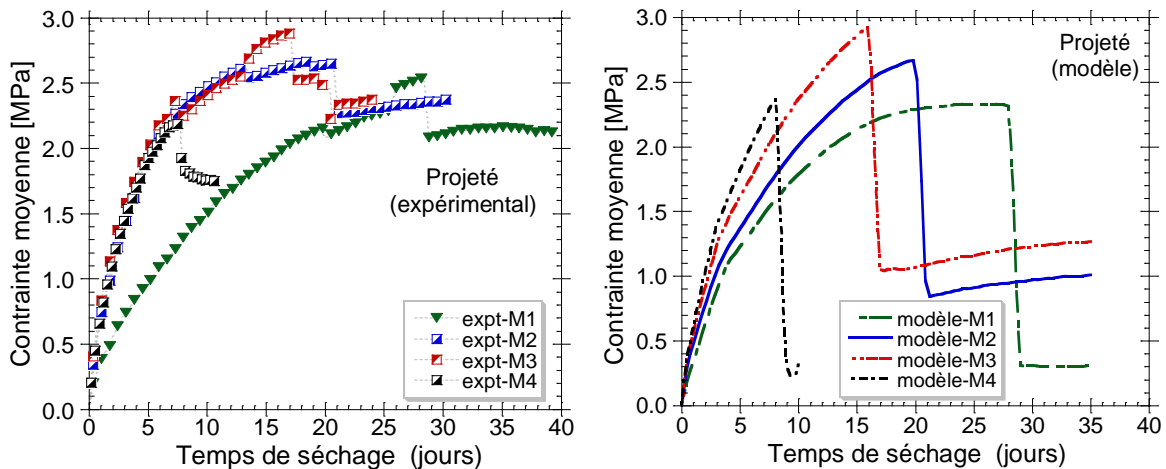
Fig. A.5 Évolution de la contrainte moyenne après 3 jours de mûrissement à 100 % H.R. : comparaison des résultats expérimentaux et de la modélisation - Cas du béton projeté par voie sèche
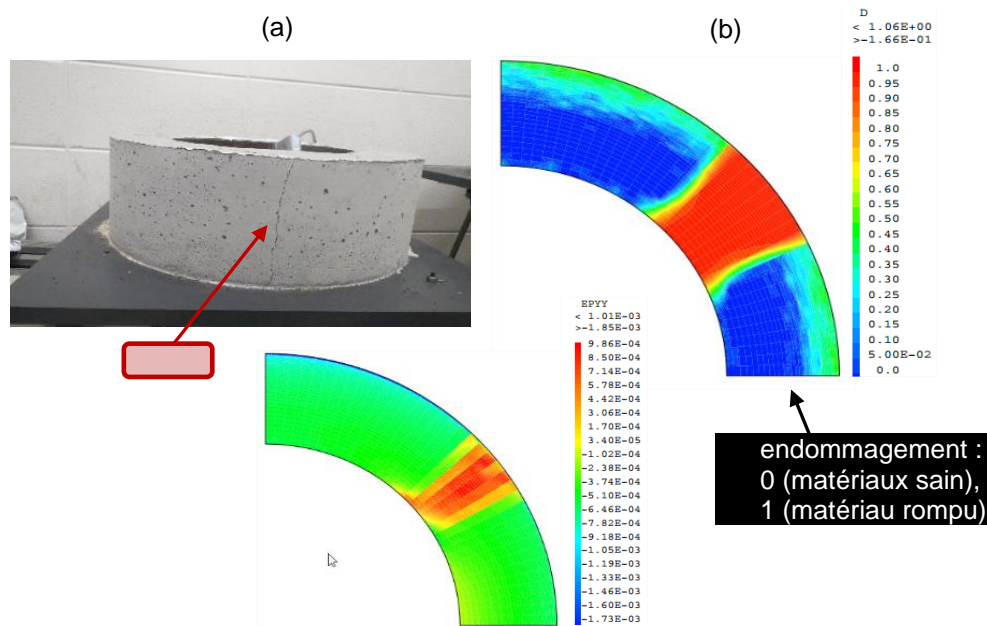
Fig. A.6 Patron des fissurations expérimental (a) et numérique (b) après 3 jours de cure

A.8 Conclusions

Cet article présente l'analyse des sensibilités à la fissuration des bétons projetés au jeune âge par une étude expérimentale et modélisation numérique. Globalement, les résultats obtenus démontrent que le retrait et le potentiel de fissuration des bétons projetés dépendent de leurs propriétés individuelles. Les résultats démontrent entre autres que le retrait dépend du rapport volume/surface exposé au séchage. Aussi, les résultats révèlent que la présence de fumée de silice augmente nettement le taux de retrait libre. On remarque que la sensibilité à la fissuration au jeune âge augmente avec l'augmentation de la quantité de ciment dans le mélange. On constate également que l'ajout de fumée de silice en remplacement partiel du ciment se traduit par la diminution de la résistance à la fissuration des bétons. Ainsi, on observe que pour les mélanges sans fumée de silice, le faible rapport eau/ciment augmente le risque de fissuration par retrait. Enfin, le modèle développé permet de faire un choix sélectif des matériaux de réparations moins vulnérables face à la fissuration. Dans ce modèle, seuls le retrait endogène, la perte de masse et les propriétés mécaniques doivent être connus. Ces résultats serviront à tous les domaines utilisant le béton projeté afin de produire des bétons plus robustes et résistant à la fissuration.

A.9 Remerciements

A.10 Références

[3] S. Girard. 2013. Etude du bilan deformationnel des bétons projetés, MSc Thesis, Université Laval, Quebec, Canada, pp. 124 pages. (in French)

[9] ACI-506R-16. 2016. Guide to Shotcrete, American Concrete Institute, Farmington Hills, USA, pp. 40 pages.

[33] F. Benboudjema. 2002. Modélisation des déformations différées du béton sous sollicitations biaxiales. Application aux enceintes de confinement de bâtiments réacteurs des centrales nucléaires, PhD Thesis, Université de Marne la Vallée, Champs-sur-Marne, France, pp. 254 pages. (in French)

[55] Z. Bažant, L. Najjar. 1971. Drying of concrete as a nonlinear diffusion problem, Cem. Concr. Res., 1(5), 461-473.

[57] B. Menu, M. Jolin, B. Bissonnette. 2017. Studies on the influence of drying shrinkage test procedure, specimen geometry, and boundary conditions on free shrinkage, Adv. Mater. Sci. Eng., 2017(Article ID 9834159), 9.

[75] A.B. Hossain, J. Weiss. 2004. Assessing residual stress development and stress relaxation in restrained concrete ring specimens, Cem. Concr. Compos., 26(5), 531-540.

[120] F. Modjabi-Sangnier, A. Ghezal, B. Bissonnette, M. Jolin. 2008. Réduction du potentiel de fissuration des bétons de réparation: approche quantitative de la notion de compatibilité, Transports Québec, Proceedings of the 13e Colloque sur la progression de la recherche québécoise sur les ouvrages d'art, Québec, Qc., pp. 8. (in French)

[121] L. Molez. 2003. Comportement des réparations structurales en béton: couplage des effets hydriques et mécaniques, PhD Thesis, École normale supérieure de Cachan - ENS Cachan, France, pp. 249 pages. (in French)

[122] F.-J. Ulm. 1999. Couplages thermochémomécaniques dans les bétons(un premier bilan), (1161-028X), Etudes et recherches des Laboratoires des ponts et chaussées. Série Ouvrages d'art, Paris, France, pp. pages. (in French)

[123] P. Acker. 1987. The mechanical behavior of concrete: contributions of the physico-chemical approach, PhD Thesis, École nationale des ponts et chaussées, Champs-sur-Marne, France, pp. 121 pages.

[124] J. Mazars. 1984. Application de la mécanique de l'endommagement au comportement non linéaire et à la rupture du béton de structure., PhD Thesis, Université Pierre et Marie Curie-Paris 6, Paris, France, pp. 283 pages. (in French)

Appendix B Mixture Constituents

Type GU Cement used in this study

Ciment Québec

CERTIFICAT D'ANALYSE

Ciment à usage général type | **GU** | *Mars 2017*

Essais physiques

Temps de prise Vicat (minutes)
Initial...120
Final 260

Finesse
Blaine (m²/kg) 392
Retenu 45 µm (%) 5

Expansion
à l'autoclave (%) 0.10

Teneur en air (%) 6

Résistance à la compression (MPa)
3 jours 24.7
7 jours 29.1
28 jours (Fév. '17) 36.4

Expansion des barres de mortier
à 14 jours (%)..............................0.008

Analyses chimiques (%)

SiO_2 .... 19.0
Al_2O_3 .... 4.9
Fe_2O_3 .... 3.8
CaO 60.5
CaO libre.. 1.2
MgO.. 2.6
SO_3 .... 4.1
Perte au feu 1.8
Insolubles 0.5
Alcalis (équivalent Na_2O)................. 0.97

Composition Minéralogique
C_3S 51.4
C_2S 15.7
C_3A 6.7
C_4AF... 11.4

> *Par la présente, nous certifions que le ciment livré est conforme aux exigences de la norme CSA A3000-13 section A3001-13, type GU.*

Pour tout renseignement concernant ce certificat d'analyse, veuillez contacter nos services techniques au (418) 329-2100.

GUCsaFr

145, boul. du Centenaire • Saint-Basile (Québec) G0A 3G0 • Canada • Tél.: 418 329-2100 • Téléc.: 418 329-3436   **Synergia**   **ISO 9001**

SiLICIUM QUÉBEC SEC

CERTIFICAT D'ANALYSE
FUMÉE DE SILICE RÉGULIÈRE

ASTM C1240-15 SPÉCIFICATIONS STANDARDS		*Limites*	*Analyse de 2016*
PHYSIQUE	Indice d'activité pouzzolanique, 7 jours	*> 105*	**139**
	Surface Spécifique BET (m^2/g) *	*> 15*	**19**
	Densité (g/cm^3) *	*-*	**2.22**
	Finesse, retenu sur 45 µm (325 mesh) (%) *	*< 10*	**2.7**
CHIMIQUE	Perte au feu (PAF) (%) *	*< 6.0*	**2.7**
	Humidité (%) *	*< 3.0*	**0.13**
	Dioxyde de silicium (SiO$_2$) (%) *	*> 85*	**94.5**
	Chlorure - soluble à l'acide (% par poids)	*-*	**0.10**
	Alcalis totaux (%)	*-*	**0.67**

* Analyses faites par un laboratoire externe

CSA A3001-13 - SPÉCIFICATIONS		*Limites*	*Analyse de MARS 2017*
PHYSIQUE	Expansion à l'autoclave (%) *	*< 0.2*	**-0.042**
	Finesse, retenue sur 45 µm (325 mesh) (%)	*< 10*	**4.63**
	Tendance à capter l'air	*Pas de bulles*	**Pas de bulles**
CHIMIQUE	Perte au feu (PAF) (%)	*< 10*	**2.93**
	Dioxyde de silicium (SiO$_2$) (%)	*> 85*	**94.1**
	Trioxyde de soufre (SO$_3$) (%)	*< 1.0*	**0.27**

* Analyses faites par un laboratoire externe

ANALYSE DE PRODUCTION		*Analyse de MARS 2017*
PHYSIQUE et CHIMIQUE	Carbone libre (C) (%)	**2.58**
	Chlorure (Cl-) (%)	**0.22**
	Densité Apparente (g/L)	**154**
	Humidité (%)	**0.64**
	Oxyde d'Aluminium (Al$_2$O$_3$) (%)	**0.22**
	Oxyde de Calcium (CaO) (%)	**0.61**
	Oxyde de fer III (Fe$_2$O$_3$) (%)	**0.10**
	Oxyde de Magnésium (MgO) (%)	**0.28**
	Pentoxyde de phosphore (P$_2$O$_5$) (%)	**0.13**
	Oxyde de Potassium (K$_2$O) (%)	**0.59**
	Oxyde de Sodium (Na$_2$O) (%)	**0.20**

COMMENTAIRES :

La fumée de silice rencontre les spécifications de "Silica Fume Used in Cenmentitious Mixtures of ASTM C1240-15" et de "Cementing Materials and Blended Supplementary Cementing Materials of CSA A3001-13" pour le type SF.

RAPPORT PRÉPARÉ PAR :	DATE :	VERSION :
	3 mai 2017	**2**

SILICIUM QUÉBEC S.E.C. , 6500 Yvon-Trudeau, Bécancour, QC Canada G9H 2V8

Chemical analysis of the fly ash

LAFARGE
NORTH AMERICA

Lafarge Material Performance Center	1263 Lakeview Drive	Romeoville, IL 60446	1-630-243-4699

FLY ASH SOURCE: PRESQUE ISLE CLASS C
COMPOSITE DATE: 1-Mar-16 to 31-Mar-16
SAMPLE IDENTIFICATION: PIS1160301-0331

SPECIFICATIONS

CHEMICAL ANALYSIS			ASTM C 618 CLASS C	AASHTO M 295 CLASS C
SiO2 (silicon dioxide), %	=	36.79		
Al2O3 (aluminum oxide), %	=	18.62		
Fe2O3 (iron oxide), %	=	5.55		
SiO2+Al2O3+Fe2O3, %	=	60.96	50 Min	50 Min
CaO (calcium oxide), %	=	21.33		
MgO (magnesium oxide), %	=	5.18		
SO3 (sulfur trioxide), %	=	2.22	5.0 Max	5.0 Max
Moisture content, %	=	0.15	3.0 Max	3.0 Max
Loss On Ignition, %	=	1.08	6.0 Max	5.0 Max
Na2O (sodium oxide), %	=	4.50		
K2O (potassium oxide), %	=	0.72		
Total Equivalent Na2O, %	=	4.55		

PHYSICAL ANALYSIS				
Fineness, amount retained on #325 sieve, %	=	7.3	34 Max	34 Max
variation, points from average	=	-2.5	5 Max	5 Max
Density, Mg/m3	=	2.7		
variation from average, %	=	1.2	5 Max	5 Max
Strength Activity Index with Portland Cement at 7 days, % of cement control	=	104	75 Min	75 Min

Cement: LafargeHolcim Ste.Genevieve Type I/II

Water Requirement % of cement control	=	95	105 Max	105 Max
Soundness, autoclave expansion or contraction, %	=	0.07	0.8 Max	0.8 Max

The test results for this composite sample comply with the applicable specifications of ASTM C 618 and AASHTO M 295. This fly ash source is approved for use by the following state agencies:

5/1/2016
Report Date

ASTM C 618 Note 1 - Finely divided materials may tend to reduce the entrained air content of concrete. Hence, if a mineral admixture is added to any concrete for which entrainment of air is specified, provision should be made to ensure that the specified air content is maintained by air content tests and by use of additional air-entraining admixture or use of an air-entraining admixture in combination with air-entraining hydraulic cement.

Technical data sheet: sand from Lafarge

FICHE TECHNIQUE LAFARGE GRANULATS QUÉBEC

SITE: SABLIÈRE ST-GABRIEL   **PRODUIT:** AG2556 SABLE À BÉTON

DATE: 13 janv. 2014   **RÉSERVE:** 1-13

	NOMBRE ÉCH.	CSA A23.2-1A, 2A, 5A ANALYSE GRANULOMÉTRIQUE																	Module de finesse
		TAMIS (MM)												TAMIS (µM)				
	1	150	112	80	56	40	31.5	28	20	14	10	5	2.5	1.25	630	315	160	80	
RÉSULTATS	MOYENNE										100	93	84	70	50	25	9	2.4	2.68
	ÉCART-TYPE																		
EXIGENCES	LIMITE SUP.										100	100	100	90	65	35	10	3.0	3.1
	LIMITE INF.										100	95	80	50	25	10	2	0	2.3

RÉSULTATS ESSAIS PHYSIQUES

NUMÉRO ET DESCRIPTION ESSAI	RÉSULTAT	EXIGENCE	EFFECTUÉ PAR	DATE
LC 21-255 VALEUR AU BLEU DE MÉTHYLÈNE	0.04	≤0.20%	Solmatech	16 janv. 2014
LC 21-101 MICRO DEVAL GRANULATS FINS	18.1%	≤30%	LAFARGE GRANULATS	17 janv. 2014
CSA A23.2-23A MICRO DEVAL GRANULAT FIN	9.1%	≤20%	LAFARGE GRANULATS	17 janv. 2014
CSA A23.2-7A INDICE COLORIMÉTRIQUE	1	≤3	LAFARGE GRANULATS	17 janv. 2014
LC 21-080 FRIABILITÉ DES GRANULATS FINS	19.8	≤40%	LAFARGE GRANULATS	17 janv. 2014
LC 31-228 MATIÈRES ORGANIQUES	0.03%	≤0.8%	Solmatech	16 janv. 2014
CSA A23.2-3A TENEUR EN MOTTES D'ARGILE	0.23%	≤1.0%	LAFARGE GRANULATS	17 janv. 2014
CSA A23.2-4A PARTICULES LÉGÈRES	0.0%	≤0.5%	LAFARGE GRANULATS	17 janv. 2014
CSA A23.2-6A DENSITÉ GRANULAT FIN (BRUT)	2.677		LAFARGE GRANULATS	17 janv. 2014
CSA A23.2-6A DENSITÉ GRANULAT FIN (SSS)	2.693		LAFARGE GRANULATS	17 janv. 2014
CSA A23.2-6A DENSITÉ GRANULAT FIN (APP)	2.721		LAFARGE GRANULATS	17 janv. 2014
CSA A23.2-6A ABSORPTION GRANULAT FIN	0.60		LAFARGE GRANULATS	17 janv. 2014
CSA A23.2-9A DURABILITÉ MGSO4	7.13	16	LAFARGE GRANULATS	16 janv. 2014
CSA A23.2-10A MASSE VOLUMIQUE (TASSÉE)	1806.5		LAFARGE GRANULATS	17 janv. 2014
CSA A23.2-10A MASSE VOLUMIQUE (NON-TASSÉE)	1631.1		LAFARGE GRANULATS	17 janv. 2014
CSA A23.2-14A RÉACTION ALCALIS-GRANULATS	0.003%	<0.040%	GROUPE QUALITAS	23 mars 2013
CSA A23.2-5A PERTE AU 80µM	2.4%	3.0 Max	LAFARGE GRANULATS	17 janv. 2014

Technical data sheet: sand from Sables L.G.

FICHE TECHNIQUE DES GRANULATS (COMPILATION QUALITATIVE)

Type de matériaux :	Sable à béton	Calibre:	0-5 mm	Date:	05/01/16
Provenance :	Sables L.G.	Classe granulaire:		Usages prévus:	Béton de ciment
	St-Hippolyte, Québec	Classement :	1		

Granulométrie (A 23.2-2A)		% passant en mm													% passant en um			
Saison 2016	Nombre d'éch.	112	80	56	40	31.5	28	20	16	14	12.5	10	5	2.5	1.25	630	315	160	80
	2											100	100	85	63	43	27	9	2.8
Norme	Limite inf											-	95	80	50	25	10	2	0.0
BC 80um-5mm	Limite sup											100	100	100	90	65	35	10	3.0

Caractéristiques intrinsèques	Norme d'essai	Résultats	Exigences		Date	Effectué par
Micro-Deval (MD)	LC 21-101 /A23,2-23A	21,0% / 11,9%	≤30%		16 05 01	Inspec-sol inc.
Friabilité	LC 21-080	29.4%	≤ 40%		16 05 01	Inspec-sol inc.

Caractéristiques complémentaires	Norme d'essai	Résultats	Exigences		Date	Effectué par
Mottes d'argiles et part friables (%)	CSA A23.2-3A	0.1	≤1,0		16 05 01	Inspec-sol inc.
Particules légères (%)	CSA A23.2-4A	0.1	≤ 0,5		16 05 01	Inspec-sol inc.
Propreté (particules < 80 um) (%)	CSA A23.2-5A	2.9	< 5,0		16 05 01	Laboratoire central
Densité relative brute/sss/app	CSA A23.2-6A	2,718 / 2,737 / 2,771	NA		16 05 01	Inspec-sol inc.
Absorption	CSA A23.2-6A	0.71	NA		16 05 01	Inspec-sol inc.
Indice colorimétrique	CSA A23.2-7A	1	< 3		16 05 01	Inspec-sol inc.
Module de finesse	CSA A23.1	2.73	2,3 à 3,1		16 05 01	Laboratoire central
Perte au MgSO4 (%)	CSA A.23.2-9A	5.2	< 16		16 05 01	Inspec-sol inc.
Masse volumique tassée & non tassée	CSA A.23.2-10A	1837 / 1696	NA		16 05 01	Inspec-sol inc.
Sédimentométrie au 2 um (%)	ASTM D-422	1	< 3		16 05 01	Inspect-Sol inc.
Potentiel de réactivité alcalis granulats	CSA A.23.2-14A	0.017	< 0,040%		16 04 20	Qualitas

CARRIÈRES LAURENTIENNES

17250, Côte St-Antoine
Mirabel (Québec)
J7J 2G9
Tél : (450) 432-4317
Fax : (450) 432-9765

CARRIÈRES Laurentiennes
CARRIÈRES UNI-JAC INC.

ESSAIS SUR GRANULATS

Client:		
Projet : Qualitatif 2016	Usage proposé :	BÉTON / ENROBÉS BITUMINEUX

Matériau : Pierre concassée	Calibre :	5-10 mm
Source : Carrières Laurentiennes	Endroit :	Mirabel

GRANULOMÉTRIE			PROPRIÉTÉS PHYSIQUES ET MÉCANIQUES					EXIGENCES	*
Tamis	% passant		Propreté		CSA A23.2-5A	1.3	%	≤ 1.5	1
(mm)	mesuré	exigences	Masse volumique	tassée	CSA A23.2-10A	1631	kg/m^3		1
				non tassée	CSA A23.2-10A	1561	kg/m^3		1
			Densité sèche		CSA A23.2-12A	2.786			1
			Densité S.S.S.		CSA A23.2-12A	2.802			1
			Densité apparente		CSA A23.2-12A	2.830			1
			Absorption		CSA A23.2-12A	0.56	%		1
			Los Angeles (B2)		LC 21-400	17.5	%	≤ 35	2
14	100	100	Los Angeles (C)		CSA A23.2-16A	18.1	%	≤ 50	2
10	90	85-99	Micro-Deval (E)		LC 21-070	5.5	%	≤ 15	1
5	8	1-15	Micro-Deval		CSA A23.2-29A	6.1	%	≤ 17	1
2.5	2	0-3	Micro-Deval + Los Angeles		LC 21-070 + LC 21-400	23.0	%	≤ 40	1
1.25			Fragmentation		LC21-100	100	%	100	1
0.630			Particules	plates	LC 21-265	10.6	%	≤ 25	1
0.315				allongées	LC 21-265	25.9	%	≤ 40	1
0.160				plates/allongées	LC 21-265	5.6	%		1
			Particules	plates	CSA A23.2-13A	10.4	%	≤ 25	1
				allongées	CSA A23.2-13A	25.8	%	≤ 45	1
				plates/allongées	CSA A23.2-13A	5.6	%	≤ 20	1
0.080	1.3	0-1.5	CPP		LC 21-102	0.52		≥ 0.45	3
			Nombre pétrographique		CSA A23.2-15A	111		< 125	2
			Réaction alcalis-granulats		CSA A23.2-14A	0.021	%	< 0.040	2
			Mottes d'argile et particules friables		CSA A23.2-3A	0.20	%	≤ 0.3	2
			Teneur en particules légères		CSA A23.2-4A	0,0	%	≤ 0.5	2
Labo. no. :			Gel/dégel (non confiné)		CSA A23.2-24A	1.6	%	< 6	2

*Remarques :

    Essais effectués par :

    1: Laboratoire PM FABRICATION INC.

    2: Laboratoire EXP

    3 : Centre de technologie minérale et de plasturgie inc.

Date :   2016-05-10

Technical data sheet: coarse aggregate from Lafarge

FICHE TECHNIQUE LAFARGE GRANULATS QUÉBEC

SITE: CARRIÈRE MIRABEL   **PRODUIT:** AG1527 10-2.5MM BÉTON CALCAIRE

DATE: 31 mai 2013   **RÉSERVE:** 1-2013

CSA A23.2-2A ANALYSE GRANULOMÉTRIQUE

	NOMBRE ÉCH.	TAMIS (MM)													TAMIS (µM)				Module de finesse
		200	150	112	80	56	40	28	20	14	10	5	2.5	1.25	630	315	160	80	
RÉSULTATS PRODUCTION	MOYENNE									100	88	14	4	3				1.2	
	ÉCART-TYPE																		
EXIGENCES CSA A23.2	LIMITE SUP.									100	100	30	10	5				2.0	
	LIMITE INF.									100	85	10	0	0				0.0	

RÉSULTATS ESSAIS PHYSIQUES

NUMÉRO ET DESCRIPTION ESSAI	RÉSULTAT	EXIGENCE	EFFECTUÉ PAR	DATE
CSA A23.2-3A MOTTES D'ARGILE	0.09%	≤0.3%	LAFARGE GRANULATS	31 mai 2013
CSA A23.2-4A PARTICULES LÉGÈRES	0.0%	≤0.50%	LVM	31 mai 2013
CSA A23.2-5A PERTE AU 80µM	1.20%	≤2.0%	LAFARGE GRANULATS	31 mai 2013
CSA A23.2-9A MGSO4	2.6%	≤12%	LAFARGE GRANULATS	19 janv. 2013
CSA A23.2-10A MASSE VOLUMIQUE (NON-TASSÉE)	1661 kg/m^3		LAFARGE GRANULATS	31 mai 2013
CSA A23.2-10A MASSE VOLUMIQUE (TASSÉE)	1448 kg/m^3		LAFARGE GRANULATS	31 mai 2013
CSA A23.2-12A DENSITÉ GROS GRANULATS (BRUTE)	2.772		LAFARGE GRANULATS	4 juin 2013
CSA A23.2-12A DENSITÉ GROS GRANULATS (SSS)	2.784		LAFARGE GRANULATS	4 juin 2013
CSA A23.2-12A DENSITÉ GROS GRANULATS (APP)	2.815		LAFARGE GRANULATS	4 juin 2013
CSA A23.2-12A ABSORPTION GROS GRANULATS	0.39%		LAFARGE GRANULATS	4 juin 2013
CSA A23.2-13A PARTICULES PLATES (MÉTHODE B)	23.6%	≤25%	LAFARGE GRANULATS	8 avr. 2013
CSA A23.2-13A PARTICULES ALLONGÉES (MÉTHODE B)	37.9%	≤40%	LAFARGE GRANULATS	8 avr. 2013
CSA A23.2-14A RÉACTION ALCALIS-GRANULATS	0.019	<0.040%	LVM	28 mars 2011
CSA A23.2-15A ANALYSE PÉTROGRAPHIQUE	100	≤125	LVM	5 juin 2013
CSA A23.2-16A LOS ANGELES (GRADE D)	25.1%	≤50%	LAFARGE GRANULATS	31 mai 2013
CSA A23.2-24A GEL ET DÉGEL	5.0%	≤6%	LAFARGE GRANULATS	19 janv. 2013
CSA A23.2-29A MICRO DEVAL GROS GRANULATS (Grade 6.4)	12.5%	≤17%	LAFARGE GRANULATS	31 mai 2013
LC 21-070 MICRO DEVAL (GRADE E)	7.0%	≤15%	LAFARGE GRANULATS	31 mai 2013
LC 21-400 LOS ANGELES (GRADE C1)	19.30%	≤35%	LAFARGE GRANULATS	31 mai 2013
MICRO-DEVAL + LOS-ANGELES	26.3	≤40%	LAFARGE GRANULATS	31 mai 2013
LC 21-102 COEFFICIENT POLISSAGE PAR PROJECTION	0.49	≥0.45	CTMP	2 mai 2012
LC 21-100 PARTICULES FRACTURÉES	100%	100%	LAFARGE GRANULATS	31 mai 2013

Technical data sheet: Shrinkage-reducing admixture

Peramin® SRA 40

Shrinkage reducing agent

Updated : 03/2013

Description

Peramin® SRA 40 is a polyols based additive in powder which reduces mainly drying shrinkage.

Compatibility

Peramin® SRA 40 is compatible with the majority of admixtures used in drymix mortars and specially with **Peramin® CONPAC and SMF.**

Laboratory trials are advised before any industrial use.

Application

Dry-mortar industry

Concrete

Specifications

	Datas	Methods
Appearance	Powder	Visual
Active Matter (%)	58 - 64	PEROU012*
Bulk Density	0.55 - 0.75	PEROU007*
Granulometry (% > 600 µm)	< 3%	PEROU010*
pH (5% solution)	6 - 8	PEROU008*

* Internal methods

Dosage

Depending on the application, the dosage of **Peramin® SRA 40** varies from 1% to 5% by weight of hydraulic binder.

Packaging

• Pallet of 20 sacks of 25 kg

Conditions of storage

• Shelf life : 12 months in unopened bags, between 5°C and 35°C.
• The product may absorb moisture and should be stored in dry area.
• Opened bags should be carefully resealed and used within a short period of time.

# Technical data sheet: Crack-reducing admixture

Drying Shrinkage

MasterLife CRA 007 admixture reduces the drying shrinkage of concrete relative to a plain reference mixture as measured by the ASTM C 157/C 157M test method. The reduction in drying shrinkage is similar to that obtained with conventional shrinkage-reducing admixtures. However, MasterLife CRA 007 admixture provides a greater reduction in the potential for cracking and initial crack width should cracking occur. As shown in the pictures, concrete specimens treated with MasterLife CRA 007 admixture showed a ten-fold reduction in initial crack width compared to plain concrete or conventional shrinkage-reducing admixture-treated concrete specimens, when tested in accordance with ASTM C 1581/C 1581M.

CRA-treated concrete
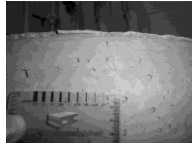
Crack width ≈ 100 µm (0.1 mm)

Untreated or SRA-treated concrete
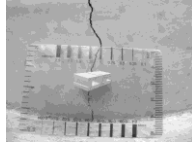
Crack width ≈ 1,000 µm (1 mm)

Guidelines for Use

Dosage: The recommended dosage range of MasterLife CRA 007 admixture is 1.0 to 2.0 gal/yd³ (5.0 to 10.0 L/m³), depending on the specific application. However, dosages outside of this range may be required depending on the level of shrinkage reduction and crack control desired. A reduction of mix water content equivalent to the dosage of MasterLife CRA 007 admixture utilized is recommended.

Mixing: MasterLife CRA 007 admixture may be added to the concrete mixture during the initial batch sequence or at the jobsite. If the delayed addition method is used, mixing at high speed for 3 to 5 minutes after the addition of MasterLife CRA 007 admixture will result in mixture uniformity.

Product Notes

Corrosivity – Non-Chloride, Non-Corrosive: MasterLife CRA 007 admixture will neither initiate nor promote corrosion of reinforcing steel, prestressing steel or of galvanized steel floor and roof systems. Neither calcium chloride nor other chloride-based ingredients are used in the manufacture of MasterLife CRA 007 admixture.

Compatibility: MasterLife CRA 007 admixture is compatible with all BASF water-reducers, mid-range water-reducers, high-range water-reducers, set retarders, and accelerators. MasterLife CRA 007 admixture should be added separately to the concrete mixture to ensure desired results.

Odor: A slight odor may be noticed when MasterLife CRA 007 admixture is used in concrete placed in confined areas. This non-harmful odor is an aromatic indication that the admixture is in the concrete.

Storage and Handling

Storage Temperature: MasterLife CRA 007 admixture is a potentially combustible material with a flash point of 189 °F (87 °C). This is substantially above the upper limit of 140 °F (60 °C) for classification as a flammable material, and close to the limit of 200 °F (93 °C) where DOT requirements would classify this as a combustible material. Nonetheless, this product must be treated with care and protected from excessive heat, open flame or sparks. For more information refer to the Safety Data Sheet. MasterLife CRA 007 admixture should be stored at ambient temperatures above 35 °F (2 °C), and precautions should be taken to protect the admixture from freezing. If MasterLife CRA 007 admixture freezes, thaw and reconstitute by mild mechanical agitation. **Do not use pressurized air for agitation.**

Shelf Life: MasterLife CRA 007 admixture has a minimum shelf life of 24 months. Depending on storage conditions, the shelf life may be greater than stated. Please contact your local sales representative regarding suitability for use and dosage recommendations if the shelf life of MasterLife CRA 007 admixture has been exceeded.

Durability

MasterLife CRA 007 admixture can be used in combination with other BASF durability-enhancing products such as MasterFiber® products, MasterLife CI 30 corrosion inhibitor, MasterLife SF 100 silica fume, MasterLife 300 D integral waterproofing admixture, and MasterLife ASR 30 alkali-silica reaction inhibitor to provide extended service life of concrete structures exposed to aggressive environments.

Packaging

MasterLife CRA 007 admixture is available in 55 gal (208 L) drums and 275 gal (1040 L) totes.

Related Documents

Safety Data Sheets: MasterLife CRA 007 admixture

Additional Information

For additional information on MasterLife CRA 007 admixture or its use in developing concrete mixtures with special performance characteristics, contact your local sales representative.

The Admixture Systems business of BASF's Construction Chemicals division is the leading provider of solutions that improve placement, pumping, finishing, appearance and performance characteristics of specialty concrete used in the ready-mixed, precast, manufactured concrete products, underground construction and paving markets. For over 100 years we have offered reliable products and innovative technologies, and through the Master Builders Solutions brand, we are connected globally with experts from many fields to provide sustainable solutions for the construction industry.

Limited Warranty Notice

BASF warrants this product to be free from manufacturing defects and to meet the technical properties on the current Technical Data Guide, if used as directed within shelf life. Satisfactory results depend not only on quality products but also upon many factors beyond our control. BASF MAKES NO OTHER WARRANTY OR GUARANTEE, EXPRESS OR IMPLIED, INCLUDING WARRANTIES OF MERCHANTABILITY OR FITNESS FOR A PARTICULAR PURPOSE WITH RESPECT TO ITS PRODUCTS. The sole and exclusive remedy of Purchaser for any claim concerning this product, including but not limited to, claims alleging breach of warranty, negligence, strict liability or otherwise, is shipment to purchaser of product equal to the amount of product that fails to meet this warranty or refund of the original purchase price of product that fails to meet this warranty, at the sole option of BASF. Any claims concerning this product must be received in writing within one (1) year from the date of shipment and any claims not presented within that period are waived by Purchaser. BASF WILL NOT BE RESPONSIBLE FOR ANY SPECIAL, INCIDENTAL, CONSEQUENTIAL (INCLUDING LOST PROFITS) OR PUNITIVE DAMAGES OF ANY KIND.

Purchaser must determine the suitability of the products for the intended use and assumes all risks and liabilities in connection therewith. This information and all further technical advice are based on BASF's present knowledge and experience. However, BASF assumes no liability for providing such information and advice including the extent to which such information and advice may relate to existing third party intellectual property rights, especially patent rights, nor shall any legal relationship be created by or arise from the provision of such information and advice. BASF reserves the right to make any changes according to technological progress or further developments. The Purchaser of the Product(s) must test the product(s) for suitability for the intended application and purpose before proceeding with a full application of the product(s). Performance of the product described herein should be verified by testing and carried out by qualified experts.

Technical data sheet: Polymer (Etonis® 850)

POLYMER MODIFICATION OF SHOTCRETE

ETONIS® brand products are polymer modifiers that WACKER has developed specifically for modifying concrete. One important application of these products is in shotcrete for tunnel construction.

Processing Advantages

The most important advantage is the considerable reduction in rebound, which significantly shortens application times, thereby lowering system costs. In addition, ETONIS® can also be used universally for wet-mix or dry-mix methods, and can be processed using conventional techniques and standard equipment.

- Significant reduction in rebound
- Adhesion properties of the concrete are outstanding on critical and/or damp substrates
- Optimized flow properties make materials easier to pump
- Excellent processability without separating
- Contains no solvents or plasticizers, making it highly safe for the groundwater
- Can be adjusted for a low water-cement ratio
- Optimizes construction site logistics, reduces overheads for transportation and waste disposal and conserves natural resources

Shotcrete lining

Benefits in hardened concrete:

When distributed in the hardened cement matrix, the polymer forms resin domains, thereby ensuring good resistance to hydrostatic pressure and aggressive media such as gases. This effect is further enhanced by the reduced tendency of ETONIS®-enhanced concrete to crack. The excellent compaction properties of the polymer-modified fresh concrete along with the ability to adjust the water-cement ratio to a lower value result in outstanding ultimate strength.

- Improved resistance to sulfate and CO_2 (carbonation)
- Permanent waterproofing against hydrostatic pressure
- Reduced crack formation

Do you have any questions or ideas? If so, please contact us at **www.wacker.com/etonis**

Technical data sheet: high range water-reducing admixture

EUCON 37
High Range Water Reducer - Superplasticizer

DESCRIPTION

EUCON 37 is a high range water-reducing admixture. It may be added to the concrete at the job site or at the ready mix concrete plant. EUCON 37 is formulated to retain plastic consistancy for 30-60 minutes after dosing depending on the initial slumps, dosage rates, and ambient temperature. No chlorides are used in its formulation; consequently, it is recommended for prestressed concrete. It is also compatible with air-entraining agents, waterproofing agents, calcium chloride and many other admixtures; however, each material should be added to the concrete separately.
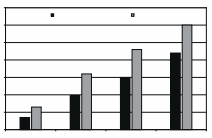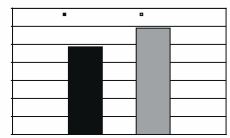
PRIMARY APPLICATIONS

• High performance concrete
• General ready mix concrete
• Heavily reinforced concrete

• Flatwork and mass concrete
• Minimum water content concrete
• Low water/cement ratio concrete
• High slump, flowable concrete

FEATURES/BENEFITS

• Produces low water content and low water/cement ratio concrete allowing higher strengths
• Produces flowing concrete with better than normal strengths
• Aids in concrete placement and reduces labor cost
• When used in precast work with Type I cement will produce the high early strengths

TECHNICAL INFORMATION

Performance Data:

The following test results were achieved using typical ASTM C 494 mix design requirements, 517 lb/yd³ (307 kg/m³) cement content and similar (± 0.5)% air content. These results were obtained under laboratory conditions with materials and mix designs meeting the specifications of ASTM C 494. Changes in materials and mix designs can affect the dosage response of EUCON 37.

PACKAGING

EUCON 37 is packaged in bulk, 275 gal (1041 L) totes, 55 gal (208 L) drums and 5 gal (18.9 L) pails.

SHELF LIFE

2 years in original, unopened package.

SPECIFICATIONS/COMPLIANCES

• Fully complies with the requirements of ASTM C 494, Types A & F admixtures.
• Fully complies with the requirements of AASHTO M 194.
• ANSI/NSF STD 61

DIRECTIONS FOR USE

EUCON 37 can be added to the initial batch water or directly on the freshly batched concrete and mixed for approximately 5 minutes or 70 revolutions. However, better results have been observed batching directly on the freshly batched concrete. It should not come into contact with dry cement or other admixtures until mixed thoroughly with the concrete batch.

EUCON 37 is typically used at dosages of 6 to 18 oz per 100 lbs (400 to 1170 mL per 100 kg) of cementitious material. Other dosages are acceptable with prior testing and confirmation of the desired performance with specific materials being used.

For any concrete application including Self-Consolidating Concrete (SCC), the dosage of EUCON 37 will vary depending on the mix design, local materials, and individual needs of the concrete producer. Trial mixes should be run to verify plastic and hardened performance with local materials. If the material gradations are not optimum for SCC, a viscosity modifier may be used to improve the quality of the mix. Please consult a local Euclid Chemical Sales Professional for trial mixtures and dosage recommendations.

EUCON 37 is compatible with most admixtures including air-entraining agents, accelerators, most water-reducers, retarders, shrinkage reducers, corrosion inhibitors, viscosity modifiers, and microsilica; however, each material should be added to the concrete separately.

Figure 1: Recommended Dosage of Eucon 37 to achieve flowable concrete (7 - 9"/ 180-230 mm slump)

Initial Slump, inches (mm)	Dosage Range of Eucon 37, oz/cwt (mL/100 kg)
4 (100)	8 - 10 (520 - 650)
3 (75)	10 - 12 (650 - 780)
2 1/2 (65)	12 - 14 (780 - 910)
2 (50)	14 - 16 (910 - 1040)
1 1/2 (40)	16 - 18 (1040 - 1170)

Placement

Concrete treated with EUCON 37 may be placed in the same fashion as conventional concrete.

Formwork

Forms for walls or narrow sections must be watertight, strong and have good bracing. During the "flowing period", when the concrete is at a slump of 7" to 9" (180-230 mm), the concrete will exert a higher pressure at the base of the form than conventional concrete. Formwork for slabs is the same as for conventional concrete.

PRECAUTIONS / LIMITATIONS

• Care should be taken to maintain EUCON 37 above freezing; however, freezing and subsequent thawing will not harm the material if thoroughly agitated. Never agitate with air or an air lance.
• Keep concrete from freezing until a minimum strength of 1000 psi (7 MPa) is reached.
• In all cases, consult the Material Safety Data Sheet before use.

Rev. 1.13

The Euclid Chemical Company
19218 Redwood Rd. • Cleveland, OH 44110
Phone: [216] 531-9222 • Toll-free: [800] 321-7628 • Fax: [216] 531-9596
www.euclidchemical.com

An RPM Company

Technical data sheet: Polymer (Etonis® 850)

The Euclid Chemical Company

EUCON AIR MAC12
AIR ENTRAINING AGENT FOR CONCRETE

EUCLID CHEMICAL

DESCRIPTION

EUCON AIR MAC12 is formulated for use as an air entraining admixture for concrete of all types and is manufactured under rigid control which assures uniform and precise performance. EUCON AIR MAC12 adds microscopic air bubbles in concrete and is acceptable to use in all types of concrete, including mixtures that have been traditionally difficult to entrain air. EUCON AIR MAC12 does not contain added chlorides and will not promote the corrosion of steel.

PRIMARY APPLICATIONS

• Ready mix concrete
• Structural concrete
• Mass concrete

• Paving concrete
• All exterior concrete subjected to freeze/thaw cycling

FEATURES/BENEFITS

• Provides a stable air void system with proper bubble size and spacing.
• Improved air-void system protects concrete against damage caused by repetitive freeze/thaw cycles.
• Concrete is made more resistant to de-icing salts, sulfate attack and corrosive water.

• Reduces bleeding and segregation of concrete.
• Less mixing water can be used per yard (meter) of concrete with improved placeability.

TECHNICAL INFORMATION

Typical Engineering Data

Specific Gravity..................................... 1.01
% of solids by weight............................ 15.0
pH... 11.0

EUCON AIR MAC12 is an aqueous solution compound of synthetic chemicals. It is compatible with the full range of Euclid admixtures and concrete mixes containing calcium chloride, water reducing admixtures, retarding admixtures, or high range water reducers.

PACKAGING

EUCON AIR MAC12 is packaged in bulk, 275 gal (1041 L) totes, 55 gal (208 L) drums and 5 gal (18.9 L) pails.

SHELF LIFE

2 years in original, unopened package.

SPECIFICATIONS/COMPLIANCES

EUCON AIR MAC12 meets or exceeds the requirements of the following specifications:
• ASTM Specification C 260
• AASHTO Specification M 154

Appendix C Supplementary Test Data

Properties of fresh cast shotcrete

Mix	Slump (mm)	Air content (%)	Unit weight (kg/m³)
0.45 w/cm	140.0	9.0	2261.2
0.60 w/cm	240.51*	0	2347.5

*flow test

Tensile creep data of the dry-mix shotcretes with 16% and 25% cement* from the ring tests - evolution of the (a) specific creep deformations, (b) creep coefficients
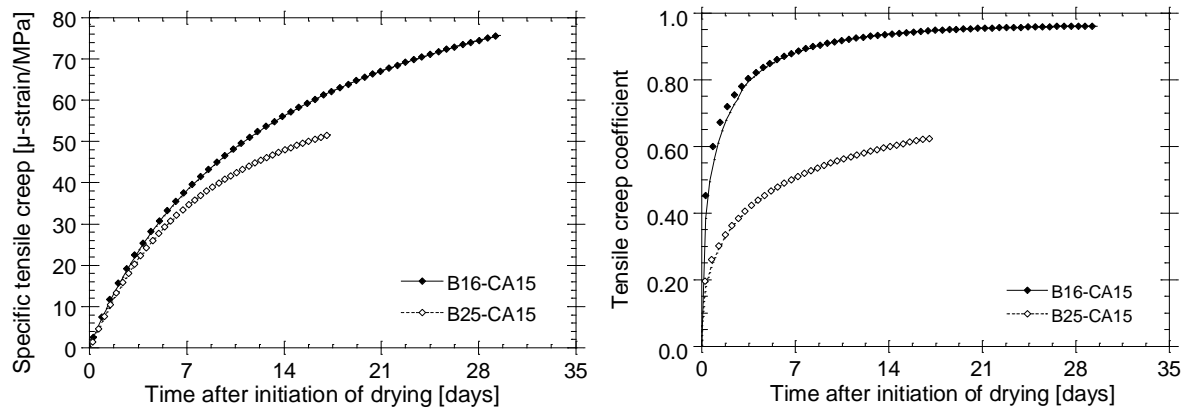

Tensile creep data of the dry-mix shotcretes with 16% and 25% cement* from the ring tests - evolution of the (a) total creep deformations, (b) the tensile creep strain-to-shrinkage ratios
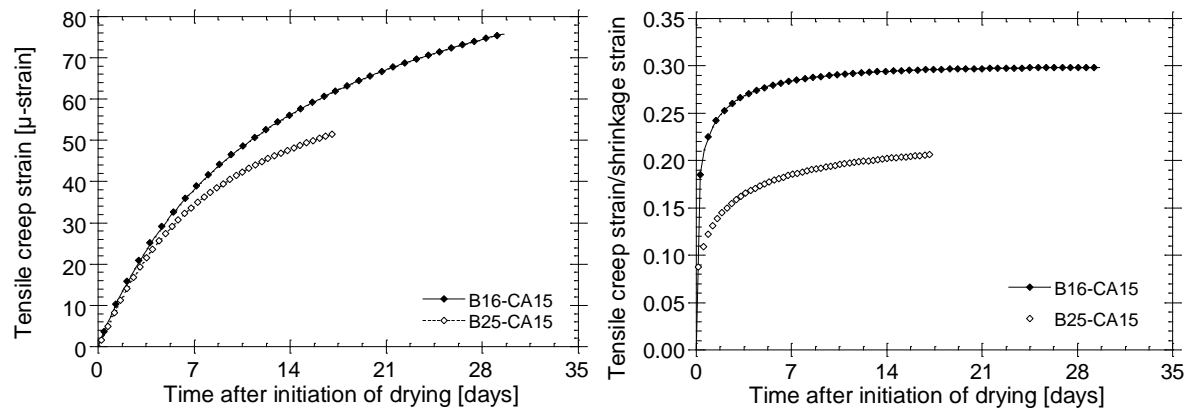
* by weight of the total dry ingredients

179

Tensile creep data of the dry-mix shotcretes with 16% and 25% cement* from the ring tests - evolution of the (a) tensile stress relaxation, (b) stress-strength ratio
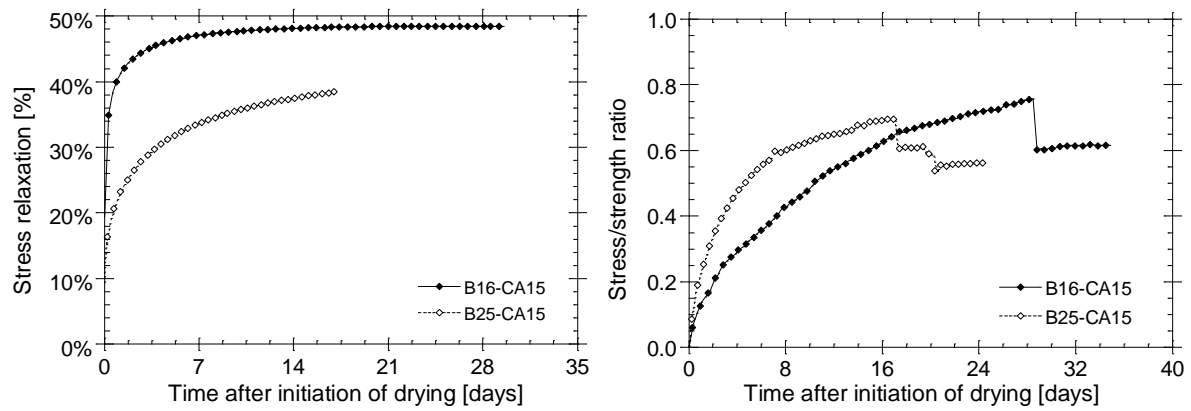
Spraying of the ring specimens using the inclined overhead method

Ring specimens during moist curing

---

* by weight of the total dry ingredients

Appendix D Numerical modelling parameters

Damage law parameters (Cast3M - CEA)

Mixtures	E_∞ (GPa)	A_t	B_t	A_c	B_c	β	k_0	l_c (mm)
C1	30.0	0.9	8000	1.276	1768	1.06	$1.10E^{-4}$	30
C2	28.8	0.9	8000	1.276	1768	1.06	$1.10E^{-4}$	30
M1	28.2	0.9	8000	1.276	1768	1.06	$1.10E^{-4}$	30
M2	32.6	0.9	8000	1.276	1768	1.06	$1.10E^{-4}$	30
M3	37.8	0.9	8000	1.276	1768	1.06	$1.10E^{-4}$	30
M4	28.6	0.9	8000	1.276	1768	1.06	$1.10E^{-4}$	30